CLINICAL AND GENETIC HETEROGENEITY OF HUMAN CATARACT

Peter James Francis BM BSc(Hons) FRCOphth

A thesis submitted to the University of London for the degree of

Doctor of Philosophy

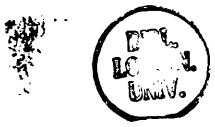

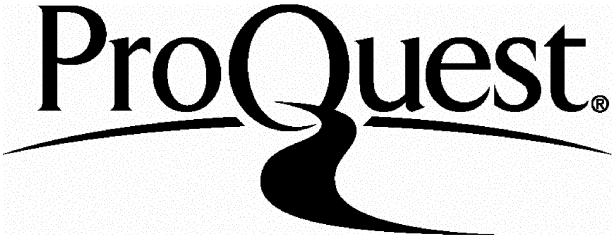

ABSTRACT:

Background: Human inherited congenital cataract is phenotypically heterogeneous most likely reflecting a complex underlying genotype. The visual prognosis for childhood cataract of all aetiologies is poor. There is however very limited information about the outcome of patients with isolated congenital cataract.

Aims: (1) to establish the phenotypic variability of human inherited cataract (HIC).

(2) to determine the visual outcome and surgical complications.

(3) to identify and characterise novel genes implicated in cataract.

Methods: HIC families were identified from hospital databases. All individuals provided a history and underwent an ocular examination. Linkage analysis, mutation detection and functional analysis of mutations identified were undertaken using appropriate expression systems.

Results: (1) 586 individuals (284 affected) from 76 pedigrees participated. Cataract phenotypes could be categorised as one of ten distinct phenotypes. (2) The visual outcome and surgical complication rate was found to be significantly better in our group of isolated cataracts when compared to congenital cataracts of all aetiologies. (3) Novel cataract loci were identified on (*a*) 12q and different missense mutations in the *MIP* gene identified in two families. Functional analysis showed that the mutants abolish the water channel function of the protein. (*b*) 2q. Candidate gene screening of the 2q locus did not reveal a mutation within the γ-crystallin gene cluster. (*c*) Xp. (*d*) 11p. (*e*) 10q. (*f*) 11q.

(4) Linkage to known cataract loci was excluded in two other families.

Conclusions: This study has enabled categorisation of HIC into ten phenotypes. It has shown that patients have better visual and surgical outcomes than those with cataracts of other aetiologies probably due to the lack of attendant developmental abnormalities and because surgery may often be delayed. Four novel cataract loci have been identified. The recognition of mutations in MIP confirms the importance of this protein in both normal lens physiology and cataractogenesis. Furthermore, the functional analyses provide a molecular basis for the cataracts observed.

Contents:

Page

List of tables

Page

List of figures

Introduction

Material and methods

Results

Glossary of terms

ADCC	autosomal dominant congenital cataract
APC	anterior polar cataract
BCVA	best corrected visual acuity
BMIP/hMIP	bovine MIP/human MIP
Cat^{Fr}	Fraser mouse
HIC	human inherited cataract
kDa	kilo-Daltons
lop	lens opacity mouse
MIP	the major intrinsic protein of the lens
NDI	nephrogenic diabetes insipidus
NHS	Nance-Horan syndrome
OMIM	Online Mendelian Inheritance in Man
PCR	polymerase chain reaction
PIC	polymorphic information content
PPC	posterior polar cataract
RD	retinal detachment
RT	room temperature and pressure

Contact details:

Peter J Francis BM BSc FRCOphth

Wellcome Clinical Research Fellow, Institute of Ophthalmology
and
Honorary Specialist Registrar, Moorfields Eye Hospital, London

Work:

Department of Molecular Genetics,
Institute of Ophthalmology,
University College London,
11-43 Bath Street,
London EC1V 9EL

email: p.j.francis@hgmp.mrc.ac.uk

telephone: 0207 608 4033 or 0585 688847

Home:

Flat 3,
12 Bulstrode Street,
Marylebone,
London W1U 2JF

email: peterjamesfrancis@ukonline.co.uk

telephone: 0207 935 0822

Acknowledgements

My thanks go to my supervisors, Professor Shomi Bhattacharya and Mr Tony Moore for their support and guidance throughout the project and to Dr Peter Agre for inviting me to his laboratory to perform the expression studies. I also acknowledge my colleagues, Dr Vanita Berry and Ms J-J Chung with whom I worked closely alongside. The work presented in this thesis is aupported by Wellcome Trust Grant 053416/Z/98. I would also like to thank all the families without whom the project would not have been possible.

I also acknowledge the following consultants and colleagues for their help in facilitating patient ascertainment or for identifying probands:
Miss G Adams and Messrs J Dart, J Lee, J Sloper, J Stevens, S Tuft and Professor P Khaw, Moorfields Eye Hospital; Mr J Ainsworth, Birmingham and Midland Eye Hospital; Mr G Brice, Research Nurse, St George's Hospital; Mr M Clarke, Newcastle; Mr J Feddow, Derriford Hospital, Plymouth; Mr Kinnear, London; Mr R Kumar, George Elliott Hospital, Nuneaton; Dr M Lees, Clinical Genetics, Hospital for Sick Children, Great Ormond Street, London; Professor E Maher, Birmingham Women's Hospital, Birmingham; Messrs Orr and Suriningham, Queens Medical Centre, Nottingham; Mr A Quinn, Royal Devon and Exeter Hospital, Devon; Mr Rubasingham, King's Mill Hospital, Sutton-in-Ashfield; Miss S Vickers, Sussex Eye Hospital, Brighton; Mr H Wilshaw, Birmingham and Midland Eye Hospital.

I would also like to acknowledge Mr Wagih Aclimandos for lending the portable slit lamp and Dr Brian Clark, Moorfields Eye Hospital for helpful discussions and in the preparation of the lens specimens and Mr Philip Ball, Senior Medical Illustrator, Addenbrooke's Hospital, Cambridge for his help and advice in preparing the some of the illustrations for this thesis.

Publications arising from the project:

Francis PJ, Chung J-J, Yasui M, Berry V, Wyatt MK, Wistow G, Moore AT,

Bhattacharya SS, Agre P

Functional impairment of lens aquaporin in two families with

dominantly inherited cataracts

Human Molecular Genetics Sept 2000; 9(15): 2329-2334

Berry V*, Francis PJ*, Kaushal S, Moore AT, Bhattacharya SS

*these individuals have contributed equally to this paper

Missense mutations in the human *MIP* gene, encoding the major intrinsic protein of the lens, underlie

autosomal dominant "polymorphic" and lamellar cataracts on 12q

Nature Genetics May 2000; 25(5): 15-17

Francis PJ, Berry V, Moore AT, Bhattacharya SS

Lens biology, development and human cataractogenesis

Trends in Genetics, May 1999; 15(5): 191-6

Francis PJ, Ionides ACW, Berry V, Bhattacharya SS, Moore AT

Visual outcome in patients with isolated autosomal dominant congenital cataract

Ophthalmology 2001 (in print)

Francis PJ, Berry V, Kaushal S, Moore AT, Bhattacharya SS

Missense mutations in the *MIP* gene, encoding the major intrinsic protein of the lens (Aquaporin-0),

underlie cataracts in humans

Book chapter, Kluwer Academic/Plenum, London (2000)

Francis PJ, Berry V, Bhattacharya SS, Moore AT

Congenital progressive polymorphic cataract caused by a mutation in the major intrinsic protein of the lens, MIP (AQP0)

British Journal of Ophthalmology, December 2000; 84(12): 1376-1379

Francis PJ, Berry V, Bhattacharya SS, Moore AT

The genetics of childhood cataract

Journal of Medical Genetics, July 2000; 37(7): 481-8

Francis PJ, Berry V, Bhattacharya SS, Moore AT

The role of the lens in anterior segment development

Ophthalmic Genetics 2001 (in print)

Ionides ACW, Francis PJ, Berry V, Mackay D, Shiels A, Bhattacharya S, Moore AT

Clinical and genetic heterogeneity in autosomal dominant congenital cataract

British Journal of Ophthalmology 1999; 83(7): 802-808

Berry V, Mackay D, Francis PJ, Shiels A, Moore AT, Bhattacharya SS

Connexin 50 mutation in a family with congenital "zonular nuclear" pulverulent cataract of Pakistani origin

Human Genetics, 1999; 105(1-2): 168-70

Francis PJ, Moore AT

The Lens (Invited editorial)

Eye 1999; 13: 393-4

Presentations arising from the project:

Association for Research in Vision and Ophthalmology, 1999,

poster

Connexin50 mutation in a family with congenital "zonular nuclear" pulverulent cataract of Pakistani origin

Berry V, Mackay D, Francis PJ, Shiels A, Moore AT, Bhattacharya SS

Association for Research in Vision and Ophthalmology, 1999,

oral presentation

Clinical and genetic heterogeneity of autosomal dominant cataract (ADCC)

Francis PJ, Berry V, Mackay D, Shiels A, Moore AT, Bhattacharya SS

Annual Congress of Ophthalmology (UK), Cardiff, 1999,

poster

Identification of the genetic mutations underlying autosomaldominant congenital cataract

Francis PJ, Ionides ACW, Berry V, Mackay D, Shiels A, Moore AT, Bhattacharya SS

Childhood Vision Research Society Meeting, Institute of Child Health, 1999

oral presentation

Clinical and genetic heterogeneity of non-syndromic autosomal dominant cataract (ADCC)

Francis PJ, Berry V, Ionides ACW, Mackay D, Shiels A,

Bhattacharya SS, Moore AT

European Paediatric Ophthalmology Group, Strasbourg, 1999

oral presentation

Clinical heterogeneity and visual outcome in inherited cataract

Francis PJ, Ionides ACW, Berry V, Bhattacharya SS, Moore AT.

Association for Research in Vision and Ophthalmology, 2000

oral presentation

Missense mutations in the human MIP gene (AQP0) underlie polymorphic and lamellar cataract families mapped to chromosome 12q

Berry V, Francis PJ, Kaushal S, Moore AT, Bhattacharya SS

Association for Research in Vision and Ophthalmology, 2000

poster

Mutation screening in a family with "coralliform" cataract that maps to human chromosome 2q

Francis PJ, Berry V, Moore AT, Bhattacharya SS

Molecular Biology and Physiology of Water and Solute transport meeting, Goteborg, Sweden, 2000

oral presentation, plenary session and poster

Missense mutations in the human MIP gene (AQP0) underlie cataract development in humans

Francis PJ, Berry V, Kaushal S, Moore AT, Bhattacharya SS

European Paediatric Ophthalmology Group, Cambridge, 2000

oral presentation

Identification and functional characterisation of mutation in lens aquaporin in two families causes dominantly inherited human cataracts

Peter Francis, Vanita Berry, Jean-Ju Chung, Masato Yasui, M. Keith Wyatt, Graeme Wistow, Anthony Moore, Peter Agre, Shomi Bhattacharya

American Society of Human Genetics, Philadelphia, 2000

oral presentation

Functional impairment of lens aquaporin in two families causes dominantly inherited human cataracts

Peter Francis, Vanita Berry, Jean-Ju Chung, Masato Yasui, M. Keith Wyatt, Graeme Wistow, Anthony Moore, Peter Agre, Shomi Bhattacharya

Annual Congress of Ophthalmology (UK), Birmingham, 2001

oral presentation

Characterisation of the genes responsible for inherited cataract

Peter Francis, Vanita Berry, Alex Ionides, Shomi Bhattacharya, Anthony Moore

Annual Congress of Ophthalmology (UK), Birmingham, 2001

poster

Functional analyses of mutations in the MIP gene that cause cataracts in humans

Peter Francis, Vanita Berry, Jean-Ju Chung, Masato Yasui, M. Keith Wyatt, Graeme Wistow, Anthony Moore, Peter Agre, Shomi Bhattacharya

Invited presentations:

Southampton Eye Unit, March 2000

South Western Ophthalmic Society Meeting, Barnstable March 2000

Preface and Statement of Originality

"We shall not cease from exploration.
And the end of all our exploring will be to arrive where we started,
and know the place for the first time" – T.S. Eliot

During the preparation of this thesis, rapid and significant advances in the world of genetics have been seen; indeed the Millenium year was greeted by the publication of the draft sequence of the human genome. The large number of genes now implicated in human disease have meant that new linkages have begun to assume lesser impact with more emphasis on the functional implications of mutations (*functional genomics*) and the advent of *proteomics*.

Given this context, this project has evolved from linkage analysis-based to a more functional approach. Nevertheless, our strategy to unravel the complex genetics of age-related cataract by first identifying the genes responsible for its childhood counterpart (a Mendelian disorder) remains essentially reductionist in approach.

The work presented in this thesis submitted for the degree of doctor of philosophy is my own composition and save as otherwise stated the data presented herein is my own original work.

To Beth

1. Introduction

1.1 Congenital cataract: general features

Cataract is the term used to describe opacification of the crystalline lens of the eye. Opacities vary in morphology, are often confined to a portion of the lens and may be static or progressive. Cataract reduces optical performance, most commonly manifested by decreased visual acuity, glare and decreased contrast sensitivity. The condition is only treatable at present by surgical removal. In adults, cataract is the commonest cause of visual impairment world-wide[1].

Congenital cataract is the commonest treatable cause of childhood blindness in Europe and the USA with a prevalence of 1-6 cases per 10 000 live births[2,3]. Presentation is most usual in early infancy, with static or slowly progressive lens opacities that are most commonly bilateral and symmetrical. The degree of deprivational amblyopia that arises without appropriate management depends upon the position of the opacity within the lens and the density of opacification[4]. In general, the more posteriorly located and dense an opacity, the greater the impact on visual function[4]. It is estimated that despite surgical removal and subsequent optical correction, a third of patients with congenital cataract will remain legally blind[5].

Inherited cataract accounts for around half of all congenital cataracts[6] and is a recognised feature of almost two hundred genetic diseases[7], including galactosaemia, Nance-Horan and Down syndromes. In most instances, however, cataract is inherited non-syndromically as an isolated abnormality (figure 1). In non-consanguineous populations, the majority of inherited cataract shows autosomal dominant inheritance. Many apparently sporadic congenital cataracts might also have a genetic basis[6,8].

Nettleship and Ogilvie published the first description of a family with inherited cataract in 1906[9]. Later, Nettleship described a genealogically distinct family with a similar phenotype. This family was re-investigated in 1963, and the disease shown to co-segregate with the Duffy blood group locus[10]. This became the first human autosomal disease to be genetically linked when in 1968, the Duffy locus was assigned to chromosome 1[11].

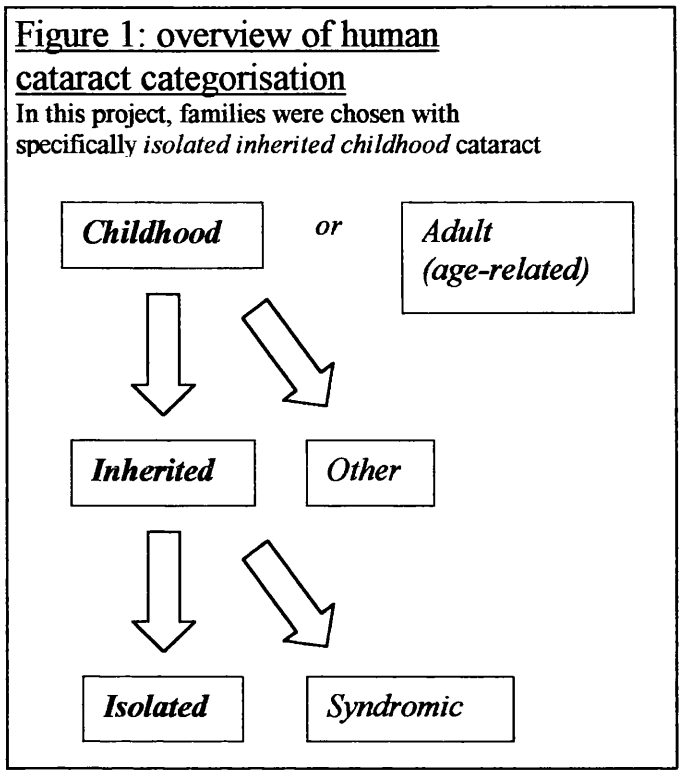

It is now evident that inherited congenital cataract is both phenotypically and genetically heterogeneous. Furthermore, recent advances in our understanding of the genetics of human cataract, in particular this inherited congenital form, together with the development of an array of animal models have provided valuable new insights into normal vertebrate lens biology and the mechanisms that underlie cataract formation.

Current knowledge of the lens is extensive. This introduction is therefore tailored to provide specific details to appreciate the questions addressed by this project, the strategy (for example the construction of a candidate gene list) and to interpret results obtained.

1.2 Lens morphogenesis and anatomy

Studies of lens embryology and gene expression have made important contributions to our current understanding of the developmental periods during which the lens is susceptible to adverse influences, thus helping to explain the observed spatial and temporal patterns of cataract. In the human, lens organogenesis (figure 2) begins in the 4mm embryo (fourth week of gestation) with thickening of the surface ectoderm overlying the optic vesicle to form the epithelial cells of the lens placode[12 13]. Invagination of this area produces the lens pit, which closes over to form the lens vesicle. A temporary connection with the surface ectoderm is retained (the lens stalk).

Cells lining the posterior wall lose their nuclei and rapidly elongate, obliterating the cavity of the vesicle to form primary lens fibres[13-15]. Secondary lens fibres are subsequently produced throughout life by division of anterior lens epithelial cells in the equatorial zone of the lens and form lamellae, compacting more central fibres[16 17]. Mature lens fibres do not divide and there is minimal turnover of their protein constituents. Points at which secondary lens fibres come into apposition result in lines of optical discontinuity or "sutures"[18]. A capsule of mesenchymal origin surrounds the lens. Successful organogenesis results in a transparent biconvex lens suspended in the eye by zonular ligaments, between the aqueous humour and the vitreous body. Exchange of waste products and nutrients occurs with the aqueous humor across the semi-permeable lens capsule[19].

Secondary lens fibre formation does not result in optical homogeneity. Instead, concentric zones of varying refractive index develop whose interfaces can be clearly delineated[20 21]. The zones correspond to different developmental stages, although controversy remains about their precise nature.

1.2.1 Lens anatomy and optics

Clinically, the lens has a convenient geography (figure 3). It has an equator and the summit or centre of each of its two convex faces, front and back, are described as the anterior and posterior poles respectively. Several zones or regions of the lens are identifiable (figure 4), which are consistent with the chronology of lens development. In practice however, it can be quite difficult to discern the

Figure 2: lens development

In humans, lens organogenesis begins in the fourth week of gestation with *a*, thickening of the surface ectoderm overlying the optic vesicle to form *b*, the lens placode; *c*, this area begins to invaginate (the lens pit) and eventually closes overto form *d*, the lens vesicle; *e*, cells lining the posterior wall of the lens vesicle rapidly elongate to form the primary lens fibres (embryonic nucleus). Thereafter, throughout life, secondary lens fibres differentiate from equatorial epithelial cells forming concentric lamellae around the embryonic nucleus

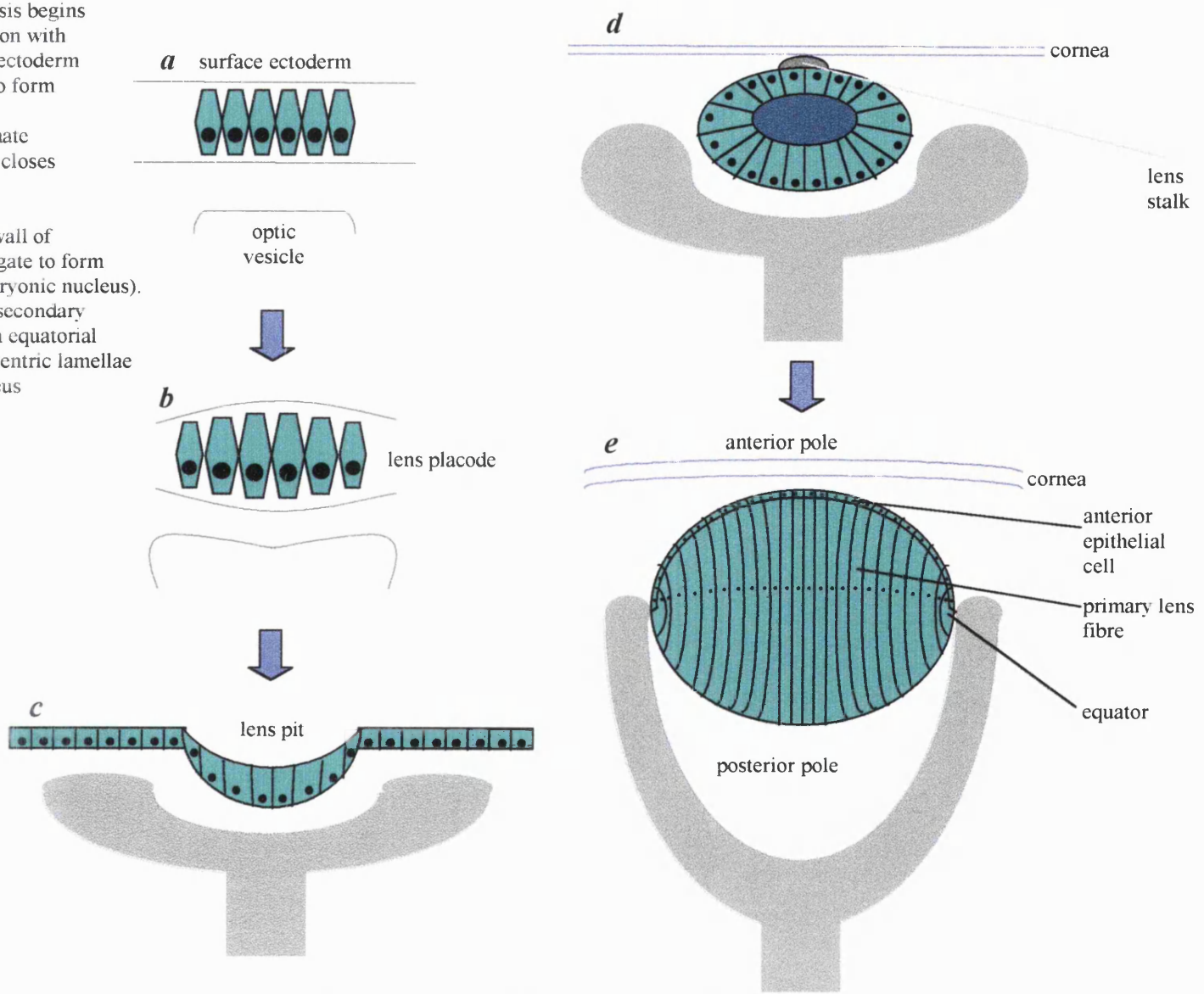

boundaries of these zones with any degree of accuracy[12]. A nomenclature that best reflects the cataract phenotypes observed, and one that has a biochemical and histological basis, proposes that the lens consists of two parts: the nucleus, which is the total lens at birth, comprising embryonic and fetal parts, and the cortex that is laid down subsequently[22]. Cortical lens matter directly adjacent to the capsule is sometimes called "subcapsular".

The optics of the lens can be described by "thin lens" mathematics. Figure 5 shows how incident light is brought to a focus. The normal human eye has an overall refractive power of about 58 dioptres. The cornea contributes the largest component and the lens about 19 dioptres. Changes in the tension of the suspensory ligaments, which are under neuromuscular control, allow the lens to change shape. This process, known as accommodation, alters the power of the lens and enables light incident from close objects to be brought to a focus on the retina[23 24].

1.3 Molecular and cell biology of the lens

1.3.1 Developmental regulators

The lens forms through a temporally and spatially regulated pattern of differentiation, co-ordinated by several growth factors, fibroblast growth factors FGF1, -2, -3 and activin, and homeobox transcription factors *PAX6*, *SIX3*, *SIX5* and *PITX3*. The roles of *PAX2*[25], *OPTX2* and retinoic acid in transcriptional regulation are less well established. In turn, the presence of the developing lens appears to be crucial for the normal development of other ocular structures.

The presence of transcripts of three subtypes of FGF in the developing optic cup and vesicle[26] suggests an important role for these growth factors in normal lens development. There is evidence now that lens fibre differentiation and subsequent survival is dependent upon their activity[27].

PAX proteins are multifunctional transcription factors, critical for numerous developmental processes in animals[28]. All share a similar strucutre defined by paired, homeo- and octa- domains. PAX6, encoded by a gene on 11p13, is essential for early eye determination[29], the specification of ocular

Figure 3: gross anatomy of the adult lens, *a*, in transverse section; *b*, quarter segment removed to show developmental stages (reproduced from Harding, 1991)

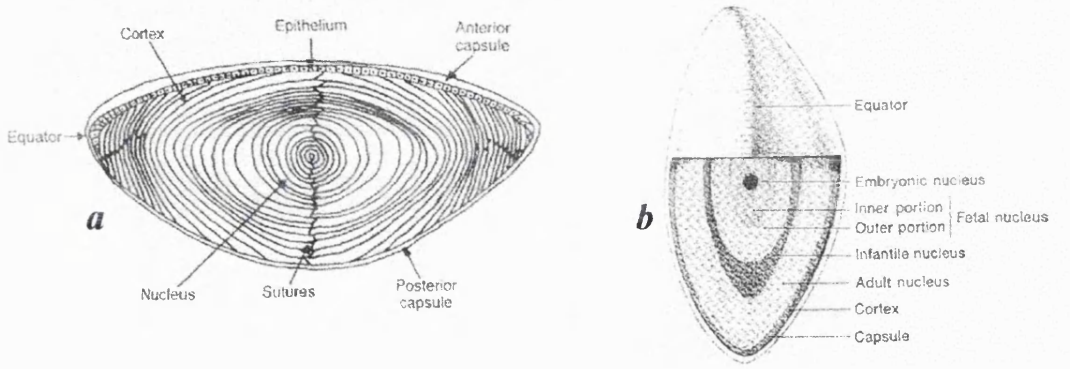

Figure 4: the adult lens consists of clinically discernable regions *a*, lens viewed anteroposteriorly; *b*, lens in cross-section

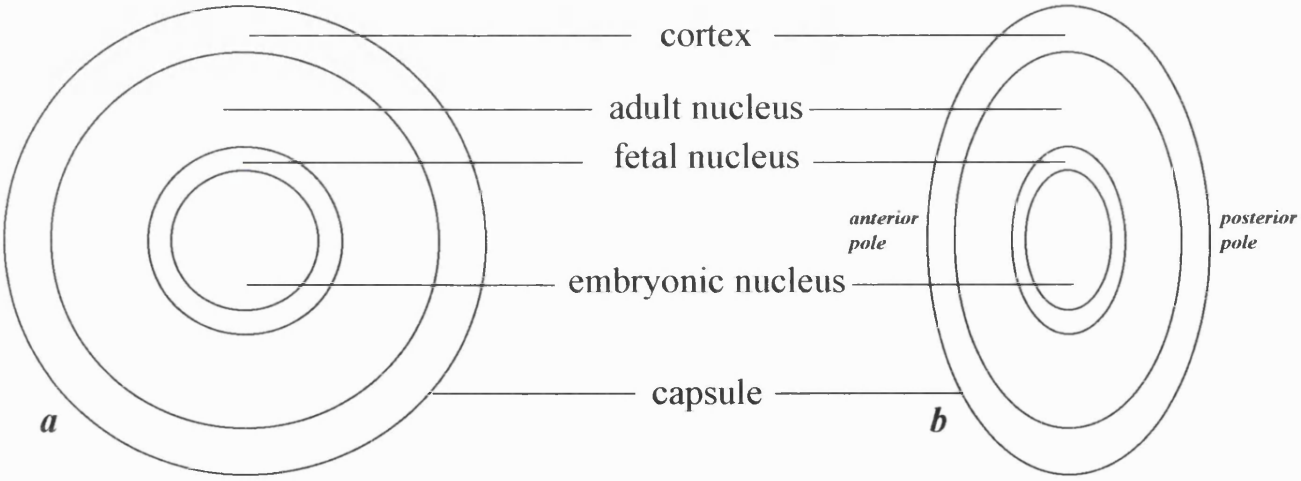

Figure 5: the optics of the human lens can be described by thin lens theory. The cardinal rays of light (drawn) from an object are brought to a focus on the retina

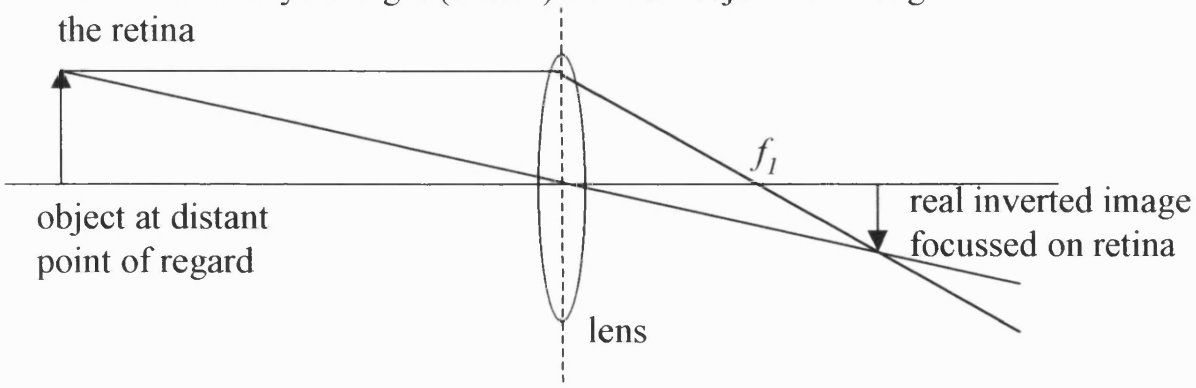

tissues and normal eye development in vertebrates[30]. Heterozygous mutations in *PAX6* are associated with abnormalities in vertebrates such as aniridia and microphthalmia[30 31]. Homozygous *PAX6* mutations are lethal and are associated with severe brain defects and a complete absence of the eyes[32]. Furthermore, targeted expression of the Drosophila *PAX6* homologue, *eyeless*, produces supernumerary eyes, suggesting that *PAX6* is a key regulatory gene for eye morphogenesis[33].

The precise role of *PAX6* in later ocular development is not completely known. It appears to be involved in the regulation of lens crystallin expression both as an activator[34 35] and a repressor[36]. Indeed, mutations resulting in premature truncation of the PAX6 protein have recently been implicated in the development of human cataract.

Of the other homeobox (*HOX*) genes, *PITX3* (10q25) is expressed in lens placode and forming lens pit[37]; *SIX3* is expressed in the optic vesicle and anterior neural plate[38] and *OPTX2* is expressed in the lens placode and optic vesicle. All appear to play important sequential roles in the induction of eye and lens development. *SIX5* is not expressed during this developmental process but has been detected in adult anterior epithelial lens cells, where the dysfunction of its protein product has been implicated in the development of human cataract[39].

Retinoic acid (RA) has been shown to play an important role in vertebrate development, cellular growth and differentiation by respecifying the anterior-posterior axis, stimulating mirrored axis duplication and modulating *HOX* gene expression. RA has also been implicated in the control of the differentiation of pluripotential germ-layer cells with excess or insufficient concentrations resulting in the abnormal development of certain structures including amongst others, the eye[40].

Cellular signalling by RA and its isoforms (retinoids) is transduced by direct binding of RA transcription factors (RAR's, retinoic acid receptors)[41] to RA and retinoid X response elements (RARE's and RXRE's respectively) in the promoter regions of target genes or by regulating production of secondary transcription factors, such as AP-2[42]. At present, the chromosomal localisation of three RAR's is known in humans; the cellular retinoic acid binding proteins (CRABP) –1 and –2 have been assigned to 15q24 and 1q21.3 respectively[43] and retinoic acid induced –2 (*RAI2*)

to Xp22[44]. Expression of these proteins in the lens is not established however ectopic expression of CRABP-1 in lens epithelial cells is cataractogenic in mice, hypervitaminosis A in late human fetal life induces congenital cataract formation[45] and retinoic acid has been directly implicated as a regulator of crystallin expression[46].

Transparency of the lens results from the highly ordered arrangement of the macro-molecular components of constituent cells and the regular arrangement of lens fibres. Mature lens fibres are hexagonal in cross-section (figure 6), and being devoid of nuclei and organelles to reduce light scattering, are metabolically inactive. Protein accounts for a third of the wet weight of the lens, nearly double that found in other tissues[47].

Lens cell physiology is entirely directed to the maintenance of this architecture serving to minimise oxidative stress (catalase[48], glutathione redox cycle[49] and the mercaptopuric pathway), and changes in hydration and electrolyte imbalance[50]. Metabolic activity is highest in the lens epithelium, an elaborate system of gap junctions allowing communication with the metabolically inert cells deep within the lens[47].

1.3.2 Crystallins

Crystallins, the main cytoplasmic proteins, are a heterogeneous group of highly stable water-soluble molecules thought originally to be selectively expressed in the lens to provide transparency[51 52]. It is now clear that crystallins are found in many tissues where they subserve other functions[53 54]. For example, αB-crystallin is now known to be a member of the small (<30kDa) heat shock protein family where it has roles in many tisues protecting cells from stress[55]. Interestingly, there is now convincing evidence that in addition to its role in lens transparency, α-crystallin also functions as a molecular chaperone guiding the correct packing of other crystallins and folding of the cytoskeleton[56]. This multiple use of a distinct protein encoded by a single gene, termed "gene sharing", seems likely to be widespread in the lens, cornea and other ocular tissues[57]. In humans, crystallins are categorised into α, β and γ subgroups. β- and γ-crystallin are closely related globular proteins whose two domain structure is distinguished by four, stable, torqued β-pleated sheets known as "greek key motifs". These

Figure 6: lens fibre connexins and connexon formation

a, mature lens fibres are hexagonal in cross-section and at least in part transparency is achieved by their resultant tight and regular packing; *b*, highlights adjacent sections of two lens fibre cell membranes where connexin proteins have assembled to form hetero-hexamers (connexons). By associating with a connexon on the other membrane (gap junction) ions and solutes may pass between cytoplasms

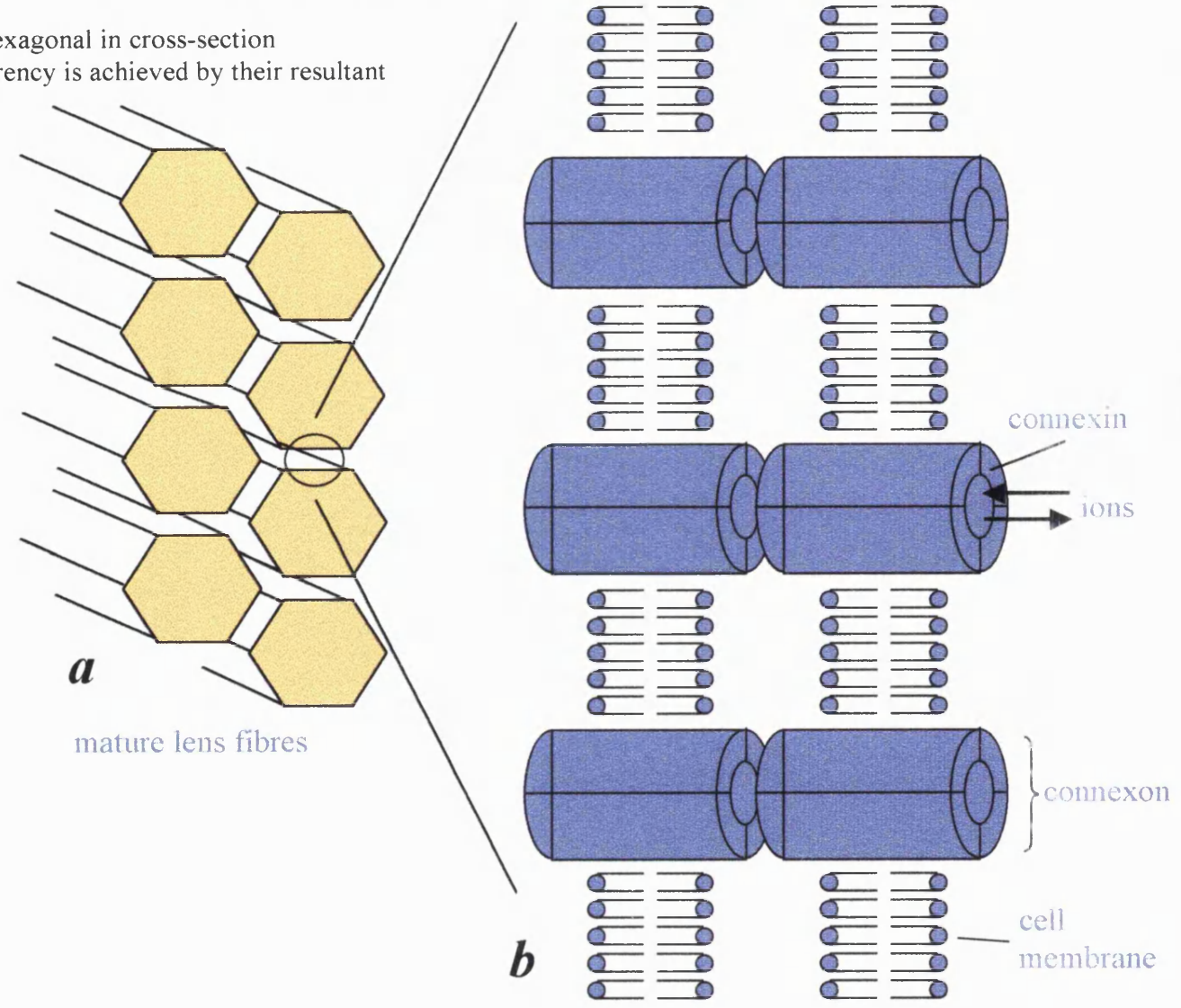

motifs enable crystallin molecules to associate in highly compact oligomers whose light-scattering properties are further reduced by the internalisation of all hydrophobic residues[52]. The α-crystallin molecule does not contain these motifs suggesting that it is not closely related to β- and γ-crystallins[54].

1.3.3 Cytoskeleton

The structural framework of the cuboidal lens epithelial cells is composed of cytoskeletal proteins typical of most mammalian cells[58]; actin-based thin filments, microtubules and vimentin based intermediate filaments. However, secondary lens fibre differentiation, elongation and compaction are accompanied by radical alterations in the expression of several components of this cytoskeletal architecture. Immunocytochemical and *in situ* hybridisation indicate that these cytoskeletal proteins disappear from the fibre cell shortly after differentiation[59 60] and are replaced by CP49 (phakinin) and CP115/CP95 (filensin) which assemble to form a novel structure referred to as the beaded filament[61]. This structure differs from other intermediate filaments and appears to have the ability to interact with α-crystallin. The role of α-crystallin, the most abundant protein in the lens, is not yet clear, but its function as a chaperone protein has recently been linked to the dynamics of mammalian cytoskeleton assembly because correct folding of cytoskeletal proteins is dependent upon its presence[62 63].

1.3.4 Membrane proteins

Maintenance of lens cell homeostasis is reliant upon the presence of an extensive array of membrane channels comprising "thin" and "gap" junctions. Thin junctions regulate the highly selective transfer of water molecules across cell membranes. In the human lens, by far the most abundant of these junctional components are MIP, the major intrinsic protein of the lens (previously referred to as MP26)[64] and LIM-2 (variously referred to as MP19, MP20, MP18 and MP17)[65-68]. LIM-2 is the most abundant integral membrane protein of the lens, first described as a fibre-specific component of bovine lens[69]. Its function remains unknown, though it has been shown to co-localise with gap junctions in distinct regions of the lens and some role in gap junction formation or maintenance is suggested[70]. Recently, mutations in the gene encoding the murine homologue, *Lim-2*, have been shown to result in cataractogenesis in the *To3* mouse model[71].

1.3.4.1 The major intrinsic protein of the lens (MIP): Aquaporin-0 (AQP0)

A significant advance in cataract genetics was the discovery that the *Cat*^{Fr} (*Fraser* originally *Shrivelled*[72]) and *Cat*^{lop} (lens opacity mutation mouse[73]) phenotypes result from mutations in the murine *Mip* gene, localised to 10q, a region syntenic with human chromosome 12q[74 75].

Cytogenetically, the position of the human gene homologue, *MIP*, primarily and abundantly expressed in the lens, has been refined to 12q14. Its protein product, the major intrinsic protein of the lens (MIP/AQP0) belongs to the aquaporin family of channel proteins crucial for controlling the influx and efflux of water across cell membranes[76]. Numerous other aquaporins have been identified and the widespread presence of these channels suggests an important physiological role[77]. For these reasons, the *MIP* gene is considered a strong candidate for human cataractogenesis in families that are linked to 12q14.

1.3.4.1.1 Spontaneously-occurring murine *Mip* mutants

The *Cat*^{Fr} mouse (also known as *Cat2*^{Fr}, *Shrivelled* or *Svl*, as wrinkling of the lens capsule is also observed) has a transposon-induced splice site mutation that results in the replacement of the C-terminus with 55 novel amino acids. The genomic structure of the Fraser mouse *Mip* gene is shown in figure 7, below. The mouse transposable element, *ETn* (*embryo transposon*) inserts into intron 3 and thus, the translated hybrid protein consists of the products of exons 1, 2, 3 and a 5' section of the transposon (sequence alignment indicates that this section is identical to the long terminal repeat, LTR, of *ETn*). It appears that the *Cat*^{Fr} lens adopts an alternative polyadenylation signal close to an in frame stop codon within the LTR sequence. Exon 4 is not translated though the contribution of the insert results in a protein almost the same length (261 amino acids) as that of the wild-type (263 amino acids)[75]. The resulting fusion protein lacks most of the sixth transmembrane and carboxy-terminal domains of the wild-type AQP0, including a major phosphorylation site at serine 235.

Figure 7 : genomic structure of the *Cat*^{Fr} *Mip* gene showing the mouse transposable element *Etn* inserted within intron 3

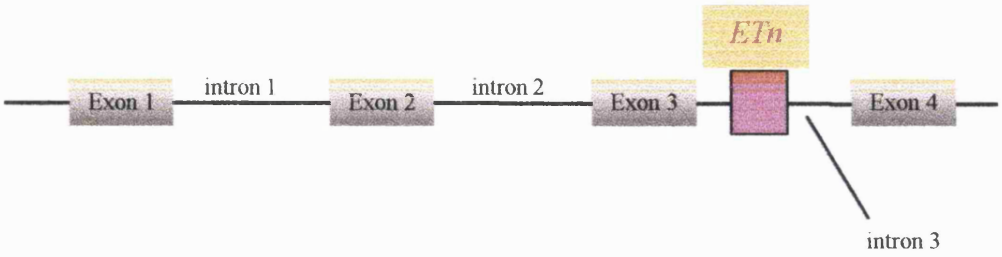

Mouse transposable elements have been shown to disrupt several other mouse genes including those for the muscle chloride channel in myotonic (*adr*) mice, leptin in obese (*ob2J*) mice and Fas antigen in lymphoproliferation (*lpr*) mice[78]. However the *Cat*^{Fr} mutant appears to be the only example where a portion is actually translated into protein. Whether the AQP0-LTR fusion protein impacts on water transport, results in a targeting defect or has a direct cytotoxic effect is unknown.

The *lop* mouse (*lens opacity*) has a dominant missense mutation. A G→C transition at nucleotide 151 results in a non-conservative amino acid substitution at position 51 (Ala51Pro). Sequence comparison with other species show that at this position, alanine is the consensus residue whereas proline is never encoded. The mutation appears to result in mis-targeting of the protein and accumulation in the endoplasmic reticulum of the lens fibre cell[75]. The precise mechanism by which this results in cataract formation is not known.

In both *Cat*^{Fr} and *lop* mutants, lens opacification is first observed near the anterior pole at embryonic days 13 and 14 which progresses to involve the whole lens. In mice homozygous for the mutations, lens fibre degeneration and a concomitant reduction in overall lens volume are also seen (figure 8)[79].

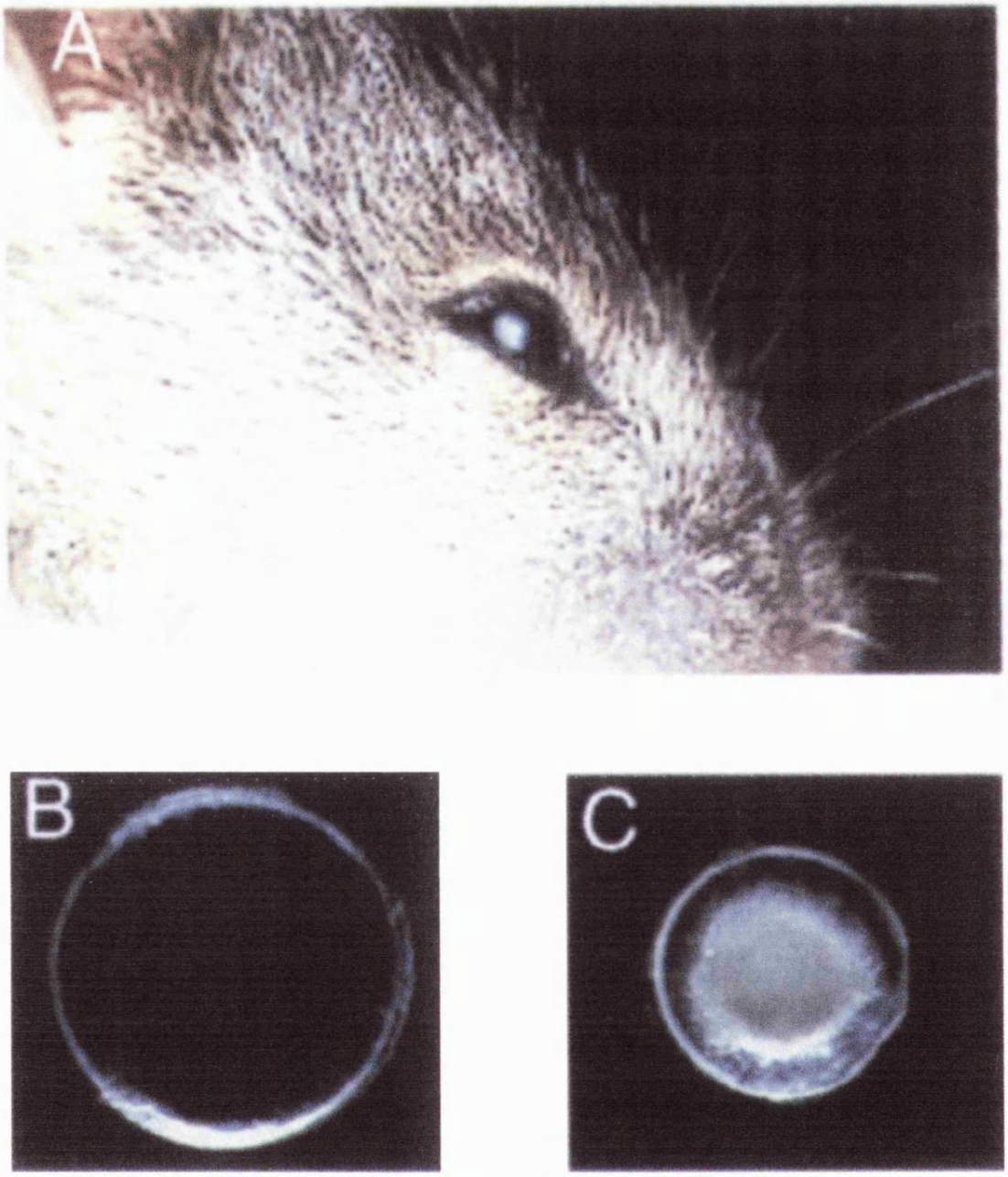

Figure 8: the Fraser mouse is a spontaneously occurring dominant mouse cataract model in which the mouse transposable element *ETn* has inserted into intron 3 of *Aqp0*, the mouse homologue of the human lens-specific aquaporin *AQP0/MIP*. The resulting protein consists of the products of exons 1, 2 and 3 and a portion of *ETn*. Exon 4 is not transcribed.
A, mice heterozygous for the mutation have lens opacities;
B, shows a cross-section through a clear normal mouse lens
C, shows a similar section through a lens from the Fraser mouse. Marked lens opacification is seen. In this mouse, homozygous for the mutation, a reduction in overall lens volume is also observed.
(by courtesy of Prof P. Agre)

1.3.4.1.2 The aquaporin gene superfamily

The aquaporin gene superfamily encodes over 150 transmembrane proteins that are ubiquitously expressed in almost all tissue types and have been identified in mammals, fish, reptiles, plants[80], bacteria[81], yeast[82] and protozoa[83]. With the exception of aquaporin-6[84], all aquaporins localise to the cell membrane. The amino acid signature of the aquaporins is the N-P-A amino acid sequence motif[77]. Aquaporins share a significant degree of sequence conservation suggesting that the proteins subserve not only a critical physiological role, but also how important amino acid sequence conservation is to the function of the molecule.

Figure 9 shows two plants of the genus, Arabidopsis thaliana, propagated hydroponically[85]. The morphology of the left-hand plant expressing antisense RNA to aquaporin Piplb (which regulates root water uptake) is identical to the control (right) except for the compensatory five-fold amplification of root arborisation.

In many instances a cell may express several different aquaporins[86]. The tissue distribution of aquaporins in the eye is shown in figure 10.

Nature has achieved in aquaporin proteins the seemingly impossible functional combination of a molecule that is able to transport water molecules in a highly selective manner[77]. Cryoelectron crystallographic analysis has taken appreciation of the structure of human aquaporin-1 to a resolution of 4.5Å where it is possible to predict that water selectivity is conferred by the narrowness of the channel. Furthermore water molecules pass as a chain through the channel linked by hydrogen bonding, except where two asparagine molecules protrude. These residues interrupt the chain, thus inhibiting proton transit through the molecule[87].

Figure 9: over one hundred and fifty members of the aquaporin gene family have now been identified in animals, bacteria and plants. A graphic example of their roles in water homeostasis is shown here. ***a***, shows a four month old wild-type *Arabidopsis thaliana plant* propogated hydroponically showing root arborisation proportionate to leaf area; ***b***, in contrast, this plant is expressing antisense RNA to the plant aquaporin *Pip1b*, which facilitates root water uptake – a compensatory five-fold increase in root arborisation.
(by courtesy, Prof P. Agre)

Figure 10: the aquaporin family of proteins mediate the bi-directional flux of water across cell membranes. In the eye there is a high degree of tissue-specific expression. Image shows sagittal section through the human eye transecting the optic nerve and cornea

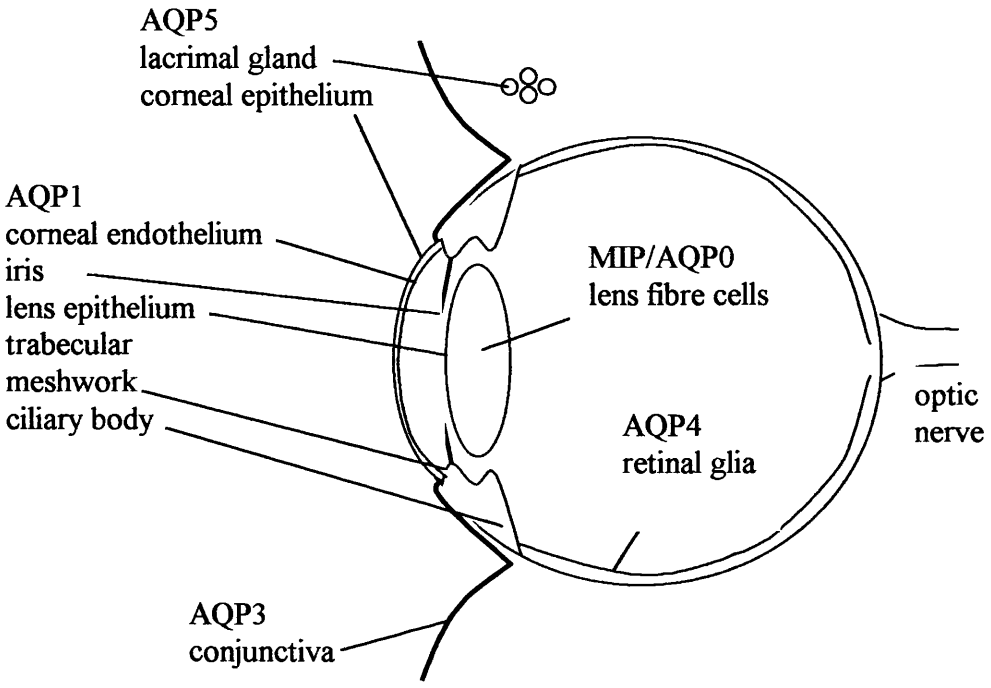

It is clear however that certain aquaporins can be shown experimentally to be permeable to other solutes (glycerol and carbon dioxide), probably because their central pore is wider and lacks the structure that confers water-selectivity. The physiological significance of these multi-functional "aquaglyceroproteins" (AQP–3, AQP-7, AQP-9 in humans) is not known[88 89] but the abundance of such polypeptides in the basolateral membranes of cells lining kidney collecting ducts and nasopharyngeal mucosa implicates important roles in renal water reabsorption and mucosal secretions respectively[76 90].

1.3.4.1.3 The roles of aquaporins in mammals

Aquaporins have been implicated in renal water secretion and reabsorption, cerebrospinal fluid and aqueous humor fluid dynamics, lacrimation, the generation of pulmonary secretions[91]. Pathophysiologically, it is hypothesised that aquaporins play a critical role in many conditions resulting in abnormal fluid retention, for example congestive cardiac failure[76].

1.3.4.1.4 Human aquaporin mutations

Of the ten aquaporins identified[92], only aquaporin-2 has so far been implicated in human disease. Expression of AQP2 is restricted to the principal cells of the renal collecting system. In response to the hormone vasopressin (anti-diuretic hormone or ADH) acting through a basolateral membrane *V2* receptor, intracellular vesicles containing AQP2 have been shown to redistribute to the cell surface thus facilitating water transport. In nephrogenic diabetes insipidus (NDI) the kidney is insensitive to vasopressin resulting the secretion of large volumes of dilute urine[93]. A number of patients with recessive NDI have now been identified, the majority of which have mutations in residues in the aqueous pore domains of the AQP2 protein[94]. In some cases abnormal trafficking of the protein is also seen, usually resulting in sequestration of the mutant in the endoplasmic reticulum and subsequent degradation. In the heterozygous state, enough wild-type functional AQP2 reaches the membrane (figure 58).

A single family with dominantly inherited NDI was recently identified with a mutation in the C-terminus of AQP2. In this instance, the mutant protein is appropriately translated and normally trafficked from the endoplasmic reticulum to the Golgi apparatus. However, here it co-oligomerises with the product of the normal allele, thereby restricting trafficking of both polypeptides[76,95] explaining the dominant nature of the mutation.

The Colton blood group antigens are now known to be polymorphisms of aquaporin-1 present in the red blood cell membrane. Interestingly, the null-phenotype, in which aquaporin-1 function is

abolished by mutations that can be shown *in vitro* to reduce erythrocyte resistance to changes in osmolarity, does not result in a clinically recognisable phenotype[96]. This evidence has lead some to raise the possibility that some aquaporins are physiologically redundant whereby other mechanisms are able to compensate for their dysfunction. Our evidence that mutations in aquaporin-0 underlie cataract formation (details below), runs contrary to this and serves to confirm the important physiological role of these proteins.

1.3.4.1.5 MIP (AQP0), the founder aquaporin

The human *MIP* gene encoding MIP (AQP0) is located on 12q14, close to several of the genes encoding the other aquaporins (see table 1) suggesting that may in part the family has evolved by duplication. The coding sequence consists of four exons which obey the ATG start codon and CT/AG rule. The 5' promoter region contains TATA and GC boxes.

Table 1: chromosomal locations of human aquaporins

Aquaporin	Chromosomal location
MIP (AQP0)	12q14
AQP1	7p14
AQP2	12q13
AQP3	12q13
AQP4	18q11.2-q12.1
AQP5	12q13
AQP6	12q13
AQP7	9p13
AQP8	-
AQP9	-

MIP is synthesised as a 26kDa pre-cursor degraded to a 22kDa functional protein. Individual MIP molecules co-oligomerise to form homo-tetramers, which are transported to the cell membrane. In

contrast to some other channel proteins, where such association is essential for the formation of a central pore or channel, monomeric MIP, like other aquaporins, has the capacity to transport water[64]. Thus, tetramer formation may confer additional protein stability allowing for example, more hydrophilic aspects of the protein to be internalised to the core of the oligomer.

The aquaporins share a high degree of sequence homology and it is predicted that all aquaporins share a common topology consisting of six transmembrane domains joined by five connecting loops (figure 11). Aquaporin-1 is perhaps the best-characterised member of the family. Functional and three-dimensional reconstructions of AQP1 suggest that the monomeric protein assumes an hourglass configuration (figure 12) formed by its six highly tilted transmembrane α-helices. Folding in this way is thought to bring into close proximity amino acids E17, Q101, N76, N192 and E142 (the equivalent of E134 in MIP) in the core of the protein. This provides a chain of polar residues from the cytoplasmic to the extracellular spaces that may form the water channel. T146 (the equivalent of T138 in MIP) may lie close enough to Q101 to participate in or stabilise the channel[77]. Central depressions on both the extra- and intra-cellular aspects of the molecule are hypothesised to form the entrance and exits for the water molecules[97].

1.3.4.1.6 Water channel properties of MIP and its role in the lens

Since the cloning of MIP cDNA[98], the role of MIP in the lens has been debated. Sequence homology with other aquaporins suggests the protein functions primarily as a water channel. Immunolocalisation studies of *Xenopus laevis* oocytes injected with bovine MIP cRNA show that the protein is targeted to the plasma membrane. When compared with water-injected (negative control) oocytes, MIP-expressing oocytes consistently exhibit a reversible (bi-directional) fourfold increase in osmotic water permeability, P_f, by a facilitated energy-independent pathway (qualitatively similar to other aquaporins) while showing no evidence of ion channel activity[64]. Thus MIP may contribute to the maintenance of lens transparency by enhancing uptake of intercellular water by adjacent lens fibre cells.

Figure 11: Domain structure of the aquaporins. Protein modelling suggests that the mature protein consists of six transmembrane domains.

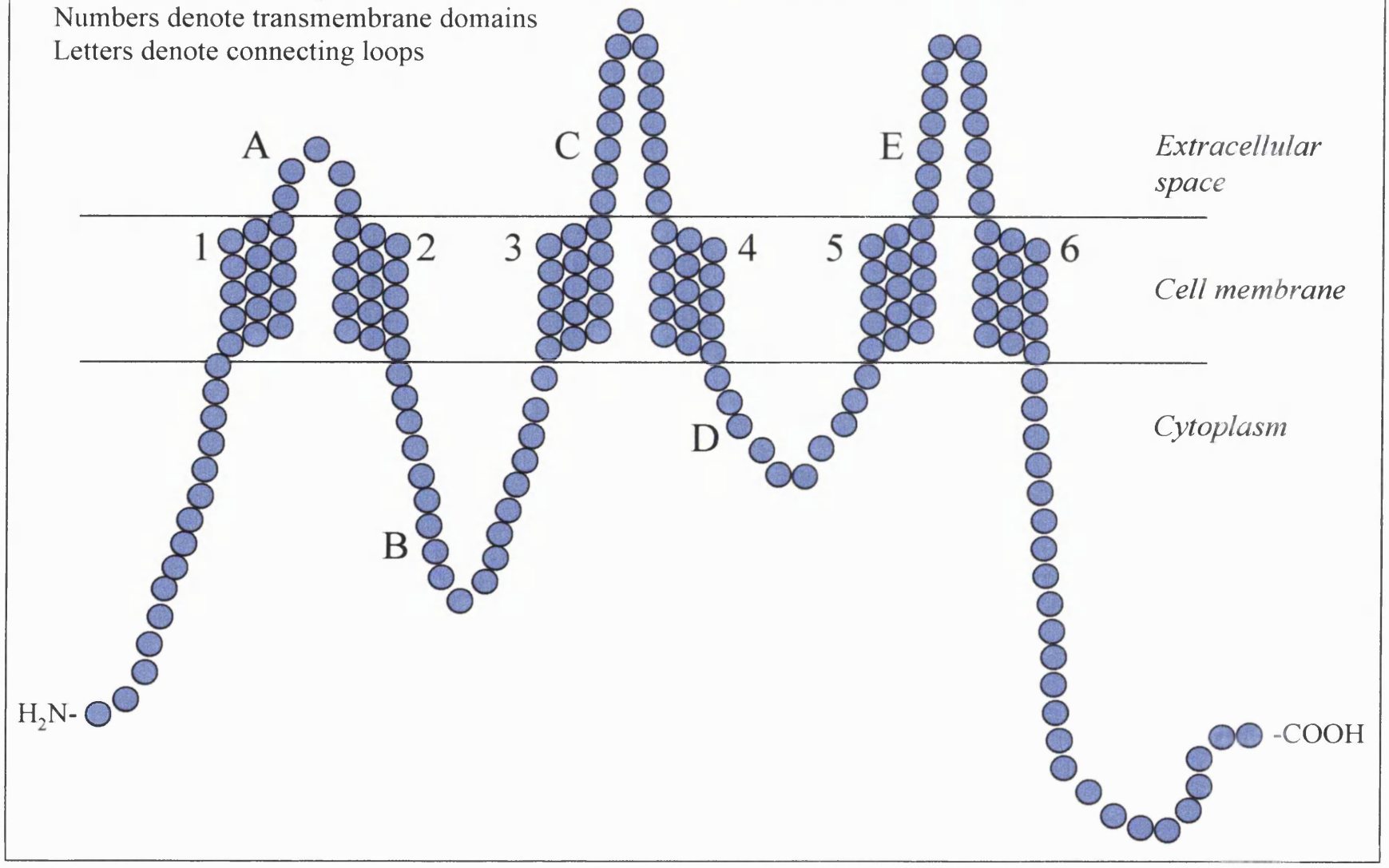

Figure 12: structure of MIP/AQP0

a, at the cell membrane, the protein is predicted to consist of six tilted transmembrane helices (blue checked bars) joined by intervening loops (continuous and dotted black lines)
b, folding in this way is thought to create an "hourglass" shape with a central water channel
c, finally individual AQP molecules co-oligomerise to form homotetramers at the cell membrane

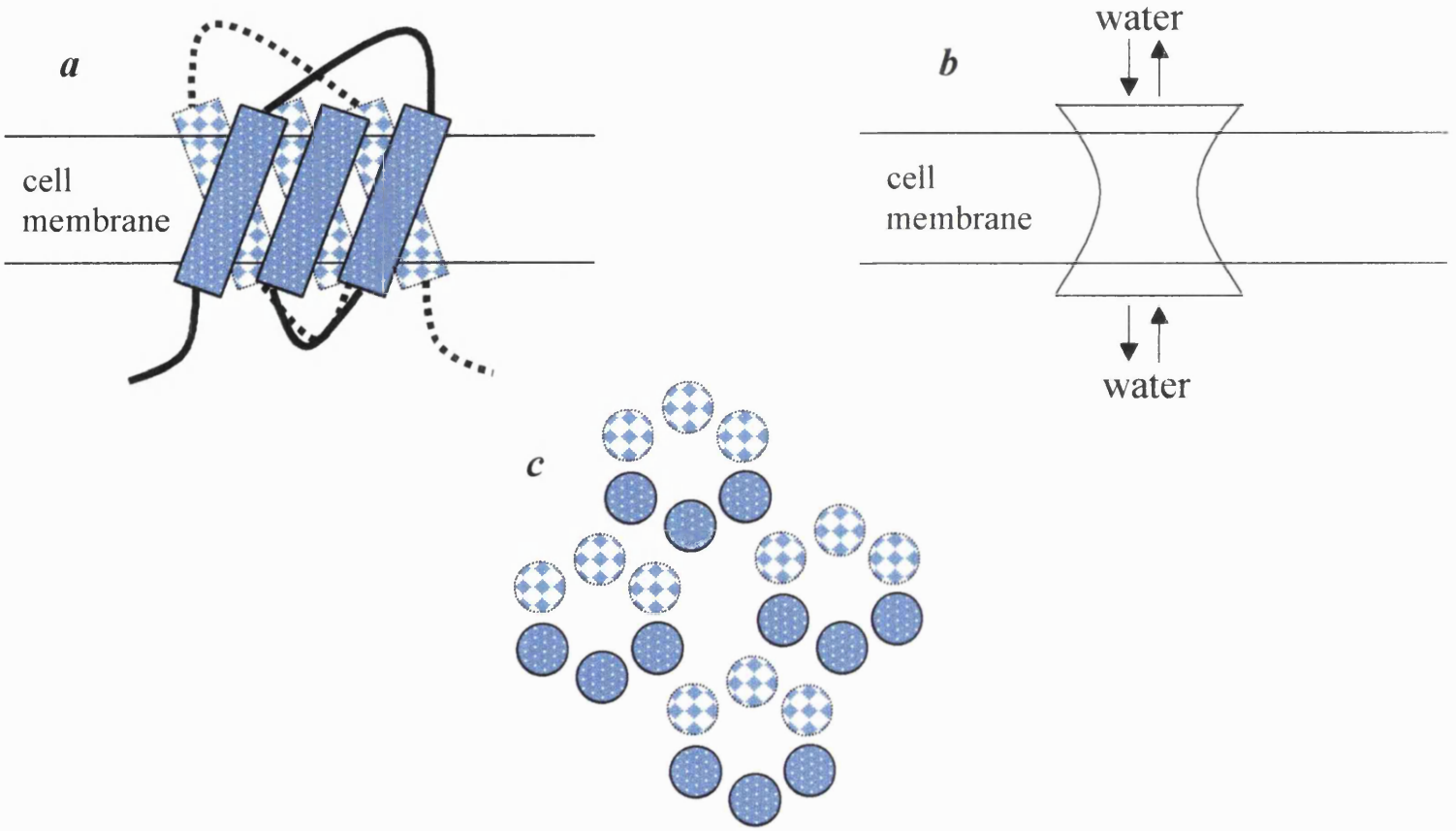

The P_f of MIP is strikingly low compared to other aquaporins, for example, AQP1which is located in the lens anterior epithelial cells and exhibits a more than 30-fold increase in P_f. Such close proximity of MIP-expressing cells to AQP1-expressing cells suggests functional cooperativity though this has yet to be elucidated[64]. This relatively low level of water transport mediated by MIP has led some to suggest other roles for the protein in the lens. Indeed, since MIP constitutes greater than 50% of the lens fibre cell membrane protein, it is possible that the molecule subserves an additional structural role.

The localisation of MIP in gap-junctional plaques suggest that the protein may have a second role in cell-to-cell coupling[99-101]. Indeed the surface topology of MIP molecules has recently been proposed to contribute to this function and may enable direct transfer of water molecules between the cytoplasms of adjacent cells[102].

1.3.4.1.7 The *Xenopus laevis* oocyte expression system

Xenopus oocytes are large, robust single cell systems whose cellular translational apparatus can be harnessed to express a variety of proteins by cRNA micro-injection. The cells do not express native aquaporins, have a low basal water permeability and traffic exogenous aquaporins to the plasma membrane, features that have made oocytes the gold standard system for the qualitative and quantitative examination of aquaporin water functionality. The experimental protocol is detailed below (see Materials and Methods). In overview, harvested oocytes are micro-injected with cRNA. Once the relevant aquaporin has been expressed, oocyte volume swells when exposed to hypo-osmolar conditions (figures 13 and 14). Such swelling is reversible and linear over time allowing a calculation of aquaporin-related water transport to be made.

Figure 13: Oocyte swelling. Transfer of an oocyte expressing aquaporin at its cell surface from *a*, an isotonic to *b*, a hypotonic environment will result in the aquaporin-mediated flux of water molecules down the osmotic gradient into the cytoplasm.
This change in volume is measurable and reversible.

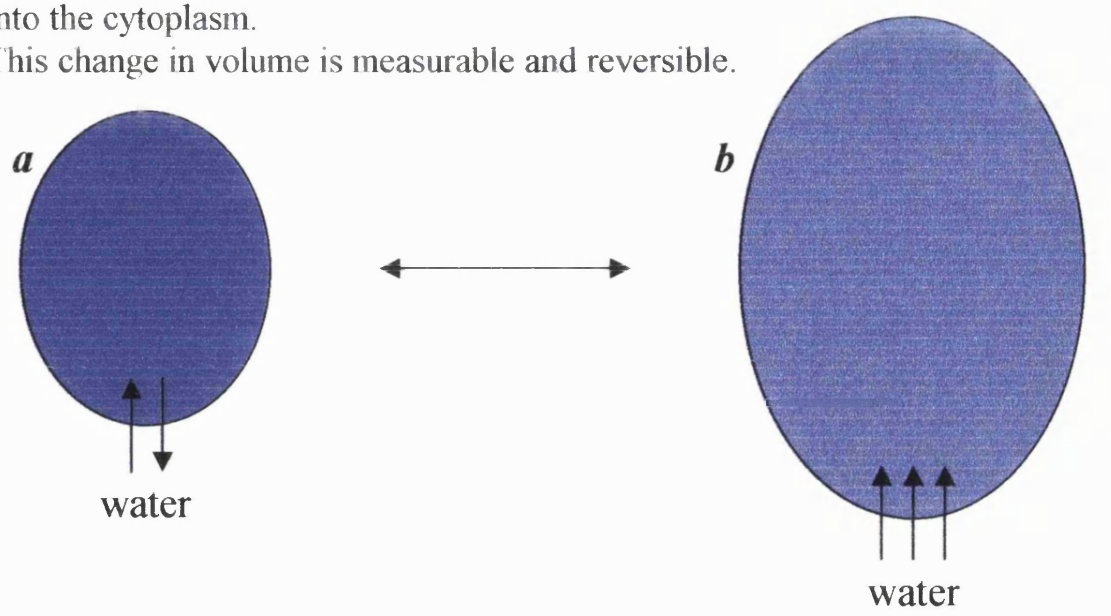

1.3.4.2 Gap junctions

Gap junctions allow ions, second messengers and small metabolites to be shared between cells. These intercellular channels are formed from two oligomeric membrane protein assemblies, called connexons, which span the plasma membranes of two adjacent cells to join in a narrow extracellular "gap" [103](figure 6). Connexons are formed from connexins, a highly related multigene family with at least 13 members[104]. Connexins 46 and 50 are found in the human lens. Considerable progress has been made in our understanding of the complex molecular switches that control the formation and permeability of these channels. Furthermore, analysis of the mechanisms of channel assembly has revealed the diversity of inter-connexin interactions and provided insights into the selectivity of their gating behaviour[105]. Orthologs of human connexin 43 have been shown to be expressed in bovine, ovine and murine lens[106] in addition to the smooth muscle myocardium of the heart[107]. This connexin should therefore be considered a candidate for human cataractogenesis.

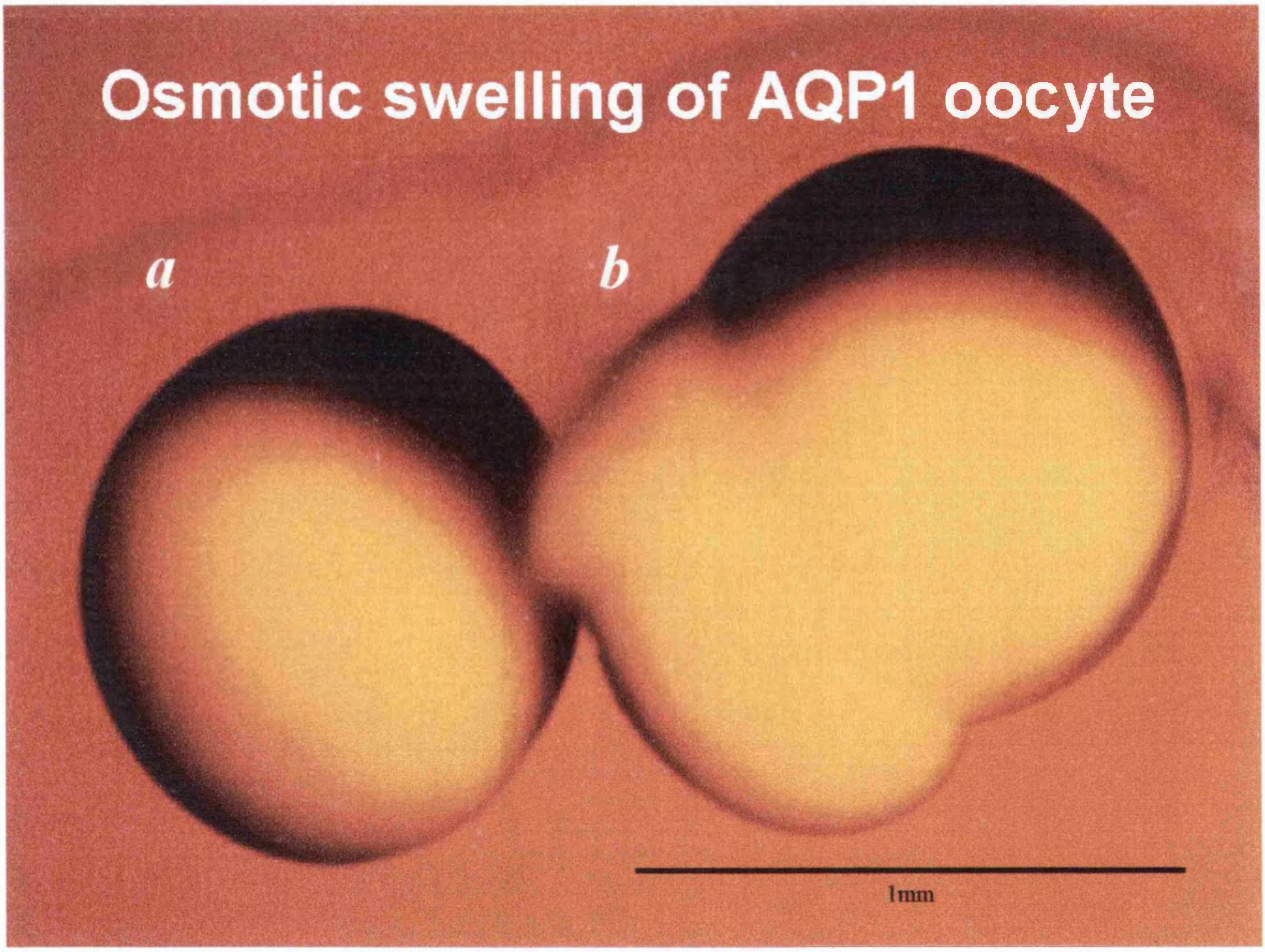

Figure 14: montage of the same oocyte which has been micro-injected with 5ng human aquaporin-1 mRNA and has been shown by Western blotting and immunofluorescence to have translated and targeted to the membrane mature AQP1 protein, *a*, in isotonic media (resting on orange background, white illumination); *b*, after 20secs transfer to hypotonic media. Marked swelling is observed, indeed the left-hand portion of themembrane has ruptured.
(by courtesy Dr M. Yasui)

Numerous other less well characterised membrane channels and proteins are known and summary of these may be found in the candidate gene list (table 6).

1.3.5 Novel lens epithelial specific proteins

Using a subtractive cDNA cloning strategy, a novel lens epithelial specific protein, LEP503, has been identified. The 6.9kDa protein of unknown function is encoded by a gene on human chromosome 1 with two exons. The deduced protein sequences show high identity between mouse, human and rat. Western blot analysis and immunolocalisation studies show that LEP503 is expressed in the lens epithelium most abundantly in the immediate postnatal period[108].

1.4 Mouse models of cataractogenesis

Animal models (figure 15) are valuable tools with which to study human disease[109]. The detailed information available regarding eye development in the mouse and the fact that cataracts are easily identified in this animal, make it an ideal candidate for the study of cataractogenesis. Furthermore, the extensive regions of synteny that exist between the human and mouse genomes facilitate comparative mapping and enable identification of novel candidate loci for human cataract. Studies of the molecular and developmental pathobiology of mouse cataract models are also likely to reveal mechanisms underlying human cataract development.

While spontaneous mouse cataract mutants are recognised, new strains can be developed by irradiation (X-ray, γ-ray) or by the use of chemical agents such as ethylnitrosourea. In most instances, dominant mutations are generated, a corollary of the inheritance pattern observed in humans and suggestive that the mutated genes encode proteins with structural roles. A notable exception is the Nakano (nct) mouse, where the cataract is due to a recessive mutation mapped to chromosome 16. At present, no suitable candidate gene has been identified, though biochemically, defects in lens Na-K-ATPase enzyme activity are suspected[110].

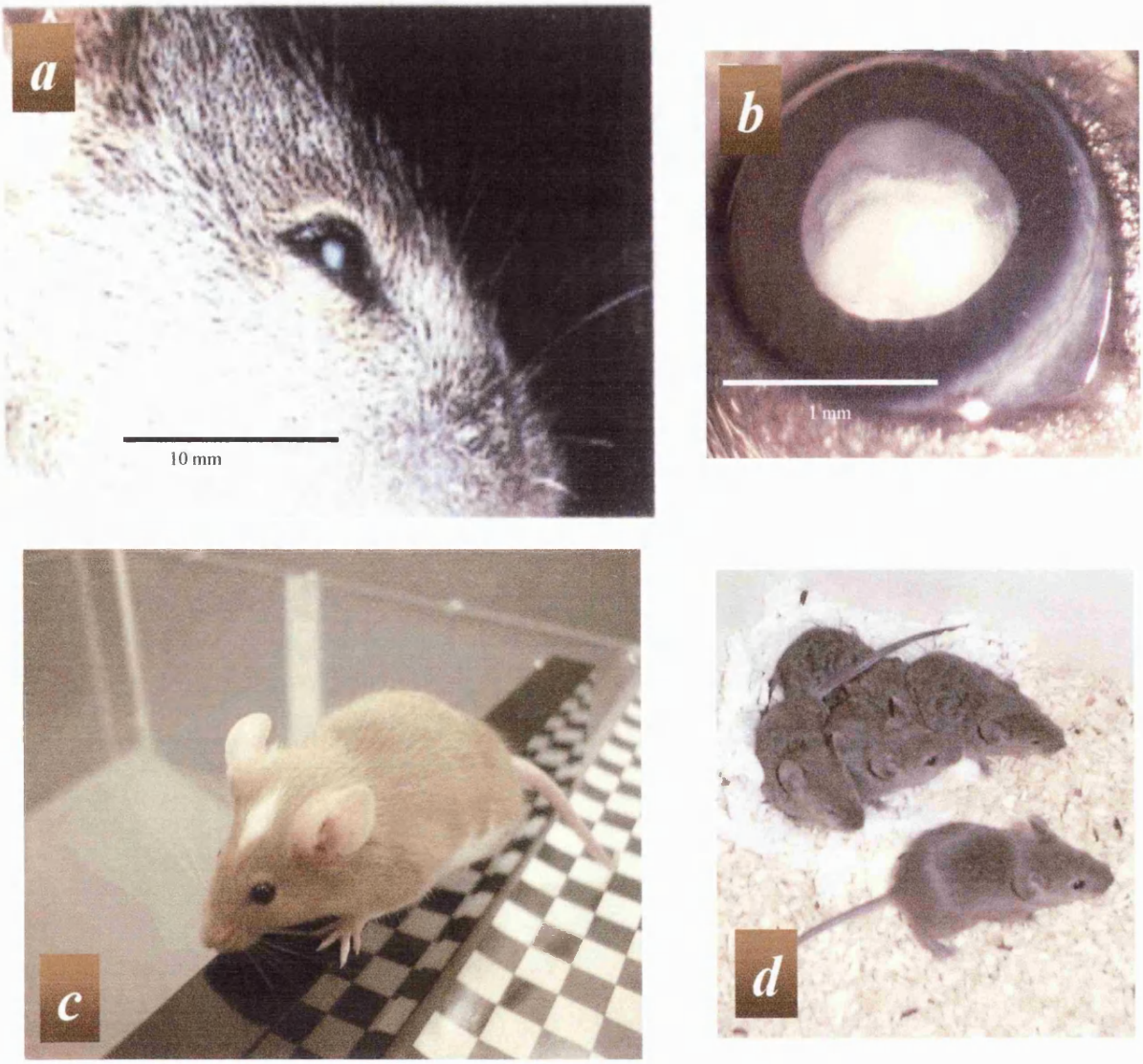

Figure 15: mouse cataract models:
a, the Fraser mouse with lens opacity *(image courtesy of Prof P. Agre)*
b, mouse eye with dense mouse cataract viewed through dilated pupil;
c, a method of detecting visual compromise. A mouse with good vision sees the apparent black edge of the "visual cliff" and will not cross, in contrast to a mouse with poor vision moving by proprioception and touch alone moving across the perspex surface unperturbed;
d, a litter of mice with dominantly inherited cataract
(images B, C, D courtesy of Dr C. Thaung)

Almost one hundred cataract mutants have now been engineered with abnormalities of development[111], immunity[112], growth[113] and physiology (defects in membrane transport[114], cytoskeleton[115] and cytoplasmic proteins[116-118]). It is reassuring that the genetic defects so far identified (table 2) mirror those implicated in human cataract. For example, mouse γ-crystallin[119] and connexin[120] gene mutations result in phenotypes not dissimilar to their human counterpart. The data confirm the crucial role that studies of mouse models will play in revealing human cataractogenic mechanisms. However, it will be only be known with hindsight whether many more of these laboratory-induced strains will be found to parallel spontaneously occurring mutations or whether transgenic models will prove more informative. A listing of mouse mutants is shown in table 3.

Table 2: mouse cataract mutations

Mouse Model	**Mutated Mouse Gene**	**Mouse Phenotype**	**Reference**	**Human Phenotype**
No2	*connexin 50*	nuclear	120	pulverulent
Cat2^{t}	*γE-crystallin*	total opacity with microphthalmia	119	Coppock-like
Cat2^{elo}	*γ-E crystallin*	eye lens obsolescence (microphakia)	121	
ak	*Pitx3*	aphakia	122	total
α3	*α3-connexin (connexin 46)*	nuclear	123	pulverulent
Po	*βA3 crystallin*	nuclear	124	sutural
lop18	*αA-crystallin*	nuclear	125	zonular central nuclear
Philly (Phil)	*βB2-crystallin*	nuclear	126	cerulean / Coppock-like

Table 3: mouse cataract mutants (on this and next page)

Mouse Chromosome	Mutant	Phenotype	Genetic Defect	Human Synteny
1	*Cat2^{t}*	total opacity with microphthalmia	*cryge*[119]	CRYG / CCL[110 127]
	Cat2^{nop}	nuclear opacity	*crygb*[119]	
	Cat2$^{ENU-436}$		*cryga*[119]	
	Cat2^{nz}	nuclear zonular		
	Cat2^{ns}	nuclear and anterior sutural		
	Cat2^{ro}	radial opacity		
	Cat2^{no2}	nuclear opacity 2		
	Cat2^{tol}	total opacity with lens vacuoles		
	Cat2^{elo}	eye lens obsolescence(microphakia)	*γ-E crystallin* single nucleotide deletion predicted to destroy the 4th greek key motif[121]	
2	*Lop4*	speckled nucleus	*cp49*	filensin on chromosome 20[110]
	Sey	small eye	*Pax6*[30]	11p13
	Cm	coloboma		20p12[128]
3	*No2*	nuclear opacity		1q21[120]
4	*Cur*	cataract and curly whiskers[129]		9
	Tcm	total cataract with microphthalmia		8q[130]
	dyl	dysgenic, recessive[131]		
5	*Philly (Phil)*[132]	nuclear opacity	*βB1-crystallin*[126]	β-crystallin on 22q[133]
	Npp	nuclear and posterior polar		4 (p16-q21)[129]
7	*To3*	total opacity	*Lim2, MP10*[129]	

Mouse Chromosome	Mutant	Phenotype	Genetic Defect	Human Synteny
10	*Cat^{Fr}*	progressive lens fibre degeneration	*MIP*	MIP on 12q[74 134 135]
	Cat^{lop}	and opacity beginning anteriorly		
	Cat-3^{vao}	cataract with vacuoles anteriorly		12q22[136]
	Cat-3^{wl}			12q21[137]
	To2 or Cat5	total opacity		6q21-q27[127]
	Cat-3	total cataract and microphthalmia		12q[138]
12	*Or*			14q24[139]
14	*rlc*	ruptured lens induced cataract		13q11-12[140]
16	*Opj*			16p or 22q CATM locus at the t(2;16) breakpoint near 16p13.3 or mutation in *CRYM* on 16p13.11-p12.3[129]
	Coc			3q2[141]
17	*Lop18*	lens opacity	*αA-crystallin*	21q22[125]
19	*ak*	aphakia[142]	*Pitx3*[122 143]	10
X	*Xcat*	primary fibre cell degeneration resulting in nuclear opacity		Xp22.1-p22.3 near Nance-Horan locus[144]

Unassigned mutants:

Mi (microphthalmos)[145], *opb (open brain)*[146], *ey1 (eyeless)*[147 148], *nct/ cac/Cat^{na} (Nakano cataract, recessive)*[149 150], *Em (Emory cataract)*[151], *Lop2, 3, 5, 6, 7, 8, 9, 10 (lens opacity)*[152], *Acc, Apc-1, Apo, Apoc (anterior polar cataracts), Asc-1 and –2 (anterior sutural cataracts), Cad (milky white cataract)*[153].

1.5 The molecular genetics of inherited cataract

In 1963, Renwick and Lawler described in their seminal publication the co-segregation of inherited cataract with the Duffy blood group locus[9 10]. This became the first autosomal disease to be genetically linked in man when in 1968, the Duffy locus was assigned to chromosome 1[11]. Subsequent development of advanced molecular biological techniques has facilitated the identification of a large number of independent cataract loci and mutations. In most cases a candidate gene approach has been used once linkage has been established. There are however several practical considerations when mapping human cataract genes. A significant proportion of cataract mutations appear *de novo* often making family size small. Whilst penetrance in all phenotypes is high, expressivity, age of onset and rate of progression are variable making careful ophthalmic evaluation critical. In addition, surgical modification of the disease and the absence of reliable reproducible qualitative and quantitative measures of the disorder can hamper appropriate classification.

1.5.1 Mapped genes

A complete listing of the mutations so far implicated in human cataract is given in table 4 below.

1.5.1.1 Connexin genes

The report of the co-segregation of pulverulent cataract with the Duffy blood group locus in a single English kindred[10 11] has been described above.

Recently, the Duffy blood group locus has been refined to 1q22-23[154] and lies close to the *gap junction α-8* (*GJA8*) gene at 1q21.1. *GJA8* encodes connexin protein 50 which primarily and abundantly expressed in human lens[155] and therefore is considered a strong candidate gene for human cataractogenesis. Indeed a missense mutation (C→T transition at nucleotide 262) in this

Table 4: identified human cataract mutations: *all mutations are autosomal dominant*

Locus	Gene	Protein	Mutation	Number of Mutations	Phenotype	OMIM Number	Reference
1q21-q25	*GJA8*	Connexin 50	missense	2	pulverulent	600897 (11622)	[75]
2q33-q35	*CRYGC*	γC-crystallin	missense	1	Coppock-like	604307 (123660)	[156 157]
2q33-q35	*CRYGC*	γC-crystallin	missense	1	aceuliform	604307	[157]
2q33-q35	*CRYGD*	γD-crystallin	missense	1	nuclear	123690	[158]
3q21-q22	*CP49*	BFSP-2	missense/ deletion	2	lamellar/nuclear	603212	[159 160]
10q24-25	*PITX3*	Pitx3	missense	1	total	602669	[37]
13q11-q13	*GJA3*	Connexin 46	missense	2	pulverulent	121015 (601885)	[161]
17q11.1-q12	*CRYBA1*	βA3 crystallin	splice site	1	sutural	600881	[162]
21q22.3	*CRYAA*	αA-crystallin	missense	1	zonular central nuclear	123580	[163]
22q11.2	*CRYBB2*	βB2-crystallin	chain termination	1	cerulean	123620 (601547)	[164]
22q11.2	*CRYBB2*	β-crystallin	missense	1	Coppock-like	604307	[165]

gene has been shown to underly cataract formation in this family. The mutation results in the substitution of serine for proline at codon 88, which lies within the phylogenetically conserved second transmembrane region of the protein[166]. A feature of the mature lens cell is its metabolic inactivity. It is likely therefore that the connexin 50 mutation results in altered function with subsequent disruption of cell homeostasis observed as a loss of clarity. Further evidence to implicate this protein in human cataractogenesis has been provided by the identification of another mutation in an ethnically unrelated family (Pakistani) with pulverulent cataract[167], predicted to disrupt connexon-connexon interactions by altering the electrical charge distribution in the extracellular loop of the protein.

A mutation in the gene coding for another gap junction protein, connexin 46, has recently been shown to underlie pulverulent cataract development in two families linked to 13q[168]. In the first family, an A to G transition at nucleotide 188 results in the non-conservative substitution of serine for asparagine at codon 63[161]. This missense mutation lies in the first extracellular loop of the protein, believed to mediate the intermembrane coupling of connexon hemi-channels[169]. In the second family, insertion of a cytosine after nucleotide 1137 is predicted to cause a frame shift immediately after codon 379. This results in the mis-translation of the final 56 amino acids and the addition of 31 amino acids to the C-terminus of the mutant protein before an in-frame translation stop codon is detected. Further evidence of the importance of connexin 46 in human cataract is provided by the report of a third mutation, C560T (P187L), in a family also with pulverulent cataract[170].

1.5.1.2 Crystallin genes

The γ-crystallin gene cluster located in region 2q33-35 consists of genes γ-A, -B, -C, -D, -E, -F and a gene fragment γ-G (figure 16). Only γ-C and γ-D encode abundant proteins while γ-E and γ-F are pseudogenes by virtue of in-frame stop codons (the γ-F lacks a promoter as well). The Coppock-like cataract (pulverulent) was mapped to chromosome 2q33-35 close to the γ-D and γ-E genes[171] and a number of sequence changes identified in and around the γ-E pseudogene TATA box. These were considered by the authors to be mutations and were predicted to result in an order

of magnitude increase in promoter activity raising the level of expression of this gene to 30% of that of the γ-D gene. The resultant mutant protein is a 6kDa N-terminal γ-crystallin fragment, the accumulation and precipitation of which was thought likely to cause cataract[156]. The activation of a pseudogene in this way was regarded as a unique pathogenic mutational mechanism. Recently however, similar sequence changes were identified in a panel of control patients suggesting in fact that they represented polymorphisms of no functional significance. Indeed, a missense mutation in γ-C crystallin has now been shown to be responsible for the disease in this family[157].

Figure 16: the γ-crystallin genes on 2q33-35

The cluster consists of 7 genes: γC and γD are abundantly expressed in the lens. γE and γF are pseudogenes and are not thought to be expressed. γG is a non coding gene fragment

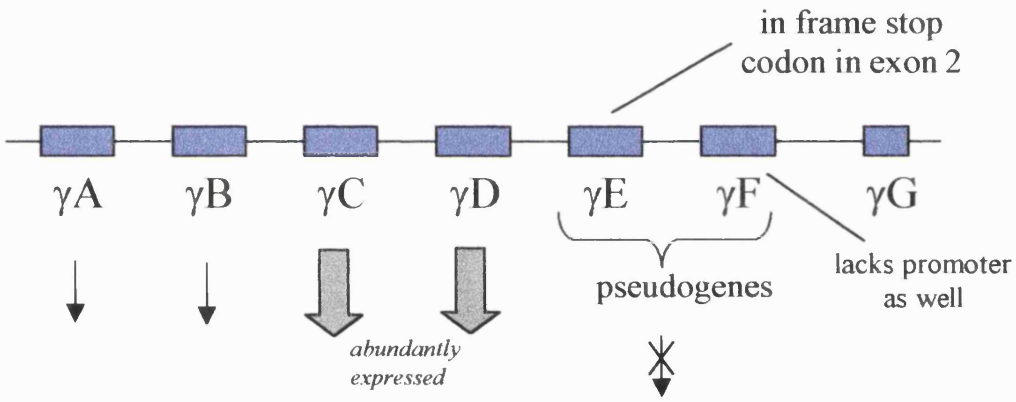

Two forms of congenital cataract, cerulean and pulverulent, have been mapped to a region of chromosome 22q that contains three β-crystallin genes[164 165] and missense mutations identified in the crystallin βB2 gene. This finding is consistent with the fact that only its protein product is highly expressed in the adult lens. The G to A transition in the antisense strand of the first nucleotide of codon 155 creates a stop codon that truncated the protein by 51 residues. Significantly, linkage to this and the 17q24 loci have been excluded in other families with cerulean cataract confirming that a further gene(s) remains to be identified in this form of cataract.

More recently, a missense mutation in the crystallin αA gene has been identified[163] in a family described as having congenital zonular nuclear opacities. The nucleotide transition results in the substitution of an arginine at position 116 for a more negatively charged sulfhydryl-group-forming

cysteine. It is hypothesised that this change increases α-crystallin aggregation or interferes with chaperone activities.

A large Danish family with nuclear cataract has been assigned by linkage studies to the interval 1pter-1p36, within which lies the gene ENO1[172]. This gene has been considered a candidate because, by the process of "gene sharing" (described above), it encodes not only red cell enolase 1 but also τ-crystallin. However, despite its widespread expression within the lenses of vertebrate species, τ-crystallin is not expressed in the human lens. Indeed, the only family described with hereditary red cell enolase deficiency shows no evidence of cataract. Linkage to the 1p36 locus has also been shown in a family with posterior polar cataract[173]. This suggests that either two genes lie within this locus or, more interestingly, that distinct mutations within a single gene have resulted in the different phenotypes observed. While the chromosomal location of many of the other crystallin genes is now known, no mutations causing cataract have yet been identified.

1.5.1.3 Transcription factors

The identification of a mutation in the human gene PITX3 in a family with total cataract is the first to implicate a developmental regulator gene with congenital cataract. PITX3 is a member of the homeobox gene family RIEG/PITX and has been localised to chromosome 10q24-25. A G to A transition was identified that results in the substitution of serine for asparagine at codon 13. The mutation is not within the crucial homeodomain of the protein but does occur in a highly conserved position and is purported to result in the modulation of a DNA-binding site or inhibition of protein-protein complex formation[37].

1.5.1.4 Genes encoding cytoskeletal proteins

The mature lens fibre cell cytoskeleton consists of a unique intermediate beaded filament configuration formed by the association of BFSP-2 (CP49 or phakinin) and filensin. The recent identification of two mutations in the *BFSP-2* gene (missense: C to T in exon 4 resulting in R287W[159]; deletion: Δ233 ref [160]) strongly suggests mutations in its companion filensin, which maps to chromosome 20, will soon be reported.

1.5.2 Other chromosomal loci

Congenital cataract families have been mapped to several loci within which as yet no candidate gene has been identified. Two families with autosomal dominant cataract have shown linkage to the 1p36 locus, the first with a posterior polar phenotype (Z_{max}=3.48, θ=0)[173] and the other a large Danish family named Volkmann (Z_{max}=14.04, θ_{male}=0.025, θ_{female}=0), with progressive zonular and nuclear opacities (probably pulverulent)[172]. In the latter family, a mutation was sought in τ-crystallin, which is not expressed in the human lens but lies within this locus. Perhaps, not surprisingly, no mutation was identified. Another Danish family, first reported by Marner[174], with primarily lamellar cataract, shows strong linkage to the haptoglobin locus on 16q22.1 (Z_{max}=8.33, θ=0.05)[175].

Another three families with dominantly inherited cataracts have been mapped to chromosome 17. The first, with anterior polar cataract, shows linkage to 17p13 (multipoint lod score=5.2)[176], the second with lamellar opacities maps to 17q11-q12 (Z_{max}=3.9, θ=0)[177], distinct from the third family with the blue-dot phenotype, mapped to 17q24[178].

Anterior polar cataract has also been reported in association with an apparently balanced chromosomal translocation t(2;14)(p25;q24)[179]. Following the recognition of a female with multiple abnormalities, including congenital cataract in association with a terminal deletion of

chromosome 14, it has been argued that a cataract locus must therefore reside in the region 14q24[180].

The recognition of another family with a reciprocal translocation has identified a further cataract locus on 16p[181]. In this family, a balanced translocation, t(2;16)(p22.3;p13.3), was observed in four individuals; three had partial trisomy 2p derived from this translocation and two individuals had a normal karyotype. All patients with translocations had cataracts and those with the normal karyotype had not, suggesting the cataract-causing gene lay in the region 16p13.3. Other chromosomal regions 2q23, 4p14, 11p13, 18q11-12 are also considered to have significant relationships with congenital cataracts though no candidate genes have been identified[182].

Autosomal recessive forms of inherited cataract have been reported in several genealogically distinct populations[6] and seem particularly prevalent in the Japanese. Linkage to the I- blood group (at 9q21) has been suggested (Z_{max}=3.4, θ=0)[183 184].

1.5.2.1 X-linked cataract

The existence of X-linked non-syndromic congenital cataract remains contentious. A number of pedigrees have been reported, though in many, other modes of inheritance appear more likely. The recognition of chromosomal deletions of varying size in this region and the resulting phenotypes observed, suggest that a cataract locus may reside within the region Xp22.3-p21.1[185]. It has been suggested however that X-linked cataract is either synonymous with or closely related to the Nance-Horan syndrome, mapped to Xp.

NHS (OMIM 302350) is a rare X-linked disease characterised by severe congenital cataract with (a) microcornea or microphthalmia, (b) distinctive dental anomalies (crown shaped permanent teeth), (c) evocative features, (d) anteverted pinnae of the ears, and (e) mental retardation in some. Cataracts are fully penetrant in heterozygous females and are confined to the posterior Y-sutures[186-188]. The variable phenotype has led some to suggest that NHS is a contiguous gene syndrome but there is little genetic evidence to back this up[189].

Table 5: mapped loci for human ADCC without candidate genes

Phenotype	Locus	Inheritance	OMIM Number	Reference
Volkmann (pulverulent)	1p36	autosomal dominant	115665	172
Posterior polar	1p36	autosomal dominant	116600	173
Unknown	6, I-blood group locus	autosomal recessive	110800	190
Anterior polar	14q24	translocation	115650	179
Unknown	16p13.3	translocation	156850	181
Marner	16q22.1	autosomal dominant	116800	175
Posterior polar	16q22.1	autosomal dominant	116800	175
Anterior polar	17p13	autosomal dominant	601202	176
Zonular-sutural (lamellar)	17q11-12	autosomal dominant	600881	177
Cerulean	17q24	autosomal dominant	115660	178
Posterior polar	20p12-q12	autosomal dominant		191
Sutural (lamellar) *(possibly synonymous with Nance-Horan syndrome)*	Xpter- Xqter *(the recognition of various deletions probably refine the region to Xp22.3-21.1 refs* [185 193]*)*	X-linked recessive	302200	192

Linkage studies have refined the NHS disease locus to a 3.5cM interval on Xp22.2 between the microsatellite markers DXS1053 and DXS443[194 195], a region syntenic with the mouse cataract disease locus *Xcat*[196]. The gene responsible has not been identified. Recently, the *RAI2*, retinoic acid induced gene 2, has been excluded[194]. Figure 17 shows the relevant region of the X chromosome with disease intervals that coincide with the NHS disease interval. Several diseases with certain similar features have been mapped to intervals that coincide (oral-facial-digital syndrome OMIM 311200; non-specific X-linked mental retardation 19, OMIM 300114) raising the possibility that they are allelic.

1.5.2.2 Other cataract genes

Linkage exclusion data on other families with autosomal dominant cataract have been reported, strongly supporting the supposition that several cataract genes remain to be identified[197].

1.5.3 Cataract in complex anterior segment anomalies

1.5.3.1 *PAX6*, Aniridia, Peter's and Rieger's syndromes

Studies confirm the key role of normal lens development in directing eye embryogenesis[198 199]. It is not surprising therefore that cataract is found in association with microphthalmia, microcornea, persistence of the pupillary membrane and certain corneal dystrophies.

Furthermore, syndromes resulting from abnormalities of those factors that regulate eye development are also associated with cataract. Aniridia, in which partial or total absence of the iris is associated with a number of other ocular (foveal hypoplasia, peripheral retinal detachment and cataract) and systemic abnormalities (most importantly Wilm's tumour), is known to result from a variety of mutations within the homeobox gene, *PAX6*[35]. There are several other homeobox genes

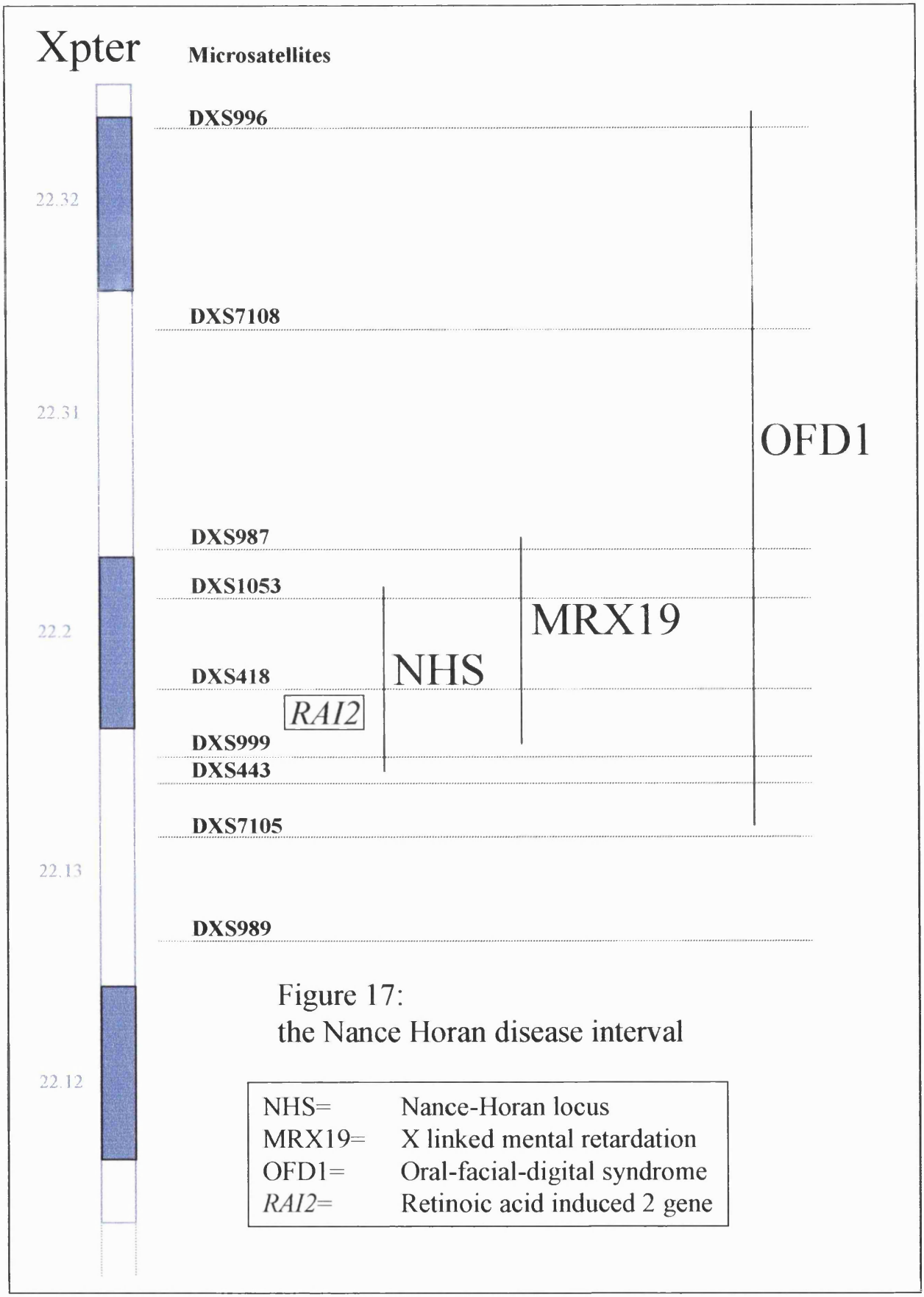

Figure 17:
the Nance Horan disease interval

NHS=	Nance-Horan locus
MRX19=	X linked mental retardation
OFD1=	Oral-facial-digital syndrome
RAI2=	Retinoic acid induced 2 gene

that are essential for early eye determination[29], the specification of ocular tissues and eye development in vertebrates[30].

A point mutation in the *PAX6* gene (Arg26Gly) is also responsible for Peter's anomaly, in which variable adhesions are observed between the cataractous lens, iris and an area of corneal endothelial defect. A mutation that results in Ser353Ter substitution underlies the syndrome of congenital cataract and late-onset corneal dystrophy[7].

Rieger's syndrome, in which cataract, glaucoma and a spectrum of anterior segment dysgeneses are found in association with characteristic facies and hypodontia, is genetically heterogeneous. Family studies and analysis of cytogenetic abnormalities in certain individuals have revealed that mutations within the homeobox gene *PITX2/RIEG1* on 4q25 underlie most cases[200]. A family with anterior segment mesodermal dysgenesis, ASMD (cataract, corneal opacity and anteriorly placed Schwalbe's line) also maps to the Rieger locus on 4q. The possibility that this form of ASMD is in fact a Rieger variant is given weight by the report of another family with ASMD with a mutation in the homeobox gene *PITX3* on 10q[37].

A second Rieger locus on 13q14 has been identified but no gene yet implicated[201]. Interestingly, several eye disorders associated with primary congenital glaucoma including the Rieger eye anomaly have been mapped to 6p25, suggesting that either they are allelic, or a cluster of "eye" genes resides in this region. In support of the former, mutations in the transcription factor, forkhead-related activator, *FREAC-7/FOXE-2* (drosophila homologue *FKHL7*), have recently been shown in patients with Rieger's anomaly, Axenfeld anomaly and iris hypoplasia.

1.5.3.2 Nanophthalmos and microphthalmia

Nanophthalmos or "simple microphthalmia"[202] is an uncommon ocular condition characterised by a small eye with (a) a reduced axial length, (b) high hyperopia (+7.00 D to + 13.00 D), (c) a high lens/eye volume ratio, and (d) a high incidence of angle closure glaucoma[203 204] and (e) characteristic yellow macula pigmentation, chorioretinal folds and crowded optic discs[205]. Ocular

ultrasound commonly reveals a thickened sclera composed of abnormal collagen fibrils[206] which may obstruct the outflow of blood through the vortex veins resulting in recurrent or persistent choroidal effusions and non-rhegmatogenous retinal detachments[207]. The surgical management of patients with this condition is complex as sight threatening posterior segment complications commonly complicate cataract and glaucoma surgery[208].

Nanophthalmos, which is usually isolated and bilateral may be inherited as a sporadic, autosomal dominant or recessive condition. Linkage analysis of a single dominant family has assigned a locus (NNO1) for nanophthalmos to 11p13 (an interval close to but excluding the *PAX6* gene)[203]. No candidate gene is known to lie within the disease locus, though it is possible that elements that regulate and control *PAX6* expression may lie within the *NNO1* region (V van Heyningen, personal communication).

Nanophthamos has been reported as an autosomal recessive trait in association with a progressive pigmentary retinal degeneration (characterised by nyctalopia, visual field restriction and cystic macular degeneration and atrophy)[209]. No association with cataracts has yet been reported.

Nanophthalmos is distinct from the more common congenital microphthalmia (CMIC) which often occurs in association with other ocular (coloboma, cataracts, sclerocornea) and systemic abnormalities (cardiac defects, cleft lip). Other microphthalmia phenotypes include congenital cystic eye, anophthalmos and microphthalmos (small eye)[210]. Linkage analysis of a single Pakistani family has assigned a locus for recessive microphthalmos to 14q32 (excluding the *CHX10* and *MITF* gene loci)[211].

Strong candidate genes and loci for other families with these conditions include *PAX6 (*11p13, ***small eye*** mouse), NNO1 (11p13), arMi (14q32, recessive microphthalmia locus), *CHX10* (14q, ***ocular retardation*** mouse), *MITF* (14q, ***microphthalmia*** mouse), OPTX2 (14q), *EYA1* (***eya***, drosophila ***eyes absent*** mutant).

1.6 Candidate genes for human isolated cataract

When applying positional cloning techniques, as in this project, it is critical to construct a complete list of all possible genes that could be implicated in the disease of interest. Such a list can be drawn up for congenital cataract, the backbone of which will recognise the increasing genetic heterogeneity of the condition and include all mapped loci and mutations. Any other gene expressed in the lens should be considered. However, by limiting the remit of this project to families with cataract present in isolation, genes expressed in a lens-specific manner or highly expressed in the lens assume greater importance. These will include those described above which control lens development and growth (the developmental regulators), the structural proteins in the lens (the crystallins, the cytoskeletal proteins), the membrane proteins and any genes identified in animal models of cataract. The current list of candidate genes and loci for human inherited cataract is shown below in table 6. A continuing problem is that most studies of tissue expression do not include the lensand thus some candidates may be overlooked.

Table 6: cataract candidate genes and loci (listed by chromosomal locus) (on this and next two pages)

Location	Symbol	Name
1p36	CCP	*cataract, posterior polar type*
1p36	CCV	*cataract, Volkmann type (pulverulent)*
1p36	FTH1	ferritin heavy chain polypeptide 1
1p36	SCNN1d	non-gated sodium channel 1d
1p32	FKHL-7	forkhead-like factor-7 transcription factor
1p31-22	CRYZ	crystallin, ζ
1q21-25	CAE1, CX50 CZP1	connexin 50 *cataract, zonular pulverulent 1*
1q32.2	PROX1	developmental regulator
2p25	CAP1	*cataract, anterior polar 1*
2p22.3	CATM	*cataract (with microphthalmia)*
2q31	Sp3	*MIP* gene regulatory factor
2q33-35	CRYGA	crystallin γA
2q33-35	CRYGB	crystallin γB
2q33-35	CRYGC	crystallin γC
2q33-35	CRYGD	crystallin γD
2q33-35	CCL	*cataract, Coppock-like (nuclear)*
2q33-35	CRYGEP1	crystallin, γE pseudogene 1
2q33-35	CRYGFP1	crystallin, γF pseudogene 1
2q34-36	CRYGBA2	crystallin βA2
3q21-25	CP49	phakinin, beaded filament structural protein LIFL-2
3	CRYGS	crystallin γS
4q28-31	PITX2/RIEG1	RIG/PITX homeobox gene
6q	CX43	connexin 43
10p13	VIM	vimentin
10q25	PITX3	RIEG/PITX homeobox gene
11p13	PAX-6	PAX homeobox gene
11q21.1-23.2	CRYA2	crystallin α2
12q13-14	MIP, AQP0	major intrinsic protein, aquaporin

Location	Symbol	Name
13q11-12	CX46, CZP	connexin 46, *cataract, zonular pulverulent 2*
14q24	CAP1	*cataract, anterior polar 1*
15q24	CRABP1	*cellular retinoic acid binding protein-1*
16p13.3	CATM	*cataract (with microphthalmia)*
16p13.11-12.3	CRYM	crystallin μ
16q21.1	CTM	*cataract, Marner type (pulverulent)*
17p13-12	CAP	*cataract, anterior polar*
17p13	SERCA 2b and 3	sarcoplasmic reticulum Ca^{2+} -ATPases
17p13	12-LOX	12-lipoxygenase
17p13	15-LOX	15-lipoxygenase
17q11.1-12	CRYBA1	crystallin βA1
17q11-12	CCZS	*cataract, zonular sutural (lamellar)*
17q24	CCA1	*cataract, cerulean 1*
19	KCNC3	K-gated channel AFO55989
19q11.2	SIX3	Dystrophia myotonica gene
19q13.3-13.4		Kv3.3 K channel
19q13.4	LIM2	lens integral membrane protein 2
20q13.2	hDRK1	Kv2.1 K channel
20	CP115, LIFL-H	filensin
21q22.3	CRYA1	crystallin α1
22q11.2-12.1	CRYBB1	crystallin βB1
22q11.2-12.1	CRYBB2	crystallin βB2
22q11.2-12.1	CRYBB2P	crystallin βB2 pseudogene
22q11.2-12.1	CRYBB3	crystallin βB3
22q11.2-12.1	CRYBA4	crystallin βA4
22q		*cataract, cerulean 2*

Other candidates known to be expressed for which the chromosomal location is unresolved:

IRK1CIC-4 Cl channel

Potassium channel KCNB1 AFO26005

Potassium voltage gated channel (delayed rectifier) subfamily S, member 3 locus 3790

δEF-1Ca activated K channel AF026002.1

Chloride ion induction system AF026003.1

MIF, macrophage inhibitory factor, early lens development

Aldose reductase

Retinoic acid

Thiol transferase

Mercaptopuric pathway

Glutathione reductase

Syntaxin 4

Cl channel protein AAB88807

Chloride channel CLC4 AF170492.1 AAD50981

Dihydroxyacetonephosphate acyltransferase

Lens epithelial cell protein AAD38378

EYA2, EYA3 and EYA4 proteins

Lens epithelial derived growth factor

1.7 Inherited non-syndromic cataract phenotypes

Classification of human inherited cataract is difficult because of the wide variation in morphologies observed though a number of observers have proposed classification systems[197 212-219]. The lens develops by the formation of an embryonic nucleus during morphogenesis, around which lens fibres are deposited throughout life, initially forming the fetal nuclear region and thereafter the cortex (figures 3 and 4). Animal models suggest that the genes so far implicated in cataractogenesis are expressed in a time-ordered, sequential fashion[110]. Categorisation therefore, more weighted towards the location of opacification rather than appearance will accommodate these developmental considerations and best reflect the underlying genotype. Such a system is also clinically convenient.

1.7.1 Nuclear cataract

Cataract affecting the nucleus is common and suggests an abnormality of gene expression in early development. Opacities are inherited in an autosomal dominant manner and may be confluent or discrete. Affected individuals show bilateral symmetrical involvement with variable expressivity. An exception is the pulverulent cataract where the type and distribution of the opacities can vary not only between family members but also between eyes of the same patient[197].

Pulverulent cataract derives its name from the dust-like "pulverised" appearance of the opacities, which can be found in any part of the lens. Largely historical attempts have been made to sub-classify this form of cataract to reflect possible aetiologic differences. The first detailed description of an affected family was published by Nettleship in 1906[9]. In this, the Coppock family, the cataract was confined to the embryonic nucleus and has been termed central pulverulent[220]; in all probability, the phenotype described as Doyne's discoid cataract[221 222]. The Coppock family has not been the subject of a published linkage study, unlike the genealogically unrelated pedigree whose cataract has been described as Coppock-like[213 221 223], which has been linked to the crystallin gene cluster region on 2q. It is of note that the Coppock phenotype and the cataract investigated by Renwick and Lawler in the "Ev family from Southern England"[10 224] have

become synonymous in the literature. However, the latter involves the larger fetal nucleus with opacification increasing in density towards the periphery and is therefore identical to the family with zonular pulverulent cataract described by Poos[225 226].

Many other families with pulverulent cataract have now been described[9 227-229]. It is clear is that significant intra- and inter- familial variation, both in the distribution of the cataract and the degree of opacification, distinguish this phenotype from all others.

1.7.2 Lamellar cataract

The concentric deposition of secondary lens fibres that occurs during growth of the normal lens results in the formation of lamellae. Opacities confined to a specific lamella therefore reflect a short period of developmental disturbance (usually during the foetal period) resulting in usually symmetrical bilateral lens opacification. Lamellar cataracts have also been called zonular, perinuclear, polymorphic[230] or Marner's cataract[174]). Commonly, cataract occurs at the anterior and posterior Y sutures and may be associated with cortical riders. The degree of opacification is variable and visual acuity may be well preserved or reduced enough to require surgical intervention[231].

1.7.3 Cortical cataract

Cataract limited to the cortex is rare and differs from lamellar cataract since opacification is limited to a sector of outer cortical, often inferior, lens fibres, adjacent to the lens capsule. The nucleus is unaffected. The pathogenesis is unknown but its distribution, early onset and subsequent progression suggest an abnormality of the later stages of lens development.

1.7.4 Polar cataract

The presence of families with cataract limited to either the anterior or posterior pole is less amenable to explanation in terms of lens development. Anterior polar cataracts are bilateral,

usually symmetrical, well-circumscribed lens opacities that are rarely progressive and can be inherited as dominant, recessive or X-linked traits[179 218]. Larger opacities often have a pyramidal shape, the apex of which may extend into the anterior chamber[173 176 197]. Associations with microphthalmia[232] and astigmatism[233] implicate a gene involved in anterior segment development. Visual function is usually well preserved[234].

Families with posterior polar cataracts are less common. Affected individuals have bilateral, symmetrical lens opacities, which are usually inherited as a dominant trait. Since opacification is close to the optically crucial, nodal point of the eye, vision is commonly reduced[5]. In some families, progressive accumulation of further posterior cortical opacities can lead to total cataract formation[173 222 224 235].

1.7.5 Blue dot cataract

The blue-dot cataract, first described by Vogt[236] is not truly congenital, but develops in childhood and progresses through early life[237]. The discrete pinhead-shaped blue-white opacities are distributed throughout the lens becoming more numerous in the cortex where they may form large cuneiform (wedge-like) shapes in the mid-periphery. Within a pedigree, this phenotype is consistent in its distribution but variable in its severity. Acuity is usually well preserved; cataract extraction, if necessary, only being required in adult life and associated with a good outcome[220 238].

1.7.6 Coralliform cataract

A peculiar and rare form of cataract, "coralliform", originally described by Nettleship[239], is characterised by finger-like protuberances extending from the nucleus that resemble sea coral[222 240]. The visual impact is variable but cataract extraction is usually required in the early years of life.

1.7.7 "Total" cataract

"Total" cataract, that is lens opacity apparently affecting both nuclear and cortical regions, has been reported in families both with autosomal dominant[37] as well as X-linked recessive congenital cataract[185]. It has also been reported as the end result of the progression of the phenotypes outlined above.

Other phenotypes have been described in isolated cases, but not documented in families.

1.8 Genotype-phenotype correlations

Development and growth of the lens throughout life seem to rely upon the sequential time-limited expression of a number of genes. The spatial and temporal patterns of cataract observed are, therefore, likely to be consequent upon the expression of a mutant form of one of these genes. So far, consistent with this view, no single gene has been implicated in two widely-varying patterns of cataract, though several genes, for example, the genes encoding connexins 46 and 50 are observed to produce the same phenotype. While it seems likely that different mutations in the same gene would cause cataracts of the same general pattern, mapping of both posterior polar and pulverulent zonular nuclear cataracts to 1p36 and evidence from other genes, for example peripherin/RDS, mutations within which cause retinitis pigmentosa[241], cone-rod dystrophy[242] and other retinal degenerations.[243], suggest that this mught not be the case in every instance.

The manner by which mutations in lens genes result in cataract formation has yet to be established. Dysfunction of any element essential for the maintenance of transparency to visible light could result in opacification. With current evidence, it is tempting to speculate that this may occur in three ways. A mutant protein, for example a crystallin, may lose its optical properties or fail to interact appropriately with its intracellular environment. The failure of mutant proteins such as cytoskeletal proteins, to facilitate crystallin packing may result in loss of optical homogeneity. Disturbances in transmembrane signal transduction, for example due to mutated connexin proteins,

may result in disturbances of cell homeostasis, the accumulation of abnormal precipitates or frank disruption of cell architecture. It is possible to envisage how such mutations may result in some of the patterns of cataract observed. How polar cataracts form and why opacification may in some cases progress, is less well understood.

It is apparent that whilst each phenotype may be mapped to more than one locus, no single gene has been implicated in more than one phenotype. This is interesting because it suggests not only that novel linkage will be found for nuclear, lamellar, coralliform and cortical cataracts, but also because it provides an insight into the spatial and temporal expression patterns of lens genes.

The identification of further novel mutations in the genes coding for the crystallins, lens cell membrane and cytoskeletal proteins as well as genes expressing factors that regulate development is likely. Furthermore, a diverse collection of animal cataract models (mostly mice) has been developed. The high degree of synteny between human and mouse genomes suggests that linkage studies in these pedigrees will reveal many further candidate loci for human disease.

1.9 Management and visual outcome from congenital cataract

Surgery is advocated for those cataracts causing significant visual compromise[5]. Complications are more common in children than adults, reflecting both the technical problems associated with surgery on the infant eye and the more marked inflammatory and healing responses of the young. Late complications such as glaucoma, retinal detachment and corneal decompensation may be more frequent because children have many post-operative years to live[244]. The reported incidence of glaucoma, both open and closed angle ranges from 6-24%(ref. [245 246]). There are no reliable statistics for the incidence of retinal detachment (RD) after paediatric cataract surgery but it has been estimated that the mean interval from cataract extraction to RD is around thirty years[247]. It has also been suggested that the detachment rate in children following cataract surgery is similar to that in adults but the incidence of this complication in childhood is likely to be an underestimate given the relatively short follow-up periods of most studies[245].

Despite surgical intervention and appropriate optical correction, up to one third of patients with bilateral congenital cataracts will remain legally blind[5]. Even the most optimistic studies suggest that only 32% of patients will achieve a visual acuity of 20/40 or better[248]. Deprivational amblyopia is the major cause of poor outcome[249-251]. Early treatment (within six weeks of birth) appears to result in a better visual outcome than later surgery at least for lens opacities that are complete or very dense at birth[252]. Less severe lens opacities may have a better outcome if surgery is delayed until later childhood.

In most studies (table 7), outcome and complication rates have been generated from consecutive series of patients with infantile cataracts of all aetiologies[253-256]. In only one recent study were the results of surgery for isolated and syndromic cataract compared. In this retrospective analysis of 46 patients, children who underwent surgery for isolated cataract appeared to have a better visual outcome than those with cataract associated with a syndrome.

1.9.1 Genetic counselling for congenital cataract

Genetic counselling in congenital cataract is usually straightforward when the abnormality is confined to the lens and there is a positive family history. Most families show autosomal dominant inheritance and the status of at risk individuals can readily be assigned by careful slit lamp examination after pupillary dilatation. Variability in disease expression is common and asymptomatic individuals should not be assumed to be unaffected. X-linked and recessive forms of inherited cataract are rare and may be recognised when there is an appropriate family history.

Genetic counselling in isolated cases is more problematic. Most unilateral cataract is non-genetic but patients with bilateral cataract in whom there is no family history should undergo further investigation to elucidate the cause[5]. Firstly, both parents and any siblings should undergo dilated slit lamp examination to exclude mild congenital opacities; the presence of such opacities will confirm the familial nature of the cataract and allow accurate counselling of recurrence risks.

Table 7: visual outcomes from congenital cataract surgery

Study	Number of patients	Patient groups	Best corrected visual acuity (%)		
			Better than 20/40	20/50-20/100	Worse than 20/200
Lorenz et al (1991)[253]	11	Bilateral cataract of all aetiologies	32	46	22
Neumann et al (1993)[257]	14 eyes	Bilateral cataract of all aetiologies	64	27	27
Bradford et al (1994)[258]	23	Bilateral cataract of all aetiologies	43	43	14
Ainsworth et al (1997)[259]	50	Bilateral cataract of all aetiologies	Mean visual acuity 20/30		
Yamamoto et al (1998)[254]	95	Bilateral cataract of all aetiologies	25	75	
Spierer et al (1998)[255]	36	Isolated congenital cataract	32	32	36
	10	Syndromic congenital cataract	0	69	31
Zwaan et al (1998)[260]	276	57% traumatic, 37% infantile (syndromic and isolated), 6% secondary cataracts	44	27	29
Cavallaro et al (1998)[261]	23 eyes	43.5% traumatic, 17.4% lamellar, 39.1% other	78	22	
Sharma et al (1999)[262]	28	43.6% congenital, 28.2% traumatic, 28.2% developmental	70% with visual acuity of 6/18 or better		

If other family members are normal the child should be reviewed by a dysmorphologist or paediatrician to rule out any other clinical features that may suggest a multisystem disorder associated with cataract. Routine investigations include plasma urea and electrolytes, urinary amino acids (to exclude Lowe's syndrome in male infants), urinary reducing sugars (to exclude galactosaemia) and a screen for congenital infection, particularly rubella[5]. Other investigations may be required depending on other clinical findings. In the absence of a family history and where investigations prove normal, the risk of recurrence in subsequent pregnancies is extremely small.

When counselling adults with congenital cataract about the risk to their offspring, it is again important to review other relatives and where possible examine clinical records to exclude any syndromic forms of cataract or non-genetic aetiology. In adults without a family history, the risk of having an affected child is very small if the cataract is unilateral. The risk is higher in bilateral cases as some may represent new autosomal dominant mutations; the precise risk is difficult to quantify. Many of the adults seeking advice will have had multiple operations in childhood and still have severe visual impairment; they may have reservations about putting their own child through a similar experience. However, improvements in cataract surgery and optical management have resulted in greatly improved visual outcome and multiple operations are rarely necessary[263]. This improved prognosis should be discussed and it is important that the newborn child is examined by an ophthalmologist in the first few weeks of life to exclude cataract as the long term prognosis in infants that require early surgery is improved if surgery is performed promptly.

1.10 Strategies for identifying human disease genes

The problems facing those interested in identifying human disease genes are firstly one of scale – the human haploid genome consists of 3 x 10^9 base pairs divided amongst 22 autosomes and sex chromosomes X and Y- and secondly one of complexity – only 5-10% of the genome codes for functional genes, the remainder has uncertain function, partly consisting of repeated DNA sequences. A detailed analysis of the structure and function of the human genome is beyond the scope of this discussion. Several excellent accounts are available[264].

There are in essence two broad approaches employed to identify human disease-related genes: functional cloning and positional cloning.

1.10.1 Functional cloning

Functional cloning has largely been limited to biochemical defects or inborn errors of metabolism where the precise biochemical defect has been established. Evidence implicates a particular gene as a "candidate" for the disease and it may then be screened.

1.10.1.1 Functional candidate gene cloning

This method extends the scope of functional cloning. Again, the precise defect need not be known. A candidate gene list is constructed based on the observed abnormality for example, hyperferritinaemia suggests genes involved in iron metabolism. Additionally, candidates may be human homologs of genes implicated in animal models of disease, for example, the Fraser mouse and *MIP* (discussed earlier), or from genes implicated in similar human disease phenotypes. Each gene can then be screened directly.

1.10.2 Positional cloning

Positional cloning assumes no functional information about a gene or its protein products, but relies instead on locating the gene solely on the basis of map position using genetic linkage analysis. The aim of genetic mapping is to assign the disease locus to the smallest genetic interval by identifying recombination events in the pedigree[265]. Several strategies may then be employed to identify the disease-causing gene[264].

1.10.2.1 Positional candidate cloning

With collective efforts to decode the human genome[266], this methodology has become increasingly powerful. Once linkage analysis has refined the disease interval to its smallest, a genome database search can be undertaken to identify "candidate" genes within the region. The ideal candidate is one that lies within interval and is expressed in the tissue of interest[266]. The identification of a number of large, extended pedigrees with isolated human inherited cataract facilitated the use of this technique in this project as it was possible to construct a candidate list primarily consisting of genes expressed principally in the lensand genes homologous to those implicated in animal models of cataractogenesis.

1.10.2.2 Physical mapping

This strategy has become less popular as more genes are identified. However, it may be the only option where either no mutation is found in candidate genes or no candidates can be identified. A map of the sub-chromosomal region is constructed by screening the libraries available from the genome centres. The relevant clones (packaged within suitable vectors, YAC and BAC, yeast and bacterial artificial chromosomes respectively) are freely available. These can be ordered sequentially by identifying overlapping segments using several methods including *end probes*, fingerprinting, colony hybridization and STS content (an STS or sequence tagged site: a polymorphic DNA sequence that allows comparison between physical, genetic and genomic maps[267]). High resolution physical maps

can then be created by cloning the DNA into smaller fragments in higher fidelity vectors for example, bacterial and P1-derived artificial chromosomes (BACs and PACs respectively)[268 269]. Coding regions within the contig are then identified by one or more of a variety of methods: ESTs (expressed sequence tag, a type of STS, derived from cDNA libraries of expressed sequences[270]) exon trapping, CpG island mapping and computer-assisted sequence analysis.

1.10.3 The positional candidate approach

1.10.3.1 Genetic markers

A genetic marker is any heritable character that may be used to track the inheritance of a particular segment of DNA. Linkage analysis further requires that a marker can be easily studied, for example DNA from a blood sample or buccal smear.

In order to detect recombinants and non-recombinants between marker and disease loci in the progeny, at least one of the parents must be doubly heterozygous, that is possess two different alleles at each marker locus. Thus, a marker's usefulness or informativeness depends on the number of its alleles and their gene frequencies in the population. Informativeness is quantified by its polymorphic information content (PIC)[265]. The PIC measures the probability that the marker will be heterozygous in the parent so that it will be informative in the children and is described by the equation,

$$PIC = 1 - \sum_{i=1}^{n} p_i^2 - \sum_{i=1}^{n-1} \sum_{j=i+1}^{n} 2p_i^2 p_j^2$$

where p_i and p_j are the population frequencies of the ith and jth alleles.

Informativeness is maximised if the marker has many alleles, which are equally represented in the general population. Efficient linkage analysis requires genetic markers with PIC values above 0.70.

As has been described much of the human genome consists of tandemly repeated sequences of DNA and these have been well-categorised (table 8).

Table 8: repeated DNA sequences in the human genome[271]

Class	Repeat size (basepairs)	Location
Satellite DNA		
α	171	Centromeric heterochromatin
β	68	Centromeric heterochromatin
Satellite 1	~35	Centromeric heterochromatin
Satellite 2	5	All chromosomes
Satellite 3	5	All chromosomes
Minisatellite DNA		
Telomeric family	6	Telomeres
Hypervariable family	~15	All chromosomes
Microsatellite DNA	1-4	All chromosomes

It has been long recognised that the number of repeats at a certain point in the genome may vary between individuals and *de facto* may be utilised as a polymorphic marker. This feature is not only heritable but also shows a low spontaneous mutation rate ($5 \times 10^{-4} - 10^{-5}$) making such repeats ideal. The broad dispersal of highly polymorphic microsatellite DNA repeats (either di-, tri- or tetra-nucleotide) in the human genome together with their relative ease of detection has lead to the wide acceptance of these as markers used for linkage studies.

1.10.3.2 Genetic maps of the human genome

The identification of a large number of these genetic markers has lead several authors to compile marker maps that span the known genome (relevant genetic maps utilised in the project are shown below in table 9).

Table 9: marker maps of the human genome[272]

Research grouping	Year of publication	Number of markers
Co-operative human linkage center (CHLC)	1994	1123
Genethon	1994	2066
CHLC/Genethon/Centre d'Etude du Polymorphisme Humain (CEPH)	1994	5840
Genethon	1996	5264

1.10.3.3 Linkage analysis

At the pachytene phase of meiotic cell division, homologous pairs of maternal and paternal chromosomes, lying in close apposition, become physically connected at specific points (chiasmata) and a reciprocal exchange or recombination of genetic material is observed[273]. Chiasmata are thus the physical expression of a crossover point. Since two genes lying far apart on a chromosome are more likely to be separated by a recombination event than genes in close proximity, the result is not only the introduction of enormous genetic variation but also the non-random assortment or recombination of genetic material. Linkage analysis is the measurement of this process detected as non-random segregation of loci in offspring[274]. Two genetic loci are said to be linked if they segregate together in pedigrees more often than by chance.

The mathematical measure of linkage is the lod score (Z), which is the $\log_{10}$ of the odds that the two loci are linked at a certain recombination fraction (θ) rather than unlinked. The two loci are regarded as linked at $\theta=0$ and independently assorted at $\theta = 0.50$.

A lod score of zero indicates that assumptions of linkage or no linkage are the same. A positive lod score favours linkage. A negative lod score provides evidence against linkage. In human genetic linkage analysis, there is a relatively low prior probability (approximately 1 in 50 chance) that two loci chosen at random are unlinked. Therefore, conventionally a lod score of three or more (odds in favour of linkage are more than 1000:1) which equates to an overall probability of linkage of greater than or equal to 95% is regarded as significant. A lod score of –2 or greater provides significant evidence that two loci are unlinked. A major advantage of the use of lod scores is that if a single gene is implicated in a disease, Z values from different pedigrees may be added. Several widely available computer programs are available for example the FASTLINK package which includes the MLINK two-point lod score calculation program[275].

Extended, multigenerational families are the most efficient for human linkage studies since the yield of informative chromosomes is higher and it is often possible to infer parental phase information from the determination of grand-parental genotypes. Furthermore, the utilisation of single kindreds minimises the possibility that genes at more than one locus might be involved.

Linkage analysis may be undertaken between a disease locus and a single polymorphic genetic marker (two-point) or several (multi-point)[275 276]. A detailed discussion of the merits and drawbacks of each may be found elsewhere though the advent of dense highly informative marker maps has rendered multi-point linkage analysis relatively obsolete. Its utilisation in this project was reserved for instances where it was important to define the disease interval and when markers proved uninformative for a particular family.

Once a disease gene has been successfully assigned to a particular sub-chromosomal region, the genetic interval may be refined by genotyping with further markers to discover the boundaries within which no recombination events are observed or by examining linkage disequilibrium between the disease and the linked genetic markers. Nowadays, such strategies are often not necessary since the large number of genes whose map position has been defined means it is common to find a candidate gene within the defined disease interval (the positional candidate gene approach).

.

1.10.4 Identifying disease-causing mutations

A number of confirmatory steps must be taken to conclude that a sequence alteration in a gene is disease causing. The change must co-segregate with the disease within the pedigree and must not be present in a panel of unrelated control individuals ascertained from an ethnically similar background. Convenient methods to demonstrate co-segregation include direct DNA sequencing, single-stranded conformational polymorphism (SSCP), denaturing gradient gel electrophoresis (DGGE) or heteroduplex analysis[277]. In addition, mutations can result in the introduction or loss of a restriction enzyme binding site. Thus a mutation may be detected by digesting the relevant DNA sequence in the presence of the enzyme.

There are a number of ways that changes in the genetic code are known to produce abnormal expression of a gene (table 10) and it is highly likely that a sequence alteration detected will conform to one of these mechanisms. Finally, gene expression studies must confirm disturbed physiology of the protein of interest.

Table 10: Sequence alterations affecting the expression of a gene[271]

Sequence alteration	Example
Gene deletion	α-crystallin
Partial gene deletion	Duchenne muscular dystrophy
Gene duplication	FKHL-7
Gene translocation or inversion	Duchenne muscular dystrophy
Insertion	haemophilia A
Inhibit or prevent transcription	Fragile X
Promoter mutation	β globin
Decrease mRNA stability	Hb-Constant Spring
Inactivate donor splice site	PAX3
Inactivate donor acceptor splice site	PAX3
Activate cryptic splice site	β globin
Frameshift	PAX3
Conversion of codon to stop codon	PAX3
Missense mutation	Connexin 50
Prevent post-transcriptional processing	Familial hyperproinsulinaemia
Prevent correct cellular localisation of product	Cystic fibrosis

1.11 Aims:

(1) to establish the phenotypic variability of human inherited cataract.

(2) to determine the visual outcome and surgical complications for patients with this condition.

(3) to identify and characterise novel underlying mutations.

2. Materials and Methods

2.1 Ethical committee approval

Prior to the commencement of patient ascertainment, the ethical committee of Moorfields Eye Hospital granted approval for the study (protocol number 183).

2.2 The patient sample

The majority of probands with isolated non-syndromic congenital cataract were identified from the Moorfields Genetic Eye Database. The database is a record of patients with genetic eye disease that have attended the Moorfields Eye Hospital Genetic Clinic. The genetic clinic is a tertiary referral clinic for the purposes of genetic counseling. At the first visit, details of the proband are collected using a standardized proforma including a pedigree of the family and the address of each proband at the time of clinic attendance.

Other patients were identified from those attending the general outpatient clinics at Moorfields Eye Hospital. Several other families were identified from the genetic clinic registers of Birmingham Women's and Royal Devon and Exeter Hospitals.

2.3 Identification of families

All families with definite evidence of hereditary isolated non-syndromic cataract were considered eligible. Those with cataracts associated with either ocular or systemic syndromes were excluded.

Pedigrees were divided into two groups based on size. Families with more than eleven meioses and involvement through three or more generations were suitable for linkage analysis and every effort was made to ascertain all members. Other families were collected for the purposes of generating a large

panel suitable for mutation screening. Many sporadic cases of congenital cataract have a genetic basis and a number of these were also collected for mutation screening.

The correct current address and status of each patient was meticulously sought using the hospital information systems, general practitioner databases and directory enquiries. Each proband was sent a contact letter together with a form to be returned in an enclosed stamped addressed envelope (appendix 1). All those who consented to participate were then telephoned using the contact number they provided. Other members within a family, once identified, were contacted by letter and given the choice to participate or decline.

Appropriate consent for patients' participation was sought from relevant health care practitioners.

2.3.1 Making contact with the Coppock family

2.3.1.2 Preliminary enquiries

In 1906, Nettleship and the Right Reverend Ogilvie visited the village of Headington Quarry, about 2 miles from Oxford city center to examine a family with cataracts. Since then, no contact with the family has subsequently been described. In order to identify living members of the family for this study, enquiries were made at the Clinical Genetics Service and Eye Infirmary at Oxford. The Oxford telephone directory was used to obtain details of Coppock family members and contact letters sent to each inviting a reply.

2.3.1.2 Survey of Headington Quarry

Subsequently, through contact with a local public house "*The Masons Arms*", a visit was made and members of direct descendants of the original family examined. Indicated relationships were then cross-checked using the 1900 census information (Family Records Centre, formerly St Catherine's

House, No 1 Myddleton Street, London, EC1). The census records provide details of the names and ages of all members of each household in the UK at the time. Birth records give the place, date and parental names; death records provide date and often next-of-kin.

2.4 Examination

All participating individuals were invited to attend Moorfields Eye Hospital for an examination. Where this was inconvenient, arrangements were made for families to be examined either at their local hospital or in their home.

Prior to each examination, informed written consent was obtained. All family members, both those affected and those unaffected (including relevant spouses) underwent a full ophthalmic assessment including visual acuity (distance and near) and slit lamp examination with dilation where not contra-indicated (1% tropicamide instilled more than twenty minutes beforehand; 0.5% cyclopentolate for children under 3 years, 1% cyclopentolate for other children). Examinations at home were performed using a portable slit lamp (Clement Clarke).

Patients with glaucoma were identified if they were taking anti-glaucoma medications, had evidence of previous glaucoma surgery or a diagnosis of glaucoma documented in their hospital records. Tonometry and optic disc assessment was performed when possible.

Using a proforma, data regarding demographic details age at diagnosis, surgical procedures and complications, cataract phenotype and other relevant ocular abnormalities were collated.

All participating individuals received personal written thanks (appendix 1) and expenses were paid upon request.

2.5 Sample collection

2.5.1 For DNA extraction

20mls of venous blood were collected from each adult (10mls or less from each child) in EDTA impregnated vials using the Vacuette vacutainer blood collection system and stored at -20°C until required.

Where samples could not be collected in this manner, Cytobrushes (Medscand MD) were used to collect buccal cells. Each Cytobrush consists of a nylon brush mounted on a plastic stick. To obtain a sample, the brush was swept along the buccal mucosa for 30 seconds (3 cytobrushes per patient). Ideally, the sample was collected at least three hours after the last meal. Samples were then transferred to sterile 0.9% saline solution for carriage to the laboratory and storage at -20°C.

In several cases, usually spouses of affected family members, it was not possible for convenient arrangements to be made and in this situation patients gave their consent for blood samples to be collected at their general practitioner's surgery. Stamped addressed secured boxes were provided to ensure the safe passage of samples to the laboratory.

2.5.2 For histological analysis and creation of lens epithelial cell lines

Since the advent of small incision phacoemulsification cataract surgery for adults and lensectomy-vitrectomy for visually-significant childhood cataract, it has become increasingly challenging to obtain intact lens fibres. Where possible, groups of lens fibres usually in the form of so-called "soft lens matter" (usually cortical) were obtained at the time of surgery and placed directly into 10% formaldehyde solution. Samples were then mounted in paraffin blocks for histological analysis (my thanks to Dr Brian Clark, Consultant Pathologist, Moorfields Eye Hospital).

In contrast, the development of continuous curvilinear capsulorrhexis, enables the ready harvesting of anterior epithelial cells and these were sent to Dr Roy Quinlan, University of Dundee for transformation in immortalised cells lines.

2.6 Pedigree collation

Family pedigrees were collated using Cyrillic 2.1.3 pedigree analysis software (Cherwell Scientific Publishing Ltd, The Magdalen Centre, Oxford Science Park, Oxford OX4 4GA).

2.7 DNA extraction from venous blood

DNA extraction was performed using the Nucleon II kit (Scotlab Bioscience). Ten millilitre aliquots, thawed to room temperature were transferred to 50ml falcon tubes (Greiner) and the volume made up to 40mls by the addition of sterile reagent A (10mM Tris-HCl pH 8.0, 320mM sucrose, 5mM $MgCl_2$, 1% Triton X-100). After mixing by inversion, the mixture was centrifuged (4000 x *g*, 4 min, 4°C).

The supernatant was removed and the pellet re-suspended in 1ml of reagent B (provided) and transferred to a 2ml screw-topped centrifuge tube. 500µl of 5M sodium perchlorate was added and the sample mixed again by hand. The volume was then made up to 2.5mls by adding 24:1 chloroform:isoamyl alcohol and emulsified by inversion. 300µl Nucleon® resin (provided) was then layered on top and the mixture centrifuged (4000 x *g*, 3 min, 4°C). The aqueous phase was recovered into a universal tube and two volumes of absolute ethanol added. Mixing precipitated the DNA, which was removed with a spatula, and dissolved overnight in 400µl distilled water at 4°C in a 1.5ml-eppendorff tube.

2.8 DNA extraction from buccal swabs

Three buccal swabs (Medscand MD) taken from each patient were stored in 2.5mls 0.9% saline at –20°C. Samples were thawed to room temperature prior to extraction. A combination of inversion, vortexing and pipetting was used to suspend the buccal cells in the 0.9% saline which was then removed to a fresh tube and centrifuged at 1000 x *g* for 2 minutes. The pellet was then transferred to an eppendorff containing 600µl PBS.

DNA extraction was then performed using the QIAamp DNA mini kit. 20µl of QIAGEN protease solution (provided) and 600µl buffer AL (provided) were added and mixed by vortexing for 15 seconds. Samples were then incubated at 56°C for 10 minutes following which 600µl absolute ethanol was added and the mixture, in 700µl aliquots, transferred to a QIAamp spin column and centrifuged at 6000 x *g* for 1 minute. The flow through was discarded and 500µl buffer AW1 (provided) added to the spin column and centrifuged at 6000 x *g* for 1 minute. The flow through was again discarded and 500µl buffer AW2 (provided) added to the spin column and centrifuged at 20000 x *g* for 3 minutes. The spin column was then transferred to a fresh collection tube and centrifuged at 20000 x *g* for a further minute to remove residual buffer. 150µl of distilled autoclaved water was then added to the centre of the pellets in the spin column and the flow through collected by centrifugation at 20000 x *g* in a 1.5ml eppendorff. Typical DNA yields were 10µg/µl.

2.9 Construction of a panel of affected individuals and a panel of controls:

For the purpose of screening other ascertained families for the study that may carry a newly identified mutation, a panel was constructed which consisted of one affected and one unaffected member (where possible) of each family ascertained. 20µl of each DNA sample was diluted five-fold in dH_2O and stored at –20°C. The panel is shown in appendix 3.

In order to confirm that a mutation was not a sequence variant present in the general population, a panel of fifty (unaffected) spouses was compiled in the above fashion.

2.10 Linkage analysis

2.10.1 Polymerase chain reaction (PCR)

Detailed discussion of the principles of PCR can be found elsewhere[271]. In this work, standard parameters and reaction conditions were used and adapted where necessary.

The standard PCR mix (12μl) contained 200ng DNA, 2.5pmol of each primer, 50mM $MgCl_2$, 250μM of each dNTP and 0.6U of Taq DNA polymerase in NH_4 buffer. Standard PCR conditions were: 1 cycle at 95°C for 5 min (stage 1), 30 cycles at 95°C for 1 min, 52 or 55°C for 1 min, 72°C for 1min (stage 2), then 1 cycle at 72°C for 5 min (stage 3). PCR was performed using Hybaid Omnigene or Perkin Elmer Cetus thermal cyclers.

2.10.2 Microsatellite markers

To exclude candidate loci by linkage analysis, Online databases were consulted to identify two microsatellite markers (preferably tetranucleotides - Research Genetics and Co-operative Human Linkage Centre - spaced no more than 10cM from each other) that spanned the genetic interval. Where appropriate other markers within the interval were employed to confirm exclusion.

For the purposes of genome screening the full set of Genethon tetranucleotide microsatellite markers (Research Genetics) which are spaced at approximately 10cM interval were used.

2.10.3 DNA fractionation

2.10.3.1 Agarose gel electrophoresis

In order to visualise PCR products and restriction enzyme digests, agarose gel concentrations appropriate to the resolution required (typically 2%) were made by melting electrophoresis grade agarose (Biorad) in 1 x TAE buffer. On cooling to below 50°C 10mg/ml ethidium bromide was added and the mixture poured into a sealed casting tray containing a 10µl well-forming comb. 2µl of ficoll loading dye (15% ficoll, 50mg bromophenol blue, 50mg xylene cyanol) was added to each 10µl PCR sample immediately prior to loading. Product size recognition was aided by the use of a 1kb ladder (ϕx174/HaeIII, CibaBRL). Electrophoresis was carried out until the required resolution was achieved (rule of thumb: 5 V/cm gel). DNA was visualised on an ultra-violet transilluminator and photographed with a Polaroid MP4 camera with an orange filter and Kodak plus X-film.

2.10.3.2 SDS-polyacrylamide gel electrophoresis

50cm x 38cm gel plates (Biorad) were cleaned and assembled with 0.75mm spacers according to the manufacturer's instructions. A non-denaturing 6% polyacrylamide gel (100ml Protogel [National Diagnostics], 260ml distilled water, 40ml 10xTBE, 1400µl 25% ammonium persulphate, 160µl TEMED) was then poured between the plates and once set, pre-run in a continuous electrophoresis tank containing 1xTBE for at least 30 min. 2µl of ficoll loading dye (15% ficoll, 50mg bromophenol blue, 50mg xylene cyanol) was added to each 10µl PCR sample immediately prior to loading. Product size recognition was aided by the use of a 1kb ladder (ϕx174/HaeIII, CibaBRL). Electrophoresis was undertaken at 100W, 55°C for up to 3 hours depending on the size of the PCR products. The gel was then cut and stained for 10 min in a tank containing 3ml of 10mg/ml ethidium bromide in 1 litre 1xTBE. DNA was visualised on an ultra-violet transilluminator and photographed with a Polaroid MP4 camera with an orange filter and Kodak plus X-film.

2.10.3.3 Linkage analysis

Pedigree data was collated using the software program Cyrillic 2.1.3 (Cherwell Scientific Publishing Ltd., The Magdalen Center, Oxford Science Park, Oxford OX4 4GA). Two point and multipoint lod scores were calculated using the programs MLINK[272] and *Allegro*[278].

2.11 Sequence analysis of candidate genes

2.11.1 Primer design

PCR primers were designed whose 5′ end lay more than 30 nucleotides from the coding start (forward) and end (reverse) of an exon and which would yield an end product of between 200-400 base pairs to enable amplification of the entire coding region.

The following default parameters were used:

a) Primer lengths were designed to be unique for the human genome and varied from 17mer to 24mer, according to the formula:

$$2N(0.25)^n = 1$$

where for any given nucleic acid sequence of length, N, containing only the four normal nucleotides, the segment length, n, is necessary to define a unique sequence.

b) to avoid 3' pentamer instability, false priming, dimerisation and secondary structure formation, the pentamer ΔG was set below –8.5kCal/mol.

c) Primers with discrete 3' 7mer were preferred to avoid false priming.

d) The estimated melting point of each primer (T_m) was calculated using the formula,

$$T_m = 2°C\ x\ (A + T) + 4°C\ x\ (G + C).$$

Ideally, primer pairs were designed with similar T_m values. An annealing temperature 5°C below the estimated T_m was used as a starting point.

Online human genome databases (NCBI Genbank) were consulted to obtain the complete intron and exon sequences for each gene of interest. Where this was not readily available or only partially published, exons were reconstructed from full length mRNA and intron boundaries characterised by utilising BLAST sequence comparison software to identify human clones localised to the genomic region of interest.

2.11.2 PCR conditions

The standard PCR mix (50µl) contained 200ng DNA, 2.5pmol of each primer, 50mM $MgCl_2$, 250µM of each dNTP and 0.6U of Taq DNA polymerase in NH_4 buffer. Standard PCR conditions were: 1 cycle at 95°C for 5 min (stage 1), 30 cycles at 95°C for 1 min, 58 or 60°C for 1 min, 72°C for 1 min (stage 2), then 1 cycle at 72°C for 5 min (stage 3). PCR was performed using Hybaid Omnigene or Perkin Elmer Cetus thermal cyclers.

2.11.3 DNA purification using the QIAGEN QIAquick PCR purification kit

5 volumes of buffer PB (provided) were added to 1 volume of each sample and placed in a QIAquick spin column and centrifuged at 6000 x *g* for 60 seconds. The buffer provides the correct conditions to bind the DNA to the membrane in the spin column. The flow-through was discarded and 0.75ml

buffer PE (provided) added to the column and centrifuged 6000 x *g* for 60 seconds. The flow-through was discarded and the column centrifuged again at 6000 x *g* for 60 seconds. To elute the DNA 50μl of distilled autoclaved water was added to the centre of the spin column placed within a 1.5ml eppendorff and centrifuged at 6000 x *g* for 60 seconds.

2.11.4 Cycle sequencing

4μl of "big" dye (ABI PRISM dye terminator cycle sequencing kit with Amplitaq DNA polymerase FS) and 1.6pmol primer was added to 1μg purified DNA. The reaction performed in either a Perkin Elmer Cetus 2400 or 9600 consisted of 25 cycles (96°C for 10 sec, 50°C for 5 sec and extension at 60°C for 4 min). The mix was then held at 4°C. Samples were transferred to a 0.5ml-microfuge tube and excess nucleotides removed with an absolute and 70% ethanol wash.

2.11.5 Direct sequencing using the Sanger dideoxy chain termination method and fluorescent ABI373 sequencer

The gel plates were cleaned meticulously in non-fluorescent detergents and assembled in accordance with the manufacturers instructions. 50ml of a 6% SDS-polyacrylamide gel (40ml Sequagel-6 and 10ml Sequagel-complete, National diagnostics) was mixed with 40mg ammonium persulphate and poured between the plates. The gel, once set, was installed in the ABI sequencer and following an initial scan to exclude imperfections was pre-run for 1 hour. 4μl of formamide/EDTA loading dye was added to each lyophilised sample and the DNA denatured at 95°C for 5 min and immediately placed on ice. 1.2μl of each sample was loaded and sequence analysis undertaken over 12 hours. Data was collated and analysed using the sequencing software installed on an Apple Macintosh computer.

2.11.6 Mutation detection

2.11.6.1 Direct sequence comparison

Following the identification of a non-synonymous sequence alteration in two affected individuals from a family and its absence in an unaffected family member, DNA from the whole family was sequenced to confirmation segregation of the mutation. Furthermore, one hundred normal unrelated control individuals were also sequenced to show that the mutation alteration was not present. Final confirmation was provided by restriction digest analysis.

2.11.6.2 Restriction enzyme digestion

Restriction digests were performed according to each manufacturer's instructions as summarised in table 11 and visualised on a 2% agarose gel.

Table 11: restriction enzyme conditions

Name of enzyme	Recognition site	Consequence of mutation	Incubation Conditions	Company
AocI	↓ CCTnAGG ↑	Gain of site	37°C, 2 hours	Boehringer-Mannheim
BglII	↓ AGATCT ↑	Loss of site	37°C, 2 hours	Boehringer-Mannheim

2.11.6.3 Heteroduplex analysis

The gel plates were cleaned and assembled according to the manufacturers instructions and gels poured (see solutions section below, setting time 90 mins). Thirty samples can be loaded on one double gel rig. 5µl of loading dye was added to 10µl of each PCR sample directly prior to loading and the gels run at 120 V (best resolution) for around 24 hours depending on PCR fragment size. Gels were then cut and stained for 10 min in a tank containing 3ml of 10mg/ml ethidium bromide in 1 litre 1xTBE. DNA

was visualised on a UV transilluminator and photographed with a Polaroid MP4 camera with an orange filter and Kodak plus X-film.

2.12 Functional characterisation of the MIP mutations using a *xenopus* oocyte expression system

A general overview of the strategy is shown overleaf (figure 18). The *xenopus* oocyte expression system was chosen be cause it represents a well-validated system for the characterisation of aquaporin function[64].

2.12.1 Oocyte harvesting

Adult female *xenopus* frogs were kept in accordance with Johns Hopkins Medical Institute regulations for the care and management of animals. An adult female (10-14cms long) that had previously not undergone oophorectomy, was selected and anaesthetised by burying in ice at 4°C for 1 hour. Under sterile conditions, an oblique inguinal incision was made and the peritoneal cavity entered using blunt dissection. Approximately 400 oocytes were delivered through the incision and excised using blunt scissors to a petridish containing calcium-free OR-2 at 37°C. Peritoneal and abdominal incisions were repaired using interrupted 4-0 silk sutures and the *xenopus* allowed to recover on a slope head-up in air for 1 hour before being returned to its water tank.

The harvested oocytes were then separated into small clumps (of approximately ten) using two pairs of non-toothed forceps and transferred to a 50ml tube containing 20mls of collagenase (2mg/ml, Sigma) solution. The mixture was swirled for 1 hour or until all oocytes had separated (the collagenase solution was refreshed every 15 minutes).

The oocytes were then rinsed five times with calcium-free OR-2 and three times with MBS before being laid out once more in a petridish. Using a wide-mouthed fire-polished Pasteur pipette, healthy

Figure 18: Overview of the protocol for functional characterisation of MIP mutants using xenopus oocyte expression system

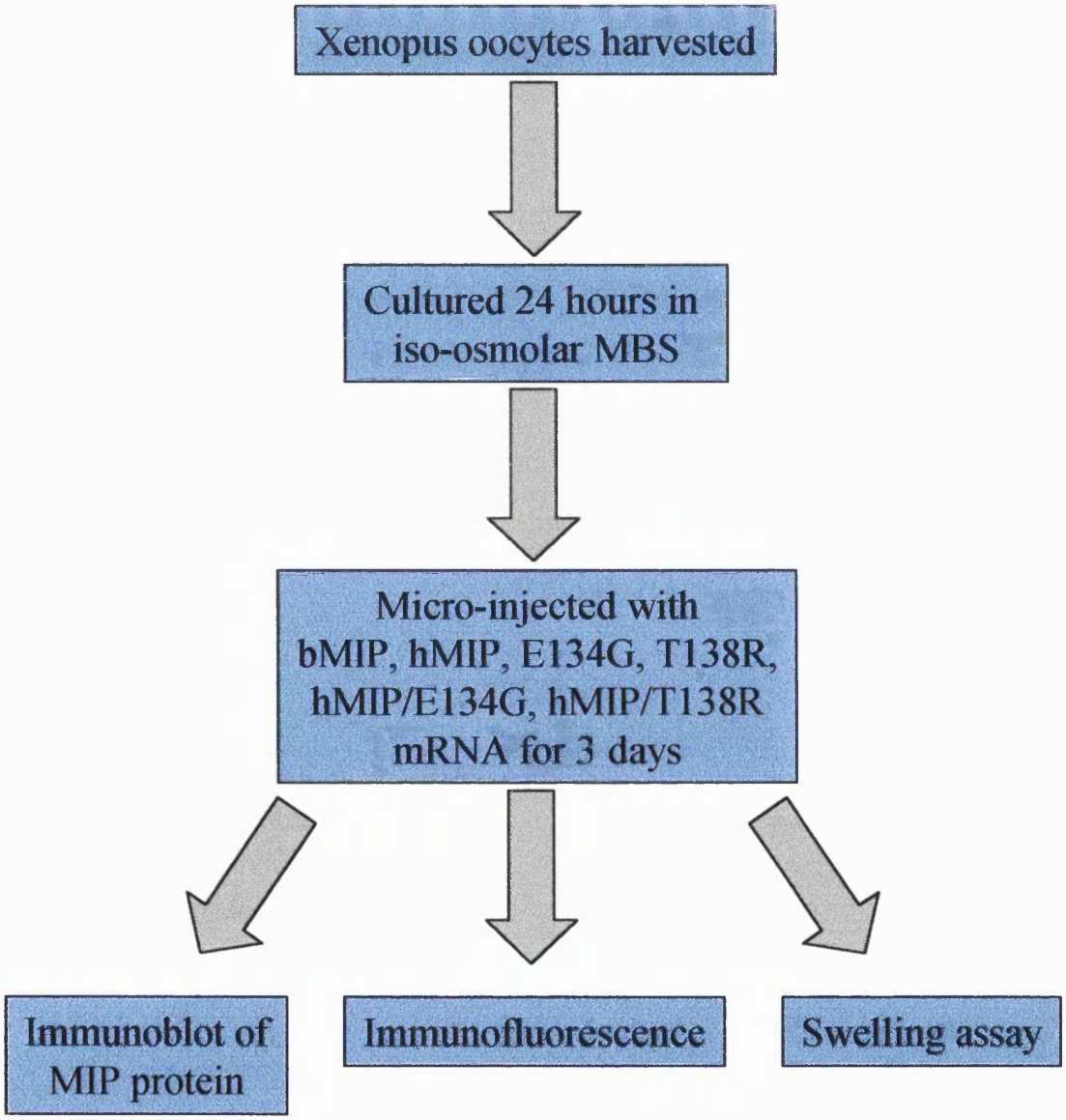

de-folliculated oocytes were selected and incubated overnight (animal poles up) in a culture dish, gently swirled on an orbital shaker at 20°C.

2.12.2 Microinjection of mRNA

Selected oocytes, cultured for 24 hours in MBS were separated into groups of twenty using a wide-mouthed fire-polished pasteur pipette and arranged on a coarse plastic mesh secured with tape to the bottom of a small petridish containing enough MBS to fully submerge all cells.

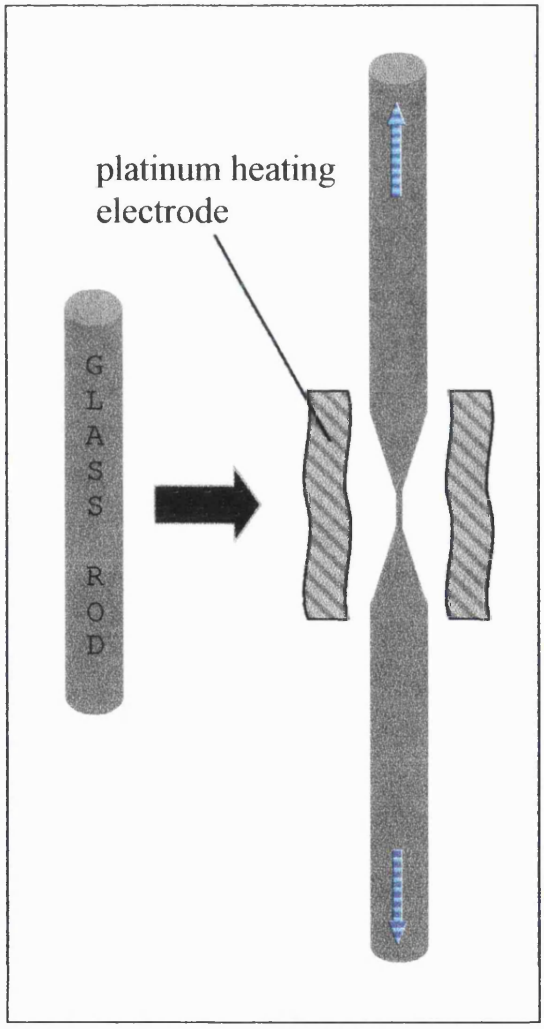

Figure 19: fashioning of glass microinjection needle
The glass rod is heated between two platinum electrodes. When the glass melts, it elongates under the weight attached to its lower end

Fine glass injection needles were fashioned by heating the centre of a 1mm glass rod to red hot and drawing out the glass to narrow its calibre as shown below (figure 19) mRNA for injection was drawn up into the needle tip containing a bung of mineral oil. By viewing through a low power biomicroscope, oocytes were carefully positioned and the needle inserted and a single injection of cRNA dissolved in 50nl water delivered. Oocytes were then cultured (as described above) for 3 days.

2.12.3 Oocyte water permeability (swelling) assay

Individual oocytes were transferred (maintaining a constant temperature of 22°C) to approximately 20ml isotonic normal saline (200mM) for 5mins using a wide-mouthed fire-polished Pasteur pipette and then to 20ml hypotonic saline (70mM) in a petridish placed for the swelling assay. Using a low-powered video biomicroscope (Axiovert135TV, Zeiss), the oocyte was briskly centred and its image focused on the television viewing screen. Measurements of the changing oocyte cross-sectional area were made using The Metamorph Imaging System 3.5 for Windows 95 (Universal Imaging Corporation, 502 Brandywine Parkway, West Chester, PA, USA). The software makes a reading every 5 seconds for 1 min. The coefficient of water permeability (P_f) was calculated from the changes in volume between 15 and 30 seconds, the initial volume (V_o = 9 x 10-4 cm^3), the initial oocyte surface area (S= 0.045 cm^2) and the molar volume of water V_w = 18 cm^3 / mol) using the equation:

$$P_f = [V_o \times d(V/V_o)dt] / [S \times V_w \times (osm_{in} - osm_{out})]$$

It is anticipated that healthy oocytes swell in hypo-osmolar conditions in a linear fashion. By plotting all volume measurements against time, unhealthy oocytes could be excluded from the assay.

Oocytes were then returned to isotonic conditions and frozen in minimal media at –20°C prior to inclusion in the immunofluorescence protocol (see below).

2.12.4 Western blotting of membrane-bound MIP protein

2.12.4.1 Sample preparation

1ml of homogenisation buffer was added to 10 oocytes and the mixture homogenised using a glass pipette before centrifugation (735 x *g*, 4°C, 5mins). The pellet containing yolk proteins was discarded and the supernatant recovered and further centrifuged (16000 x *g*, 4°C, 20mins). The lipid layer and supernatant were then discarded and the pellet containing the membrane protein fraction re-suspended in the original volume of homogenisation buffer and centrifuged (16000 x *g*, 4°C, 20mins). With the supernatant discarded the pellet was suspended in 100µl 5% SDS solubilisation buffer at 37°C for 30mins. Samples could then be stored at –20°C for later use.

Prior to gel loading, 25µl 5x Western blotting loading buffer (containing DTT) was added to each sample and heated to 60°C in a water bath for 15 minutes to ensure full protein solubilisation.

2.12.4.2 Gel electrophoresis:

The electrophoresis plates were cleaned and assembled according to the manufacturer's instructions (Mini protein II cell gel rig, Biorad) for a 1mm gel thickness. A 12% acrylamide resolving gel with 4.0M urea was poured and allowed to polymerise with the surface covered with 2ml isopropanol to ensure a smooth surface and prevent gel dehydration. With the isopropanol removed, a 4% acrylamide stacking gel with 2.0M urea was poured and a 20µl comb inserted. Once polymerised, the comb was removed and the wells immediately flushed with electrophoresis buffer.

2µl of each sample were loaded and run through the stacking gel at 100V and resolved at 200V thereafter. Details of the electrophoresis buffer are given in the solutions section below.

2.12.4.3 Protein transfer:

Transfer of protein from the gel to a nitrocellulose membrane was performed using a Transferblot SD semi-dry transfer cell (Biorad), running at 250mA for 30mins according to the diagram below (figure 20). Each fibre pad and the membrane were pre-soaked in 80ml of 80% transfer buffer, 20% methanol.

Figure 20: transfer to nitrocellulose membrane
Protein in the gel is transferred to a nitrocellulose membrane laid underneath, by electrophoresis in a semi-dry transfer cell

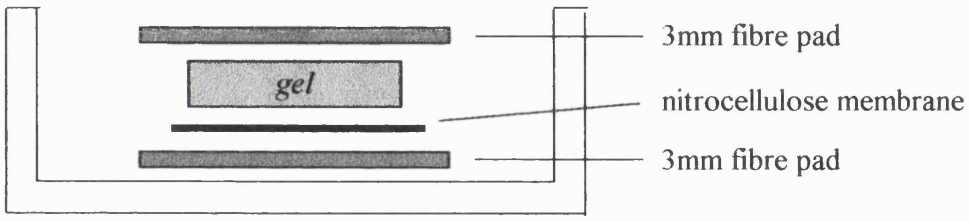

2.12.4.4 Antibody probing

Once blotting was complete, the nitrocellulose membrane was incubated at RT in 20mls of primary antibody solution (1:10000 dilution affinity purified rabbit anti-human MIP monoclonal antibody, kindly provided by Dr J Kuczak) for 1 hour, gently swirled. The membrane was then washed using 60mls wash buffer twice briefly, twice for 15 minutes then twice for 5 minutes. The membrane was then probed with the secondary antibody solution (1:100 donkey anti-rabbit Ig/HRP in 5% fat free milk, Amersham, UK) for 1 hour, gently swirled, and the washing protocol repeated.

2.12.4.5 Detection using ECL Western blotting analysis system (Amersham, UK)

All excess fluid was drained and the membrane washed in 3ml Amersham detection 1 and 2 for 1min following which it was wrapped in plastic film and exposed to film (Kodak X-OMAT AR 8x10inch) for 20sec, 1min, 5min and 30min.

2.12.4.6 Protein quantitation

To estimate the quantity of protein in the solubilised samples, electrophoresis was undertaken according to the Western blotting protocol detailed above. The gel was then immersed in 100ml of Coomassie blue dye overnight and then de-stained by washing with a 10% acetic acid 10% isopropanol solution.

2.12.5 Immunofluorescence

Five of each of the groups of oocytes (following recovery from the swelling assay) were transferred to small petridishes containing 10ml of fixing solution and incubated at RT for 4 hours. Oocytes were then transferred to fresh petridishes containing 10ml of 100% methanol and incubated for 24 hours at –20°C.

Oocytes were rehydrated by transfer to new petridishes containing 10ml PBS for 2 hours was followed by incubation in 100mM sodium borohydride ($NaBH_4$) for 24 hours at RT in a fume hood. Oocytes were recovered to 10ml PBS once more and bisected using a scalpel and incubated for 24 hours at 4°C with polyclonal antiserum specific to the C-terminal of bovine AQP0 at 1:3,000 dilution in 2% (w/v) bovine serum albumin in PBS. The sample was then washed with at least 6 changes of PBS for 36 h with gentle agitation, and incubated for 24 h in 500µl 1:100 fluorescein 5'-isothiocyanate-conjugate goat anti-rabbit IgG (40 µg/ml in PBS with bovine serum albumin).

Oocytes were mounted on microscope slides according to the Molecular Probes Slow Fade Light Anti-fade kit. Oocytes were pre-incubated with equilibration buffer for 5 minutes. Oocytes were then arranged (bisected side up) in 100µl of buffer A (previously applied) to a 0.5 mm well slide and covered with a No. 1 cover slip. Excess fluid was blotted away and the slide sealed with nail varnish applied to the edges of the cover slip. Fixed oocytes were viewed under a Zeiss Laser Scanning Microscope 410.

2.12.6 Preparation of MIP mRNA (wild-type and mutant)

2.12.6.1 Site-directed mutagenesis

0.03µg of human MIP cDNA was kindly provided by Dr G Wistow (NIH, Bethesda, Maryland, USA) using the following protocol (included here for completeness):

A lens cDNA library was prepared from RNA isolated from lenses of a 40 year old human (Life Technologies, Gaithersburg, MD) cloned into the pCMVSPORT6 vector. Expressed sequence tag (EST) analysis showed the presence of AQP0 in the library. To obtain a complete coding sequence, specific primers were designed from published genomic sequence (Accession U36308) and from EST data.

`hMIP 5': AGATCTGTGACCATCCCCCCTGCCATGTGG`

`hMIP 3': AGATCTCTACAGGGCTTGGGTGTTCAGTTC`

Template DNA was produced from $1x10^6$ cfu of the un-normalised lens library in LB/ampicillin followed by plasmid isolation using Turbo Prep (Qiagen, Valencia, CA). Amplification by polymerase chain reaction was performed using AmpliTaq (PE Biosystems, Foster City, CA) and a dilution series

of the template DNA. The product of expected size (821bp) was subcloned using the pCR2.1 TOPO cloning system (Invitrogen, Carlsbad, CA) and verified by restriction digestion and sequencing.

Bovine MIP was provided by Professor Peter Agre (John's Hopkins Medical Institute, Baltimore, Maryland, USA). Human MIP cDNA with EcoRI and BstEII linkers was cloned into pXBG cloning vector by J-J Chung (John's Hopkins Medical Institute, Baltimore, Maryland, USA), see figure 21.

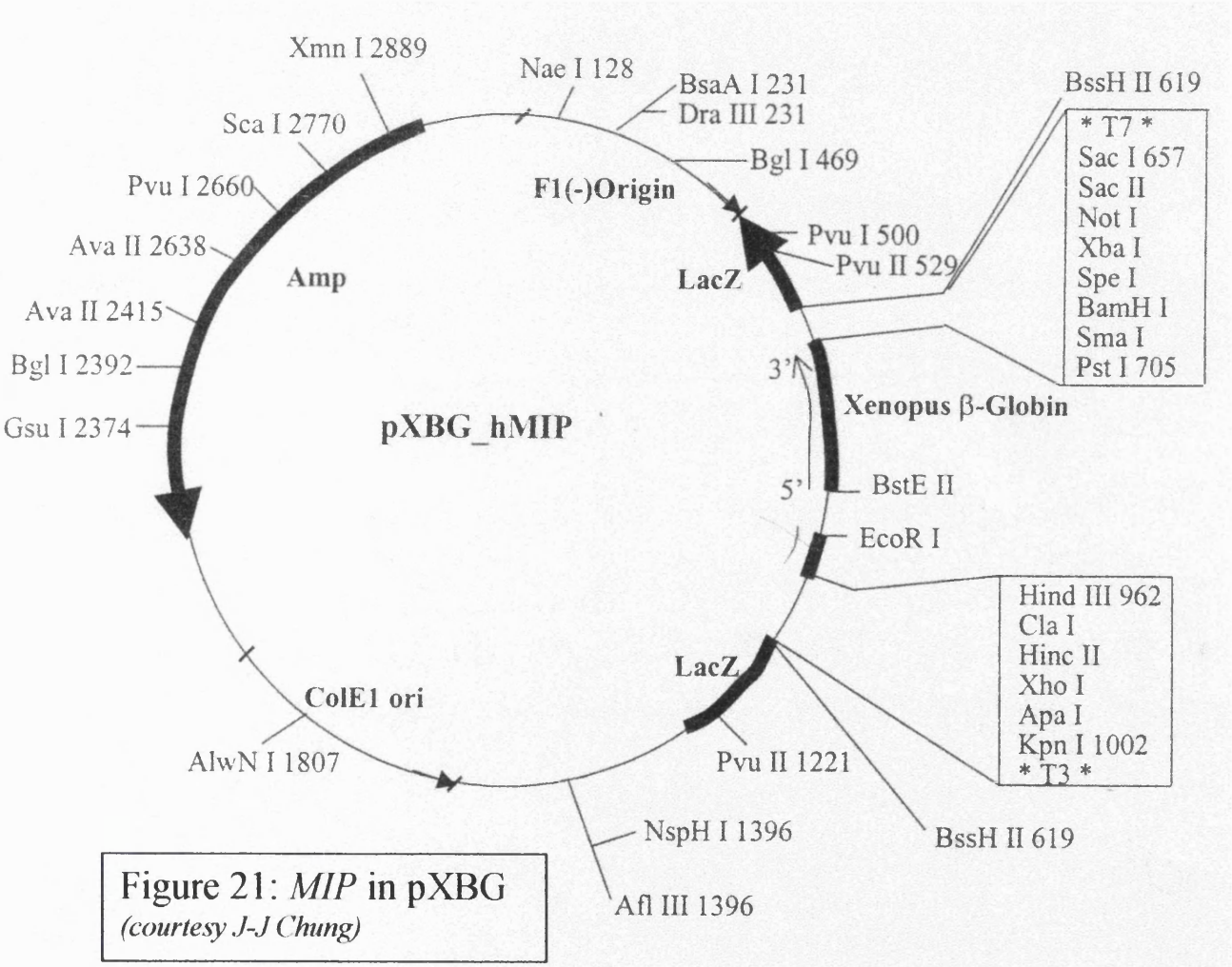

Figure 21: *MIP* in pXBG
(courtesy J-J Chung)

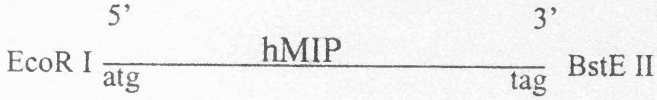

Mutations were introduced into the wild-type hMIP by site-directed mutagenesis (Chameleon Double Stranded Site-Directed Mutagenesis Kit, Stratagene Cloning Systems, 11011 North Torrey Pines Rd, La Jolia CA, USA) with specific 5'-phoshorylated primers.

E134G: CGTCAGGAAGATCCCCACTGTGGTTGC

T138R: CGAACTGGAGCCTCAGGAAGATCTCC

The presence of the mutations was confirmed by direct sequencing. An overview of the principle employed in this kit is shown in figure 22.

Step1: the plasmid containing MIP is denatured and the primers annealed

Both control and experimental reaction mixes were incubated in microcentrifuge tubes at 100°C in a water bath for 5mins and then at 25°C for 30mins.

Step 2: the new strand is extended and ligated

7µl of nucleotide mix is first added and stirred followed by 3µl of freshly prepared enzyme mix (T7 DNA polymerase, T7 DNA ligase, single-stranded binding protein, enzyme dilution buffer, provided), centrifuged (1000 x *g*, 30secs) and incubated at 37°C for 60 mins. The T4 DNA ligase was then inactivated by heating to 80°C for 15 mins.

Step 3: a restriction digest is performed with the selection restriction digest to linearise the remaining parental plasmid

20U of *ScaI* restriction enzyme was then added and the total volume made up to 60µl with dH_2O and incubated at 37°C for 1 hour.

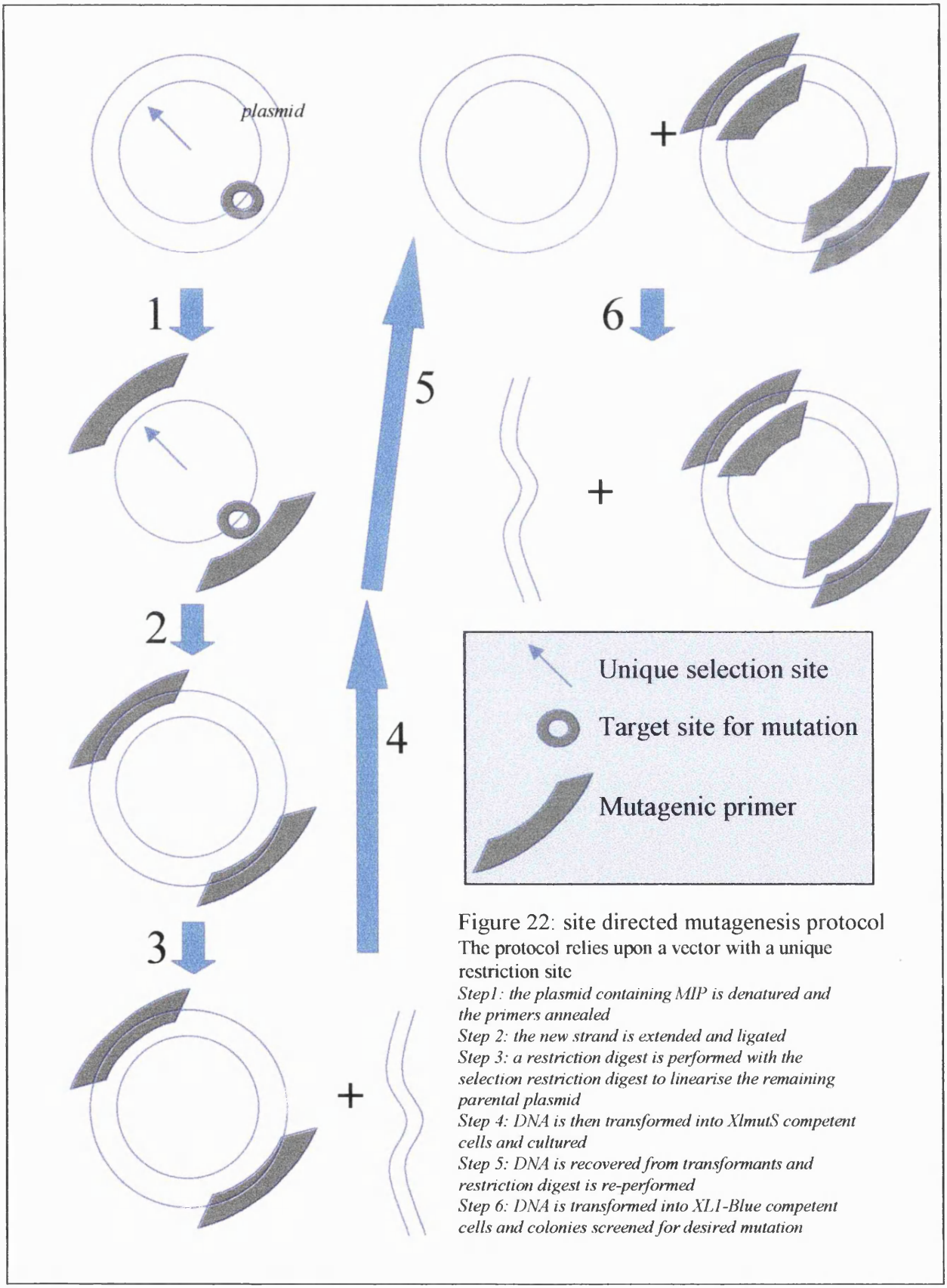

Figure 22: site directed mutagenesis protocol
The protocol relies upon a vector with a unique restriction site
Step1: the plasmid containing MIP is denatured and the primers annealed
Step 2: the new strand is extended and ligated
Step 3: a restriction digest is performed with the selection restriction digest to linearise the remaining parental plasmid
Step 4: DNA is then transformed into XlmutS competent cells and cultured
Step 5: DNA is recovered from transformants and restriction digest is re-performed
Step 6: DNA is transformed into XL1-Blue competent cells and colonies screened for desired mutation

Step 4: DNA is then transformed into XlmutS competent cells and cultured

Xl*mutS* cells on ice were gently mixed and then 90µl transferred to two Falcon 2059 polypropylene tubes (provided). 1.5µl β-mercaptoethanol was then added to each aliquot of cells and gently mixed for 10mins. 6µl of both the control and experimental reaction mixes were then added to the cells, mixed and incubated on ice for 30mins, 42°C for 45 seconds and then ice for 2mins. 0.9ml SOC medium (provided) was then added to each and the mixture incubated at 37°C for 1 hour, gently shaken.

100µl of both the control and experimental transformations were then plated onto X-gal and IPTG containing LB-ampicillin agar plates (20mg/l ampicillin) and incubated overnight at 37°C. Successful transformation yielded approximately 50% colonies displaying the blue mutation (about 500 colonies in total).

Step 5: DNA is recovered from transformants and restriction digest is re-performed

The remaining transformation mixture was plated to 3ml of 2x YT broth and incubated overnight at 37°C, gently shaken. Plasmid DNA was then isolated using QIAGEN QIAquick miniprep kit (described above).

10µl of the resulting control and experimental DNA was then digested with 20U *ScaI* restriction enzyme (together with 1µl of 10x mutagenesis buffer and 9µl dH_2O) and incubated overnight at 37°C.

Step 6: DNA is transformed into XL1-Blue competent cells and colonies screened for desired mutation

Two aliquots of 40µl of XL1-Blue competent cells, on ice, were transferred to Falcon 2059 polypropylene tubes and 0.68µl of β-mercaptoethanol added and incubated for 10mins on ice. 4µl of

each of the control and experimental reaction mixtures were added and mixed on ice for 30mins, 42°C for 45 secs, then ice for 2mins. Addition of 0.45ml SOC medium was followed by a further period of incubation at 37°C for 1 hour.

100µl of the control transformation was then plated onto X-gal and IPTG containing LB-ampicillin agar plates (20mg/l ampicillin) and incubated overnight at 37°C to verify the Lac phenotype.

5µl, 50µl and 200µl of the experimental transformation were plated onto agar plates and incubated overnight at 37°C. Colonies with the blue mutation were easily identified and plasmid DNA recovered for *in vitro* transcription using the QIAGEN QIAquick miniprep kit (described above).

2.12.6.2 Primers used for mutagenesis:

The primers used for the site-directed mutagenesis are shown in table 12.

Table 12: primers used for site-directed mutagenesis

Primer	Sequence (5' – 3')
5'hMIP	GGG GCC GCT GTG CTG TAT AGC
3'hMIP	GGC ACC CTT GAG GAC AGA CAG
MIP (T138R)	CGA ACT GGA GCC TCA GGA AGA TCT CC
MIP (E134G)	CGT CAG GAA GAT CCC CAC TGT GGT TGC

2.12.6.3 In vitro transcription:

20ng of pXBG containing human MIP with was linearised by digestion with 10µl Xba1 restriction enzyme, 10µl Xba1 buffer made up to a total volume of 100µl with dH_2O at 37°C for 4 hours. The DNA was then cleaned by one 100% and one 70% ethanol wash (described above) before re-suspension in 50µl DEPC H_2O. In vitro transcription master mix was then added and incubated for 90 mins at 37°C. Addition of 1µl of T3 RNA polymerase was followed by further incubation for 60 mins.

2.5µl RNasin and 4µl DnaseI were then added and incubated for 20 mins. The reaction was then cessated by the addition of 5µl 100mM EDTA. RNA was then cleaned up using the QIAGEN RNeasy kit.

2.13 Creation of a cDNA bank derived from mouse lens mRNA

2.13.1 Recovery of lenses

Mouse lenses were obtained from the enucleated eyes of freshly killed RDS mice. Lenses were isolated by circumferential pars plana incision followed by surgical zonulysis. Fresh specimens were "snap" frozen in liquid nitrogen and stored at –80°C before use.

2.13.2 mRNA extraction using QuickPrep Micro mRNA Purification kit (Pharmacia)

All equipment was freshly prepared, DEPC (diethyl pyrocarbonate) treated and autoclaved. The extraction buffer (guanidinium isothiocyanate-based) was equilibrated to 37°C and a 0.4 ml aliquot taken and immediately placed on ice in an eppendorff containing the lenses. The lenses were then homogenised using a plastic stick or glass pestle and mortar followed by repeated drawing through a 25 gauge needle with a two ml syringe. 0.8ml elution buffer was added to the extract and mixed thoroughly. The extracted sample was centrifuged at 6000 x *g* for 1 min in parallel with 1ml of the Oligo (dT)-cellulose slurry provided. The buffer was removed from atop the Oligo-(dT)-cellulose and 1ml of the cleared cellular homogenate added and mixed for 3 mins followed by centrifugation for 10 secs at 6000 x *g*. The supernatant was removed and 1ml of High Salt buffer added and the pellet resuspended followed by centrifugation, 6000 x *g*. This wash cycle was repeated for a total of 5 times followed by two washes with Low Salt buffer. The pellet was resuspended in 0.3ml of Low Salt buffer and pipetted to a MicroSpin column placed in a microcentrifuge tube and centrifuged 6000 x *g* for 10 secs. The flow through was discarded and 0.5ml Low Salt buffer washes repeated three times. 0.2ml

of Elution buffer (at 65°C) was then centrifuged through the column to recover the extracted mRNA in a fresh eppendorff.

10µl glycogen, 40µl potassium acetate and 1ml absolute ethanol (chilled to –20°C) was then added to the sample for 1 hour. The precipitated mRNA was then collected by centrifugation at 4°C, 6000 x *g* for 5 mins and stored at –80°C prior to use.

2.13.3 Synthesis of cDNA using 5'/3' RACE fit (Boehringer Mannheim) and Recombinant RNasin Ribonuclease inhibitor (Promega)

The cDNA synthesis mixture was pipetted into a sterile eppendorff on ice and mixed. The mixture was then briefly centrifuged and incubated at 55°C for 1 hour (synthesis stage) followed by 10mins at 65°C (inactivation stage). The newly synthesised cDNA was then stored at –20°C prior to use in PCR reactions.

2.14 Protein prediction

The Windows based protein prediction and sequence analysis software, DNAstar (DNASTAR Inc) and the online PredictProtein programs[279] (phd@maple.bioc.columbia.edu) were used to assess the effect of mutations on the structure and function of proteins.

2.15 General laboratory solutions

1xTBE

89mM Tris base

89nM boric acid

2mM EDTA

1xTAE

89mM Tris base

2mM EDTA

Phosphate buffered saline

8g NaCl

0.2g KCl

1.44g Na_2HPO_4

made up to 1 litre with distilled water

pH 7.4 with HCl

(autoclaved 20 min at 15lb/sq. inch)

Ficoll loading dye

15% ficoll

50mg bromophenol blue

50mg xylene cyanol

Formamide/EDTA loading dye

49ml formamide

1ml 0.5M EDTA

50mg xylene cyanol

50mg bromophenol blue

TE buffer

10mM Tris-HCl

1mM EDTA

pH 8.0

1 double Heteroduplex gel

Urea	15g
Water	40ml
10xTBE	6ml
MDE	50ml

Gel plug: to 1000µl of gel mix,

10µl 10% APS and 3µl TEMED

Gel: to remainder, 440µl 10% APS, 44µl

TEMED

Preparation of *xenopus* oocytes from frog:

Calcium-free OR-2

NaCl	100mM	5.8g
KCl	2.0mM	2ml 1mM stock
$MgCl_2$	1.0mM	1ml 1mM stock
Hepes	5.0mM	50ml 100mM stock
Water		914ml

pH 7.5, 200mosm

MBS (Modified Barth's solution)

NaCl	88.0mM
KCl	1.0mM
$NaHCO_3$	2.4mM
Tris-Cl	15.0mM, pH 7.6
$Ca(NO_3)_2$	0.3mM
$CaCl_2$	0.4mM
$MgSO_4$	0.8mM
Na penecillin	100µg/ml
Streptomycin sulphate	100µg/ml
pH 7.5, 200-230mosm	

Immunoblotting solutions:

Tissue homogenisation buffer

NaPO4	7.5mM
EDTA	1mM
Aprotinin	2mg/ml
PMSF (phenylmethylsulphonyl fluoride)	174mg/ml
Leupeptin	2mg/ml
Pepstatin A	2mg/ml

1ml per 10 oocytes

5% SDS solubilisation buffer (50ml)

SDS	5%
water	
Tris-HCl, pH 8.0	20mM
EDTA, pH 8.0	5mM

Western blotting:

5x loading buffer

SDS	5%
Glycerol	30%
Tris, pH 8.0	50mM
Bromophenol Blue	0.05%

12% acrylamide resolving gel with 4.0M urea

acrylamide	12%
Tris, pH 8.0	0.39M
SDS	0.1%
Urea	4.0M

TEMED 4µl (added just prior to loading)

35% APS	400µl

Made up to 6ml with water

4% acrylamide stacking gel with 4.0M urea

acrylamide	4%
Tris, pH 8.0	0.13M
SDS	0.1%

TEMED 2µl (added just prior to loading)

35% APS	200µl

Made up to 2ml with water

Electrophoresis buffer

Tris	25mM
Glycine	190mM
Na azide	1mM
SDS	0.1%

Transfer buffer

Tris, pH 7.4	20mM
NaOAc	10mM
EDTA	1.0mM
SDS	0.02%

Site-directed mutagenesis:

10x mutagenesis buffer

Tris-acetate,

pH7.5	100mM
MgOAc	100mM
KOAc	500mM

Nucleotide mix

DNTP	2.86mM
rATP	4.34mM

1.43x mutagenesis buffer

Tryptone	16g

Made up to 1l with dH_2O, pH 7.5 with 2M NaOH

Enzyme dilution buffer

Tris-HCl	20mM
KCl	190mM
β-mercaptoethanol	10mM
DTT	1mM
EDTA	0.1mM

50% glycerol

SOB medium

Tryptone	20.0g
Yeast extract	5.0g
NaCl	0.5g
1M $MgCl_2$	10ml
1M $MgSO_4$	10ml

made up to 1l with dH_2O

SOC medium

SOB medium

20% glucose	2ml

2x YT broth

NaCl	10g
Yeast extract	10g

Immunofluorescence:

Fixing solution

PIPES	80mM
Na EGTA	5mM
MgCl2	1mM
Formaldehyde	3.7%
Triton-X-100	0.2%

In vitro transcription:

In vitro transcription master mix

5x T3 reaction buffer	20µl
10x ACU (10mM) g (2mM) nucleotide mix	10µl
50mM DTT	10µl
40U/µl RNasin	2.5µl
50U/µl T3 RNA polymerase	2µl
10mM $m^7G(5')ppp(5')G$	6µl

2.16 Online databases used

Table 13: literature searching and general information:	
Human Genome Mapping Project	Http://www.hgmp.mrc.ac.uk/
Human Mutation Database	Http://www.uwcm.ac.uk/uwcm/hgmd0.html
National Center for Biological	Http://www.ncbi.nlm.nih.gov/
Information (NCBI)	
The Genome Database	Http://www.gdb.org/
Online Mendelian Inheritance	Http://www.ncbi.nlm.nih.gov/Omim/
In man (OMIM)	
Genbank	Http://www.ncbi.nlm.nih.gov/Genbank
Genethon	Http://www.genethon.fr/
Co-operative Human	Http://www.chlc.org/
Linkage Centre (CHLC)	
Entrez database	Http://www.ncbi.nlm.nih.gov/Entrez/
Whitehead Institute/MIT Genome	Http://www-seq.wi.mit.edu/public_release/bychrom.html
Sequencing Project	
ExPasy	Http://www.expasy.ch/prosite/

Table 14: Bio-Informatics and X-chromosome:	
Sanger Centre X chromosome database	http://www.sanger.ac.uk/HGP/ChrX/
MRC Human Genetics	http://www.hgu.mrc.ac.uk/
Integrated X chromosome database	http://ixdb.mpimg-berlin-dahlem.mpg.de/
Human chromosome launchpad	http://www.ornl.gov/hgmis/launchpad/
Baylor Human Genome Sequencing Centre	http://www.hgsc.bcm.tmc.edu/
Ensembl Genome Server	http://www.ensembl.org/
Predict Protein	

3. Results

3.1 Pedigrees and phenotypes

Five hundred and eighty six patients participated from 79 pedigrees (77 Caucasian, 2 Asian). Sixty five pedigrees were drawn from those areas directly served by Moorfields Eye Hospital. The remainder originated from the following counties: Kent, Hampshire, Devon, Oxfordshire, West Midlands, Greater Manchester, Merseyside, Nottinghamshire, Derbyshire, Tyneside, County Cork, and Dublin.

The median age of participants was 43 years (range 0-91). Two hundred and eighty four individuals were found to be affected, 184 unaffected and 118 were spouses. All affected individuals could be classified as one of ten different phenotypes: anterior polar, posterior polar, lamellar, nuclear, coralliform, pulverulent, blue-dot, cortical, polymorphic or lattice as shown in table 15. Cataract was fully penetrant though expressivity was variable in all pedigrees. The morphology of the cataract in affected individuals within any single pedigree was the consistent for all except the pulverulent pedigrees (see below). In only one of the pedigrees (family N) were other ocular or systemic abnormalities present.

Autosomal dominant inheritance was suspected in all but one pedigree by the presence of affected individuals in successive generations, male-to-male transmission and equal numbers of affected males and females within each family. Inheritance in family J, appeared X-linked (see results 3.6).

A complete listing of all pedigrees ascertained is shown in figure 23.

Figure 23 (on this and next pages): Pedigrees ascertained. Each pedigree is denoted by a unique identifier (a single letter for large pedigrees considered suitable for linkage analysis; a number prefixed with 'S' for small families). Standard symbol conventions are observed. Squares and circles denote males and females respectively. Blackened symbols denote affected individuals. Deceased family members have a diagonal line through them.

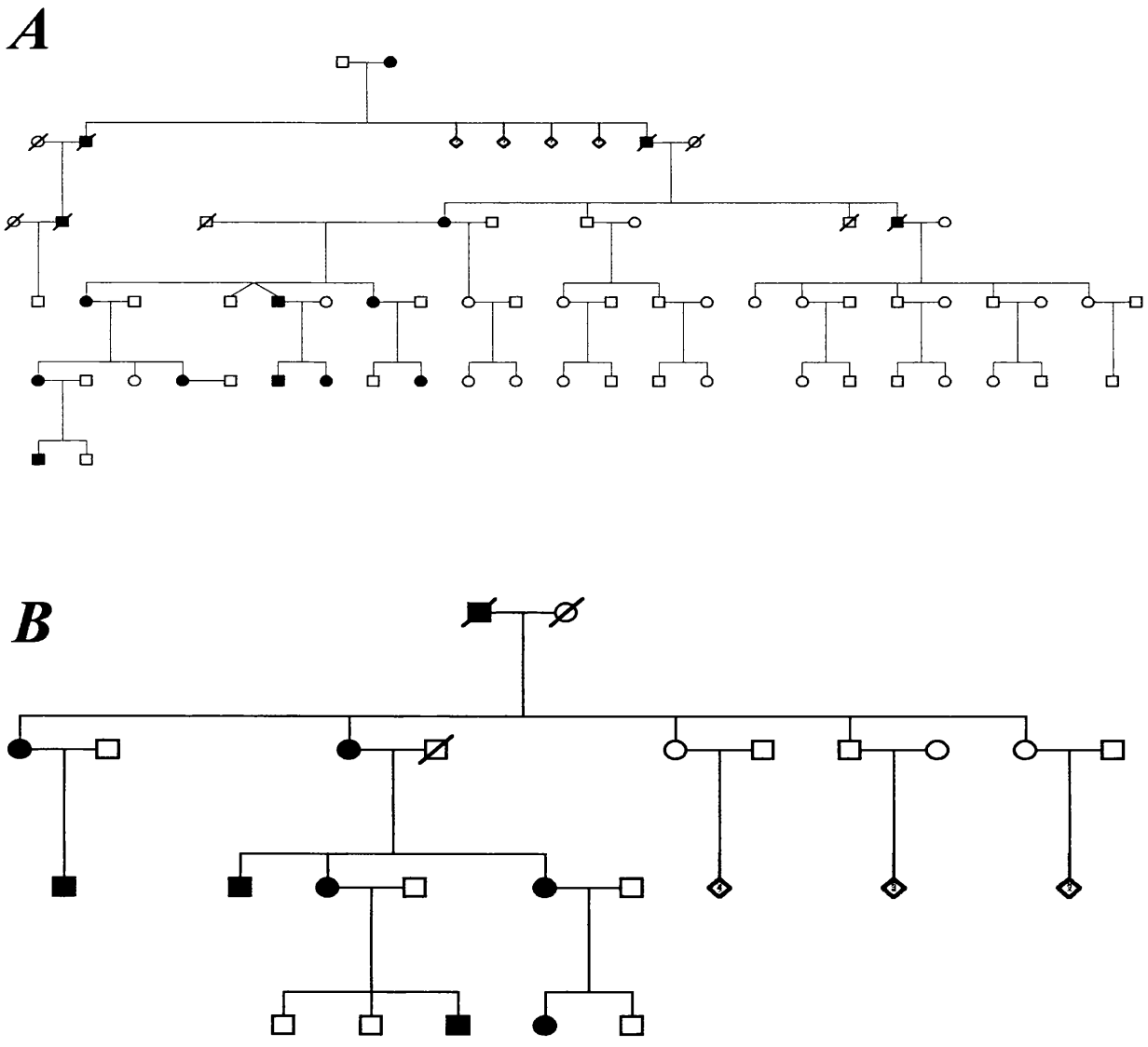

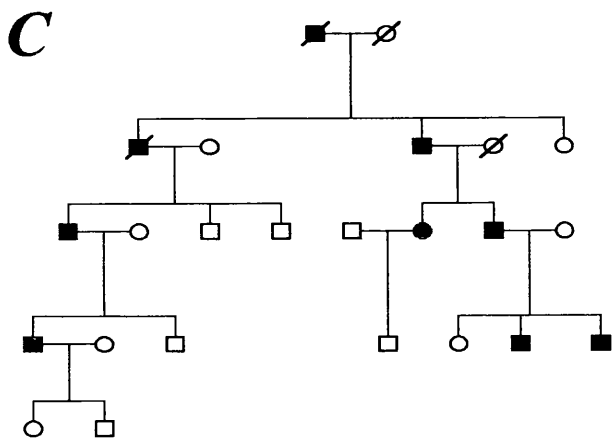
C

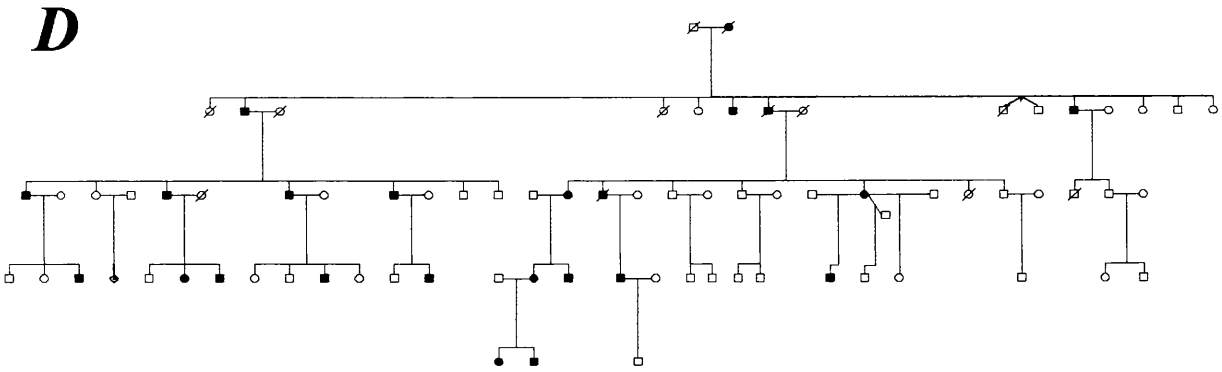
D

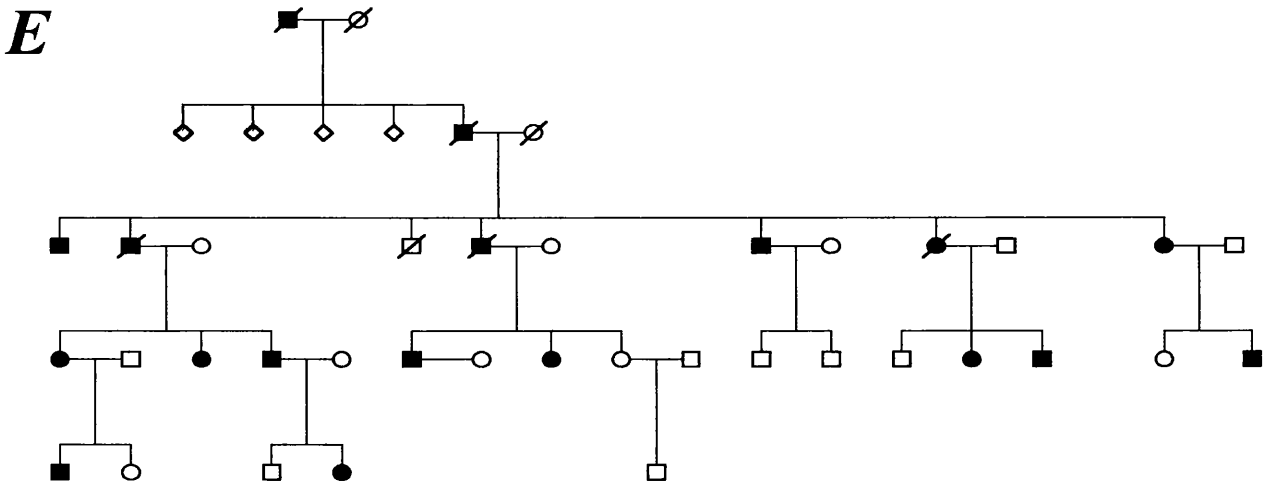
E

F

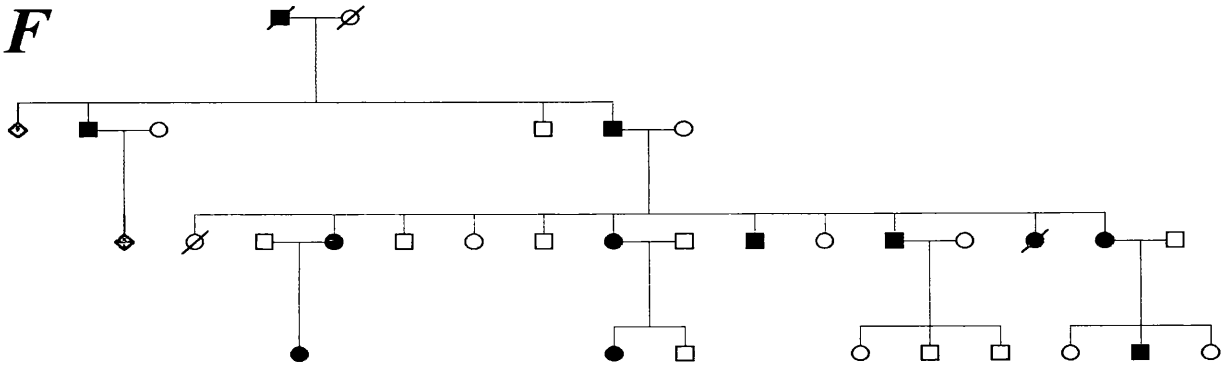

G

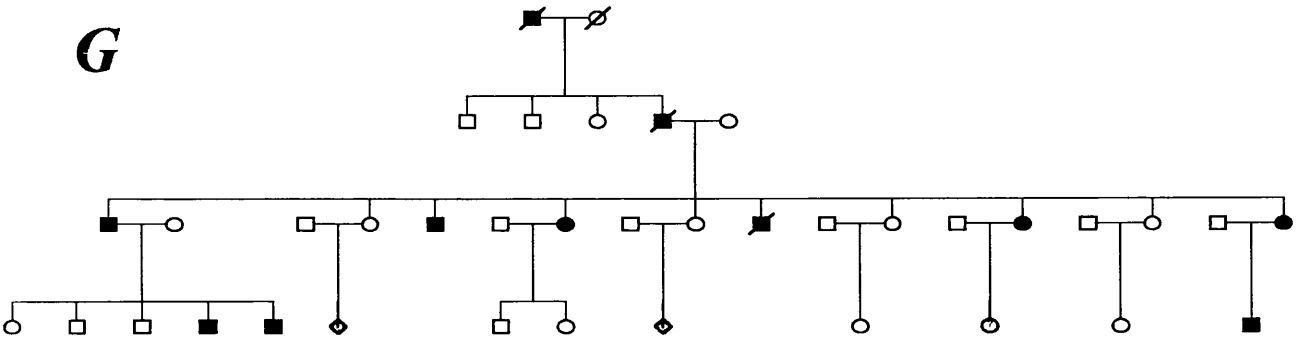

H

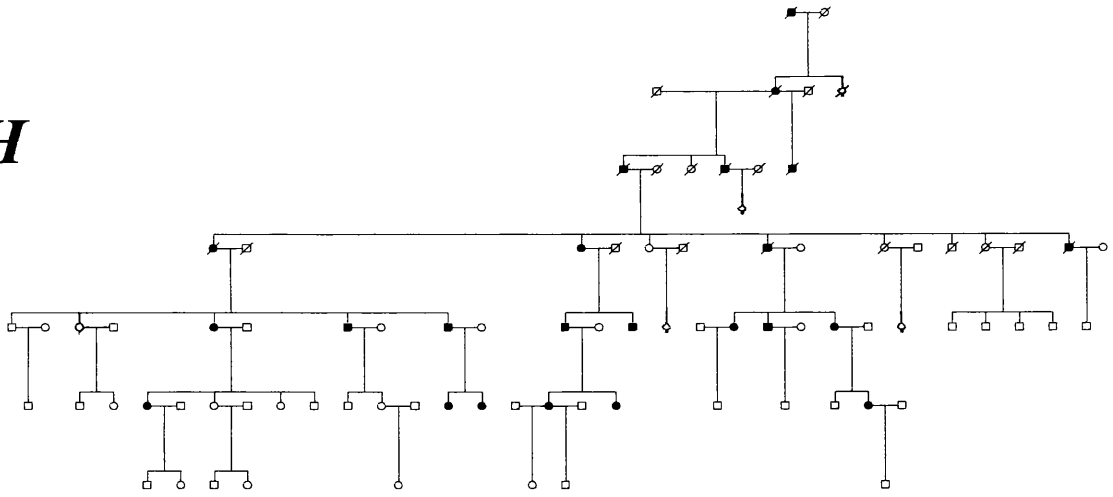

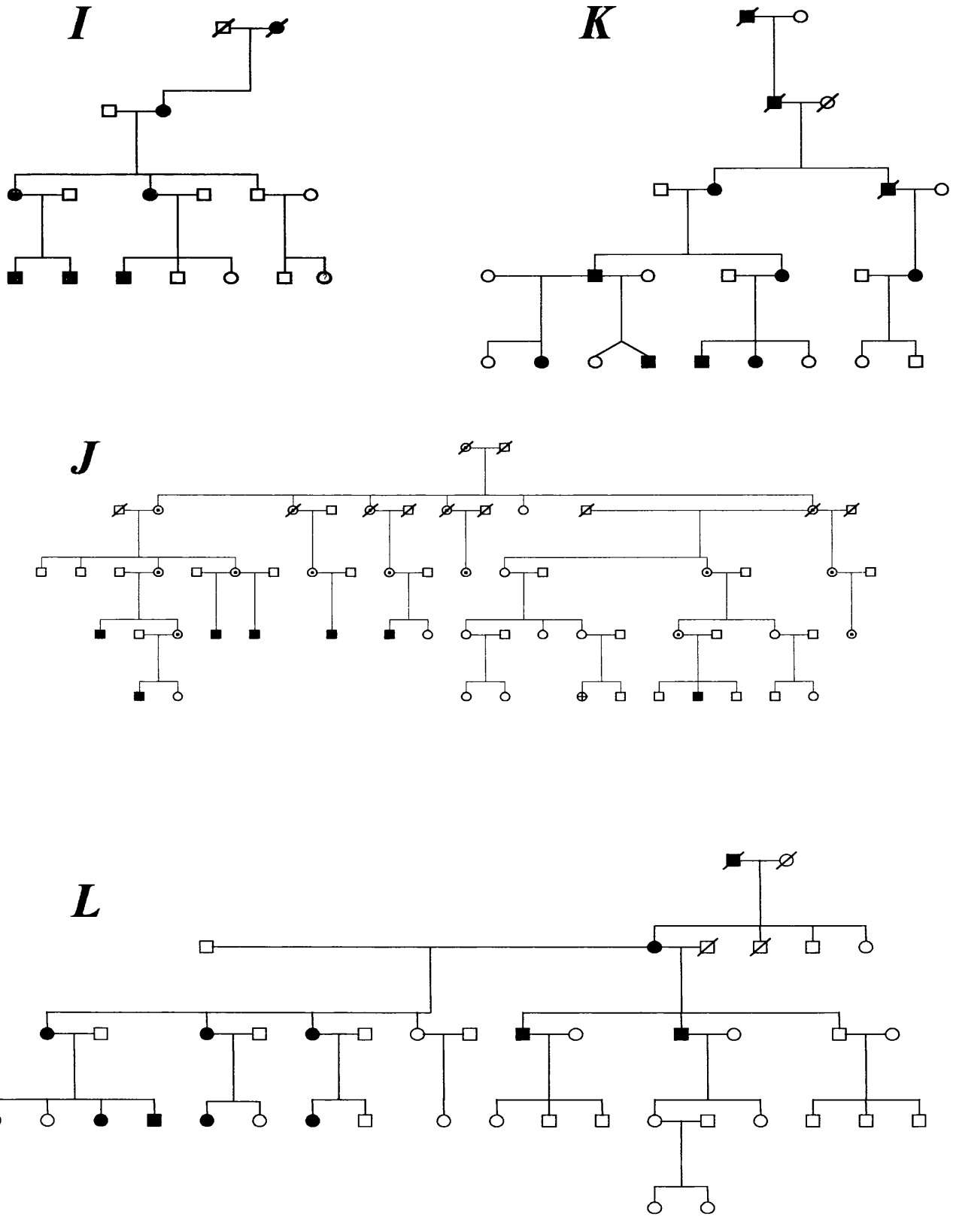
I
K
J
L

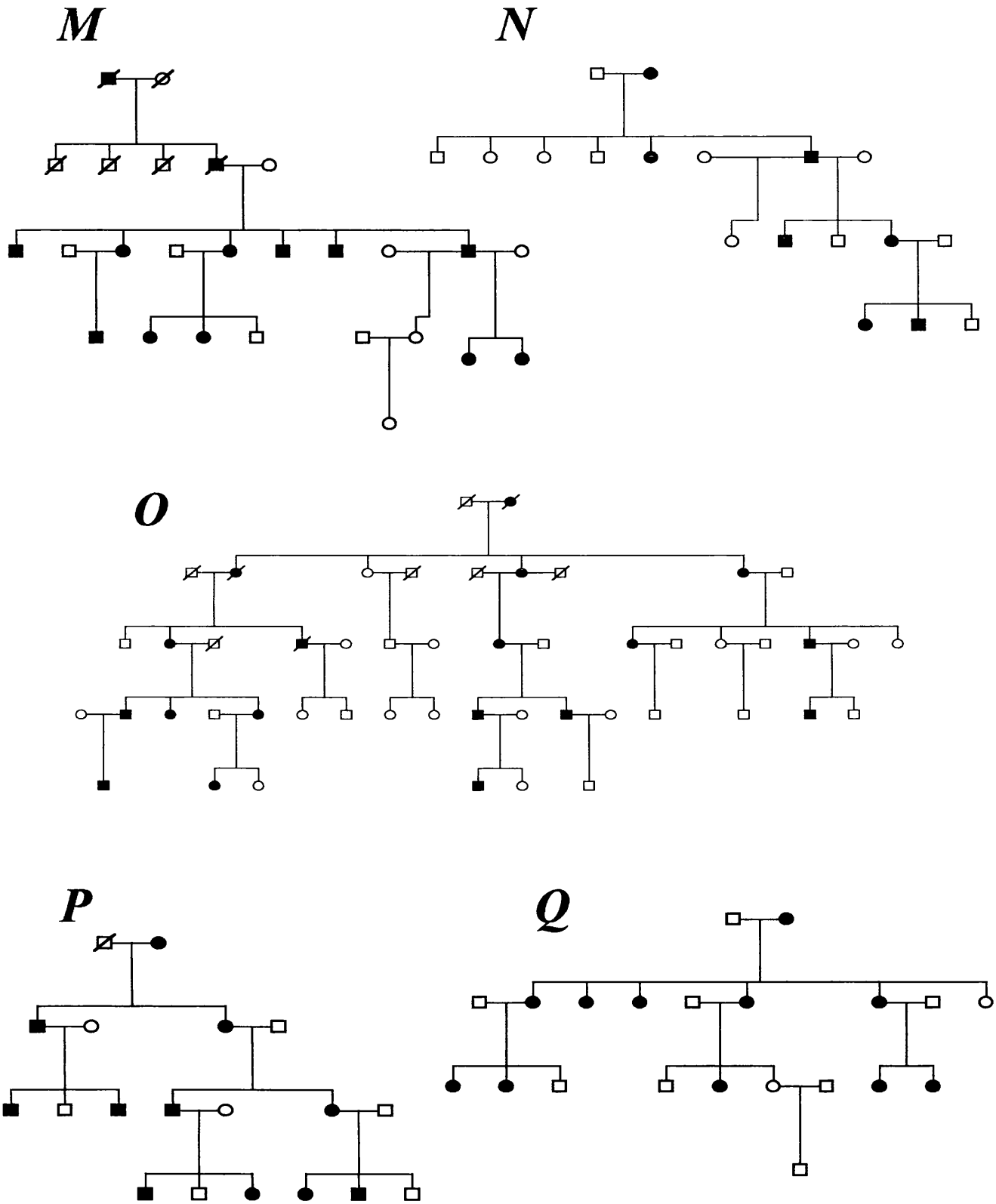
M
N
O
P
Q

S1

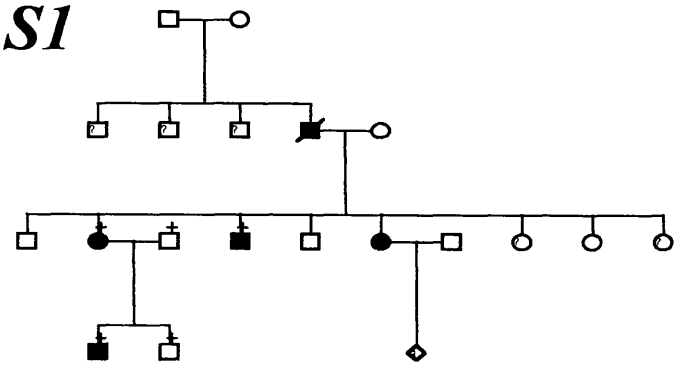

S2

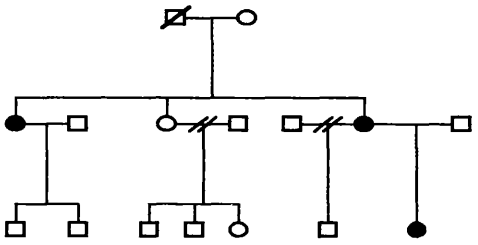

S3

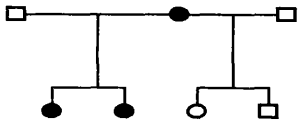

S4

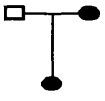

S5

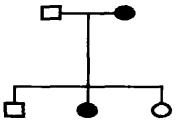

S6

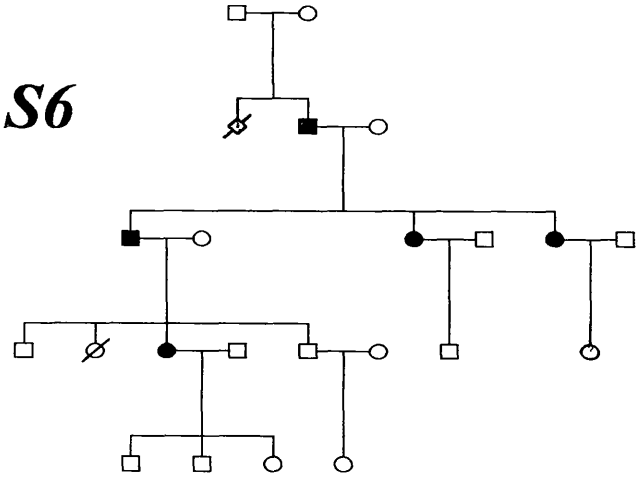

S7

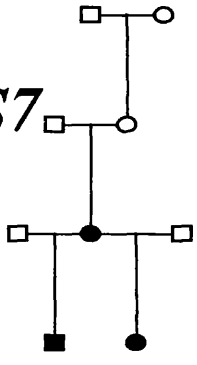

S8

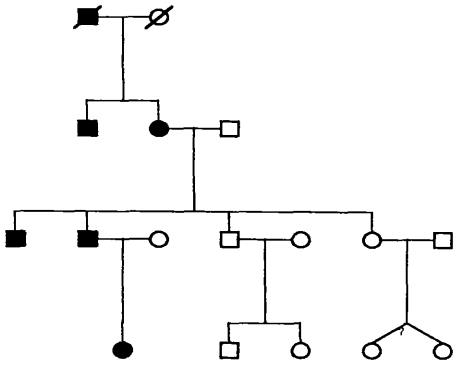

S9

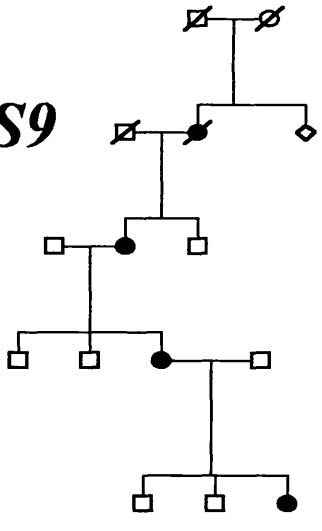

S10

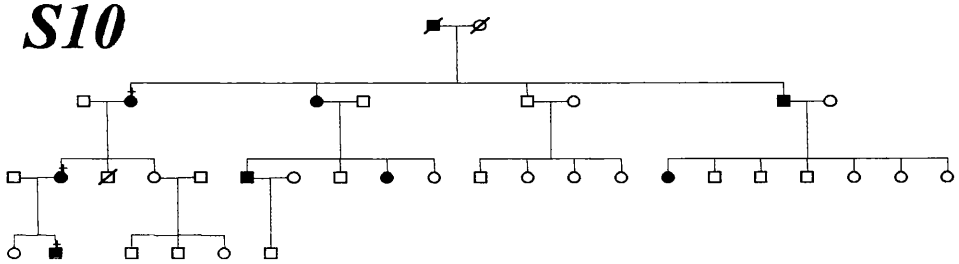

S11

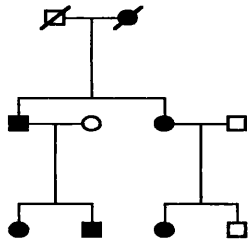

S12

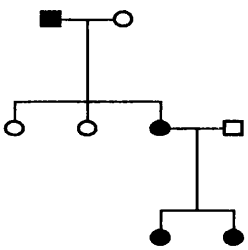

S14

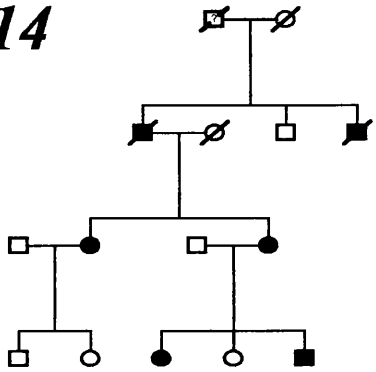

S13

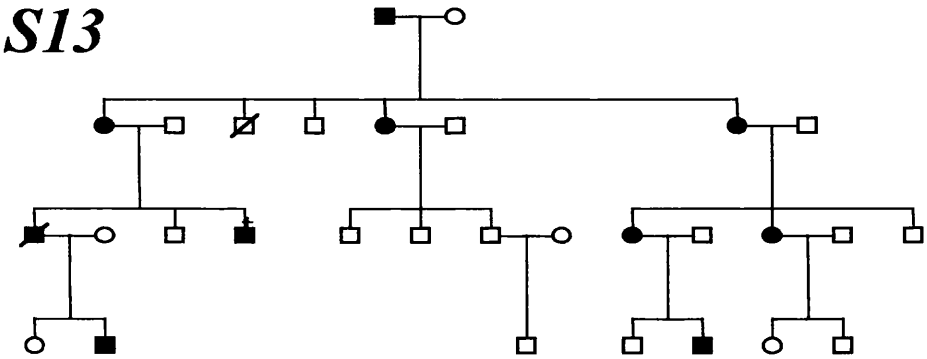

S15

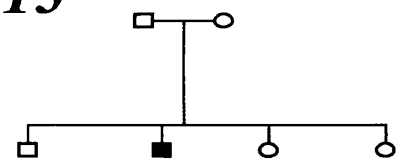

S16

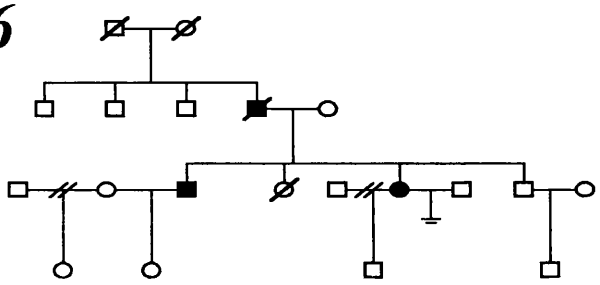

S17

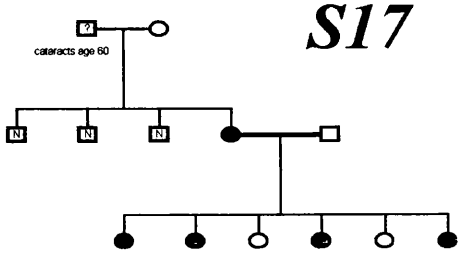

S18

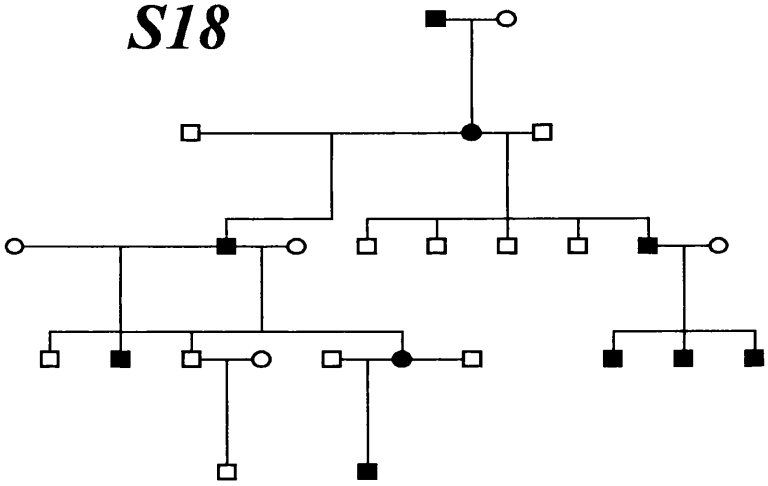

S19

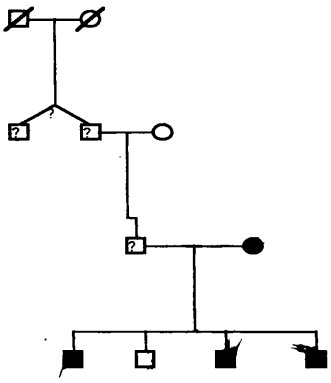

S20

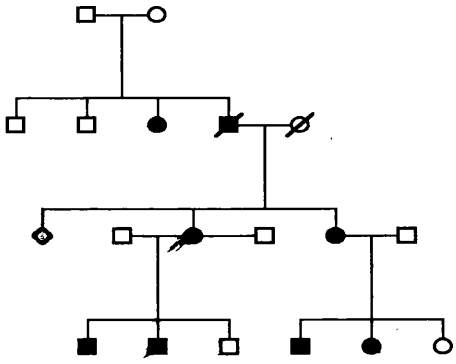

S21

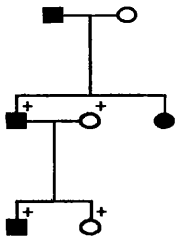

S22

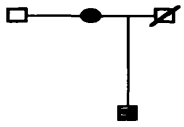

S23

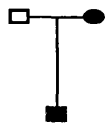

S24

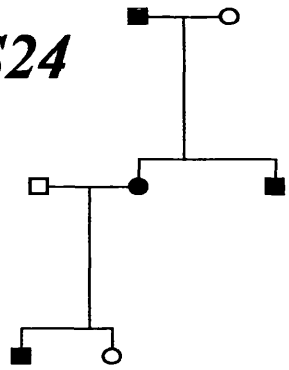

S25

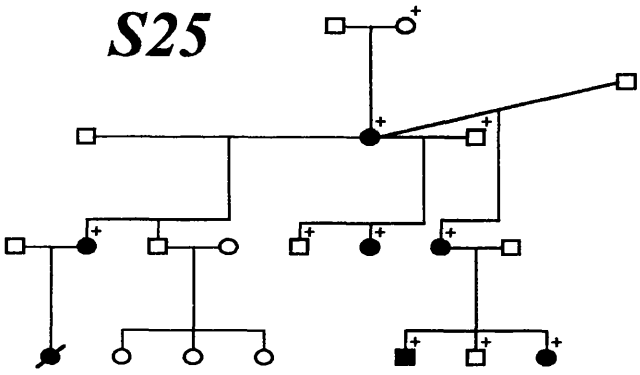

S26

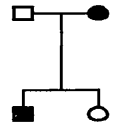

S27

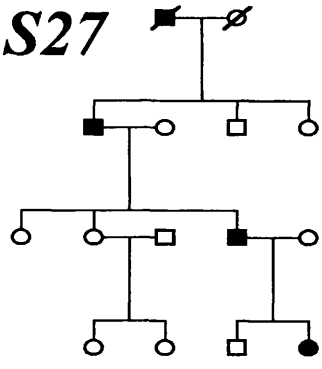

S28

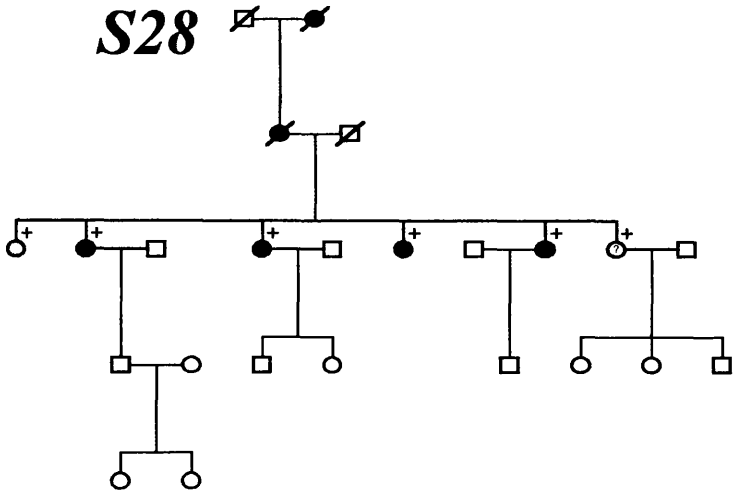

S29

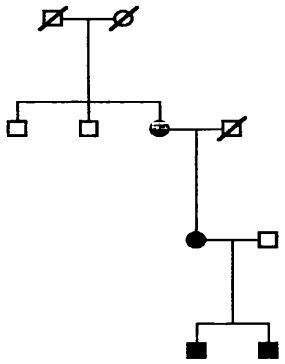

S30

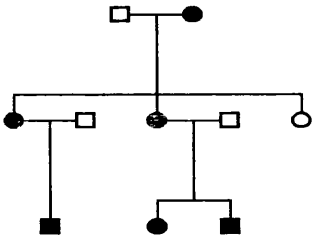

S32

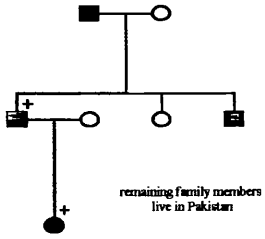

S33

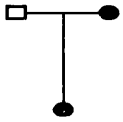

S34

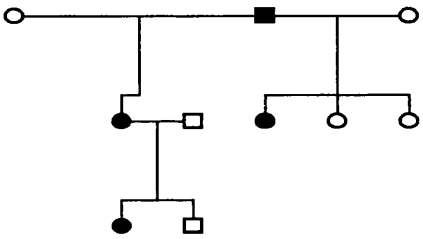

S35

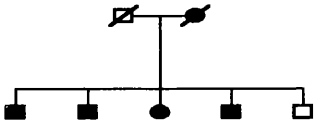

S64

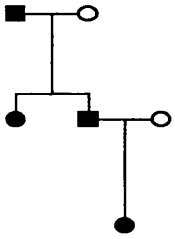

S66

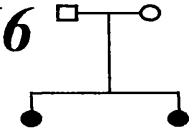

S65

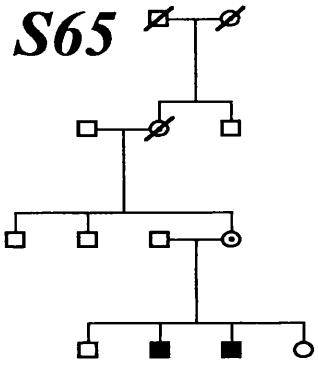

S67

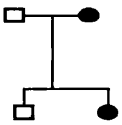

Phenotype	Number of pedigrees	Number of affected
Anterior polar	4	10
Posterior polar (stationary)	4	15
Posterior polar (progressive)	7	32
Lamellar	7	45
Nuclear	12	75
Coralliform (aceuliform)	1	7
Pulverulent	7	39
Blue-dot (cerulean)	3	10
Cortical	1	2
Polymorphic	2	14
Lattice	1	3
Total	49	252

Table 15: phenotypic distribution of patients

3.1.1 Clinical appearances

Ten phenotypes could be recognised that included all the pedigrees seen in the study. These phenotypes were anterior polar, posterior polar, nuclear, lamellar, coralliform, blue-dot (cerulean), cortical, pulverulent, polymorphic and lattice. The morphology of the cataract in affected individuals within any single pedigree was the same for all except the pulverulent and polymorphic pedigrees, varying only in the severity and density of the opacity. In pedigrees with the pulverulent phenotype there was considerable variation in the cataract morphology amongst affected individuals from the same pedigree. Penetrance was uniformly very high. Autosomal dominant inheritance was supported in many cases by affected individuals in successive generations, equal numbers of affected males and females, and the presence of male-to-male transmission.

3.1.1.1 Anterior polar cataract (figure 24*a*)

Affected individuals had bilateral, symmetrical, well-circumscribed lens opacities. Larger opacities were pyramidal in shape and extended into the anterior chamber. Microphthalmia as an associated feature was not observed.

3.1.1.2 Posterior polar cataract (figure 24*b* and *c*)

Affected individuals had bilateral, symmetrical, well-circumscribed opacities located close to the posterior pole involving the capsule and/or posterior lens cortex. Families with posterior polar cataract were much more common in our series and fell broadly into two groups, stationary and progressive. In the latter group, spreading cortical extensions of the cataract were observed that eventually became confluent to result in total cataract formation.

3.1.1.3 Nuclear cataract (figure 24*d*)

Inherited nuclear cataracts show wide clinical variation, even between members of the same family, though the distribution of opacities is consistent. In some of our families, opacification was confluent and dense whilst in others, within the same family, it was more punctate. It can be clinically difficult to determine a precise demarcation between the nucleus i.e. that part of the lens formed in utero, and the surrounding cortex laid down thereafter. However, in these families, the edge of opacification appeared to clearly delineate this transition.

3.1.1.4 Lamellar cataract (figure 24*e* and *h*)

The concentric deposition of secondary lens fibres that occurs during growth of the normal lens results in the formation of lamellae. Opacities confined to a specific lamella therefore reflect a

short period of developmental disturbance resulting in usually symmetrical bilateral lens opacification. Interestingly, in some cases cortical riders may also be observed. Lamellar cataracts are also called zonular or peri-nuclear cataract. In our families, cataract showed wide variations in expressivity, where some individuals had complete lamellar opacification whilst in others only the anterior and posterior Y sutures were opacified.

3.1.1.5 Coralliform cataract

Patients with this rare form of congenital cataract also known as aceuliform cataract, have finger-like opacities that extend from an opacified nucleus. In one of the families, no affected individuals were still phakic and description of the cataract was taken from hospital records.

3.1.1.6 Pulverulent cataract (figure 24*f, g, k* and *l*)

Pulverulent cataracts are characterised by powdery (pulverised) opacities that may be found in any part of the lens. Pedigrees affected by pulverulent cataract showed wide intra-familial variation in the cataract phenotype and although some affected individuals from these families had cataracts similar to lamellar or nuclear cataract, pedigrees were classified as pulverulent if the majority of affected individuals had fine, powdery opacities.

3.1.1.7 Blue-dot cataract (figure 24*i*)

The blue-dot or cerulean cataract is not truly congenital, but develops in childhood and progresses through early life. The discrete pinhead-shaped blue-white opacities are distributed throughout the lens becoming more numerous in the cortex where they may form large cuneiform (wedge-like) shapes in the mid-periphery. Within our pedigrees, this phenotype was consistent in its distribution but variable in its severity.

3.1.1.8 Cortical cataract (figure 24*j*)

In only one of the families studied was cataract limited to the cortex. This phenotype differs from lamellar cataract since opacification is limited to a sector of outer cortical, often superior, lens fibres, adjacent to the lens capsule. The nucleus was unaffected.

3.1.1.9 Polymorphic and lattice cataracts

These two phenotypes have not previously been described as inherited traits and are therefore dealt with in more detail in the next chapter.

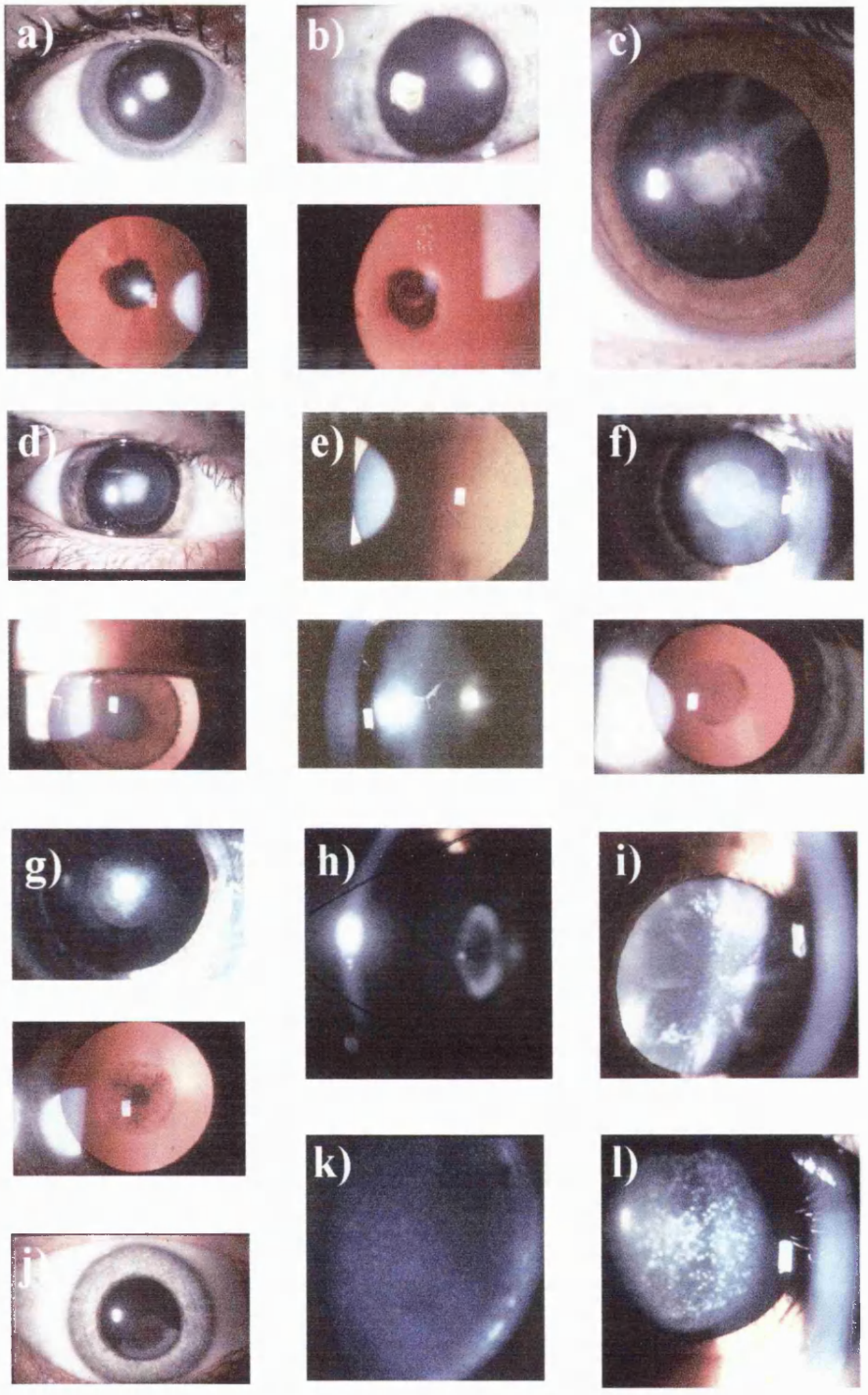

10 mm (approx)

Figure 24: autosomal dominant congenital cataract phenotypes

a) Slit lamp (above) and retroillumination (below) view of anterior polar cataract (47 year old female)
b) Slit lamp and retroillumination view of a stationary posterior polar cataract (49 year old female)
c) Slit lamp view of a progressive posterior polar cataract (9 year old female)
d) Slit lamp and retroillumination view of a dense nuclear cataract (14 year old male)
e) Slit lamp and retroillumination view of nuclear opacities (50 year old female)
f) Slit lamp and retroillumination view of the Coppock-like (pulverulent) cataract with fine nuclear opacities (24 year old female)
g) Slit lamp and retroillumination view of the Coppock-like cataract with dense central opacities (6 year old female)
h) Slit lamp view of lamellar cataract
i) Slit lamp view of a blue-dot (cerulean) cataract (32 year old male)
j) Slit lamp and retroillumination view of a cortical cataract (45 year old female)
k) Slit lamp view of a fine pulverulent cataract (32 year old male)
l) Slit lamp view of large pulverulent opacities (12 year old female)

3.2 Novel cataract phenotypes

3.2.1 Polymorphic cataract

The cataract observed in family A could not be satisfactorily placed into any previously described phenotypic category and given its variable appearance was described as "polymorphic". The cataract in this family was subsequently mapped to 12q and a mutation identified in MIP, the major intrinsic protein of the lens (see below, Results 3.4).

In the family, autosomal dominant inheritance was supported by the presence of affected male and female individuals in each generation and male-to-male transmission. The disease showed both complete penetrance and highly variable expressivity.

Opacification of the lens was bilateral in all affected cases and consisted of discrete progressive punctate lens opacities limited to mid and peripheral lamellae. In addition, some of those affected had asymmetric anterior and posterior polar opacification. One young female had predominantly cortical cataract and another had serpiginous nuclear opacities. The clinical spectrum of the phenotype is shown in figure 25. Hospital records indicated that the opacity was present at birth or developed within the first year of life. Visual acuity in the unoperated eyes of those affected ranged from 6/6 to 6/24. No affected individuals have developed strabismus or retinal detachment. There was no evidence of other ocular or systemic abnormalities.

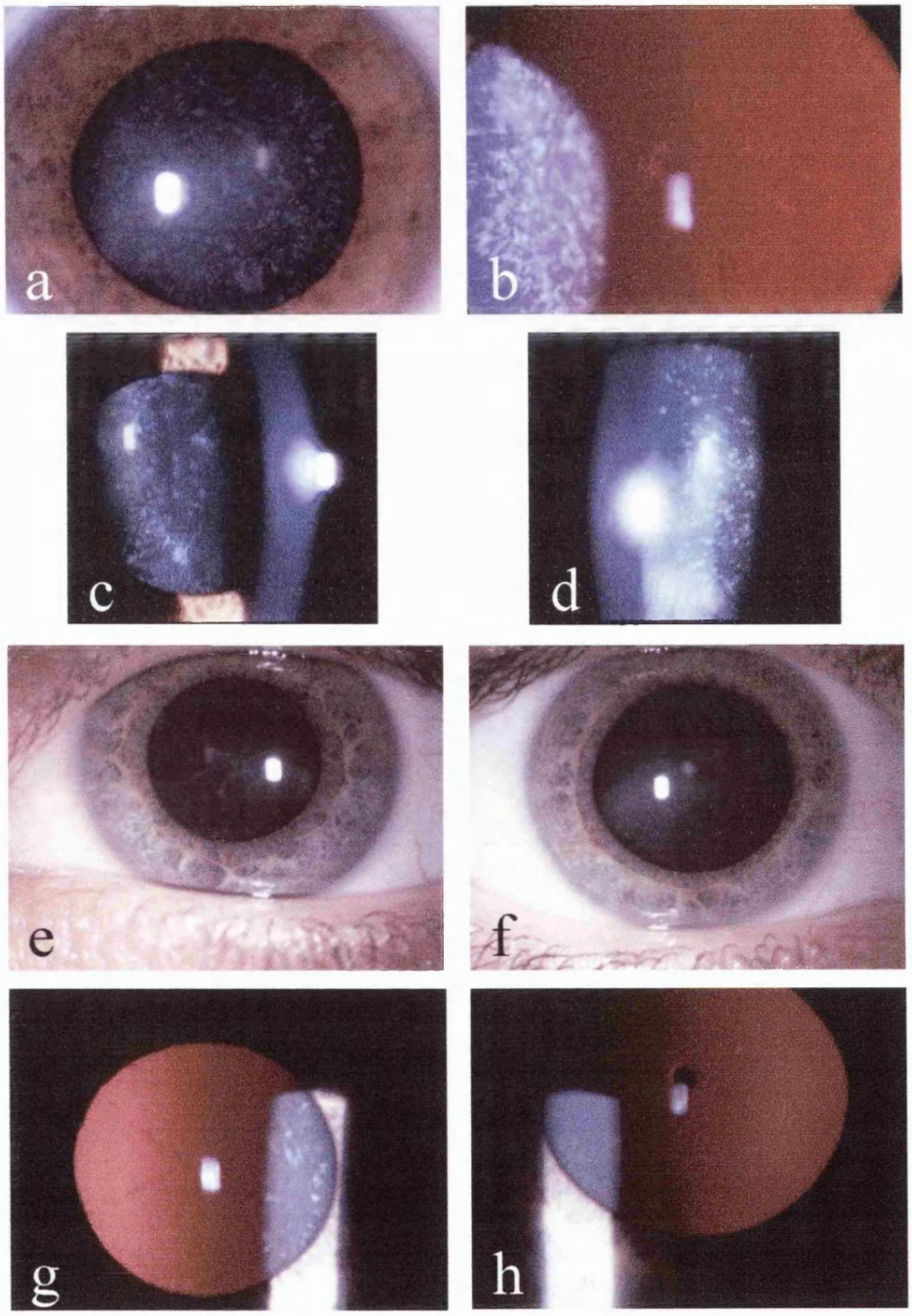

Figure 25: the polymorphic cataract phenotype.

Punctate mid and peripheral opacities in:
a direct illumination (34 year old female);
b retroillumination (same patient as *a*);
c slit beam illumination (17 year old female);
d slit beam illumination (46 year old female);
e serpiginous nuclear opacities (24 year old female);
f anterior polar cataract (same patient as *e*);
g retroillumination view of serpiginous nuclear opacities (same patient as *e*);
h retroillumination view of anterior polar cataract in patient with predominantly cortical opacification

Three individuals had undergone bilateral lensectomy in childhood, aged 1 month (left and right best corrected visual acuities 6/9, 6/12 respectively), 4 months (6/6, 6/9; subsequently developed well-controlled aphakic glaucoma) and 15 years (HM, 6/9). Right extracapsular cataract extraction had been performed on two patients in adulthood (aged 55 and 72 years, each achieving best corrected visual acuity of 6/6).

Opacification of the lens was bilateral in all affected cases and consisted of discrete progressive punctate lens opacities limited to mid- and peripheral lamellae. In addition, some of those affected had asymmetric anterior and posterior polar opacification. One young female had predominantly cortical cataract and another had serpiginous nuclear opacities. Hospital records indicated that opacification was present at birth or developed within the first year of life.

Table 16 shows that although final visual outcome for these individuals did not differ significantly from the visual acuities achieved by members of the other family with a different missense mutation in MIP, only 5 out of 10 affected had required surgery to prevent deprivational amblyopia.

Table 16: best corrected visual outcome for patients with *a*, polymorphic cataract; *b*, lamellar cataract with different missense mutation in MIP.

a

Affected individual	Age (years)	Best corrected visual acuity	
		Right	Left
II:2	72	6/12	6/6 (pseudophakic)
III:2	55	6/24	6/6 (pseudophakic)
III:4	45	6/9 (aphakic)	HM (aphakic)
III:7	45	6/9	6/9
IV:2	35	6/6	6/12
IV:4	27	6/6	6/9
IV:5	15	6/12 (aphakic)	6/9
IV:6	11	6/9 (aphakic)	6/6 (aphakic)
IV:8	16	6/6	6/6
V:2	1	-	-

b

Affected individual	Age (years)	Best corrected visual acuity	
		Right	Left
II:2	56	6/18 (pseudophakic)	6/9 (pseudophakic)
III:2	34	6/6 (pseudophakic)	6/6 (pseudophakic)
III:3	33	6/12 (pseudophakic)	6/9 (pseudophakic)
IV:1	15	CF (aphakic)	6/9 (aphakic)
IV:2	11	6/6 (aphakic)	6/12 (aphakic)
IV:3	9	6/18 (aphakic)	6/18 (aphakic)

3.2.2 Lattice cataract

Figure 26 shows examples of the fully penetrant autosomal dominant cataract phenotype evident in the three-generation family, P. All affected individuals show inter-linking progressive lines of cortical opacification. Such a pattern was clearly distinct from other phenotypes.

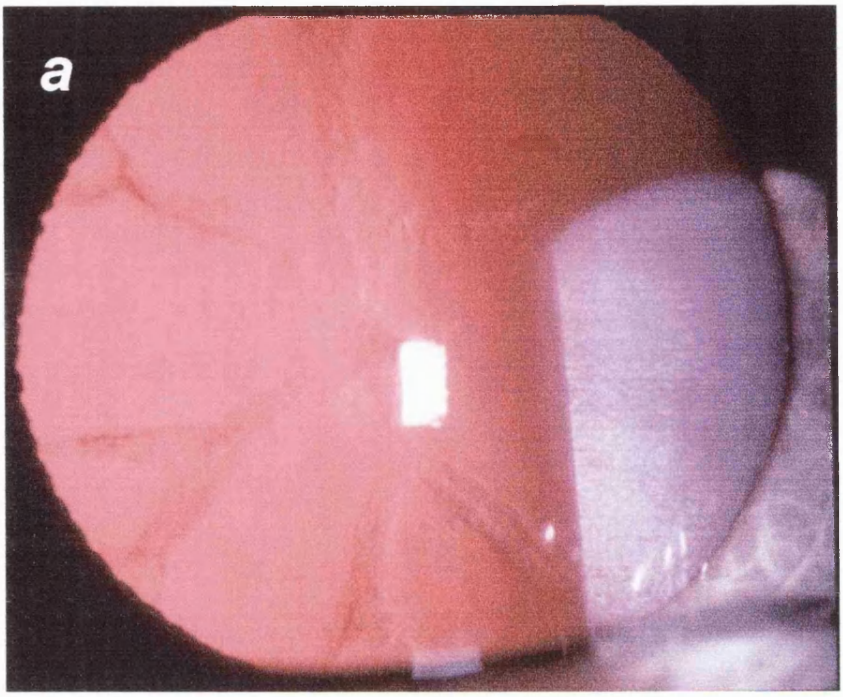

Figure 26: the lattice cataract phenotype. Intertwining bands of Anterior and posterior cortical cataract are shown (six year old female), *a*, in retroillumination; *b*, in diffuse illumination

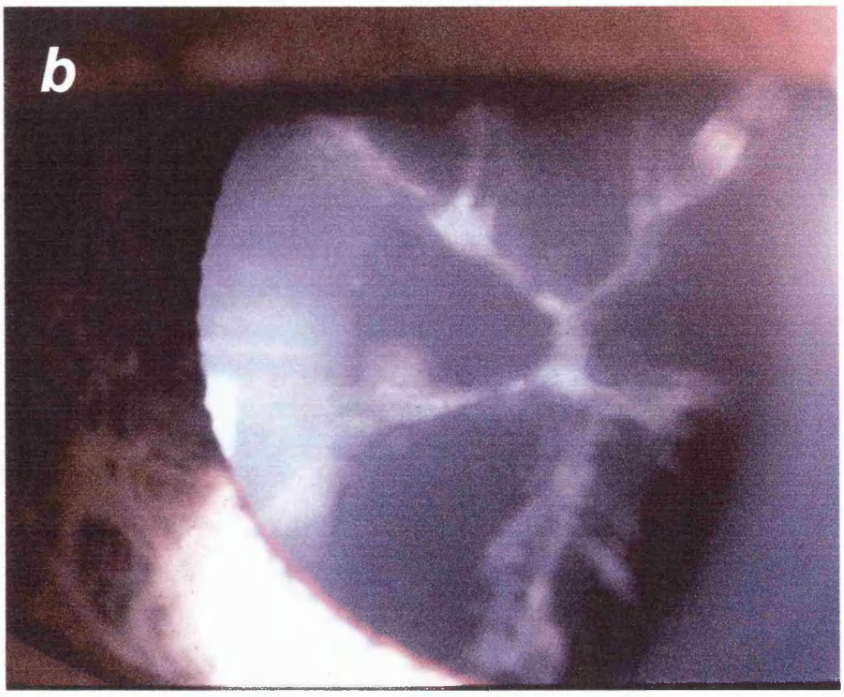

3.2.3 The search for the "Coppocks"

In 1906, Nettleship and Ogilvie published the first description of a family with isolated autosomal dominant congenital cataract. In this, the "Coppock" family, cataract was central with sutural and mid-peripheral opacities. The authors examined over three hundred individuals who all lived in Headington Quarry. Although we ascertained that members of the original pedigree had been followed for many years at the Oxford Eye Infirmary, the Coppock family had never been the subject of a linkage study.

A number of enquiries were made to trace the family. These included a search of the Oxford eye and genetic database (my thanks to Dr C Chapman and Professor A Bron for their help), a mailshot to all those surnamed Coppock who appeared in the Oxford telephone directories (my thanks to all those individuals who kindly replied). Finally a visit was made to the Masons Arms pub in Headington Quarry where it was possible to examine several of the direct descendants of the original family and also advertise for further information.

Dominantly inherited very peripheral punctate lens opacities were identified in three individuals in three generations of "Coppocks" directly descended from the family described by Nettleship and Ogilvie.

Despite these extensive enquiries no individual with the "Coppock" phenotype could be identified. Furthermore, it was concluded unlikely that any affected individual was still alive. The pedigree (family *S31*) examined is shown in figure 27.

Figure 27: Coppock pedigree.
+ symbols indicate those individuals examined
▬ denotes individual with punctate peripheral lens opacities

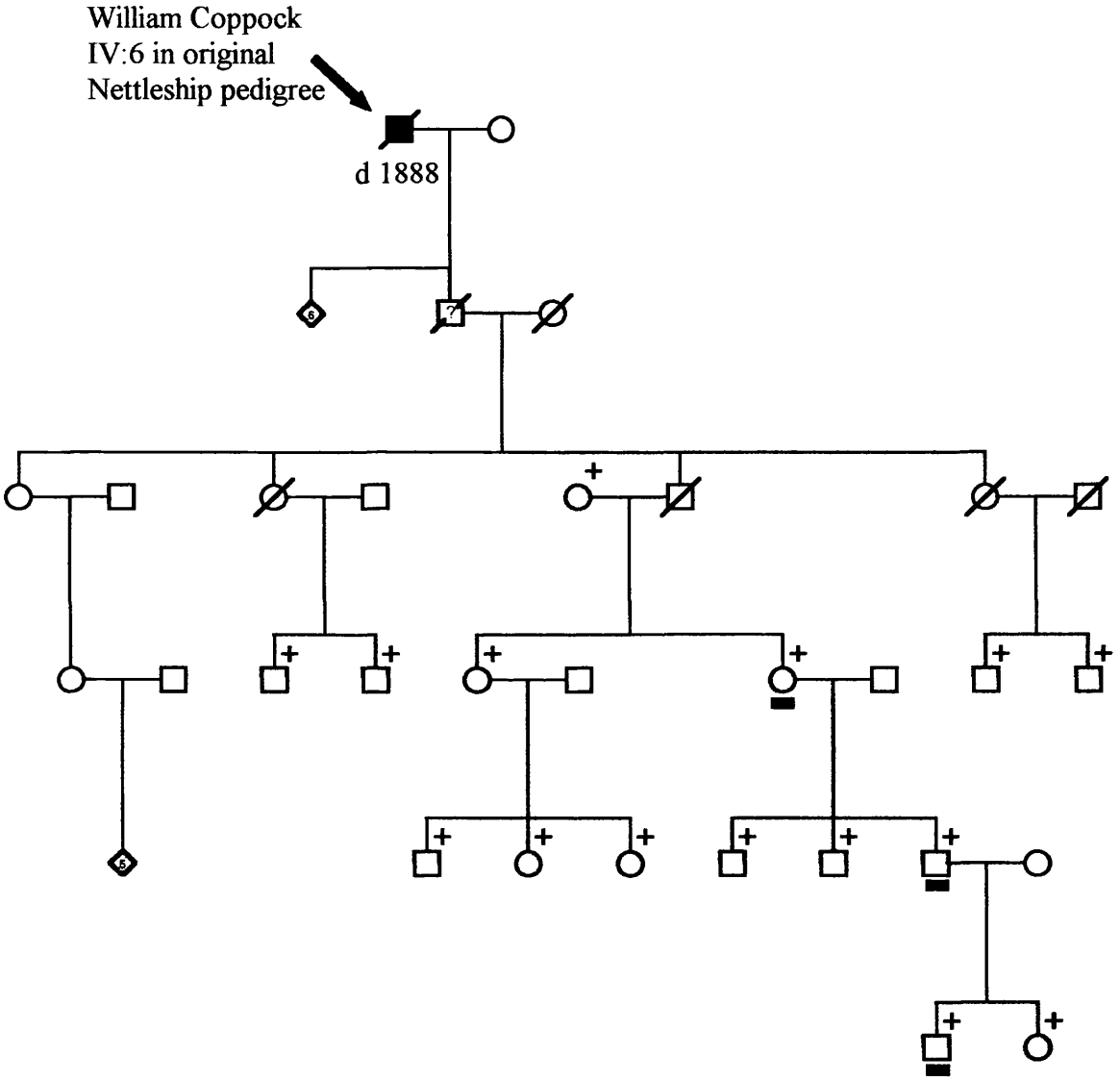

3.3 Visual outcome and complications

Two hundred and eighty seven patients with isolated human inherited cataract participated in the study. All had bilateral involvement except one patient who had a unilateral left cataract (family J, see results 3.6). One the basis of clinical and genetic information this individual was categorised as a phenocopy and was not included in the analysis.

For the purposes of gene mapping, all members of each family were screened. This revealed nine asymptomatic individuals with previously undiagnosed cataracts requiring no clinical intervention.

The 28 patients from small families that were ascertained for the purpose of generating a panel for mutation screening were excluded from analyses as were the six individuals from family N who had other severe ocular anomalies in addition to cataract.

Two hundred and fifty two individuals were therefore included, of which 211 (83.7%) had undergone cataract extraction, giving 387 eyes in total.

3.3.1 Age at diagnosis

An accurate age at diagnosis of cataract was available for 238 (94.4%) patients and of this group 201 (84.5%, 366 eyes) had undergone cataract surgery. The median age at which cataract was diagnosed was 4.2 years (range 0-51). The median age at diagnosis for those who underwent surgery was 4.0 years (range 0-72). Table 17 shows how age at surgery relates to final best corrected visual acuity.

Table 17: age at surgery and final visual acuity

Age (years) at time of surgery	Final best corrected visual acuity											
	6/5	6/6	6/9	6/12	6/18	6/24	6/36	6/60	CF	HM	PL	NP
<1	0	2	10	11	10	7	10	0	9	0	11	3
1-2	2	4	13	5	12	4	4	12	10	3	2	0
3-5	0	4	5	1	13	4	15	6	2	4	2	1
6-10	0	0	8	0	0	10	2	0	3	5	3	0
11-20	1	15	10	16	4	2	1	2	3	0	1	0
>20	4	10	10	14	29	12	3	2	1	0	0	0
All ages (%)	1.9	9.5	15.2	12.8	18.5	10.6	9.5	6.0	7.6	3.0	4.6	0.8

3.3.2 Visual outcome

A visual acuity was measurable in 216 patients (85.7%). Data were most frequently unavailable owing to the difficulty of obtaining accurate acuities in young children. A summary of the final bestcorrected visual acuity (VA) achieved is shown for each phenotype in table 18.

Table 18: final visual acuity by phenotype

Phenotype	% (all eyes) achieving final best corrected visual acuity		
	6/12 or better	6/18 – 6/60	CF or worse
Anterior polar	44.4	44.4	11.2
Posterior polar (stationary)	46.2	38.5	15.4
Posterior polar (progressive)	33.3	51.9	14.8
Lamellar	43.6	43.6	12.8
Nuclear	43.8	34.3	21.9
Coralliform (aceuliform)	83.3	16.7	0.0
Pulverulent	69.7	21.2	9.1
Blue-dot (cerulean)	66.7	11.1	22.2
Cortical	50.0	50.0	0.0
Polymorphic	58.3	25.0	16.7
Lattice	50.0	50.0	0.0
All phenotypes	50.1	35.9	14.0

Overall 50.1% (46.8% of those operated) achieved a VA of 20/40 or better, 35.9% (36.1% of those operated) a VA between 20/50 and 20/200 and 14.0% (17.1% of those operated) worse than 20/200. 14 patients (5.5%), all of whom had undergone bilateral cataract surgery, were blind as defined by WHO criteria (categories 3, 4, 5)[280], (table 19).

Table 19: patients blind by WHO criteria

Primary etiology	Number of patients
Glaucoma (bilateral)	4
Glaucoma and retinal detachment	2
Retinal detachment (bilateral)	2
Retinal detachment (unilateral) and deprivational amblyopia	1
Amblyopia or other	5
Total	14

3.3.3 Glaucoma

Eighteen patients (7.1%, 36 eyes) developed secondary glaucoma (open or closed angle). Fourteen of these had undergone multiple procedures following initial cataract extraction (table 20). Two patients with previously undiagnosed glaucoma were identified.

3.3.4 Retinal detachment

A history of retinal detachment was present in 8 patients (3.2%), with a mean age at surgery of 1.6 years and a mean time from surgery to detachment of 24.8 years (range 0-49). Details are provided in table 3.3.3a. None of those with un-operated cataracts developed glaucoma or retinal detachment.

Phenotype	Glaucoma			Retinal detachment		
	Number of affected individuals	Age at surgery of affected eye		Number of affected individuals	Age at surgery of affected eye	Interval from cataract surgery to RD
		Right	Left			
Anterior polar	2	6, 4	6, 3	1	5	40
Posterior polar (stationary)	4	1, 1, 3, 4	3, 1, 4, 3	4	3,1,1,5	10, 1, 13, 29
Posterior polar (progressive)	2	1, 1	3, 1	3	40, 40, 21	11,0,18
Lamellar	5	1, 1, 1, 13, 18	1, 5, 1, 2, 18	1	1	48
Nuclear	8	8, 1, 1, 1, 1, 1, 1, 1	8, 1, 1, 1, 1, 1, 1, 1	6	3, 1, 1, 2, 1, 1	10, 0, 49, 34, 20, 52
Coralliform (aceuliform)	2	7, 3)	7, 3	1	3	29
Pulverulent				1	7	15
Polymorphic	1	1	1			

Table 20: prevalence of glaucoma and retinal detachment by phenotype

3.4 Missense mutations in the human aquaporin AQP0 gene (*MIP*) underlie autosomal dominant "polymorphic" and lamellar cataracts on 12q

3.4.1 Linkage analysis

After excluding a number of candidate loci for cataract in family A (table 21), a positive two-point lod score was obtained using the tetranucleotide marker D12S1052 ($Z = 2.71$ at $\theta = 0$). The marker is located on chromosome 12q14 and lies genetically close and centromeric to the *MIP* gene encoding the major intrinsic protein of the lens (MIP). At 10.5cM telomeric to this marker, one definite recombination event is observed with marker D12S1064, indicating that the disease locus might lie either between these markers or centromeric to D12S1052. Lod scores for markers spanning this interval and located above marker D12S1052 are shown in table 22.

The significantly positive lod score at marker D12S1676 ($Z = 3.91$ at $\theta = 0$) and the single recombination event observed with marker D12S375 indicate that the disease locus for cataract in this family lies in the 15.5cM genetic interval encompassing MIP and bounded by markers D12S375 and D12S1064 (figure 28).

Table 21: cataract candidate gene exclusion data: two-point lod scores for linkage between the polymorphic cataract locus and candidate gene markers in family A

Marker	Candidate	LOD score (Z) at recombination (θ) of					
		0.0	0.05	0.1	0.2	0.3	0.4
D1S468	Volkmann, PPC locus	-∞	-1.49	-0.48	0.25	0.43	0.32
D1S2141	Pulverulent	-∞	-2.98	-1.78	-0.70	-0.21	-0.00
GATA124F08		-∞	-3.21	-1.94	-0.78	-0.26	-0.03
D2S427	γ-crystallin	-∞	-3.58	-2.16	-0.90	-0.33	-0.07
GATA178G09		-∞	-0.53	0.11	0.48	0.42	0.19
D3S1744	γS-crystallin	-∞	-4.30	-2.59	-1.05	-0.35	-0.04
D3S3053	Phakinin	-∞	-1.95	-1.23	-0.53	-0.20	-0.05
D3S2427		-∞	-1.53	-0.48	0.08	0.22	0.15
D4S2623	RIEG1	-∞	-0.72	-0.44	-0.19	-0.07	-0.02
D4S1644		-∞	-3.53	-2.30	-1.10	-0.50	-0.16
D10S1213	PITX3	-∞	-1.80	-1.00	-0.34	-0.07	0.02
D10S1248		-∞	-0.08	0.13	0.22	0.25	0.14
D11S1981	PAX6	-	-	-	-	-	-
ATA34E08		-∞	-2.16	-1.27	-0.47	-0.12	0.018
D11S1998	α2-crystallin	-∞	-3.91	-2.44	-1.08	-0.42	-0.10
D11S4464		-∞	-2.47	-1.36	-0.46	-0.14	-0.06

Table 22: two-point lod scores for linkage between the *CPL1* locus and chromosome 12q markers in family A. *Genetic distances shown are between adjacent markers.*

Marker	Genetic Distance (cM)	LOD score (Z) at recombination (θ) of					
		0.0	0.05	0.1	0.2	0.3	0.4
D12S375	5.0	-∞	-0.04	0.17	0.28	0.22	0.11
D12S1052	1.0	2.71	2.49	2.26	1.77	1.23	0.65
D12S1700	2.4	2.41	2.21	2.00	1.56	1.09	0.57
D12S1676	4.8	3.91	3.55	3.19	2.39	1.51	0.59
D12S92	0.0	2.77	2.56	2.34	1.86	1.33	0.72
D12S80	2.3	0.77	0.77	0.73	0.59	0.37	0.13
D12S1064		-∞	-1.31	-0.70	-0.19	0.00	0.05

Figure 28: abridged pedigree of family A showing segregation of 12q microsatellite markers, listed in descending order from the centromere. Bar beside alleles indicates disease haplotype.

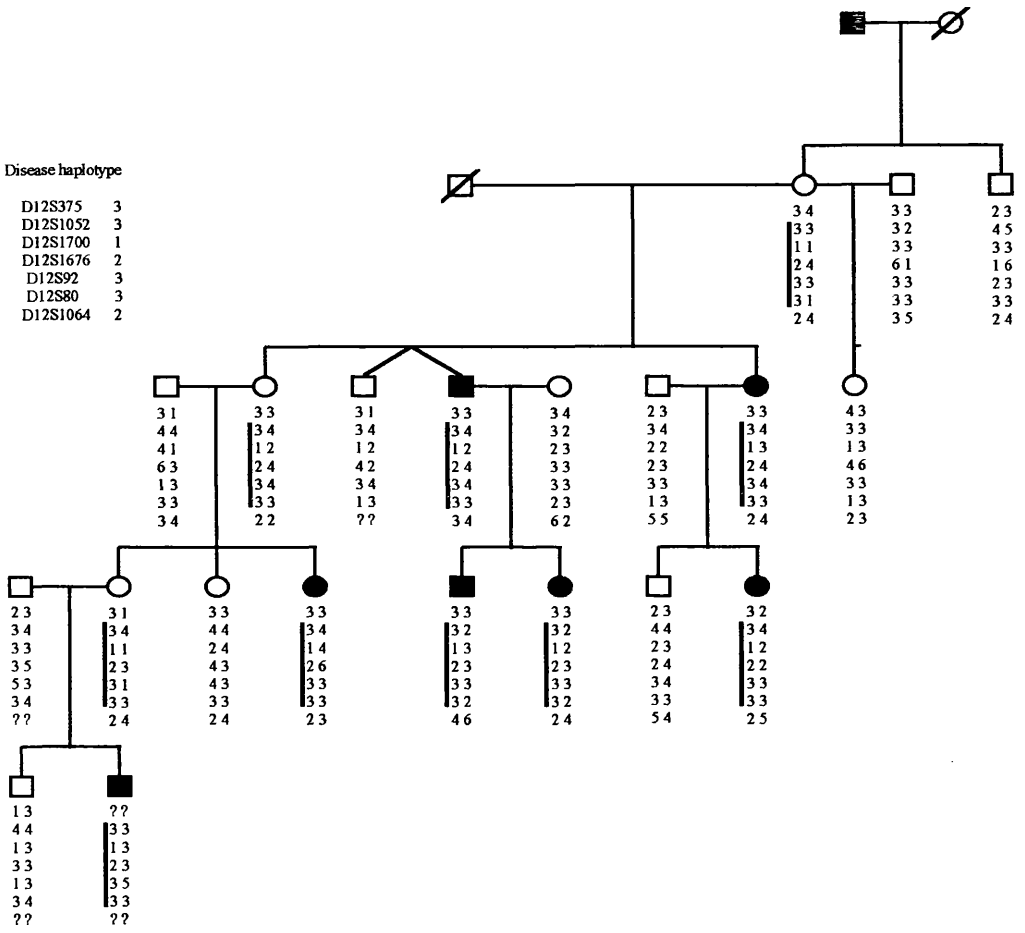

3.4.2 Sequence analysis and screening of congenital cataract panel

Sequence analysis of the *MIP* gene (PCR primers are shown in table 23) in family A revealed a missense mutation that segregated with the disease.

Table 23: PCR primers used for mutation screening of the *MIP* gene

Primer Pair	Forward primer 5' –3'	Reverse primer 5' – 3'	Anneal-ing temp (°C)
1	GTC CAC CCA GAC AAG GCC ATG	CAG CCA ACC ATT ACC GTG TTG AGT	58
2	CCT TTG CAC AGT TGC ACC CTG CG	TCC TTC CTG CTT ACC CCA AAG AG	58
3	TTA CAA CTG TGT CTT TTG CAG ATG	TGC AGT CCA CAA CCA TCC AGA AG	58
4	TAT TCC TTT TCT CTT TCT ACA GGT	AGG GAA GTT TGC ACC AAC CAG CTC	58

The C→G transition at position 3795 (exon 2) results in a threonine-to-arginine substitution at codon 138 (T138R, figure 29*b*). The mutation results in the introduction of an *AocI* restriction enzyme site (figure 31). Figure 29*c* shows a restriction fragment length analysis of *MIP* exon 2 of members of family A digested in the presence of the enzyme confirming co-segregation of disease and mutation. Only one band is seen in unaffected individuals as no digestion takes place. However, three bands arise in affected individuals. The upper band corresponds to the normal allele and has the same migration pattern as the band seen in unaffected individuals. The two other bands correspond to the two fragments generated by digestion of the mutant allele.

Screening of our panel of families with dominant congenital cataract identified one other unrelated family with a different co-segregating mutation in the *MIP* gene. In this family (J) all affected individuals were found to have an A→G transversion at position 3783 (exon 2) that results in the substitution of glutamic acid for glycine at codon 134, E134G (figure 30*b*). The mutation results in the

loss of a *BglII* restriction enzyme binding site (figure 31). Figure 30*c* shows a restriction fragment length analysis of *MIP* exon 2 of members of family J digested in the presence of the enzyme, confirming segregation disease with mutation. Two distinct bands are seen in unaffected members of the family corresponding to the fragments resulting from digestion of both alleles of exon 2. In contrast, the mutant exon of affected individuals is not digested and is seen as third band whose migration characteristics are slower than the other two bands.

To identify whether the mutation was a sequence variation present in the normal population a panel of one hundred normal controls from an ethnically similar backgound and without evidence of eye disease was constructed using spouses of individuals participating in this and other studies within the epartmnt. Examples of the restriction fragment length analyses for both enzymes are shown in figure 32. Neither mutation is a variant observed in our control population.

Haplotype analysis (figure 28 and 33) of both families indicated that the cataract locus (designated *congenital polymorphic / lamellar cataract locus 1, CPL1*) probably lies in the genetic interval D12S375-D12S1064 (15.5cM) (table 24*a*). The combined LOD score at marker D12S1676 was 6.02. A limited candidate gene screen had been performed previously on family J (table 24*b*). The cataract phenotype of family A has already been described (examples are shown in figure 25). Examples of the stationary lamellar cataract in family J are shown in figure 34.

Figure 29: antisense sequence analysis and restriction digest of *MIP* gene, family A (arrow highlights mutation):
a, unaffected individual from family A;
b, C→G transition resulting in threonine-to-arginine at codon 138 (T138R) in affected individual from family A;
c, restriction fragment-length analysis showing gain of an *AocI* site that co-segregates with affected individuals (blackened symbols) in family A.

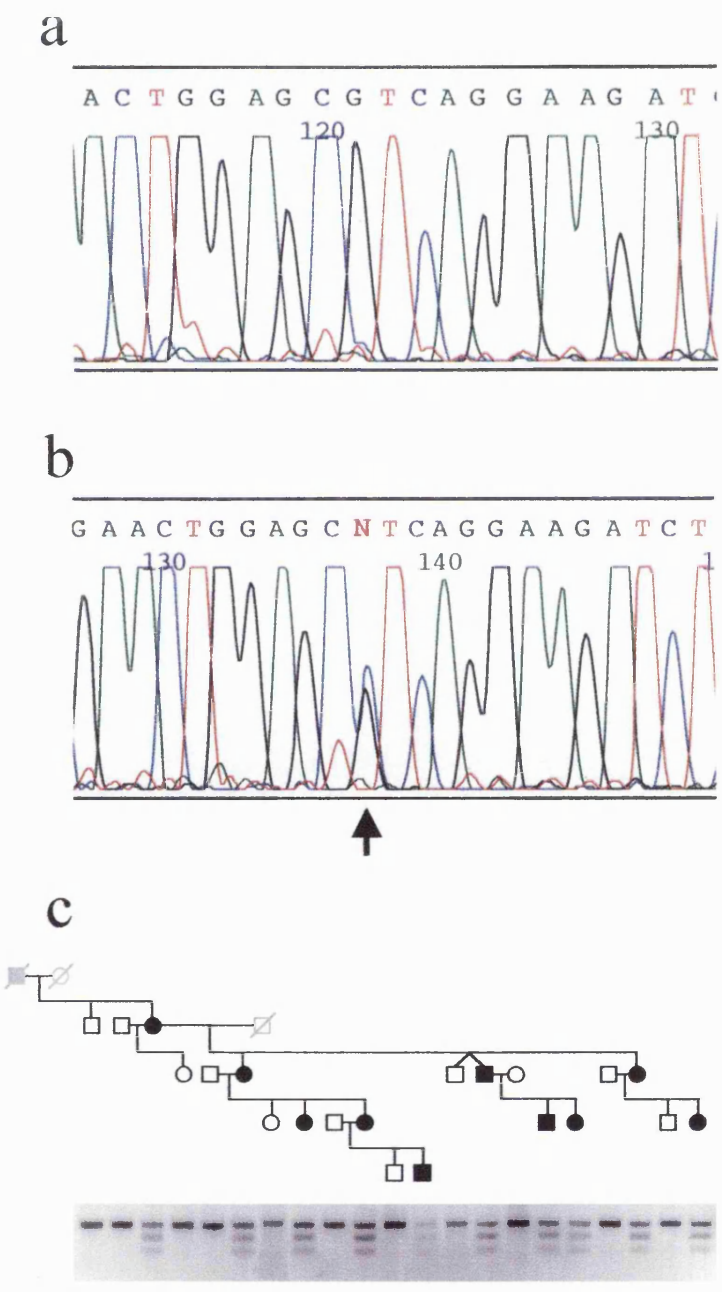

Figure 30: antisense sequence analysis and restriction digest of *MIP* gene, family J (arrow highlights mutation):
a, unaffected individual from family J;
b, A→G transversion resulting in a glutamic acid-to-glycine at codon 134 (E134G);
c, restriction fragment-length analysis showing loss of a *BglII* site that co-segregates with affected individuals in family J.

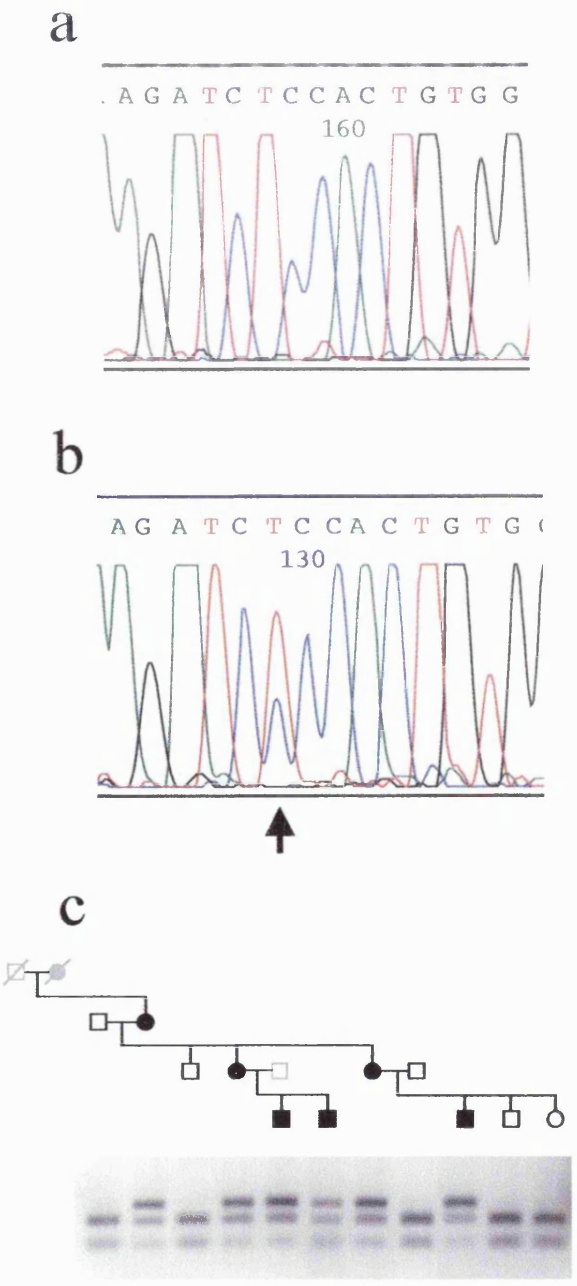

Figure 31: exon 2 *MIP* restriction maps

a, restriction map of segment of exon 2 *MIP* wild-type sequence

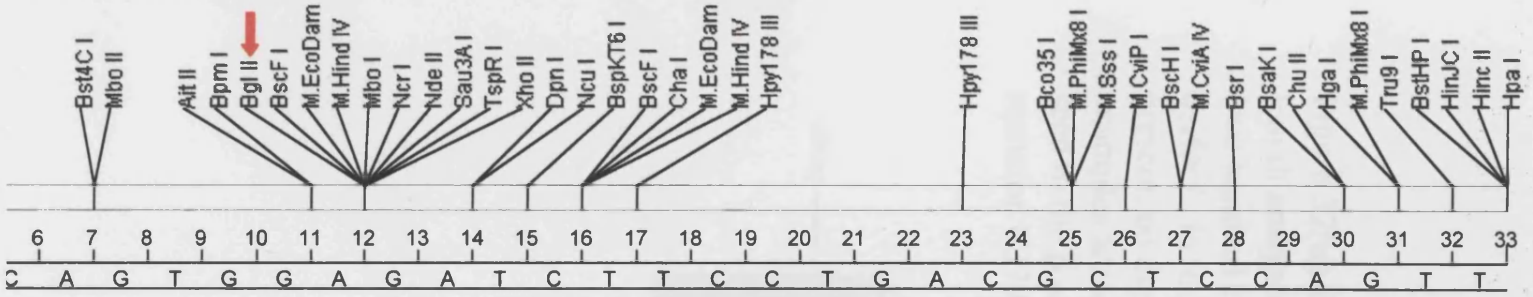

b, restriction map of segment of exon 2 *MIP* A3783G (E134G) mutant

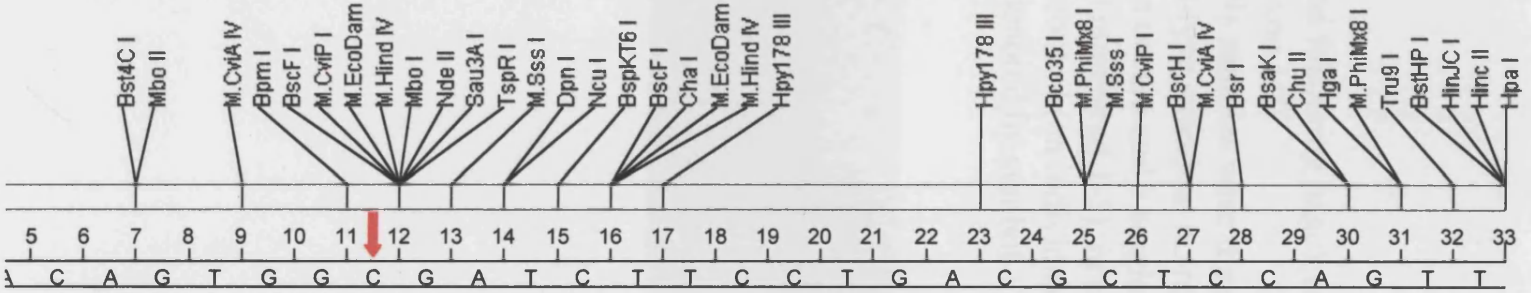

c, restriction map of segment of exon 2 *MIP* C3795G (T138R) mutant

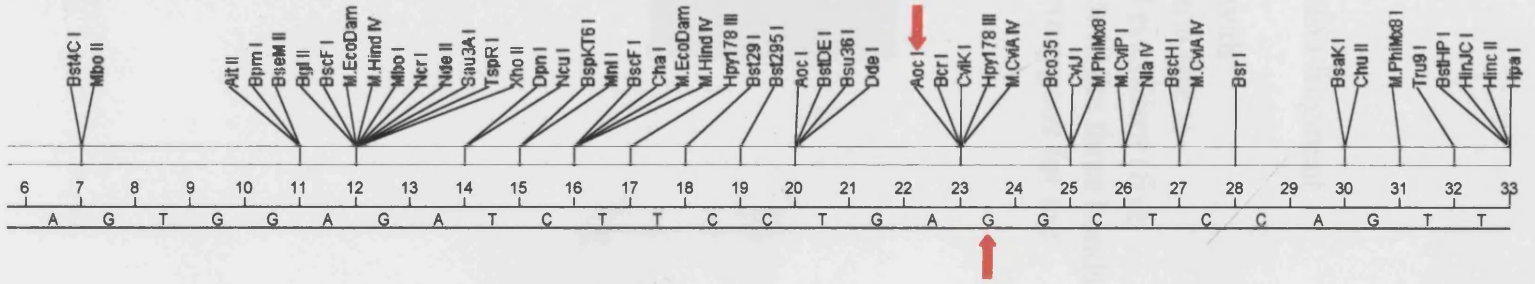

denotes relevant restriction enzyme sites and nucleotides

Figure 32(on this and following page): restriction fragment length analyses of exon *MIP*.
One hundred controls samples were digested with *a*, *Aocl*. In the wild-type situation, no restriction site is present, no digestion occurs and a single band is evident (five examples are shown numbered 1-5), in contrast to the three bands seen in the positive control (an individual heterozygous for the mutation C3795G, denoted by symbol +)

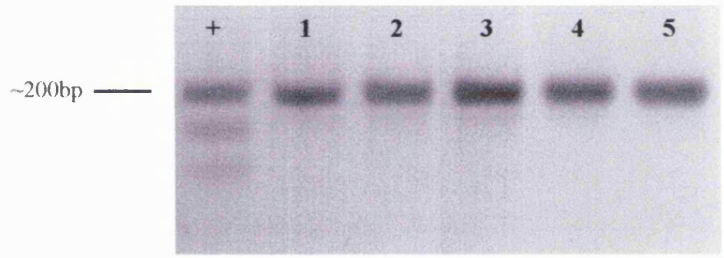

b, *BglII*. In the wild-type situation, a single restriction site is present and two bands are evident (four examples are shown, numbered 1-4), in contrast to the three bands in the positive control individual (an individual heterozygous for the mutation A3783G, denoted by symbol +).

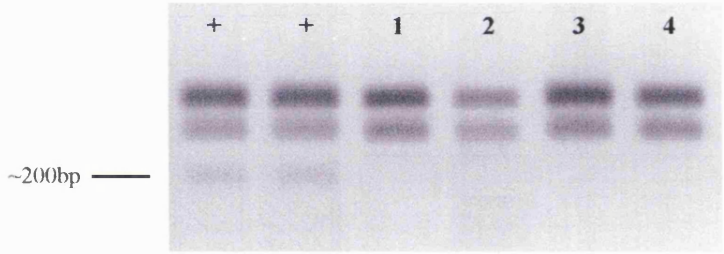

Table 24: two-point lod scores for linkage between *a*; the *CPL1* locus and chromosome 12q markers in family J, *b*; the *CPL1* locus and cataract candidate genes. *Genetic distances shown are between adjacent markers.*

a

Marker	Genetic Distance (cM)	LOD score (Z) at recombination (θ) of					
		0.0	0.05	0.1	0.2	0.3	0.4
D12S375	5.0	-∞	-3.24	-2.39	-1.33	-0.66	-0.19
D12S1052	1.0	0.90	0.84	0.77	0.61	0.44	0.24
D12S1700	2.4	0.00	0.00	0.00	0.00	0.00	0.00
D12S1676	4.8	2.11	1.93	1.74	1.34	0.90	0.45
D12S92	0.0	0.60	0.54	0.47	0.32	0.17	0.10
D12S80	2.3	0.90	0.84	0.77	0.61	0.44	0.24
D12S1064		-∞	0.65	0.79	0.74	0.53	0.27

b

Marker	Candidate	LOD score (Z) at recombination (θ) of					
		0.0	0.05	0.1	0.2	0.3	0.4
D1S468	Volkmann, PPC locus	-∞	-2.44	-1.59	-1.11	-0.37	-0.13
D1S2141	Pulverulent	-∞	-0.98	-0.51	-0.17	-0.07	-0.05
GATA124F08		-∞	-1.91	-1.12	-0.47	-0.20	-0.08
D2S427	γ-crystallin	-∞	-1.23	-0.69	-0.23	-0.04	0.02
GATA178G09		-∞	-0.52	-0.28	-0.09	-0.03	-0.01
D3S1744	γS-crystallin	-∞	-1.19	-0.68	-0.27	-0.13	-0.07

Figure 33: abridged pedigree of family J showing segregation of 12q microsatellite markers, listed in descending order from the centromere. Bar beside alleles indicates haplotype.

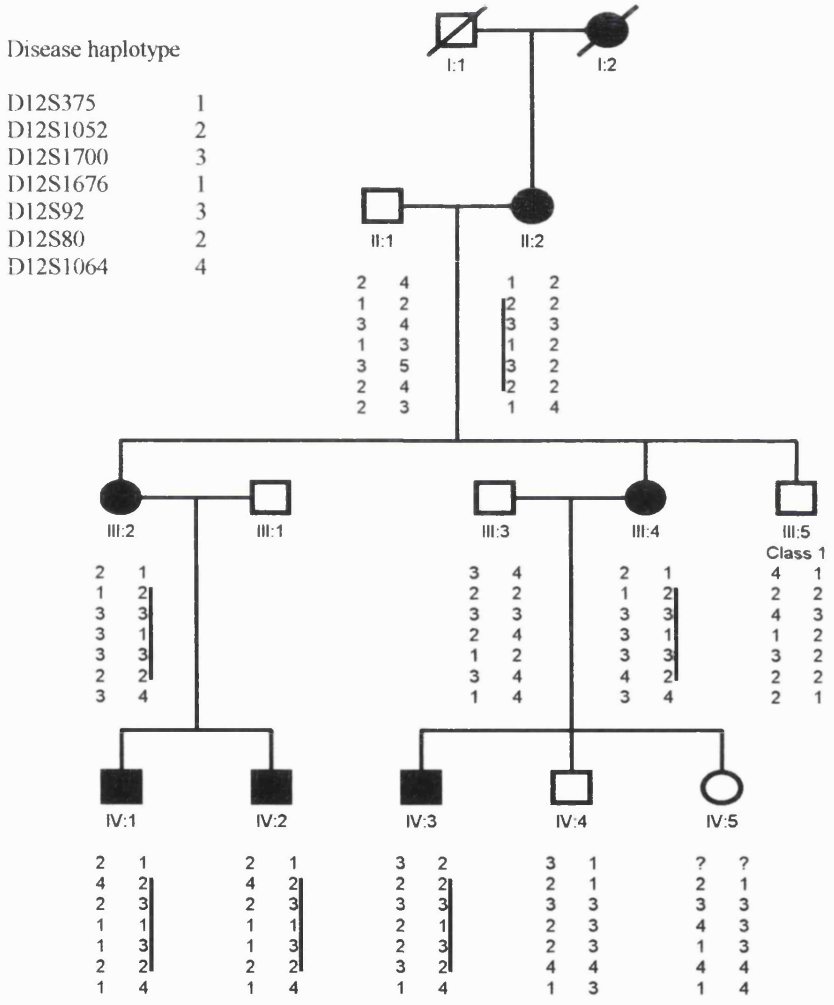

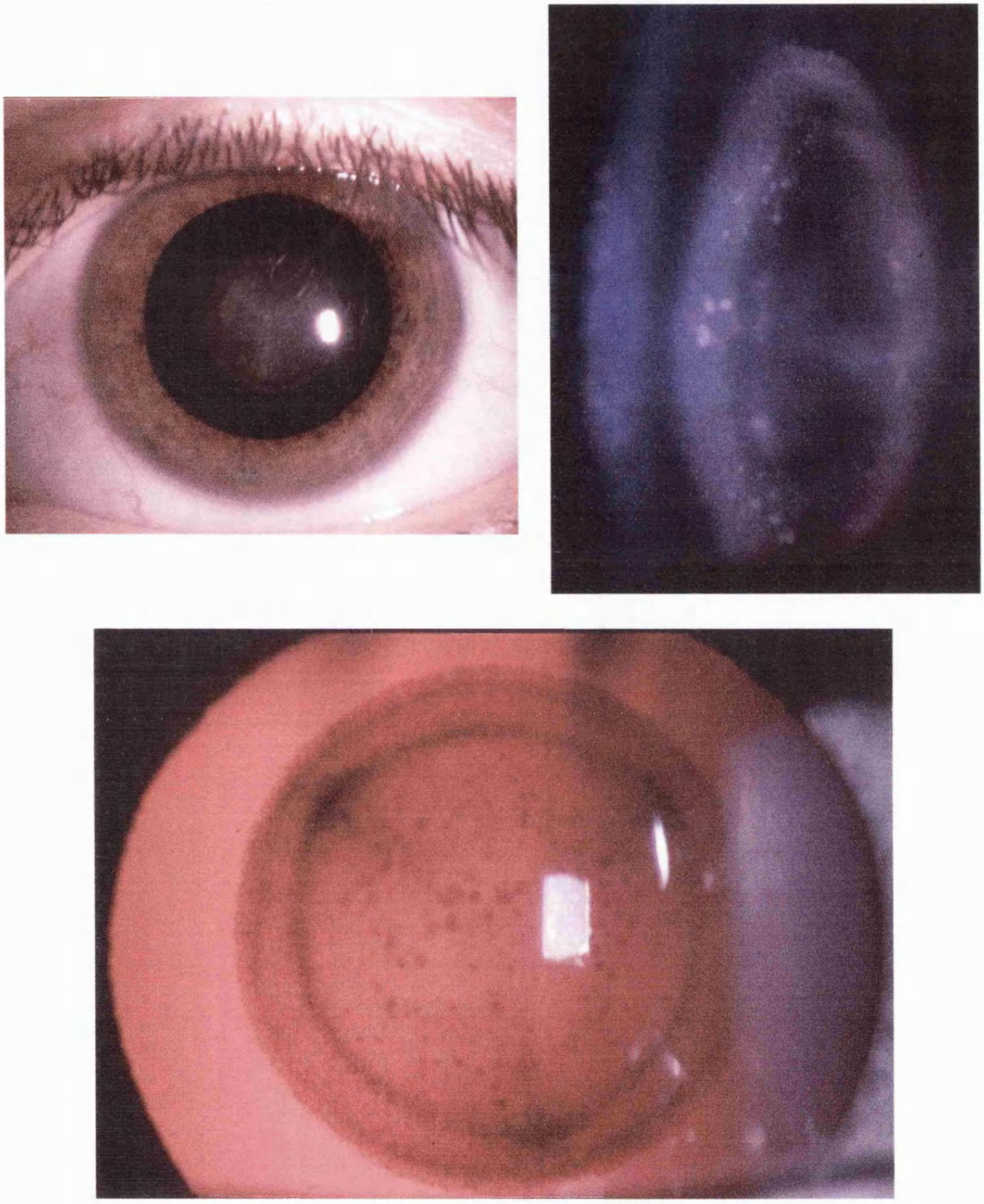

Figure 34: lamellar cataract phenotype (family J), *a*, diffuse illumination (30 year old female); *b*, oblique section through lens (9 year old male); *c*, retroillumination (same child) showing opacified lamellae and fine sutural cataracts

3.4.3 Conservation of the mutated residues amongst other human aquaporins and between MIP orthologs

The human aquaporin gene superfamily encodes ten sequence-related members (AQP -0 to -9). Figure 35 shows that Glu 134 (E) is conserved in all aquaporins except the aquaglyceroporins AQP -3, -7, -9 and that Tyr 138 (T) is conserved in all members.

Phylogenetically, both residues are highly conserved in mammals, reptiles and bacteria, suggesting their roles are critical for aquaporin function (figure 36).

3.4.4 Predictive modelling of the mutant proteins

Both missense mutations result in the substitution of amino acids in the fourth transmembrane region of the protein (figure 37) that differ in both size and charge. Substitution of negatively charged residue glutamate (E142, MIP E134) with glycine, a smaller and uncharged residue, eliminates a fixed charge lining the aqueous pathway (figure 38). Replacement of the polar residue threonine (T146, MIP T138) with the large residue arginine, introduces a strong positive charge in the channel (figure 38).

In the light of its sequence similarity to aquaporin-1, the structure of which is known from crystallographic studies, wild-type MIP is expected to have six transmembrane α-helices linked by five connecting loops (A to E). Predictions of secondary structure and hydophobicity of MIP indicate this to be the case (figure 38). Both mutations occur within the putative fourth transmembrane domain (TH4). However, they are not predicted to alter significantly the hydrophobicity of this domain or the secondary or tertiary structure of the protein (figure 38).

Figure 35: Alignment of MIP (AQP0) with other human aquaporins shows that the residues E134 (boxed) and T138 (boxed) are highly conserved. The table is organised so that the aquaglyceroproteins AQP -3, -7 and -9, which have been shown experimentally to be permeable to molecules in addition to water, appear below the hashed line.

		134	138
MIP (AQP0)	119 N T L H P A V S V G Q - A T T V	E	I F - - - - L	T	L Q F V L C I F A T Y D E R R
AQP1	127 N D L A D G V N S G Q - G L G I	E	I I - - - - G	T	L Q L V L C V L A T T D R R R
AQP2	119 N A L S N S T T A G Q - A V T V	E	L F - - - - L	T	L Q L V L C I F A S T D E R R
AQP4	148 T M V H G N L T A G H - G L L V	E	L I - - - - I	T	F Q L V F T I F A S C D S K R
AQP5	120 N A L N N N T T Q G Q - A M V V	E	L I - - - - L	T	F Q L A L C I F A S T D S R R
AQP6	133 N V V R N S V S T G Q - A V A V	E	L L - - - - L	T	L Q L V L C V F A S T D S R Q
AQP8	146 V T V Q E Q G Q V A G - A L V A	E	I I - - - - L	T	T L L A L A V C M G A I N E K
AQP3	144 A G I F A T Y P S G H L D M I N G F F D Q F I G	T	A S L I V C V L A I V D P Y N
AQP7	155 A G I F A T Y L P D H M T L W R G F L N E A W L	T	G M L Q L C L F A I T D Q E N
AQP9	145 A H I F A T Y P A P Y L S L A N A F A D Q V V A	T	M I L L I I V F A I F D S R N
Consensus	. . . . . G Q -	E	. . - - - - -	T	. Q L . L C . F A . . D . R .

Figure 36: Sequence homology comparisons between mammalian and reptilian MIP sequences Indicate that residues 134 and 138 are highly conserved (boxed)

	119														134				138																	
mouse	N	T	L	H	T	G	V	S	V	G	Q	A	T	T	V	E	I	F	L	T	L	Q	F	V	L	C	I	F	A	T	Y	D	E	R	R	N	G	R	M	G
	117																																			
rat	N	T	L	H	T	G	V	S	V	G	Q	A	T	T	V	E	I	F	L	T	L	Q	F	V	L	C	I	F	A	T	Y	D	E	R	R	N	G	R	M	G
	119																																			
human	N	T	L	H	T	G	V	S	V	G	Q	A	T	T	V	E	I	F	L	T	L	Q	F	V	L	C	I	F	A	T	Y	D	E	R	R	N	G	R	M	G
	119																																			
bovine	N	T	L	H	T	G	V	S	V	G	Q	A	T	T	V	E	I	F	L	T	L	Q	F	V	L	C	I	F	A	T	Y	D	E	R	R	N	G	R	M	G
	119																																			
frog	N	T	L	H	T	G	V	S	V	G	Q	A	T	T	V	E	I	F	L	T	L	Q	F	V	L	C	I	F	A	T	Y	D	E	R	R	N	G	R	M	G
Consensus	N	T	L	H	T	G	V	S	V	G	Q	A	T	T	V	E	I	F	L	T	L	Q	F	V	L	C	I	F	A	T	Y	D	E	R	R	N	G	R	M	G

Figure 37: MIP secondary structure predictions suggest the protein has six transmembrane domains (TM 1-6). The mutated residues reside in he two families reside in TM 4).

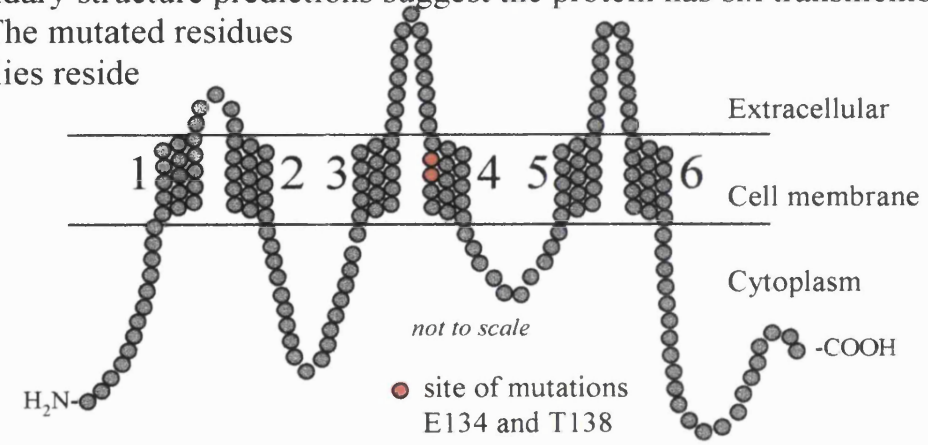

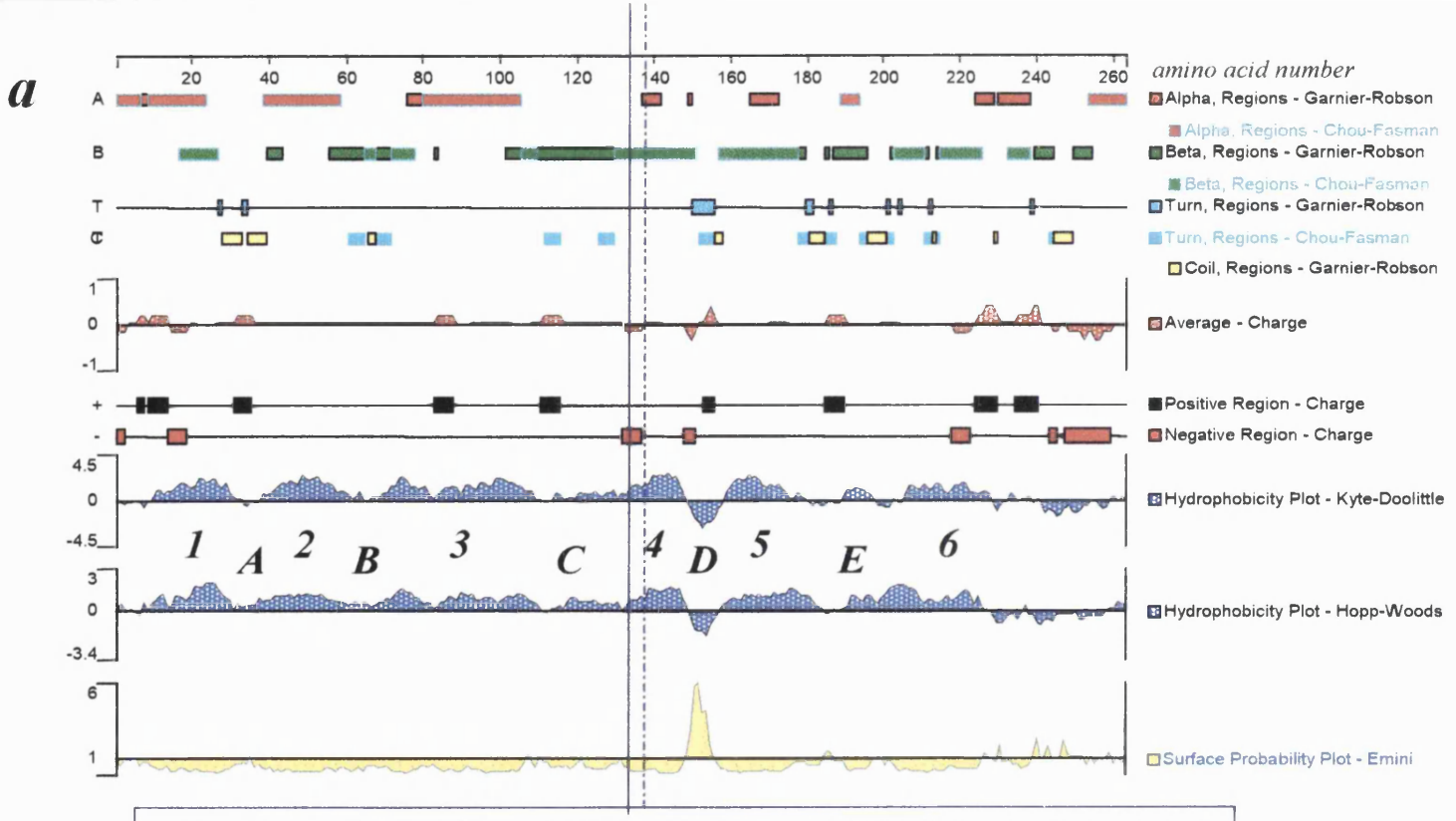

Figure 38: protein modelling of wild-type and mutant MIP/AQP0 using Protean 4.03 protein prediction software (DNAStar Inc)

a, wild-type
b, E134G mutant
c, T138R mutant

position of each mutation is shown: E134 ——————
T138 -·-·-·-·-·-·-

transmembrane regions 1-6 and connecting loops A-E are labelled

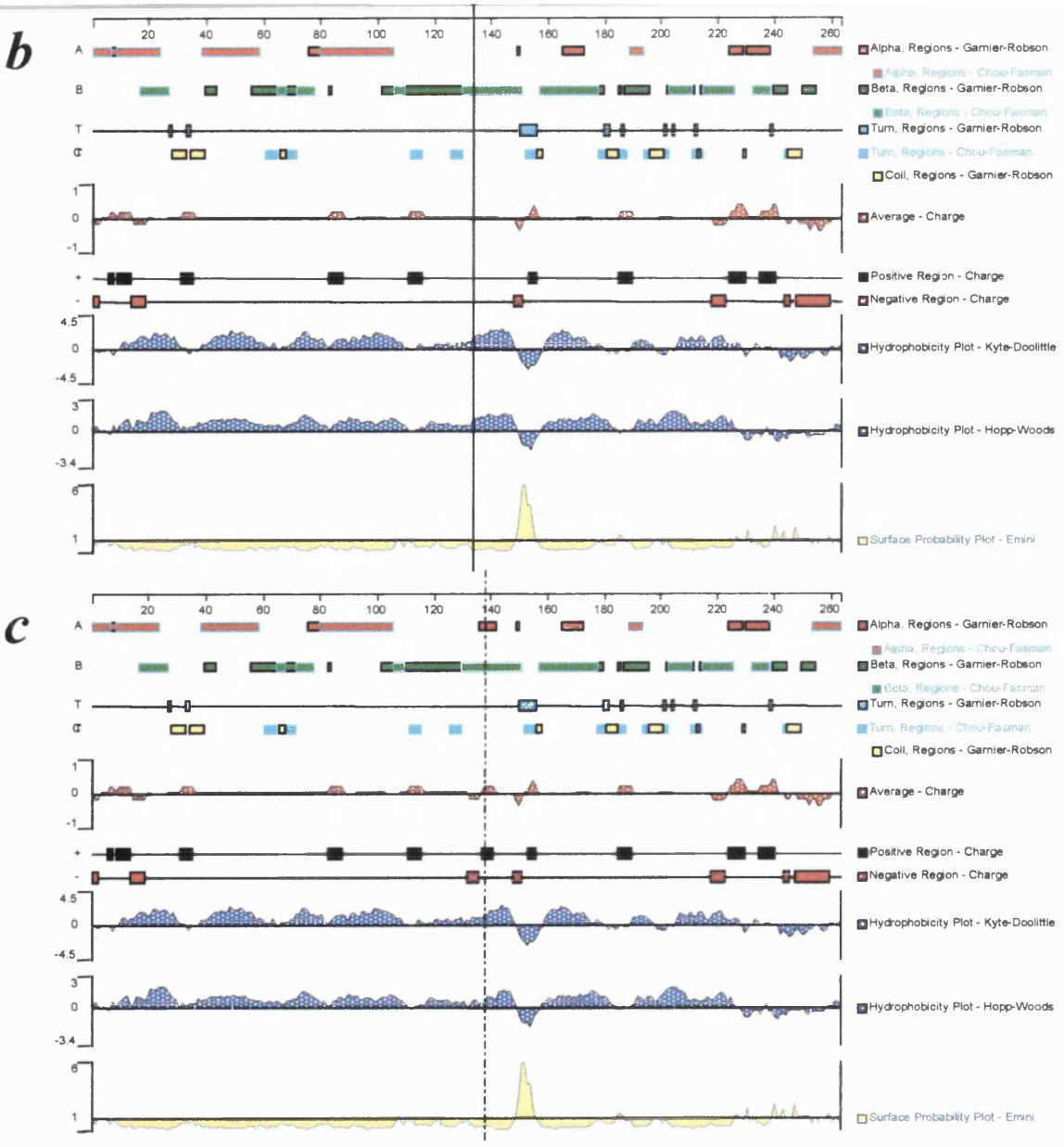
b
20 40 60 80 100 120 140 160 180 200 220 240 260
A
B
T
C
Alpha, Regions - Garnier-Robson
Alpha, Regions - Chou-Fasman
Beta, Regions - Garnier-Robson
Beta, Regions - Chou-Fasman
Turn, Regions - Garnier-Robson
Turn, Regions - Chou-Fasman
Coil, Regions - Garnier-Robson
1
0
-1
Average - Charge
+
-
Positive Region - Charge
Negative Region - Charge
4.5
0
-4.5
Hydrophobicity Plot - Kyte-Doolittle
3
0
-3.4
Hydrophobicity Plot - Hopp-Woods
6
1
Surface Probability Plot - Emini
c
20 40 60 80 100 120 140 160 180 200 220 240 260
A
B
T
C
Alpha, Regions - Garnier-Robson
Alpha, Regions - Chou-Fasman
Beta, Regions - Garnier-Robson
Beta, Regions - Chou-Fasman
Turn, Regions - Garnier-Robson
Turn, Regions - Chou-Fasman
Coil, Regions - Garnier-Robson
1
0
-1
Average - Charge
+
-
Positive Region - Charge
Negative Region - Charge
4.5
0
-4.5
Hydrophobicity Plot - Kyte-Doolittle
3
0
-3.4
Hydrophobicity Plot - Hopp-Woods
6
1
Surface Probability Plot - Emini

3.5 Functional analysis of mutations detected in the *MIP/ AQP0* gene

The *Xenopus laevis oocyte* swelling assay was employed to assess possible functional consequences of the E134G and T138R substitutions. The cDNA encoding the human MIP/AQP0 protein from a human lens library was cloned into the *Xenopus laevis* expression vector. Coefficients of osmotic water permeability (P_f) were calculated from measurements of oocyte swelling after transfer from 200 mosM to 70 mosM modified Barth's solution.

3.5.1 Preliminary experiments

AQP1 and most other mammalian aquaporins are known to exhibit a 10-20 fold increase in water permeability using this system[281]. However non-human AQP0 orthologs have previously been noted by multiple laboratories to exhibit much smaller increases in P_f[64 282 283].

In each of six experiments, (using 15 – 20 oocytes in each experimental group) oocytes injected with 5ng of human AQP0 cRNA exhibited approximately a three-fold increase in osmotic water permeability (injected P_f : control P_f ratio = 31:12). Oocytes injected with 5ng bovine AQP0 cRNA exhibited an approximately four-fold increase (injected P_f : control P_f ratio = 42:12), in water permeability (figure 39). Water and uninjected oocytes showed no increase in water permeability above basal levels.

3.5.2 Water permeabilities of oocytes expressing mutant MIP

Oocytes injected with 5ng of E134G or T138R mutant cRNA had water permeabilities similar to control oocytes. Oocytes co-injected with 5ng of wild-type AQP0 cRNA plus 5ng of E134G or T138R mutant cRNA showed intermediate water permeabilities (injected P_f : control P_f ratio = 13 :10 and 12:10 respectively).

Figure 39: osmotic water permeability of *Xenopus laevis* oocytes injected with cRNAs and incubated for three days; *a*, control oocytes were uninjected or water injected, hMIP/APQ0 (human MIP), bMIP (bovine MIP), E134G, and T138R oocytes were injected with 5ng of the indicated cRNAs. AQP0 + E134G, and AQP0 + T138R denote oocytes injected with 5ng of wild-type AQP0 cRNA and 5ng of mutant cRNA; *b*, effect of acidification of the pH on P_f.
The coefficients of osmotic water permeability were determined by the swelling assay of 15-20 oocytes after transfer from 200mosM to 70mosM modified Barth's solution. Statistical significance when compared to wild-type AQP0: (*) $p<0.01$; (**) $p<0.001$.

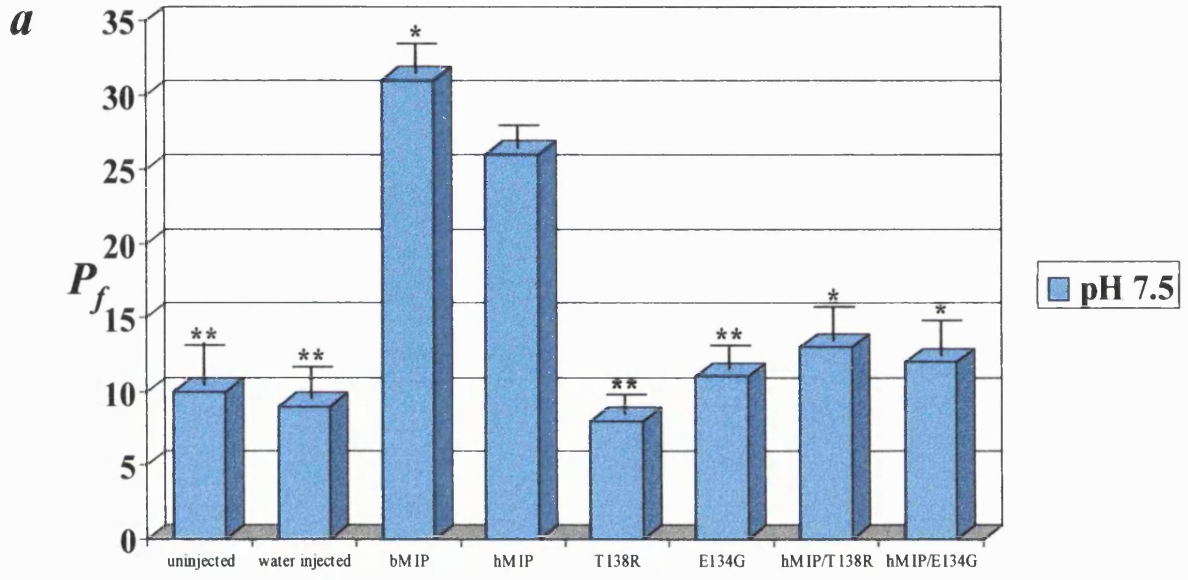

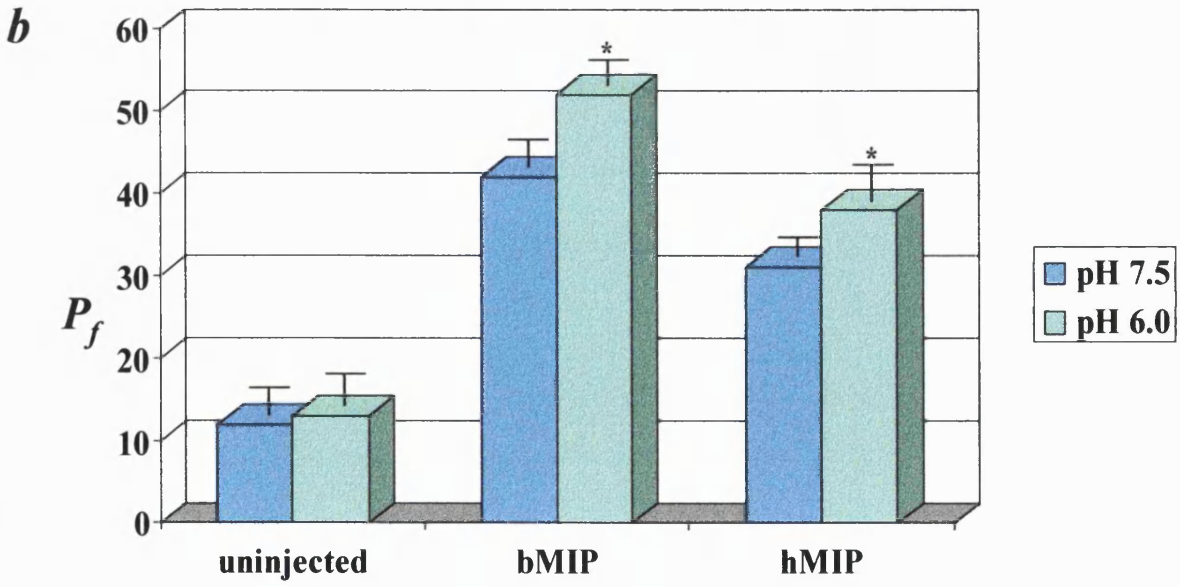

3.5.3 No change in water permeability is observed by varying injected cRNA in the range 2.5ng – 20ng

A series of experiments were performed in which the amount of cRNA injected (bMIP, hMIP, mutant MIPs) was varied (2.5ng, 5ng, 10ng, 15ng and 20ng). Within this range, for each cRNA type, no gradient in induced water permeability was observed (data not shown).

3.5.4 Acidification of the environment facilitates wild-type aquaporin-0 induced water permeability

Reducing the pH of the MBS test media to 6.0 from 7.5 increased the observed *Pf* induced by both bovine and human AQP0. T138R and E134G water permeabilities were unchanged (figure 39).

3.5.5 Western blotting of oocyte whole membrane fractions

Oocyte membranes were analysed on immunoblots incubated with rabbit antiserum specific for the C-terminus of AQP0 (figure 40). Membranes from control oocytes exhibited no immunoreactivity on immunoblots. After three days incubation, immunoblots of membranes from oocytes injected with wild-type AQP0 cRNA exhibited a strong band at 28kDa. In contrast, immunoblots of membranes from oocytes injected similarly with E134G or T138R mutant cRNA exhibited 28kDa with reduced intensity; in all experiments, the band from T138R oocytes was less intense than from E134G oocytes.

In each of four experiments, immunoblots of oocytes co-injected with wild-type AQP0 cRNA plus the E134G mutant cRNA exhibited a 28kDa band of equal or greater intensity than oocytes injected with only wild-type AQP0 cRNA. In contrast, immunoblots of oocytes co-injected with wild-type AQP0 cRNA plus the T138R mutant cRNA always had a 28kDa band of lower intensity (figure 40).

Figure 40: SDS-PAGE immunoblot of membranes prepared after the swelling assay and incubated with anti-serum specific for the C-terminus of AQP0.
Specific bands at 28kDa are shown. Sample loading was equalised based on Coomassie blue staining. Immunoblot band intensities were compared by Densitometry and normalising to wild-type AQP0 (1.0), E134G (0.6), T138R (0.5), AQP0 + E134G (1.1), and AQP0 + T138R (0.5).

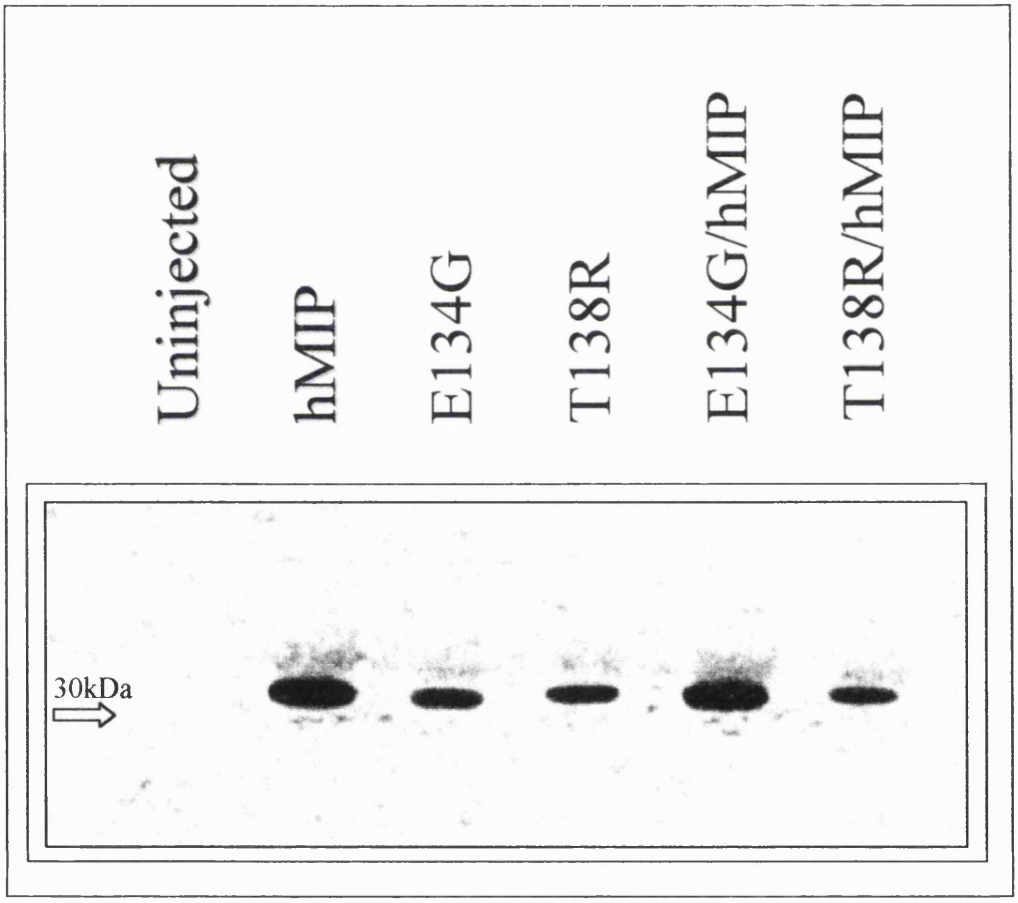

3.5.6 Immunohistochemical analyses

The likelihood that the mutant proteins fail to traffic to the oocyte plasma membrane was studied by confocal immunofluorescence microscopy (figure 41). Control oocytes exhibited negligible immunofluorescence, whereas oocytes injected with wild-type AQP0 cRNA had a sharp rim of immunofluorescence at the plasma membrane with negligible signal over the cytoplasmic space. Oocytes injected with E134G or T138R cRNA showed immunofluorescence over the cytoplasmic space but no signal at the plasma membrane. Oocytes injected with wild-type AQP0 cRNA plus E134G or T138R mutant cRNA exhibited immunofluorescence at the plasma membrane as well as over the cytoplasmic space.

3.5.7 Histology of the T138R lens

The architecture of cortical lens fibres of a patient with the T138R mutation (individual III:2) appeared normal (figure 42) when compared to a normal lens (data not shown). Importantly, there was no change in cell size or morphology and the extracellular space was not increased. The only possible abnormal finding was an increased number of "balloon" cells, suggestive of increased cellular destruction.

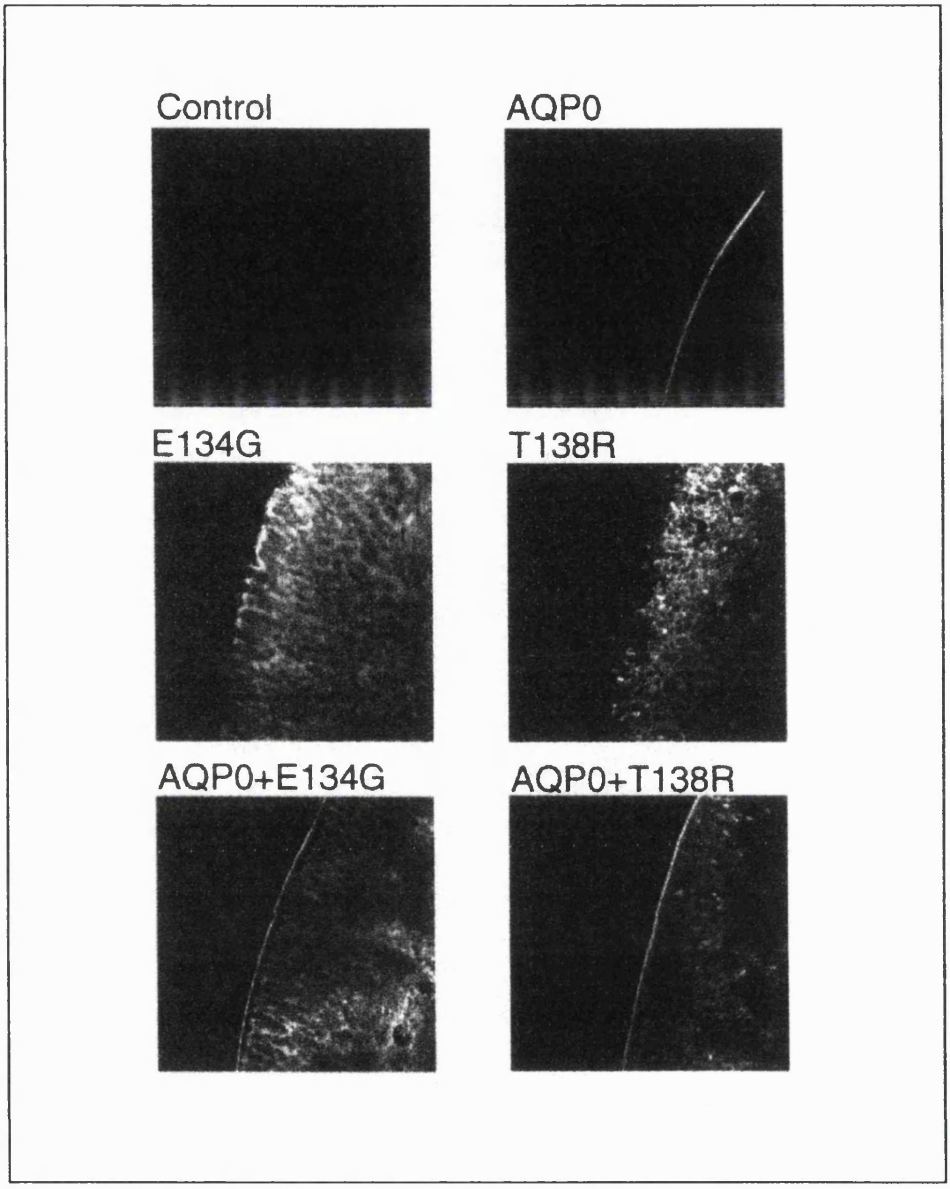

Figure 41: anti-AQP0 confocal immunofluorescence of *Xenopus laevis* oocytes injected with cRNAs and incubated for three days before fixation And incubation with antibody.
Control oocytes were injected with 50nl of water without cRNA. AQP0, E134G and T138R oocytes were injected with 5ng of the indicated cRNAs. AQP0 + E134G, AQP0 + T138R oocytes were injected with 5ng of wild-type AQP0 cRNA and 5ng of mutant cRNA. Control oocytes exhibited no immunoreactivity, whereas oocytes injected with wild-type AQP0 cRNA exhibited a sharp rim of immuno-fluorescence at the plasma membrane. Oocytes injected with E134G or T138R cRNA only exhibited immunofluorescence over the cytoplasmic space. Oocytes injected with wild-type AQP0 cRNA plus E134G or T138R mutant cRNA exhibited immunofluorescence at both the plasma membrane and throughout the cytoplasmic space.

Figure 42: histology of the MIP-T138R lens showing well preserved lens fibres of normal architecture (spaces between fibres are artefactual); *a*, longitudinal/oblique section (100x magnification), individual III:2; *b*, same lens, longitudinal section (200x magnification)

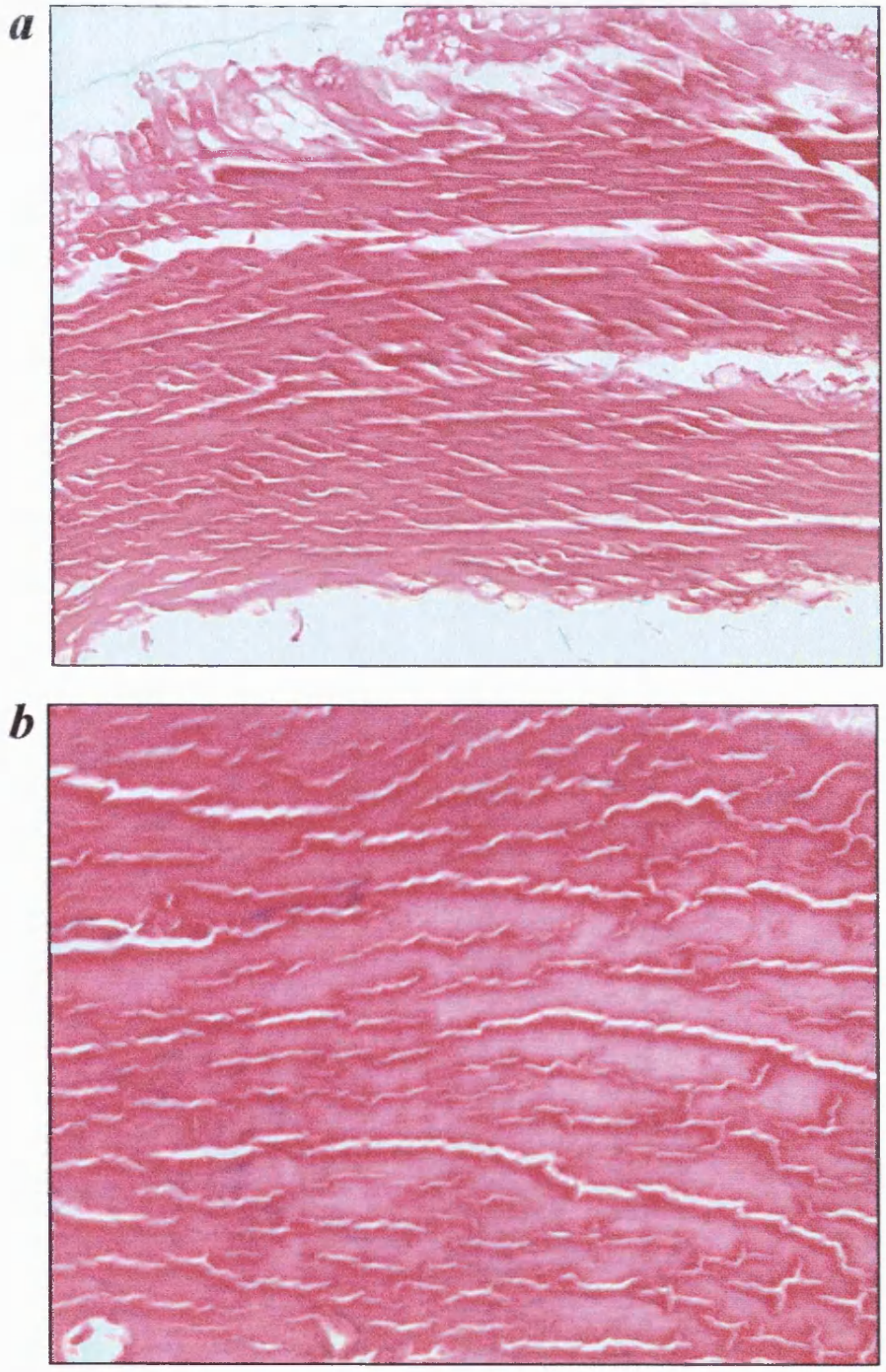

3.6 Mapping of a family with X-linked cataracts

3.6.1 Clinical evaluation

Using the Birmingham Women's Hospital Clinical Genetics Service database, details of a large four-generation family with apparently isolated autosomal dominant congenital cataract were obtained (family J). On clinical evaluation however, it became apparent that all affected males had required cataract extraction in the first few months of life with a uniformly poor outcome (table 25). This finding contrasted markedly with affected females who had very mild central nuclear opacities requiring no treatment until typically the sixth decade. Such observations raised the possibility that inheritance was indeed X-linked with full penetrance in heterozygotes. Unfortunately, none of the affected males had children and thus there had been no opportunity for male-to-male transmission.

3.6.2 The phenotype

In support of X-linked inheritance, the phenotype was distinct from any seen previously. The only phakic members of the family were female and in each, cataracts were very slowly progressive, fan-shaped and nuclear in distribution (figure 43, unfortunately, at the time of writing no individuals were available for photography). Interestingly, four of the six affected males had a ventriculo-septal defect (VSD) and other cardiac developmental anomalies. No other family members gave a history of cardiac anomalies.

The complete pedigree is shown below (figure 44, including those individuals who did not wish to participate in the analysis). Individual V:5 was designated a phenocopy since both her mother and grandmother were clinically unaffected and she had a different cataract phenotype.

Table 25: age and best-corrected visual acuity for affected individuals in family J

Pedigree number	Age in years	Right			Left		
		BCVA	Lens status	Age operated	BCVA	Lens status	Age operated
II:2	72	6/6	Pseudo-phakic	68	6/6	Pseudo-phakic	68
III:4	48	6/6	NLO		6/6	NLO	
III:6	46	6/9	NLO		6/6	NLO	
III:8	40	6/6	NLO		6/6	NLO	
III:13	75	6/9	No cataract		6/9	No cataract	
III:15	65	-	NLO		-	NLO	
III:17	60	6/12	NLO		6/12	NLO	
IV:1	23	NPL	aphakic	3 months	CF	Aphakic	3 months
IV:3	28	6/6	NLO		6/6	NLO	
IV:4	21	HM	aphakic	6 weeks			
IV:5	17	CF	aphakic	2 months	6/12	Aphakic	2 months
IV:6	20	6/36	Pseudo-phakic	1 year	6/24	Pseudo-phakic	1 year
IV:7							
IV:12	39	6/6	No cataract		6/5	No cataract	
IV:14	38	6/6	NLO		6/6	NLO	
IV:18	36	6/5	NLO		6/5	NLO	
V:1	8	6/12	aphakic	At birth	6/60	At birth	At birth
V:5	14	6/9	Fan shaped opacity		6/18	Pseudo-phakic	2 years
V:8	14	HM	aphakic	At birth	6/18	Pseudo-Phakic	At birth

BCVA= best corrected visual acuity, NLO= nuclear lens opacities

3.6.3 Linkage analysis

As an initial strategy, we performed X-chromosome linkage analysis on this family using the Genethon 10cM tetranucleotides marker set. The X-chromosome haplotype for the abridged family is shown in figure 45. Although the disease appeared fully penetrant in heterozygous females, linkage analysis was modelled as an X-linked recessive disorder. Lod scores are shown in table 26.

One recombinant (individual 34) is observed with marker DXS9902 (GATA175D03:CHLC). With marker DXSGATA124B04, two different recombinants are observed (5 and 30). Such findings raised

Figure 43: the X-linked cataract phenotype.
a, slit lamp view (diffuse illumination) of heterozygous 50 year old female showing fan of nuclear lens opacification (arrowed);
b, same eye (lower magnification), lens in retroillumination
The same pattern of opacification was observed in all heterozygous females. All hemizygous males had required cataract extraction in the first few weeks of life.

a ***b***

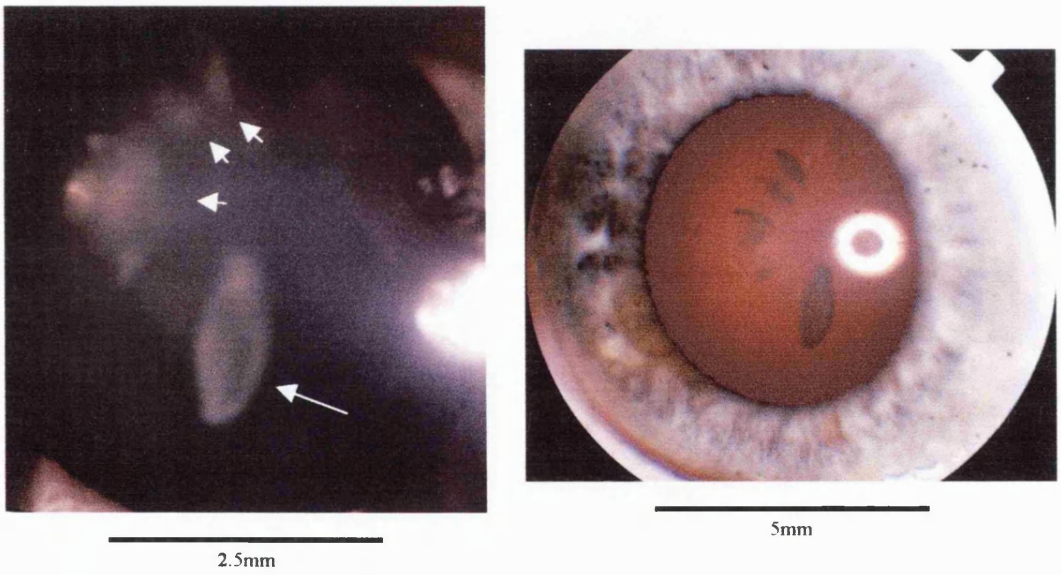

Figure 44: the unabridged X-linked pedigree

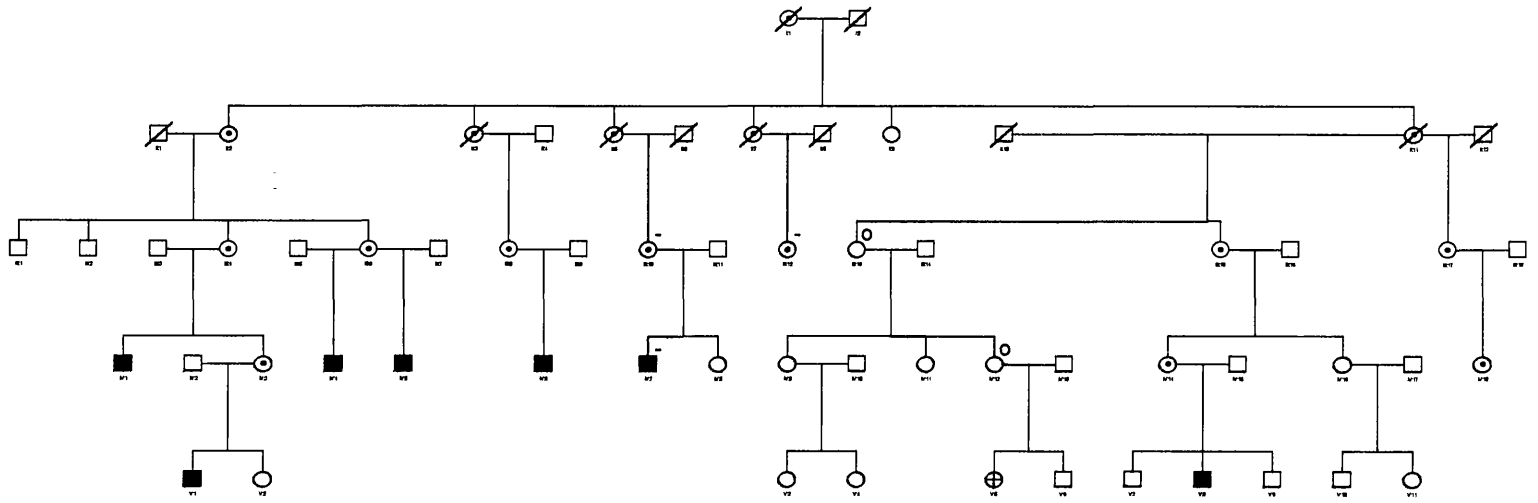

Blackened symbols denote severely affected males,
Females with mild lens opacities are denoted by symbols with central dots
+ = phenocopy
o = normal slit lamp examination
- = declined to participate

Figure 45: X-chromosome haplotype family J (abridged)

Markers listed in order from pter

(? refer to undetermined alleles)

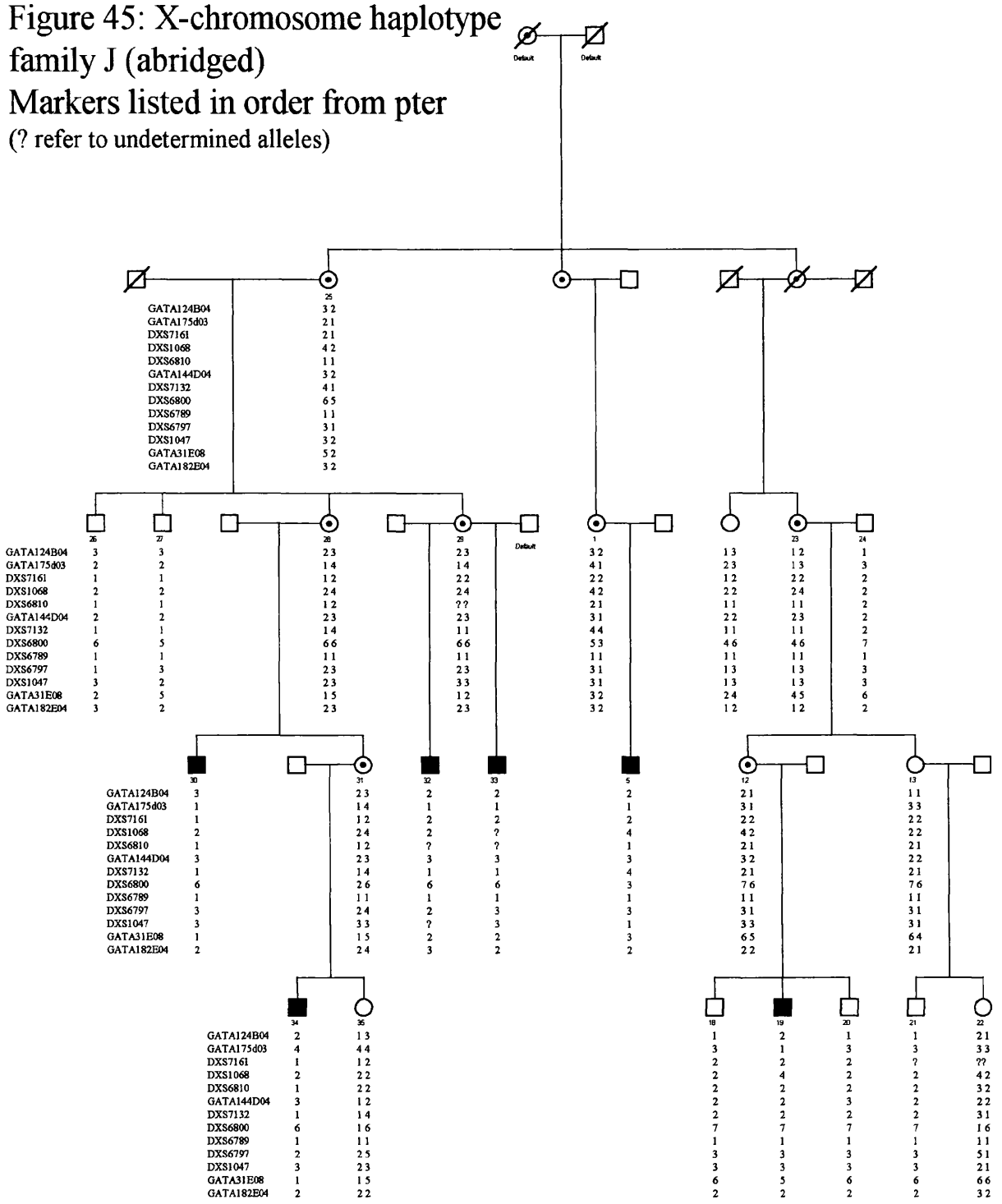

the possibility that the disease locus lies either between these markers or more likely centromeric to DXS9902, since DXSGATA124B04 is uninformative for individual 34, who may thus still be a recombinant at this map position.

Linkage analysis using markers across this interval provided strong evidence that the disease locus indeed lay centromeric to DXS9902, most probably residing between this marker and DXS999 (at which individual 34 is no longer a recombinant but a cross-over is observed with his mother, individual 28). Markers within this locus confirmed linkage of the family to this chromosomal region Xp22.13 ($Z=3.64$ at $\theta=0$ for marker DXS8036, table 27).

Interestingly, no recombinants are observed at marker DXS7103 (though critically the marker is uninformative for both individuals 5 and 34). Adjacent di-nucleotide markers excluded linkage.

Haplotype analysis of the abridged family is shown in figure 46 and lod scores for the relevant markers in table 27. A map of the region is shown in figure 47 together with multipoint linkage plot (calculated by minimizing software memory requirements by simulating genotypes using but minimum numbers of alleles.

Table 26: lod scores for linkage between the X-linked cataract locus and Genethon tetranucleotide markers for the X chromosome ordered Xpter to Xqter. Disease gene frequency 0.0001.

Marker	LOD score (Z) at recombination (θ) of										
	0	0.05	0.1	0.15	0.2	0.25	0.3	0.35	0.4	0.45	0.5
DXSGGAT3	-	-	-	-	-	-	-	-	-	-	-
DXSGATA124B04	-∞	2.25	2.16	1.93	1.64	1.33	1.01	0.70	0.42	0.19	0
DXSGATA175D03	-∞	3.14	3.04	2.78	2.45	2.08	1.67	1.22	0.77	0.35	0
DXSGATA124E07	-	-	-	-	-	-	-	-	-	-	-
DXS1068	-∞	0.78	1.08	1.12	1.06	0.94	0.78	0.60	0.40	0.10	0
DXS6810	-∞	0.60	0.72	0.70	0.65	0.56	0.47	0.36	0.25	0.13	0
DXSGATA144D04	-∞	1.27	1.49	1.44	1.28	1.05	0.78	0.49	0.23	0.06	0
DXS7132	-∞	-2.97	-1.67	-1.00	-0.59	-0.32	-0.15	-0.05	0.00	0.02	0
DXS6800	-∞	-1.30	-0.54	-0.18	0.02	0.12	0.16	0.17	0.14	0.08	0
DXS6789	0.00	0.00	0.00	0.00	0.00	0.00	0.00	0.00	0.00	0.00	0
DXS6797	-∞	-2.59	-1.37	-0.77	-0.43	-0.23	-0.17	-0.04	0.00	0.02	0
DXSGATA172D05	-	-	-	-	-	-	-	-	-	-	-
DXSGATA165B12	-	-	-	-	-	-	-	-	-	-	-
DXS1047	-∞	-3.85	-2.47	-1.71	-1.21	-0.85	-0.58	-0.37	-0.20	-0.08	0
DXSGATA31E08	-∞	-2.43	-1.06	-0.37	0.02	0.24	0.35	0.36	0.30	0.18	0
DXSGATA182E04	-∞	0.24	0.54	0.58	0.53	0.43	0.33	0.25	0.17	0.09	0
DXYS154 / SDF1	-	-	-	-	-	-	-	-	-	-	-

Figure 46: X-linked pedigree. Haplotype across disease interval

(Disease haplotype is boxed,
? refer to undetermined alleles)

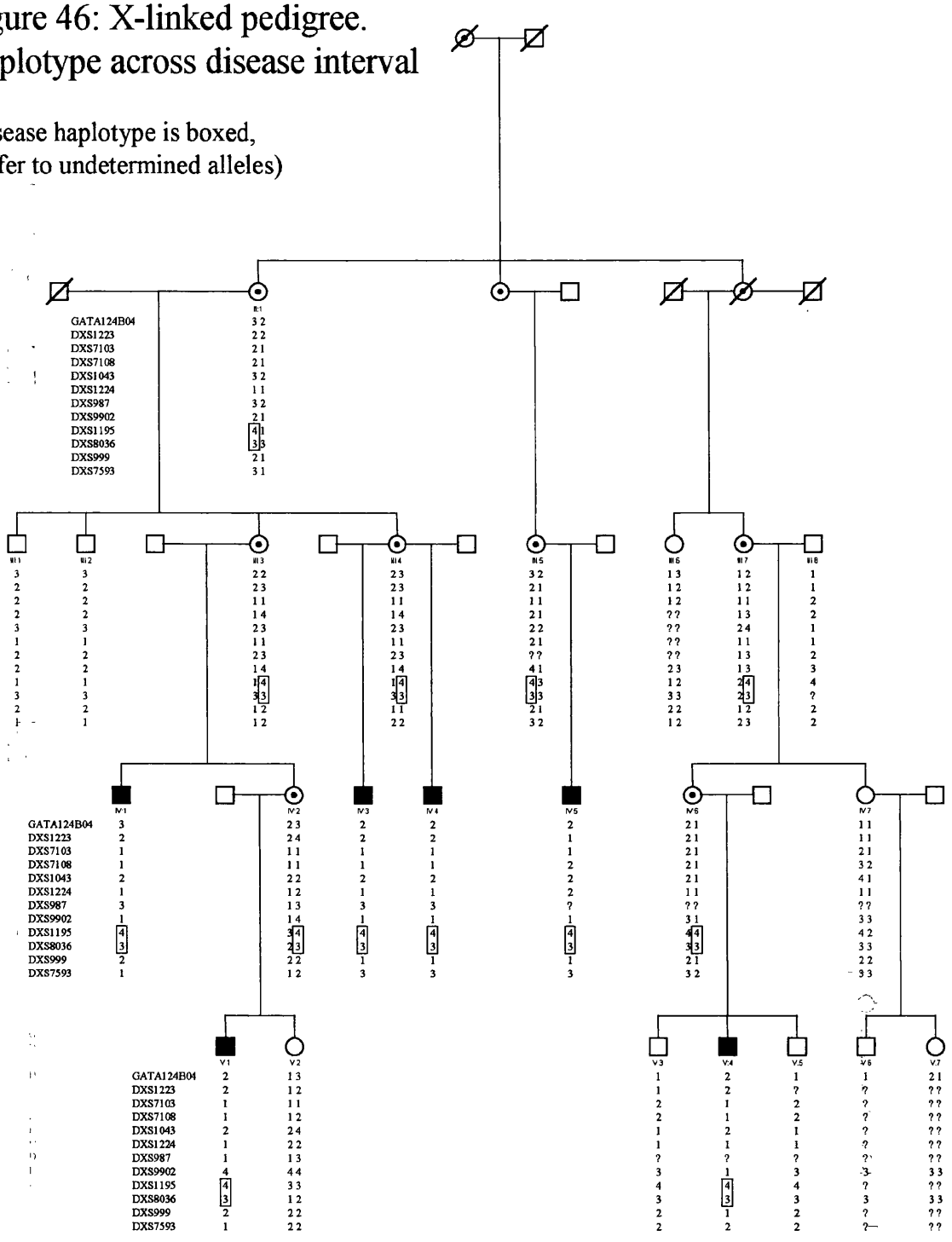

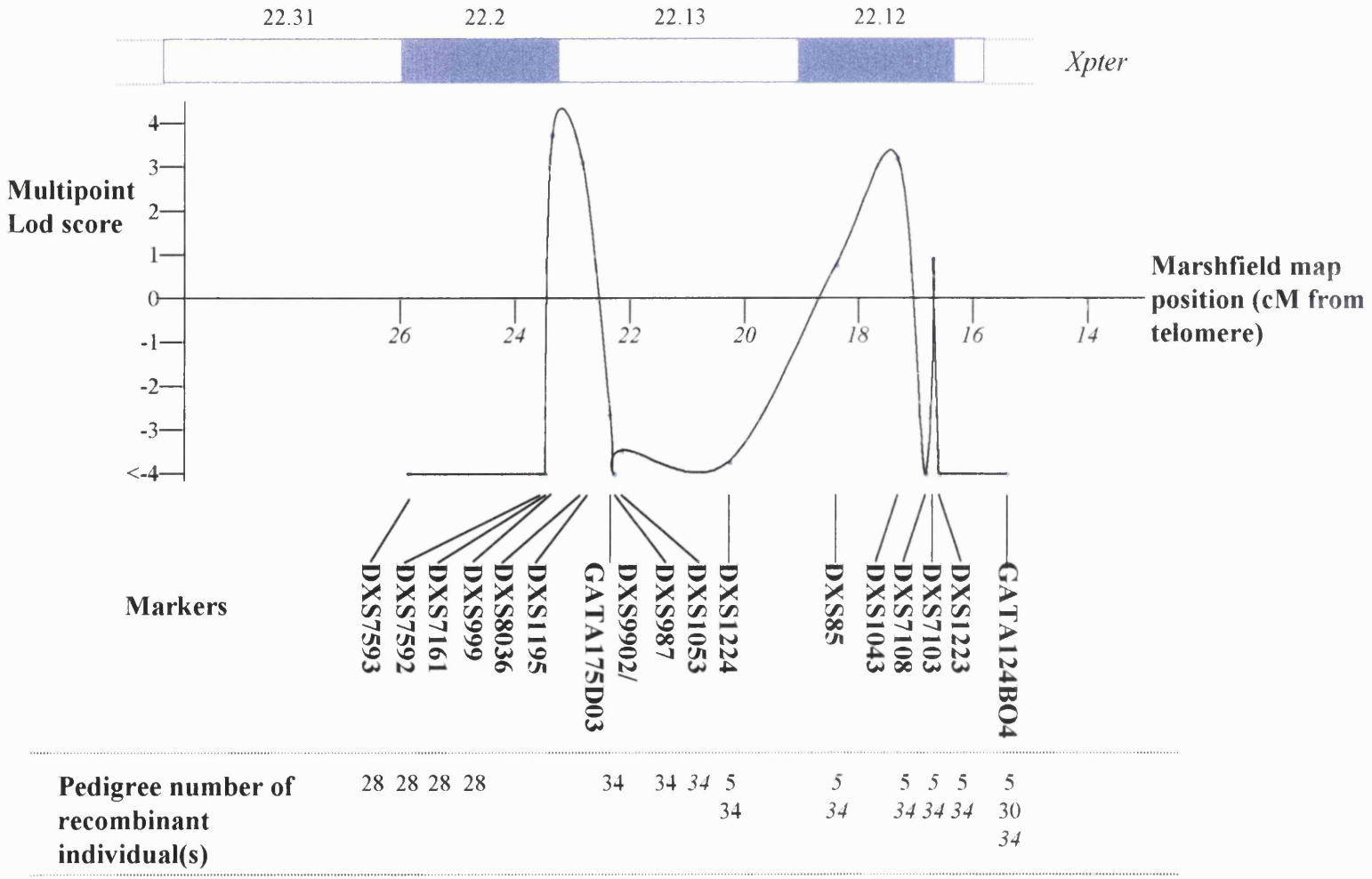

Figure 47: Xp22 ideogram, *top*, with multipoint linkage lod score plot (calculated using *Allegro* multipoint linkage analysis software, DF Gudbjartsson, Decode, Iceland) for microsatellite markers ordered from the telomere (Xpter), *below*. Marker map positions (cM) are derived from the sex averaged Marshfield map and beneath are given the pedigree numbers of recombinant individuals (figures in italics are implied recombinants on the basis of haplotype analysis with crossovers minimised.

3.6.4 Mutation screening

3.6.4.1 Identifying candidate genes within the disease interval

Using a bioinformatics approach, lists of those genes definitely within the disease interval and those close or possibly included in the locus were constructed (table 28).

Table 28: genes definitely within or possibly within the Xp22.2 disease locus (as at 29 July 2000)

The disease is indicated in instances where mutations have been identified. Strong candidates are indicated in bold.

GENE	NAME	EXPRESSION	DISEASE	Xp
DXS1053, 25.6 cM anchored marker				
CALB3	calbindin3 (vitamin D-dependent calcium binding protein)	kidney, placenta, intestine uterus		22.2
PIR	pirin			
SIGMA1B	clathrin adapter complex 1, sigma 1b			
PIGA	phospatidylinositol glycan, class A		Paroxysmal nocturnal haemoglobinuria	22.1
FIGF	c-fos induced growth factor (vascular endothelial growth factor)	heart, lung, intestine		
BMX	BMX non-receptor tyrosine kinase	bone marrow, probably		22.2
PHKA2	phosphorylase kinase, alpha 2	liver	glycogenosis	22.2-1
STAT6	signal transducer and activator of transcription			
STK9	**serine/threonine kinase 9**	**brain, lung, kidney**		**22**
CX43P	*connexin 43 pseudogene*			
RAI2	**retinoic acid induced 2**	**brain, lung, kidney, heart**		**22**
DXS999, 28.1 cM anchored marker				

Possibly within disease interval:

GENE	NAME	EXPRESSION	DISEASE	Xp
FTLL2	ferritin light polypeptide-like 2			22.3-2
GPM6B	**glycoprotein M6B**	**neurons and glia**	**excluded from Rett syndrome**	**22.2**
HCCS	holocytochrome C synthetase		excluded from Rett syndrome	22.2
MLS	microphthalmia with linear skin defects			
ZFX	**zinc finger protein**	**possibly gonadal**		**22.2-**
21.3				
HOMG			hypomagnasaemia, hypocalcaemia	22.2
INE2	inactivation escape-2	brain		22.2
KFSD	keratosis follicularis spinulosa decalvans		multiple eye probs	22.2-13
CND	corneal dermoids	cornea		22.2-1
PDHA1	pyruvate dehydrogenase E1 –alpha polypeptide-1		pyruvate dehydrogenase deficiency	22.2-1
PHEX	phosphate regulating gene		hereditary hypophosphataemia	22.2-1
PPEF1	protein phosphatase EF hand calcium binding domain		retinoschisis excluded	22.2-1
PRTS			Partington syndrome	22.2-1
RPS6KA3	serine/threonine kinase gene		Coffin-Lowry syn	22.2-1
XLRS1			retinoschisis	22.2-1
SEDL	sedlin		spondylo-epiphyseal dysplasia tarda	22.2-1
RP15			RP15	22.13-11
MEHMO			MEHMO syndrome	22.13-1
GDXY			gonadal dysgenesis	22.11-2
CA5B	**carbonic anhydrase (mitochondrial)**	**pancreas, glands, spinal cord**		**22.1**
SAT	**Spermine N(1)-acetyl transferase**			**22.1**
EIF2S3	eukaryotic translation initiation factor 2	?testis		22.2-1
CMTX2			Charcot-Marie-Tooth	22.2

GENE	NAME	EXPRESSION	DISEASE	Xp
FCP1	F-cell production 1	rbc	Heterocellular hereditary persistence of fetal haemoglobin	22.2
GLRA2	**glycine receptor (chloride channel**	**brain**		**22.1-2**
MAGEB	**family melanoma antigen**	**tumours**		**21.3**
MJD4	MJD4-PEN		Machado-Joseph Disease related 4	22.1
MLS			microphthalmia with linear skin defects	22.2
RDXP2	**radixin pseudogene 2**			**21.3**
CLCN4	chloride channel 4	skeletal muscle, brain		22.3
DXS1283E	**GS2**	**all tissues**		**22.3**
EMWX	Episodic-muscle weakness		episodic muscle weakness	22.3
IL3RA	interleukin-3 receptor	haem cells		22.3
OFD1	oral-facial digital syndrome 1		oral-facial digital syndrome 1	22.3-2
KAL1	Kallmann syndrome-1		Kallmann syndrome	22.3
OA1	Ocular albinism		OA	22.3
APXL	apical protein, Xenopus laevis-like		OA	22.3
OASD	Ocular albinism and sensorineural deafness		OA	22.3
PKX1	Protein kinase 1		chondrodysplasia	22.3
TBL1	Transducin beta like 1		OA-like + deafness	22.3
ZNFXY	Zinc finger X and Y		Opitz syndrome	22.3
ARHGAP6	**GTPase-activating protein, RHO, 6**	**all tissues, preferentially skeletal muscle, ? eye**		**22.3**
ARSD/E/F	arylsulphatase –D, -E, -F		ARSE: chondrodysplasia punctata	22.3
AMELX	**amelogenin**	**teeth**		**22.3-1**
ASMT	acetyl-serotonin O-methyltransferase	pineal and retina		22.3
ASMT 1	acetyl-serotonin O-methyltransferase-like	pineal and retina		22.3

GENE	NAME	EXPRESSION	DISEASE	Xp
GRPR	gastrin-releasing polypeptide factor	bone, brain		
PRPS2	phosphoribosyl synthetase	all tissues		22.3-2
Others:				
APT6M8-9	**ATPase lysosomal membrane sector associated protein M8-9**	**ribosomes, all tissues**		
ASSP4	arginosuccinate synthetase pseudogene 4			
COD1	cone dystrophy locus 1			22.1-3
EEF1B4	eukaryotic translation elongation factor			
ETF1P3	SUP45L4			
GAPDL10	glyceraldehyde-3-phospate dehydrogenase-like 10			
GDXY	testis-determining factor		Swyer syndrome	22.11-2
GK	glycerol kinase		glycerol kinase deficiency	22.3-3
GPXL1	glutathione peroxidase pseudogene 1			
GUCY2F	RetGC-2			
KRT18L1	keratin 19-like 1			
PFKFB1	phosphofructokinase			
PLS3	platin (T isoform)			
POLA	DNA polymerase alpha	probably lethal in hemizygous males		22.1-3
TMSL7	thymosin-like 7	brain, possibly cytoskeleton		
U2AF1RS2	U2 small nuclear ribonucleoprotein Auxiliary factor, small subunit 2			21.1
UHX1	ubiquitin carboxyl-terminal hydrolase 1	retina		21.2-2

3.6.4.2 Screening of the gene encoding the retinoic acid induced transcription factor, *RAI2*

The entire coding region (1 exon, 1960 base pairs) and 377 base pairs of the 5' upstream region were amplified with the following primers (adapted from Walpole et al.[44]).

Table 29: primers designed to amplify the *RAI2* gene

Primer pair	Forward primer 5' –3'	Reverse primer 5' – 3'	Anneal-ing temp (°C)
1	GTCTGACATAGCAACTTGGAC	CCATGGAGAGGTTCTGGGAC	60
2	TCCCTGGTTAACTAAAACGTGG	GAAAGACGTGCTGCTCCAGCAC	60
3	CTACGTCATGACCACCAGG	CACCAAGAGGGTGGCTGGTG	62
4	GTCAGCCTCCTCCTGGCTAT	GGAGCTGAACTTGGATTCAGA	60
5	CAGTCCCTATTCCCATCCCC	GCCACTGGGAAGTTTCTCCAT	60
6	CTAGACCTGTCAGTGGCAGC	CCGCCTGGGACTCGCCCAC	60
7	GCCAGCCCAACCACCCCAG	AAAGGTGGCCAGCCGTTG	60
8	GCTTTAATGGAATATTGGGTGAAT	GTGCAAACAAACATTTATTGTGAA	60
9	TAAAGTTAAAGAAAGTGAACTCCC	CACTTTGTGGCAATGAAAATAGC	60

Two affected hemizygous males and one unaffected female were amplified using each primer pair. No sequence changes were detected.

3.7 Mapping a locus for coralliform cataract

Ascertainment of a four-generation family (family C) with coralliform (synonymous with aceuliform) cataract facilitated linkage analysis. This is a branch of the family described by Nettleship, 1909[224].

3.7.1 Linkage analysis

After excluding several candidate loci (table 29), we obtained uninformative data for markers around the γ-crystallin gene cluster on 2q33. As an adjunct therefore, linkage analysis was performed using the marker D2S325 which lies within the interval. A significantly positive two-point lod scores was obtained for this marker ($Z(max)=3.47$ at $\theta=0$) and the genetic interval of the disease locus subsequently defined as D2S2261 - D2S339 (which encompasses the γ-crystallin gene cluster and the βA2-crystallin gene).

Table 30 details the two-point lod scores for linkage between the coralliform cataract locus and chromosome 2q33-35 markers.

The pedigree and disease haplotype is shown in figure 48.

Figure 49 shows a sex-averaged genetic map of the region.

Table 30: two-point lod scores for linkage between *a*, the coralliform cataract locus and candidate gene markers in family C; *b*, the coralliformcataract locus and chromosome 2q33-35 markers

a

Marker	LOD score (Z) at recombination (θ) of					
	0.0	0.05	0.1	0.2	0.3	0.4
D1S468	-∞	-2.40	-1.59	-0.91	-0.55	-0.25
D1S2141	-∞	-3.33	-2.18	-1.11	-0.56	-0.22
GATA 124F08	-∞	-2.20	-1.35	-0.57	-0.22	-0.05
D2S427	-0.05	0.01	0.05	0.09	0.10	0.07
GATA 178GO9	one allele only					

b

Marker	Genetic Distance (cM)	LOD score (Z) at recombination (θ) of					
		0.0	0.05	0.1	0.2	0.3	0.4
D2S2261	5.0	-∞	0.01	0.19	0.24	0.19	0.10
D2S118	6.0	0.00	0.00	0.00	0.00	0.00	0.00
D2S2237	2.9	1.18	1.06	0.95	0.71	0.48	0.24
D2S369	2.1	2.15	1.96	1.75	1.30	0.79	0.30
D2S325	2.1	3.47	3.14	2.79	2.03	1.22	0.45
D2S2321	1.6	3.01	2.72	2.42	1.78	1.12	0.49
D2S371	4.1	1.65	1.51	1.36	1.00	0.61	0.24
D2S2319	5.0	0.00	0.00	0.00	0.00	0.00	0.00
D2S2250	5.0	0.90	0.87	0.82	0.69	0.52	0.29
D2S339		-∞	0.14	0.51	0.62	0.43	0.17

Figure 49: linkage map of the coralliform cataract locus on 2q33-35 which spans the gamma-crystallin gene cluster.
cM values are similar for both males and females

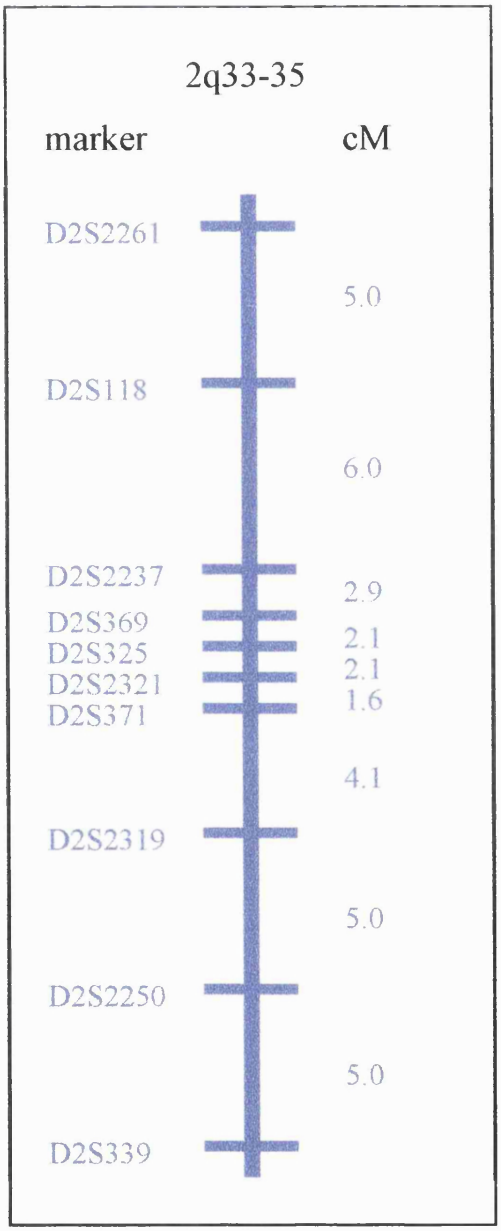

Figure 48: abridged pedigree of family C showing segregation of 2q33-35 microsatellite markers, listed in descending order from the centromere

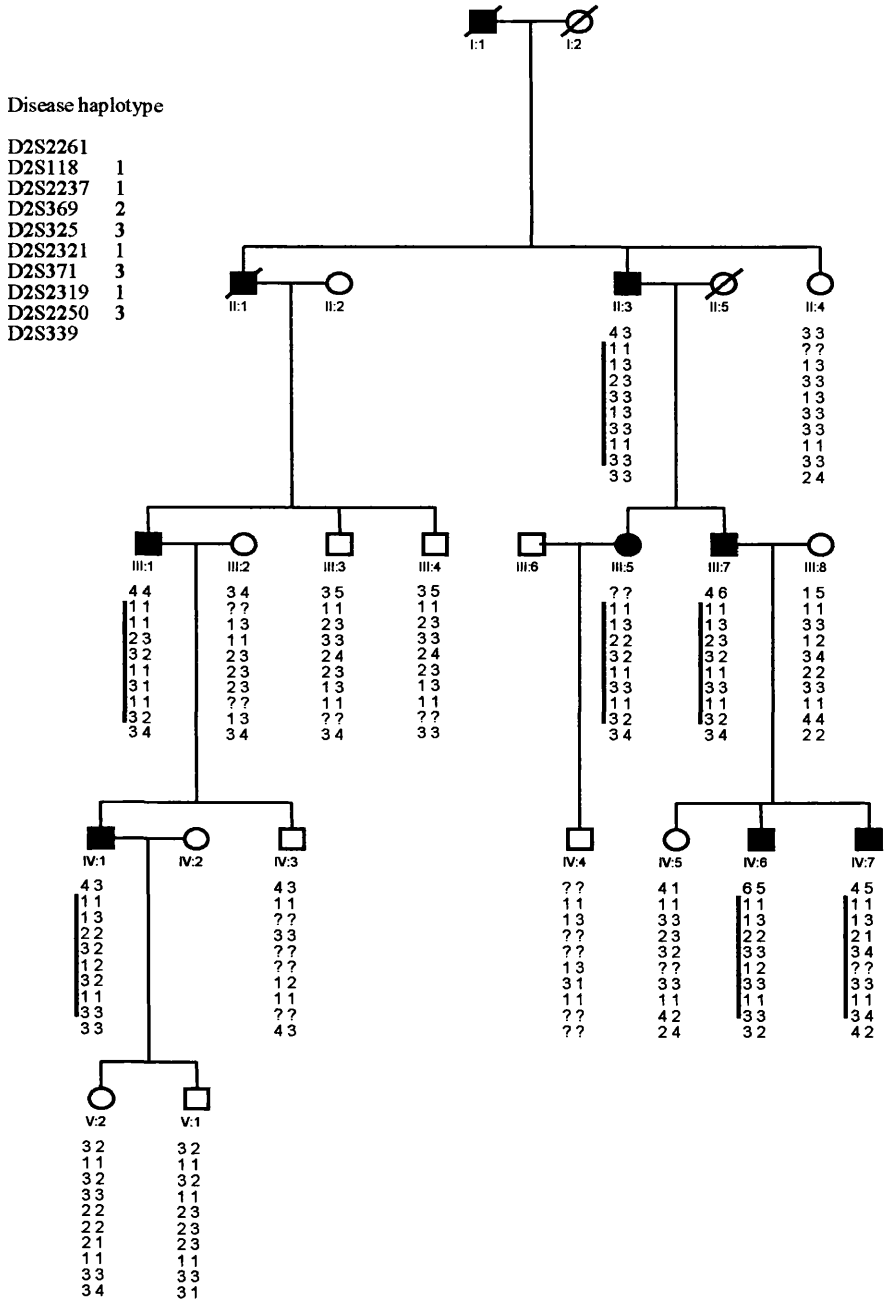

3.7.2 Mutation screening

The interval encompasses the γ-crystallin gene locus which includes genes γ-A, -B, -C, -D, -E, -F and a gene fragment γ-G. Only γ-C and γ-D encode abundant proteins in the lens while γ-E and γ-F are pseudogenes. Direct sequencing of each of the genes was undertaken in the following order of priority γ-C, γ-D, γ-A, γ-B. Table 31 below shows the primers used.

No mutation was detected in the following γ-crystallin gene: A, B, C, D. A non-segregating synonymous nucleotide polymorphism was detected in *γC* exon 3, A to G at position 507 (Arg170Arg)

Table 31: primers designed to amplify the coding regions of the γ-crystallin genes

Gene – exon	Forward primer 5' –3'	Reverse primer 5' – 3'	Annealing temp (°C)
γA – exon 1	CTA TCA TAC TAG ATG CTA ATC A	CTC GGT CCT CGT AGA AGG	52
γA – exon 2	CCA GCT GAC TGT CTA CTG T	TCA CAT GAG GAA TTA TAC GGC	58
γA – exon 3	GAC AGA CCA GCT CGC ACA	ATC ACA ACA AGG CAG GCA C	58
γB – exon 1	CAC AGC AAC CAG AAA ACA TC	CTG TCC TCG TAG AAG GTG A	58
γB – exon 2	CTC CAT GCT CCC ACA TCT T	GGA AGG CAA AGA CAG AGC C	58
γB – exon 3	TGT TTA CTC TTG CGT TTT CTG	AAG TGG AAA ACG TAA ATA CTT C	58
γC – exon 1	TGC ATA AAA TCC CCT TAC CG	CTG CAA AGG AAG AAT CGT TCC	58
γC – exon 2	ATC ACC TTC TAT GAG GAC AGG	GGG GAC TCT GGC GGC ATG	58
γC – exon 3	CCG AGT AGA CAG TCT CCC	TTG GTA GTG TTA AGC TAT TTT AA	58
γD – exon 1	GGG CCC CTT TTG TGC GG	GAA GCT CCG GGG TCC CG	60
γD – exon 2	GCC TTG CCT TGC AGA TCA	TTG AGG ATG TAC TCA CGT GG	58
γD – exon 3	CAC ACT TGC TTT TCT TCT TCT T	CAA AGG AGG ACA TAT TTC AGG	58

3.8 Mapping of a family with cataracts, nanophthalmia, retinitis pigmentosa and acute-on-chromic glaucoma

Using the Birmingham Women's Hospital Clinical Genetics Service database, details of a three-generation pedigree with apparently isolated autosomal dominant congenital cataract were obtained (family N). On clinical evaluation however, it became clear that segregating with cataract formation in the individuals were several other ocular anomalies.

3.8.1 Clinical evaluation

The fully penetrant ocular phenotype is shown in figure 50 and comprised bilateral, symmetrical nanophthalmia, microcornea, acute on chronic glaucoma in older individuals and pulverulent-like lens opacities which became visually significant by about thirty years of age. Significant variability in expressivity was observed in the degree of nanophthalmia. Fundal appearances consisted of peripheral "bone-spicule" intra-retinal pigment epithelial migration, posterior pole staphyloma with large, flat and irregularly edged optics discs. Several members of the family were attended for more extensive evaluation and the results for those affected are summarized in table 32. The ocular examinations of individuals ascribed as unaffected were otherwise normal.

Table 32: clinical evaluation of the phenotype

	III:3		IV:1		IV:2	
Status	Affected		Affected		Affected	
Age	39		14		9	
Sex	Female		Female		Male	
Operations	Bilateral cataract extraction and glaucoma filtration		Left medial rectus recession, lateral rectus resection		None	
BCVA	6/36	PL	6/9	6/18	6/9	6/9
Refraction (D=dioptres)	+13D	+14D	-0.75/ -0.25 x090	-1.00/ -0.50 x85	-4.25/ +2.00x0 80	-3.25/ +1.50x0 90
Colour vision			Normal		Normal	
Corneal diameter (mm)	8.5 h 8.25 v	8.75 h 8.25 v	9 h 8.75 v	8.75 h 8.75 v	8 h 8.25 v	8.25 h 8 v
Corneae	Clear, flat blebs superiorly		Clear		Clear	
Anterior chamber	D&Q		D&Q		D&Q	
Gonioscopy			Open (on indentation)			
IOPs						
Lens	Aphakic		Fine punctate opacities		Few punctate opacities	
Disc	Large, pale, flat, irregular borders, attenuated vasculature with abnormal branching					
Fundus	Generalised retinal thinning at posterior pole, with bone-spicule intra-retinal pigment epithelial migration pre-equatorially with demarcation line					
Axial length	22.68	18.73	23.04	22.92	22.82	22.71
Anterior chamber depth						2.41
Lens						4.55
ocular ultrasound	Posterior staphyloma right eye, retina attached, highly reflective disc, sclera appears normal thickness		No staphyloma, otherwise as for III:3		No staphyloma, otherwise as for III:3	
Photographs	Yes		Yes		Yes	
EOG Arden index	-	110% (severely reduced)	150% (sub-normal)	154% (sub-normal)	Un-reliable	Un-reliable
ERG	Severely abnormal rod and cone ERGs with only minimal responses to the brightest stimuli		Rod responses were subnormal. Cone responses were normal		All response amplitudes were subnormal	

Normal values. Refraction: 0.00 D; corneal diamter: 11.5mm ; axial length: 22.5 – 24.5mm

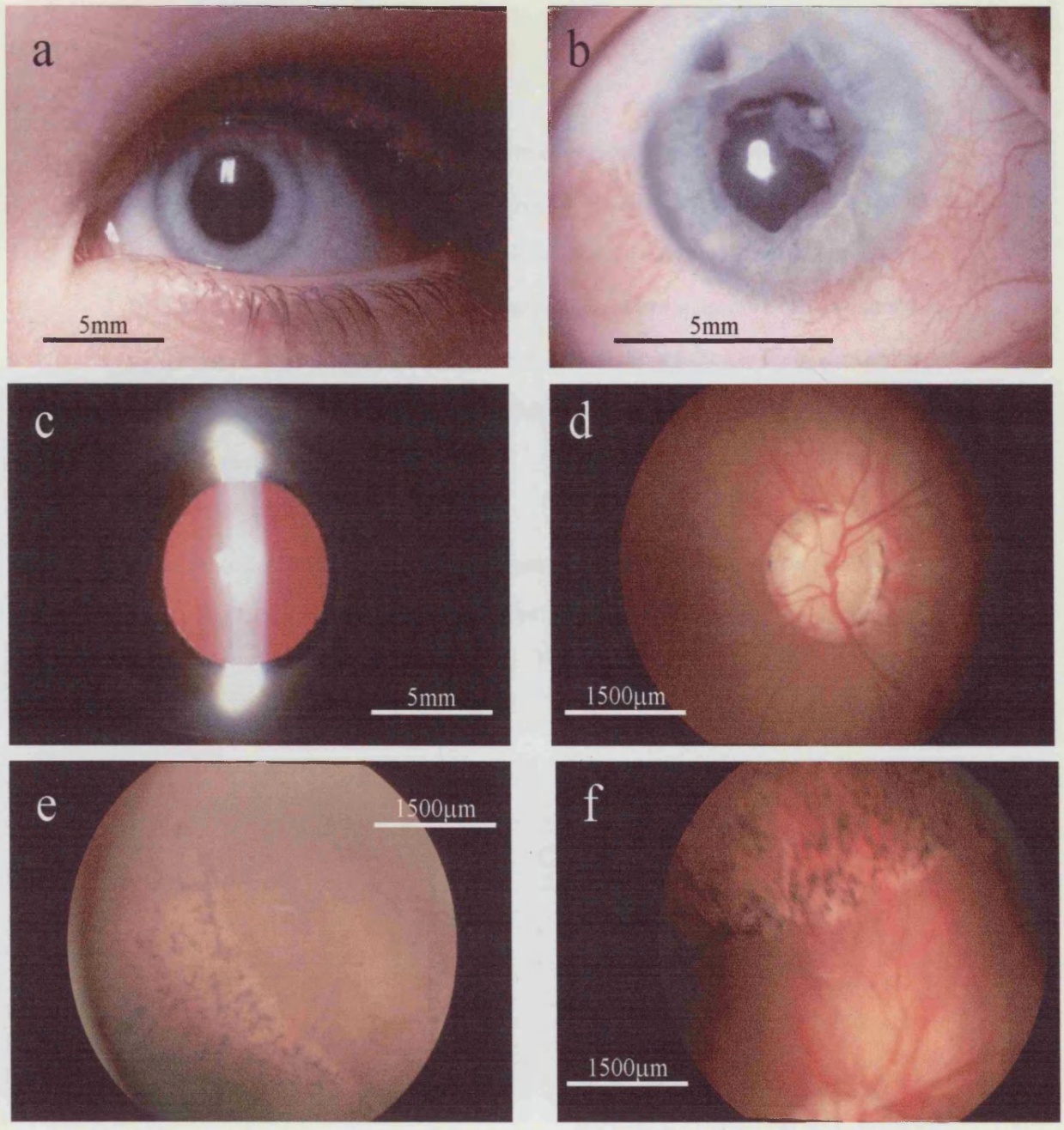

Figure 50: the phenotype: nanophthalmia, cataract, retinitis pigmentosa: *a*, the nanophthalmic eye (15 year old female);
b, consequences of glaucoma and cataract, the end point of multiple surgical procedures: aphakia, peripheral iridectomy and shallow bleb from glaucoma filtration surgery (39 year old female);
c, fine pulverulent lens opacities (15 year old female);
d, posterior pole (10 year old male) showing large flat optic disc with irregular margins, narrowed vasculature and surrounding retinal thinning;
e (10 year old male) and *f* (15 year old female), peripheral bone-spicule intrarctinal pigment epithelial migration.

3.8.2 Linkage analysis

After excluding linkage to the microphthalmia locus on chromosome 14 (table 33), significantly positive two-point lod scores were obtained for markers spanning the *NNO1* locus on 11p (Z_{max}=3.01 at θ=0 for markers D11S1765 and D11S4191, table 34) and the disease interval defined as 11pter – D11S908 (33cM). The pedigree and disease haplotype are shown in figure 51. The disease interval includes the *PAX6* gene locus. The ability to exclude this locus is limited by family size and the infomativity of adjacent markers. The results of direct sequencing of the *PAX6* gene in this family are eagerly awaited.

Figure 51: pedigree of family N showing segregation of 11p markers ordered from the telomere

(bars beside alleles indicate disease haplotype, ? refers to undetermined allele)

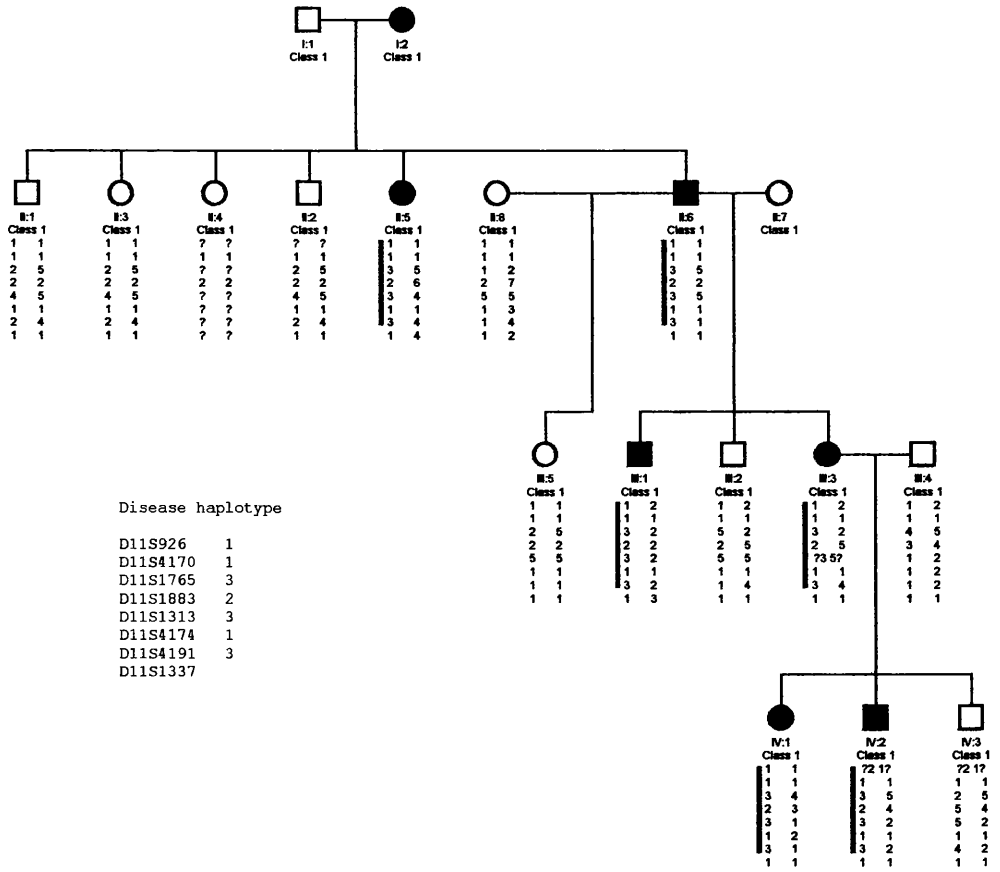

Table 33: cataract candidate gene exclusion data: two-point lod scores for linkage between the disease locus and candidate gene markers

	LOD score (Z) at recombination (θ) of										
	0	0.05	0.1	0.15	0.2	0.25	0.3	0.35	0.4	0.45	0.5
D14S267	-∞	-2.94	-1.66	-0.99	-0.57	-0.30	-0.13	-0.02	0.02	0.03	0
D14S987	-∞	-1.07	-0.70	-0.47	-0.31	-0.21	-0.12	-0.07	-0.03	-0.01	0
D14S1054	-∞	1.31	1.38	1.30	1.17	0.99	0.78	0.56	0.34	0.15	0
D14S977	-∞	0.01	0.22	0.28	0.27	0.22	0.15	0.09	0.04	0.01	0

Table 34: two-point lod scores for linkage between the disease locus and 11p markers ordered from 11pter

	LOD score (Z) at recombination (θ) of										
	0	0.05	0.1	0.15	0.2	0.25	0.3	0.35	0.4	0.45	0.5
11pter											
D11S926	0.25	0.23	0.21	0.19	0.17	0.15	0.13	0.11	0.08	0.04	0
D11S4170	One allele only										
D11S1765	3.01	2.74	2.46	2.16	1.85	1.51	1.16	0.83	0.46	0.18	0
D11S1883	0.53	0.86	0.91	0.87	0.79	0.69	0.56	0.41	0.28	0.13	0
D11S1313	2.83	2.58	2.31	2.02	1.72	1.41	1.08	0.75	0.43	0.17	0
D11S4174	One allele only										
D11S4191	3.01	2.74	2.46	2.16	1.84	1.51	1.16	0.81	0.46	0.18	0
D11S1337	1.15	1.04	0.91	0.78	0.63	0.48	0.34	0.21	0.10	0.03	0
D11S908	-∞	-0.65	-0.21	-0.02	0.06	0.08	0.07	0.03	-0.00	-0.02	0

3.9 Mapping of a family with progressive posterior polar cataract

3.9.1 Linkage analysis

After excluding several candidate loci for posterior polar cataract (table 35), significantly positive two-point lod scores were obtained in family G (progressive posterior polar cataract) with Z_{max}= 3.91 at marker D10S192 (Table 36). Figure 52 shows the pedigree with disease haplotype.

Table 35: cataract candidate gene exclusion data: two-point lod scores for linkage between the polymorphic cataract locus and candidate gene markers in family G

Marker	Candidate	LOD score (Z) at recombination (θ) of					
		0.0	0.05	0.1	0.2	0.3	0.4
D1S468	Volkmann, PPC locus	-∞	-1.49	-0.48	0.25	0.43	0.32
D16S402	PPC and	-∞	-4.37	-2.73	-1.27	-0.57	-0.17
D16S539	Marner locus	-∞	-2.99	-1.83	-0.78	-0.29	-0.06
D20S470	Putative PPC	-∞	-2.09	-1.10	-0.32	-0.07	-0.00
D20S481	locus	-∞	-4.09	-2.49	-1.12	-0.52	-0.20

Table 36: two-point lod scores for linkage between the posterior polar cataract locus and markers in family G

Marker	Candidate	LOD score (Z) at recombination (θ) of					
		0.0	0.05	0.1	0.2	0.3	0.4
AFMa053yg5	PITX3	1.31	1.34	1.17	0.81	0.46	0.15
D10S192		3.91	3.58	3.23	2.49	1.66	0.77
D10S540		0.08	0.06	0.05	0.03	0.02	0.00

Figure 52: pedigree and disease haplotype family G for 10q markers listed from the centromere

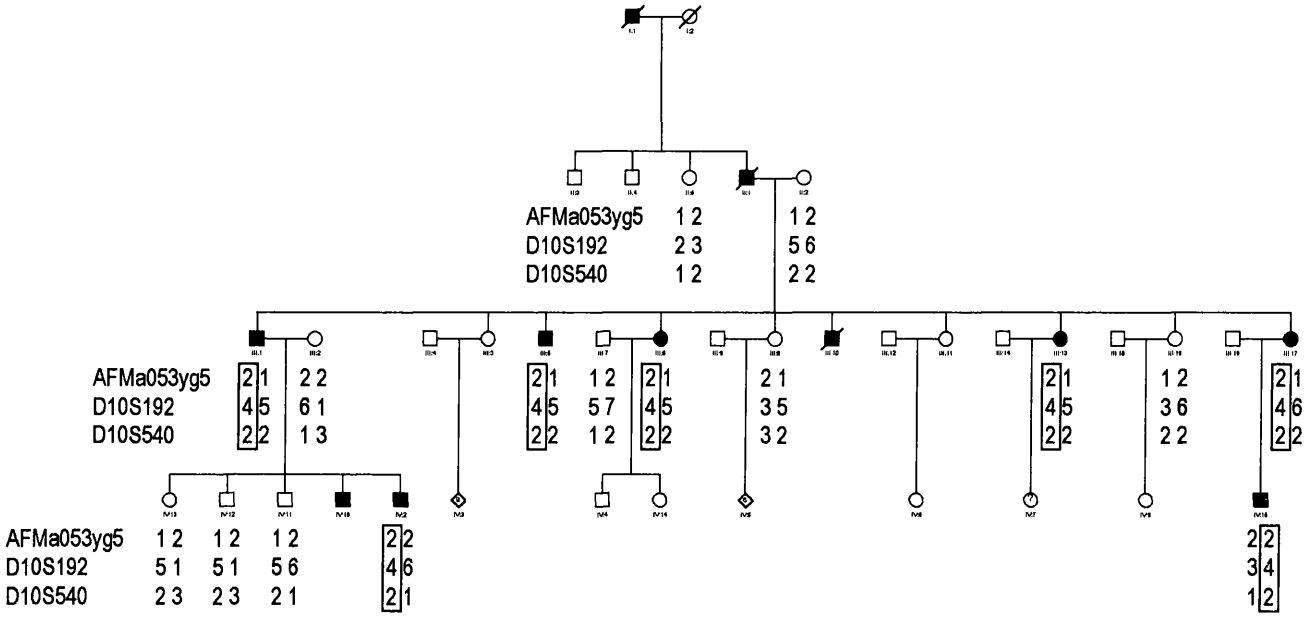

3.9.2 Direct sequencing

Exon/intron boundaries for the *PITX3* gene are not published. Using the complete CDS of the PITX3 mRNA sequence, the HGMP BLAST software identified the human PAC clone AL160011 (chromosome 10q25) as containing the complete *PITX3* coding sequence. The genomic structure of the gene could then be defined and primers designed to amplify the entire coding region (906 nucleotides, 302 amino acids, 1187 nucleotides including the 5' and 3' –UTRs, figure 53, table 37). The gene consists of 4 exons interspersed by the three short introns.

Table 37: *PITX3* primers

Gene – exon	Forward primer 5' –3'	Reverse primer 5' – 3'	Annealing temp (°C)
PITX3 exon 1	TAG CTA AGC CGG AGA TTT TTA	GAA GCT GTT ATG TCC TGC AC	55
PITX3 exon 2	AGA ATA TGC GCT GGC TTG G	GCG GGT CTG GAG AGC AT	55
PITX3 exon 3A	ACC GCC TTT CTC CCG TG	ATA AGG GCA GGA CAC GGC	60
PITX3 exon 3B	GCC GTC TCC TGC CCT TAT	AAG CCA GTC AAA ATG ACC C	58
PITX3 exon 4	GGG TCA TTT TGA CTG GCT T	AAG CGC AAC TTT GAA TCA TC	58

Direct sequencing of *PITX3* exons 3 and 4 did not reveal a sequence change. Probably owing to the high G/C content of exons 1 and 2, no sequence data is yet available.

Figure 53: *PITX3* gene structure
(derived from PAC clone AL160011)

3.10 Screening of a panel of inherited cataract patients for mutations in filensin and LEP503

3.10.1 Primers

The genes encoding the lens cytoskeletal protein, filensin is considered a strong candidate for human cataractogenesis. A recently discovered lens-epithelial specific protein LEP503 (of as yet unknown function) was also screened as a possible candidate for cataractogenesis. Primers were designed (tables 38 and 39) to amplify the entire coding regions of each gene.

Table 38: LEP503 primers

Exon	Forward primer 5' –3'	Reverse primer 5' – 3'	Annealing temp (°C)
1	CAC TAG AGG CAG CTC CCA	CTA TGC CTC CTG TTT ACT CTA	58
2	CCC AGC CCA ATT GCC ATC	TTA GAC ACT TAT AAT CTT GGG	58

Table 39: filensin primers

Exon	Forward primer 5' –3'	Reverse primer 5' – 3'	Annealing temp (°C)
1A	ATG TAC CGG CGC AGC TAC	ACT TGC TTC GGA ACT CGT C	58
1B	AGC AGC GCC ATG CCG G	TTT TAG CAG GAG TTG ACA TTC	62
2	CAT GTG AAA GCA TGG TAG TT	CAA CAC TGT AAT TAA GCT ACG	58
3	CAT TGC AGG AAG CTG ATG AAG GCC	ATC AAA CCC AAA CTG GGT TTT TC	60
4	TGA GAA TGT TTT CCC TCC CCC AA	CTG GTT TGC CTT TTC CTG CTT CA	58
5	CAT GAG TCT GAC TCT GGC CTT CT	ACG CGG CAG ACT CGA GCG TAC C	55
6	TGC CCA CAG ACA ACA ACT CTG GA	ACA CGC TCA CCT GTT GCC TTC CAA	58
7	TGA CCT CTG TTT GGC TTG TT	GTC CTC CCT CAC ATA AAA GC	55
8A	TTA TAC TTG AAT TTC TGC CTG	TTG GTG TAG AGC TCA GTG G	58
8B	TGA GAA GCC CCA AAA GAG C	ATC TTC TTT CTC CTG CAG AC	58
8C	TTA GAG AAT GGG CAG GTG G	TCT TAT AGG CCA AAG CCT TG	58
8D	CAG TGG AAG TGC TGG AAT G	ATT CCC AAG GTC CCT ATT AAT	58

3.10.2 Heteroduplex Analysis

3.10.2.1 LEP503

No heteroduplexes were detected in either exon 1 or exon 2.

3.10.2.2 Filensin

The following non-segregating nucleotide substitutions were detected in the coding region of filensin (table 40)

Table 40: filensin nucleotide substitutions

Exon	Nucleotide Substitution	Nucleotide Number	Codon	Codon Number	Amino acid	Sample Numbers (total)
6	C→T	806	AAC→AAT	268	Asn→Asn	7, 9, 25 (3)
7	G→A	1035	GGT→AGT	345	Gly→Ser	11, 15, 17, 22, 33, 37, 39, 75, 77, 93,103, 106, 108, 114, 116, 118, 131, 132, 134 (19)

Sequencing of DNA of all relatives indicated that the sequence change did not segregate with disease (data not shown). The exon 7 G76A nucleotide substitution results in the conservative substitution, G345S and would appear to be a common polymorphism. Direct sequencing of all relatives (data not shown) revealed a number of affected and unaffected individuals who were homozygous for the sequence change. Furthermore, the population prevalence of the polymorphism in our 100 controls was 22%, established by direct sequencing.

Figure 54 shows the conservation of glycine at position 345 amongst other mammalian filensin orthologs. Table 41 and figure 55 summarise the significant findings of *PredictProtein* protein prediction [279] and DNAStar Protean software respectively.

Table 41: summary of *PredictProtein* protein modelling of filensin

at codon 345	Filensin	G345S filensin
cAMP/cGMP –dependent protein kinase phosphorylation site	No	No
Protein kinase C phosphorylation site	No	Yes
Casein kinase II phosphorylation site	No	Yes
Tyrosine kinase phosphorylation site	No	No
N-myristoylation site	No	No
Coiled coil	No	No
Helix / strand / loop	No	No

Animal	% of pairwise sequence identity with human filensin
Chick	50
Rat	68
Bovine	71

Figure 54 shows that the glycine at position 345 is conserved in bovine but not in rat or chick filensin proteins (results of NCBI BLAST alignment).

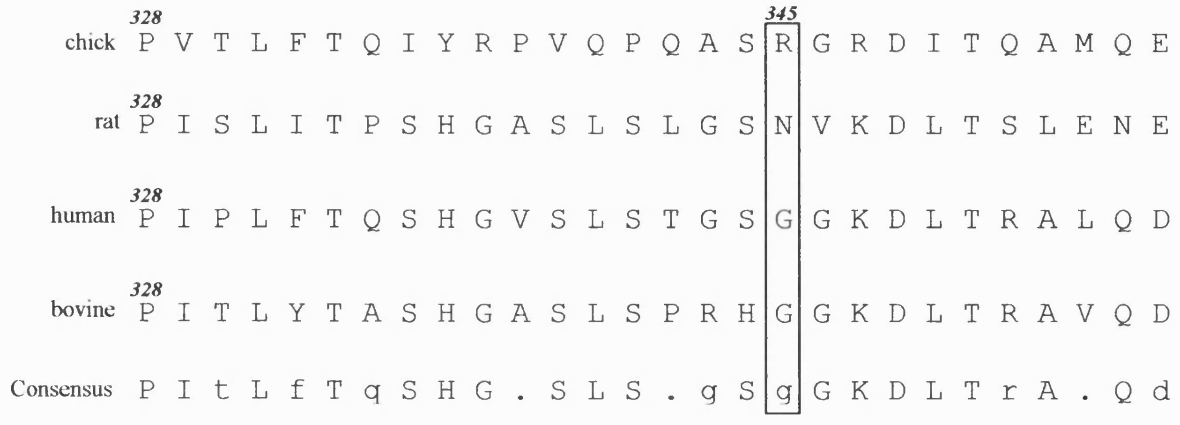

Figure 55: filensin protein modelling

a, wild-type filensin

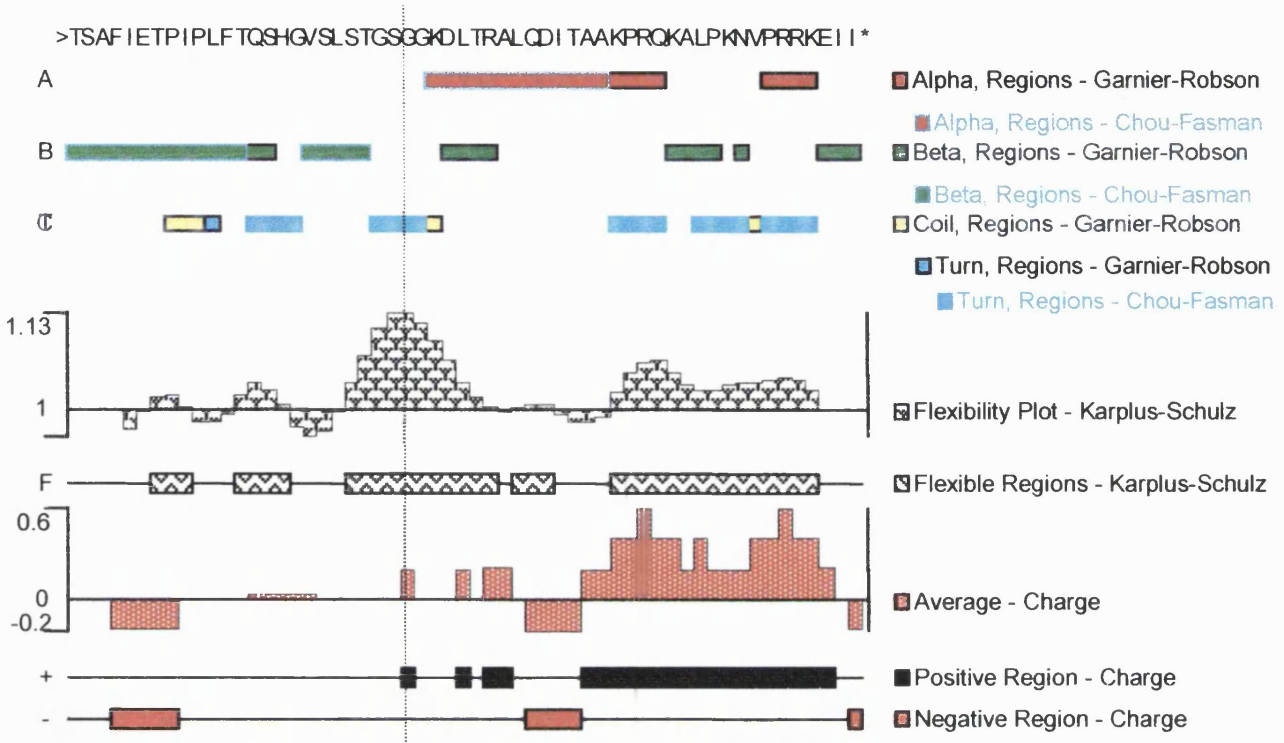

b, filensin-G345S

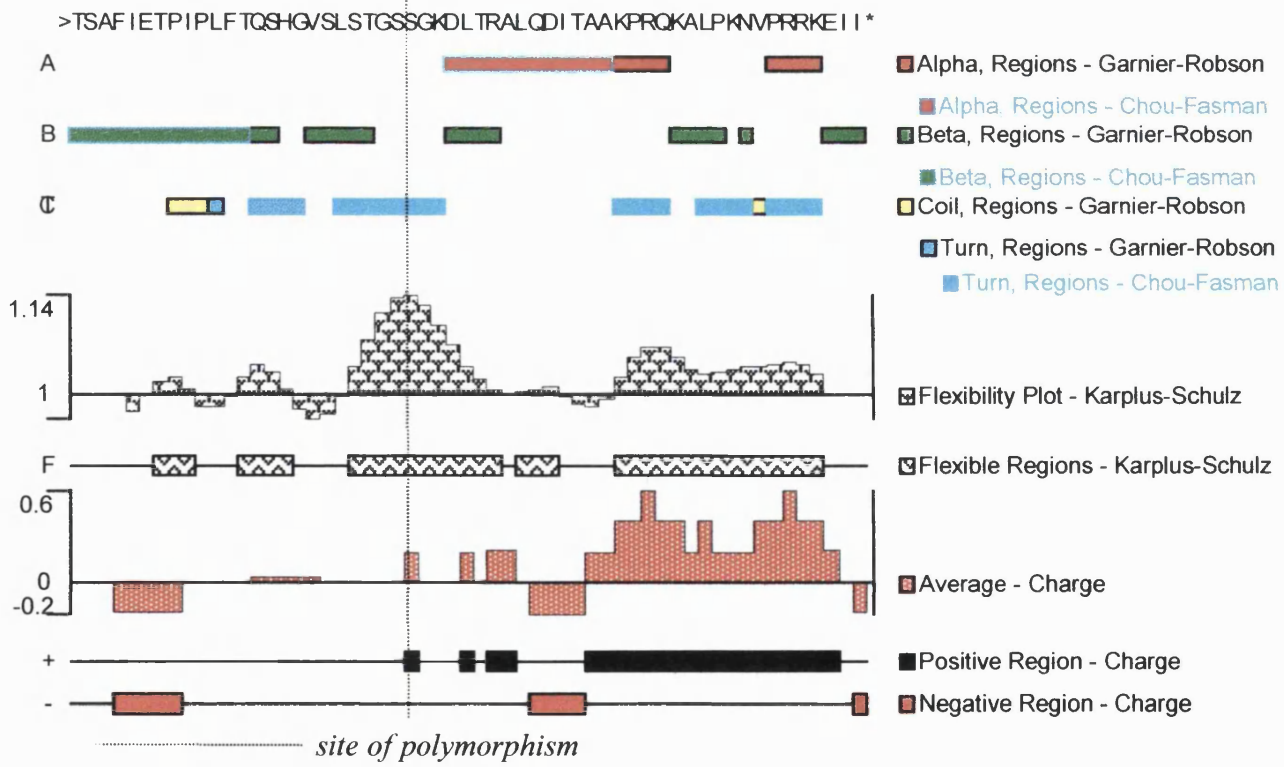

3.11 Cataract candidate gene screening

A number of families were screened for genetic linkage to candidate loci and the exclusion data is presented here.

Table 42 lists the candidate genes excluded and the tetranucleotide markers chosen that span the gene interval of interest. Marker pairs approximately 10cM apart were chosen in each case. Linkage to all cataract candidate loci was excluded in the following families: M (tables 43 and 44), E (table 45 and 46), O (tables 47 and 48).

Table 42: cataract candidate genes and loci excluded: chromosomal location, tetranuclucleotide marker pairs (with maximum amplified size)
(on this and following page)

Marker	chr	gene/locus	phenotype	Size (base pairs)
D1S468	1p36		Volkmann, posterior polar	173-191
GATA124F08	1q21	connexin50	pulverulent	229-245
D1S2141	1q21			236-263
D2S427	2q33	γ-crystallin	nuclear, lamellar,	251-263
GATA178GO9	2q33	clustter	Coppock-like	171-195
D3S1744	3q21	γS-crystallin		131-167
D3S3053	3q21	BFSP-2	lamellar/	203-245
D3S2427	3q21		sutural	203-245
D4S2623	4q28	RIEG1	Rieger's	205-241
D4S1644	4q28		syndrome	186-206
D10S1213	10q24	PITX3	total	93-133
D10S1248	10q24			241-261
D11S1981	11p13	PAX6		134-178
ATA34E08	11p13			156-171
D11S1998	11q	α2-crystallin		129-165
D11S4464	11			225-249

Marker	chr	gene/locus	phenotype	Size (base pairs)
D12S1052	12q14	MIP	polymorphic	149-165
D12S1064	12q14			173-197
D13S1493	13q11	connexin46	pulverulent	223-243
D13S894	13q11			180-200
D13S317	13q13			175-199
D13S800	13q13			259-319
D16S748	16p13	μ-crystallin		187-214
D16S764	16p13			96-116
D16S402	16q22	Marner	pulverulent	161-187
D16S539	16q22		posterior polar	148-172
D17S1298	17p13		anterior polar	246-258
D17S974	17p13		cataract	201-217
D17S1294	17q11	βA3-	sutural	248-272
D17S1293	17q11	crystallin		262-290
D17S1301	17q24		cerulean	147-163
D17S784	17q24			226-238
D19S589	19q13	LIM2		161-181
D19S254	19q13			110-150
D20S477	20q	filensin		240-268
D20S478	20q			243-275
GATA188F04	21q22	α-crystallin	central nuclear	117-193
D21S1446	21q22			209-223
GCT10C10	22q11	β-crystallin	cerulean Coppock-like	192-210

Table 43: family M lod scores for linkage to cataract candidate genes

Marker	LOD score (Z) at recombination (θ) of									
	0	0.05	0.1	0.15	0.20	0.25	0.30	0.35	0.40	0.45
D1S468	-∞	-2.60	-1.52	-0.94	-0.57	-0.32	-0.15	-0.05	0.01	0.02
D1S2141	-∞	-2.37	-1.34	-0.83	-0.52	-0.34	-0.21	-0.14	-0.08	-0.04
GATA 124F08	-∞	0.01	0.37	0.48	0.48	0.48	0.41	0.31	0.18	0.08
D2S427	-∞	-2.88	-1.77	-1.70	-0.77	-0.49	-0.30	-0.16	-0.07	-0.02
GATA 178G09	-∞	-0.49	0.2	0.5	0.64	0.68	0.65	0.56	0.42	0.23
D3S1744	One allele only									
D3S3053	-∞	-3.91	-2.51	-1.75	-1.24	-0.87	-0.61	-0.40	-0.23	-0.11
D3S2427	-∞	-0.08	0.09	0.14	0.14	0.12	0.08	0.05	0.02	0.01
D4S2623	-∞	-0.79	-0.10	0.20	0.35	0.38	0.36	0.29	0.20	0.10
D4S1644	-∞	-1.33	-0.57	-0.19	0.03	0.15	0.22	0.22	0.18	0.11
D10S1213	-∞	-2.50	-1.66	-1.21	-0.91	-0.67	-0.48	-0.33	-0.20	-0.09
D10S1248	-∞	-2.34	-1.30	-0.77	-0.44	-0.23	-0.09	-0.01	0.03	0.03
D11S1981	-∞	-0.79	-0.10	0.20	0.34	0.38	0.36	0.29	0.20	0.10
ATA34E08	-∞	0.49	0.85	0.97	0.97	0.90	0.79	0.64	0.46	0.24
D11S1998	-∞	-2.18	-1.37	-0.93	-0.65	-0.45	-0.31	-0.20	-0.12	-0.05
D11S4464	-∞	-3.61	-2.22	-1.46	-0.97	-0.62	-0.38	-0.20	-0.08	-0.02
D12S1052	-∞	-2.18	-1.37	-0.93	-0.65	-0.45	-0.31	-0.20	-0.12	-0.05
D12S1064	-∞	-1.06	-0.95	-0.01	0.16	0.25	0.28	0.28	0.20	0.16
D13S1493	-∞	-0.91	-0.42	-0.18	-0.05	0.01	0.04	0.04	0.03	0.01
D13S894	-∞	-0.55	-0.30	-0.17	-0.10	-0.05	-0.02	-0.01	0.00	0.00
D13S317	-∞	-2.05	-1.01	-0.48	-0.16	0.03	0.14	0.18	0.17	0.11
D13S800	-∞	-2.34	-1.37	-0.77	-0.44	-0.22	-0.10	-0.01	0.03	0.02
D16S748	One allele only									
D16S764	-∞	-1.11	-0.36	-0.01	0.16	0.25	0.27	0.26	0.20	0.12
D16S402	-∞	-3.63	-2.26	-1.52	-1.04	-0.70	-0.46	-0.28	-0.15	-0.06
D16S539	-∞	-0.63	-0.16	0.05	0.15	0.20	0.21	0.18	0.14	0.08

Marker	LOD score (Z) at recombination (θ) of									
D17S1298	-∞	-3.50	-2.37	-1.74	-1.30	-0.97	-0.71	-0.49	-0.30	-0.14
D17S794	-∞	-1.93	-1.16	-0.75	-0.49	-0.32	-0.19	-0.10	-0.04	-0.01
D17S1294	-∞	-2.91	-1.82	-1.24	-0.97	-0.62	-0.44	-0.32	-0.21	-0.12
D17S1293	-∞	-5.91	-3.91	-2.97	-2.04	-1.48	-1.05	-0.71	-0.42	-0.19
D17S1301	-∞	-0.48	-0.26	-0.16	-0.11	-0.07	-0.05	-0.03	-0.01	-0.00
D17S784	-∞	-4.53	-3.12	-2.32	-1.78	-1.36	-1.02	-0.72	-0.46	-0.22
D19S589	-∞	-3.63	-2.26	-1.52	-1.04	-0.70	-0.46	-0.28	-0.15	-0.03
D19S254	-∞	-1.35	-0.61	-0.24	-0.04	0.07	0.13	0.14	0.12	0.07
D20S477	-∞	-0.86	-0.40	-0.18	-0.06	0.01	0.04	0.06	0.05	0.03
D20S478	-∞	-0.20	-0.03	0.05	0.06	0.06	0.04	0.03	0.01	0.00
GATA188 F04	-∞	-0.84	-0.54	-0.35	-0.23	-0.14	-0.08	-0.04	-0.01	-0.00
D21S1446	-∞	-1.70	-0.96	-0.59	-0.37	-0.23	-0.13	-0.07	-0.03	-0.01
GCT10C10	-∞	-3.63	-2.26	-1.52	-1.04	-0.71	-0.46	-0.28	-0.15	0.06

Additional markers:

Tentatively positive lod scores are obtained for markers spanning the *PAX6* gene locus on 11p (Z_{max}=0.97 at θ=0.15 for marker ATA34E08). However the same recombinants persist for the intervening marker D11S1999 and new cross-overs appear in adjacent markers (D11S2362 and D11S1985). Table 44 summarises the lod scores for these markers.

Table 44: family M: lod scores for linkage to additional markers

Marker	LOD score (Z) at recombination (θ) of									
	0	0.05	0.1	0.15	0.20	0.25	0.30	0.35	0.40	0.45
D11S2362	-∞	-2.6	-1.52	-0.93	-0.57	-0.32	-0.18	-0.05	0.01	0.02
D11S1999	-∞	-0.79	-0.10	0.21	0.35	0.40	0.38	0.32	0.23	0.12
D11S1985	-∞	-3.75	-2.00	-1.59	-1.29	-0.83	-0.53	-0.31	-0.17	-0.07

Table 45: family E lod scores for linkage to cataract candidate genes

Marker	LOD score (Z) at recombination (θ) of									
	0	0.05	0.1	0.15	0.20	0.25	0.30	0.35	0.40	0.45
D1S468	-∞	-0.28	-0.07	-0.03	0.07	0.09	0.09	0.08	0.05	0.03
D1S2141	-∞	-2.81	-1.53	-0.87	-0.48	-024	-0.10	-0.03	-0.00	0.02
GATA 124F08	-∞	-2.85	-1.85	-0.84	-0.45	-0.22	-0.09	-0.03	-0.01	-0.00
D2S427	-∞	-2.66	-1.39	-0.75	-0.37	-0.14	0.00	0.07	0.09	0.07
GATA 178G09	-∞	-1.42	-0.90	-0.62	-0.45	-0.32	-0.23	-0.16	-0.10	-0.05
D3S1744	-∞	-0.88	-0.40	-0.15	-0.02	0.05	0.07	0.07	0.04	0.01
D3S3053	-∞	-2.78	-1.69	-1.10	-0.73	-0.46	-0.28	-0.15	-0.07	-0.02
D3S2427	-∞	-1.53	-0.80	-0.43	-0.22	-0.09	-0.02	0.02	0.04	0.03
D4S2623	-∞	-1.22	-0.58	-0.31	-0.19	-0.12	-0.08	-0.05	-0.02	-0.01
D4S1644	-∞	-0.39	-0.21	-0.15	-0.12	-0.10	-0.07	-0.04	-0.02	-0.00
D10S1213	-∞	-1.35	-0.79	-048	-0.29	-0.16	-0.08	-0.03	-0.01	-0.00
D10S1248	-∞	-1.35	-0.76	-0.44	-0.25	-0.13	-0.05	-0.01	0.00	0.00
D11S1981	-∞	-0.22	-0.04	0.03	0.05	0.06	0.06	0.05	0.04	0.02
ATA34E08	-∞	-1.65	-0.89	-0.52	-0.31	-0.18	-0.11	-0.06	-0.03	-0.01
D11S1998	-∞	-1.91	-1.00	-0.54	-0.27	-0.10	-0.01	0.03	0.05	0.03
D11S4464	-∞	-1.59	-0.86	-0.50	-0.30	-0.18	-0.11	-0.06	-0.03	-0.01
D12S1052	-∞	-2.09	-1.25	-0.79	-0.51	-0.31	-0.18	-0.09	-0.04	0.01
D12S1064	-∞	-1.73	-0.98	-0.61	-0.40	-0.26	-0.16	-0.09	-0.04	-0.01
D13S1493	One allele only									
D13S894	-∞	-0.47	-0.14	0.00	0.07	0.08	0.07	0.05	0.03	0.01
D13S317	-∞	-2.30	-1.37	-0.87	-0.55	-0.34	-0.19	-0.10	-0.04	-0.01
D13S800	-∞	-1.71	-0.89	-0.48	-0.25	-0.11	-0.04	-0.00	0.00	0.00
D16S748	-∞	-1.74	-1.01	-0.65	-0.42	-0.28	-0.17	-0.09	-0.04	-0.01
D16S764	One allele only									
D16S402	-∞	-1.82	-1.05	-0.66	-0.42	-0.26	-0.15	-0.09	-0.03	-0.00
D16S539	-∞	-0.91	-0.47	-0.28	-0.18	-0.12	-0.08	-0.05	-0.03	-0.01

Marker	LOD score (Z) at recombination (θ) of									
D17S1298	0.29	0.24	0.19	0.14	0.10	0.07	0.05	0.02	0.01	0.00
D17S794	-∞	-3.23	-1.90	-1.20	-0.76	-0.47	-0.28	-0.14	-0.06	-0.01
D17S1294	-∞	-1.96	-0.98	-0.51	-0.25	-0.11	-0.04	-0.01	-0.00	-0.00
D17S1293	-∞	-1.23	-0.64	-0.33	-0.16	-0.06	-0.02	0.00	0.00	-0.00
D17S1301	-∞	-2.00	-1.19	-0.76	-0.49	-0.30	-0.18	-0.09	-0.04	-0.01
D17S784	-∞	-0.57	0.02	0.28	0.39	0.42	0.38	0.31	0.22	0.11
D19S589	-∞	-2.36	-1.32	-0.79	-0.47	-0.26	-0.14	-0.06	-0.02	-0.00
D19S254	-∞	-0.26	-0.07	-0.01	-0.00	-0.01	-0.01	-0.01	-0.00	-0.00
D20S477	-∞	-1.45	-0.74	-0.40	-0.21	-0.11	-0.05	-0.02	-0.01	-0.00
D20S478	-∞	-4.53	-2.94	-2.02	-1.41	-0.97	-0.64	-0.40	-0.22	-0.09
GATA188 F04	-∞	-4.33	-2.66	-1.75	-1.16	-0.75	-0.45	-0.25	-0.11	-0.03
D21S1446	One allele only									
GCT10C10	-∞	-0.52	-0.23	-0.09	-0.01	0.03	0.04	0.04	0.02	0.01

Additional markers:

Inconclusive exclusion data were obtained for the 1p36 locus. Although there is no phenotypic correlation between the families an additional marker was examined which confirmed no linkage to this locus. Table 46 summarises the lod scores for these markers.

Table 46: family E: lod scores for linkage to additional markers

Marker	LOD score (Z) at recombination (θ) of									
	0	0.05	0.1	0.15	0.20	0.25	0.30	0.35	0.40	0.45
D1S243	-∞	-2.05	-1.12	-0.64	-0.35	-0.17	-0.06	-0.01	0.01	0.00

Table 47: family O lod scores for linkage to cataract candidate genes

Marker	LOD score (Z) at recombination (θ) of									
	0	0.05	0.1	0.15	0.20	0.25	0.30	0.35	0.40	0.45
D1S468	-∞	-0.57	-0.36	-0.21	-0.21	-0.18	-0.14	-0.11	-0.05	-0.01
D1S2141	-∞	-3.04	-1.92	-1.31	-0.91	-0.63	-0.42	-0.26	-0.15	-0.06
GATA 124F08	-∞	-1.34	-0.64	-0.32	-0.14	-0.05	-0.00	0.02	0.03	0.02
D2S427	-∞	-3.35	-2.12	-1.43	-0.98	-0.67	-0.44	-0.27	-0.15	-0.06
GATA 178G09	-∞	-2.19	-1.36	-0.91	-0.62	-0.41	-0.26	-0.15	-0.07	-0.02
D3S1744	-∞	-0.23	-0.07	-0.00	0.02	0.03	0.03	0.02	0.02	0.01
D3S3053	-∞	-1.19	-0.49	-0.18	-0.01	0.07	0.10	0.10	0.08	0.04
D3S2427	-∞	-2.92	-1.61	-0.93	-0.53	-0.28	-0.14	-0.06	-0.03	-0.02
D4S2623	-∞	-1.56	-0.73	-0.31	-0.07	0.06	0.13	0.15	0.13	-0.07
D4S1644	-∞	-2.44	-1.47	-0.95	-0.61	-0.38	-0.22	-0.12	-0.05	-0.01
D10S1213	One allele only									
D10S1248	-∞	-3.02	-1.88	-1.26	-0.85	-0.56	-0.35	-0.21	-0.10	-0.03
D11S1981	-∞	-1.74	-1.16	-0.84	-0.62	-0.46	-0.34	-0.23	-0.15	-0.07
ATA34E08	-∞	-0.77	-0.30	-0.10	0.00	0.04	0.05	0.05	0.04	0.02
D11S1998	-∞	0.16	0.40	049	0.49	0.45	0.38	0.30	0.21	0.11
D11S4464	-∞	-2.43	-1.60	-1.14	-0.84	-0.62	-0.45	-0.31	-0.20	-0.09
D12S1052	-∞	-1.45	-0.65	-0.26	-0.04	0.08	0.14	0.16	0.13	0.08
D12S1064	-∞	-2.76	-1.33	-0.61	-0.19	0.06	0.19	0.24	0.21	0.13
D13S1493	-∞	-1.85	-1.01	-0.59	-0.33	-0.18	-0.09	-0.04	-0.01	-0.00
D13S894	-∞	-1.89	-0.99	-0.52	-0.26	-0.02	0.01	0.01	0.01	-0.01
D13S317	-∞	-5.11	-3.36	-2.38	-1.72	-1.24	-0.87	-0.57	-0.36	-0.16
D13S800	-∞	-5.51	-3.61	-2.53	-1.81	-1.28	-0.88	-0.57	-0.33	-0.14
D16S748	-∞	-3.28	-2.16	-1.53	-1.11	-0.81	-0.57	-0.38	-0.22	-0.10
D16S764	-∞	-2.35	-1.15	-0.52	-0.14	0.08	0.20	0.24	0.22	0.14
D16S402	-∞	-0.53	-0.10	0.07	0.14	0.16	0.15	0.12	0.08	0.04
D16S539	-∞	-2.02	-1.02	-0.54	-0.25	-0.08	0.02	0.07	0.08	0.05

Marker	LOD score (Z) at recombination (θ) of									
D17S1298	-∞	-3.42	-2.17	-1.46	-1.00	-0,67	-0.43	-0.26	-0.14	-0.05
D17S794	-∞	-1.82	-1.06	-0.67	-0.44	-0.29	-0.19	-0.12	-0.07	-0.04
D17S1294	-∞	-0.01	0.22	0.31	0.32	0.30	0.25	0.19	0.13	0.06
D17S1293	-∞	-0.43	0.06	0.26	0.33	0.32	0.28	0.21	0.14	0.07
D17S1301	-∞	-3.58	-2.31	-1.61	-1.15	-0.83	-0.59	-0.41	-0.26	-0.12
D17S784	-∞	-1.59	-0.84	-0.46	-0.24	-0.11	-0.03	0.01	0.02	0.02
D19S589	-∞	-4.05	-2.46	-1.58	-1.02	-0.65	-0.39	-0.23	-0.12	-0.05
D19S254	-∞	0.89	1.21	1.28	1.23	1.11	0.95	0.76	0.53	0.28
D20S477	-∞	-2.27	-1.42	-0.96	-0.67	-0.46	-0.32	-0.20	-0.12	-0.05
D20S478	-∞	-4.75	-2.85	-1.80	-1.13	-0.67	-0.36	-0.16	-0.04	0.01
GATA188 F04	-∞	-2.31	-1.07	-0.44	-0.08	0.12	0.23	0.26	0.22	0.13
D21S1446	-∞	0.07	0.52	0.69	0.74	0.70	0.61	0.49	0.33	0.16
GCT10C10	-∞	-4.08	-2.72	-1.97	-1.48	-1.12	-0.83	-0.58	-0.37	-0.18

Additional markers:

The exclusion data for the 1p36 posterior polar cataract locus were inconclusive. Two additional markers (D1S160, D1S243) telomeric to D1S468 were therefore examined. A positive lod score (Zmax=1.28 at θ-0.15) for marker D19S254 indicated the possibility of more telomeric linkage. There is only one marker below (D19S246) and linkage is excluded. Table 48 summarises the lod scores for these markers.

Table 48: family O: lod scores for linkage to additional markers

Marker	LOD score (Z) at recombination (θ) of									
	0	0.05	0.1	0.15	0.20	0.25	0.30	0.35	0.40	0.45
D1S160	-∞	-1.18	-0.68	-0.43	-0.27	-0.17	-0.10	-0.06	-0.02	-0.01
D1S243	-∞	-1.70	-1.01	-0.64	-0.40	-0.24	-0.14	-0.07	-0.03	-0.01
D19S246	-∞	-4.55	-2.88	-1.97	-1.37	-0.95	-0.65	-0.42	-0.24	-0.11
D21S2437	-∞	-2.32	-1.40	-0.90	-0.58	-0.35	-0.20	-0.10	-0.03	-0.00
GATA129 D11	-∞	-3.77	-2.33	-1.53	-1.03	-0.67	-0.42	-0.24	-0.12	-0.04

3.12 Mapping a locus for stationary posterior polar cataract (family O)

Table 49: Genome-wide linkage search family O. Additional markers used are shown in italics

Marker	LOD score (Z) at recombination (θ) of									
	0	0.05	0.1	0.15	0.20	0.25	0.30	0.35	0.40	0.45
Chromosome 1										
D1S468	-∞	-0.57	-0.36	-0.21	-0.21	-0.18	-0.14	-0.11	-0.05	-0.01
D1S1612	-∞	-1.45	-0.73	-0.39	-0.20	-0.09	-0.07	-0.03	0.01	0.00
D1S1597	-∞	-5.00	-3.11	-2.05	-1.36	-0.88	-0.55	-0.31	-0.15	-0.05
D1S552	-∞	-3.58	-2.25	-1.55	-1.09	-0.78	-0.55	-0.37	-0.22	-0.11
D1S1622	-∞	-3.29	-2.15	-1.51	-1.08	-0.78	-0.54	-0.35	-0.21	-0.09
GATA129H04	-∞	-1.94	-0.92	-0.40	-0.11	0.07	0.16	0.19	0.17	0.11
D1S2134	-∞	-0.67	-0.22	-0.03	0.05	0.08	0.08	0.06	0.03	0.01
D1S1665	-∞	-1.46	-0.94	-0.66	-0.48	-0.35	-0.25	-0.17	-0.10	-0.05
D1S1728	-∞	-5.40	-3.60	-2.52	-1.80	-1.28	-0.88	-0.57	-0.33	-0.14
D1S551	-∞	-3.89	-2.63	-1.90	-1.40	-1.02	-0.73	-0.50	-0.30	-0.14
D1S1588	-∞	-3.72	-2.51	-1.82	-1.34	-0.98	-0.69	-0.47	-0.28	-0.13
D1S1631	-∞	-0.63	-0.36	-0.23	-0.16	-0.13	-0.11	-0.09	-0.07	-0.04
GATA176G01	-∞	-2.50	-1.51	-1.00	-0.70	-0.49	-0.34	-0.23	-0.14	-0.06
D1S534	-∞	-2.58	-1.67	-1.15	-0.81	-0.56	-0.38	-0.24	-0.13	-0.05
D1S1679	-∞	-4.40	-2.75	-1.85	-1.27	-0.86	-0.57	-0.36	-0.21	-0.10
D1S1677	-∞	-1.38	-0.83	-0.54	-0.35	-0.22	-0.13	-0.07	-0.03	-0.01
D1S1589	-∞	-3.10	-1.97	-1.35	-0.94	-0.64	-0.42	-0.26	-0.14	-0.06
D1S518	-∞	-1.75	-0.75	-0.26	0.01	0.16	0.23	0.23	0.19	0.11
D1S1660	-∞	-1.58	-0.73	-0.31	-0.07	0.06	0.12	0.14	0.12	0.07
D1S1678	-∞	-3.08	-1.99	-1.39	-1.00	-0.72	-0.51	-0.34	-0.21	-0.09
GATA 124F08	-∞	-1.34	-0.64	-0.32	-0.14	-0.05	-0.00	0.02	0.03	0.02
D1S2141	-∞	-3.04	-1.92	-1.31	-0.91	-0.63	-0.42	-0.26	-0.15	-0.06
D1S549	-∞	-0.54	-0.29	-0.17	-0.11	-0.07	-0.04	-0.02	-0.01	-0.00
D1S3462	-∞	-2.74	-1.78	-1.23	-0.87	-0.60	-0.40	-0.25	-0.14	-0.06

Marker	LOD score (Z) at recombination (θ) of									
	0	0.05	0.1	0.15	0.20	0.25	0.30	0.35	0.40	0.45
D1S235	-∞	-0.99	-0.48	-0.24	-0.10	-0.03	0.00	0.01	0.01	0.00
D1S1609	-∞	-3.06	-1.95	-1.34	-0.94	-0.65	-0.43	-0.27	-0.15	-0.06
Chromosome 2										
GATA165C07	-∞	-5.52	-3.57	-2.49	-1.78	-1.27	-0.88	-0.59	-0.35	-0.16
GATA116B01	-∞	-3.45	-2.09	-1.36	-0.88	-0.56	-0.33	-0.18	-0.08	-0.02
D2S1400	-∞	-2.69	-1.63	-1.07	-0.72	-0.47	-0.30	-0.17	-0.08	-0.03
D2S405	-∞	-0.32	-0.12	-0.04	-0.01	0.00	0.00	0.00	-0.00	-0.00
D2S1788	-∞	-2.03	-1.01	-0.49	-0.19	-0.00	0.10	0.14	0.13	0.09
D2S1356	-∞	-3.39	-2.23	-1.58	-1.15	-0.84	-0.61	-0.42	-0.26	-0.13
D2S2739	-∞	-4.68	-3.12	-2.23	-1.62	-1.16	-0.81	-0.54	-0.31	-0.14
D2S441	-∞	-1.64	-0.88	-0.51	-0.29	-0.15	-0.07	-0.02	0.01	0.01
D2S1394	-∞	-1.08	-0.58	-0.32	-0.17	-0.08	-0.02	0.01	0.02	0.02
D2S1777	-∞	-1.17	-0.67	-0.42	-0.27	-0.17	-0.10	-0.05	-0.02	-0.01
D2S1790	-∞	-0.84	-0.31	-0.07	0.06	0.11	0.12	0.11	0.09	0.05
D2S410	-∞	-2.17	-1.38	-0.98	-0.72	-0.55	-0.42	-0.32	-0.22	-0.12
D2S1328	-∞	-1.73	-1.01	-0.67	-0.48	-0.38	-0.31	-0.26	-0.21	-0.12
D2S1334	-∞	-1.99	-1.00	-0.51	-0.23	-0.06	0.03	0.07	0.08	0.05
D2S442	-∞	-0.65	-0.23	-0.06	0.02	0.06	0.08	0.08	0.06	0.04
D2S1353	-∞	-2.43	-1.42	-0.92	-0.61	-0.40	-0.26	-0.15	-0.08	-0.03
D2S1776	-∞	-2.14	-1.33	-0.90	-0.62	-0.42	-0.28	-0.18	-0.10	-0.04
D2S1391	-∞	-0.85	-0.36	-0.12	-0.01	0.07	0.10	0.10	0.08	0.04
GATA30E06	-∞	-0.47	-0.23	-0.12	-0.05	-0.01	0.02	0.02	0.02	0.02
D2S434	-∞	-1.40	-0.65	-0.27	-0.06	0.07	0.13	0.15	0.13	0.08
D2S1363	-∞	-1.50	-0.97	-0.70	-0.53	-0.41	-0.34	-0.22	-0.17	-0.09
D2S427	-∞	-3.35	-2.12	-1.43	-0.98	-0.67	-0.44	-0.27	-0.15	-0.06
GATA 178G09	-∞	-2.19	-1.36	-0.91	-0.62	-0.41	-0.26	-0.15	-0.07	-0.02

Marker	LOD score (Z) at recombination (θ) of									
	0	0.05	0.1	0.15	0.20	0.25	0.30	0.35	0.40	0.45
D2S125	-∞	-5.07	-3.28	-2.27	-1.59	-1.09	-0.72	-0.44	-0.24	-0.09
Chromosome 3										
GATA148E04	-∞	-3.36	-2.25	-1.49	-1.01	-0.68	-0.45	-0.29	-0.17	-0.07
D3S2406	-∞	-1.25	-0.48	-0.13	0.04	0.11	0.11	0.08	0.03	0.00
GATA128C02	-∞	-3.08	-2.08	-1.51	-1.12	-0.83	-0.61	-0.42	-0.26	-0.12
D3S2459	-∞	-2.18	-1.37	-0.93	-0.65	-0.46	-0.32	-0.21	-0.12	-0.06
D3S3045	-∞	-2.14	-1.17	-0.69	-0.43	-0.27	-0.18	-0.13	-0.09	-0.04
D3S2460	-∞	-1.68	-0.97	-0.63	-0.44	-0.33	-0.26	-0.21	-0.16	-0.09
D3S1764	-∞	-3.92	-2.56	-1.81	-1.33	-0.99	-0.72	-0.50	-0.31	-0.15
D3S1744	-∞	-0.23	-0.07	-0.00	0.02	0.03	0.03	0.02	0.02	0.01
D3S1763	-∞	-2.89	-1.80	-1.22	-0.88	-0.58	-0.39	-0.24	-0.13	-0.05
D3S3053	-∞	-1.19	-0.49	-0.18	-0.01	0.07	0.10	0.10	0.08	0.04
D3S2427	-∞	-2.92	-1.61	-0.93	-0.53	-0.28	-0.14	-0.06	-0.03	-0.02
D£S1311	-4.16	-0.50	-0.21	-0.07	0.01	0.06	0.08	0.08	0.06	0.04
Chromosome 4										
D4S2366	-∞	-0.19	0.17	0.28	0.29	0.24	0.17	0.10	0.04	0.00
D4S403	-∞	-5.16	-3.37	-2.37	-1.69	-1.20	-0.82	-0.53	-0.30	-0.13
D4S2639	-∞	-2.70	-1.53	-0.92	-0.54	-0.30	-0.14	-0.05	0.00	0.02
D4S2397	-∞	-0.88	-0.21	-0.08	0.21	0.26	0.26	0.22	0.16	0.08
D4S2632	-∞	-3.45	-2.09	-1.37	-0.91	-0.60	-0.38	-0.22	-0.12	-0.05
D4S1627	-∞	-0.30	0.27	0.46	0.49	0.43	0.32	0.30	0.09	0.02
D4S3248	-∞	-0.98	-0.38	-0.09	0.06	0.13	0.15	0.14	0.10	0.06
D4S3243	-∞	-2.50	-1.63	-1.07	-0.70	-0.45	-0.27	-0.15	-0.06	-0.01
D4S2361	-∞	-4.23	-2.85	-2.00	-1.41	-0.98	-0.65	-0.41	-0.22	-0.09
D4S1647	-∞	-2.26	-1.43	-0.99	-0.70	-0.49	-0.34	-0.22	-0.12	-0.05

Marker	LOD score (Z) at recombination (θ) of									
	0	0.05	0.1	0.15	0.20	0.25	0.30	0.35	0.40	0.45
D4S2623	-∞	-1.56	-0.73	-0.31	-0.07	0.06	0.13	0.15	0.13	-0.07
D4S2394	-∞	-0.98	-0.54	-0.36	-0.27	-0.22	-0.19	-0.16	-0.13	-0.07
D4S1644	-∞	-2.44	-1.47	-0.95	-0.61	-0.38	-0.22	-0.12	-0.05	-0.01
D4S1625	-∞	-2.44	-1.41	-0.89	-0.57	-0.37	-0.23	-0.15	-0.09	-0.04
D4S1629	-∞	-3.74	-2.32	-1.56	-1.08	-0.75	-0.51	-0.33	-0.19	-0.08
D4S2368	-∞	-1.91	-1.14	-0.75	-0.58	-0.34	-0.22	-0.14	-0.08	-0.03
D4S2417	-∞	-1.25	-0.73	-0.46	-0.30	-0.19	-0.11	-0.06	-0.03	-0.01
D4S408	-∞	-2.16	-1.20	-0.69	-0.38	-0.18	-0.05	0.01	0.05	0.04
D4S1652	-∞	-1.84	-0.93	-0.44	-0.15	0.03	0.13	0.16	0.15	0.09
Chromosome 5										
D5S2488		-2.06	-1.15	-0.75	-0.54	-0.42	-0.33	-0.25	-0.15	-0.08
GATA145D10	-∞	-0.25	0.20	0.37	0.43	0.42	0.37	0.29	0.20	0.10
D5S2505	-∞	-3.21	-1.81	-1.16	-0.72	-0.42	-0.22	-0.08	-0.01	0.02
D5S807	-∞	-1.41	-0.88	-0.60	-0.42	-0.28	-0.20	-0.13	-0.07	-0.03
D5S817	-∞	-1.90	-0.97	-0.55	-0.32	-0.20	-0.13	-0.08	-0.04	-0.01
GATA134B03	-∞	-2.26	-1.29	-0.76	-0.45	-0.26	-0.14	-0.07	-0.03	-0.01
D5S1470	-∞	-2.67	-1.65	-1.12	-0.79	-0.57	-0.40	-0.27	-0.16	-0.07
D5S1457	-∞	-2.22	-1.43	-1.01	-0.74	-0.54	-0.39	-0.27	-0.17	-0.08
D5S2500	-∞	-1.69	-0.89	-0.49	-0.26	-0.11	0.02	0.03	0.04	0.03
D5S1501	-∞	-1.09	-0.62	-0.39	-0.25	-0.16	-0.10	-0.05	-0.02	-0.00

Marker	LOD score (Z) at recombination (θ) of									
	0	0.05	0.1	0.15	0.20	0.25	0.30	0.35	0.40	0.45
Chromosome 6										
F13A1	-∞	-1.67	-1.10	-0.78	-0.56	-0.40	-0.28	-0.18	-0.11	-0.05
D6S1053	-∞	-1.65	-0.84	-0.44	-0.22	-0.10	-0.05	-0.03	-0.03	-0.03
D6S1031	-∞	-4.76	-3.22	-2.33	-1.71	-1.25	-0.89	-0.60	-0.36	-0.16
D6S1056	-∞	-1.87	-0.85	-0.34	-0.05	0.11	0.19	0.21	0.18	0.11
D6S1021	-∞	-1.46	-0.91	-0.61	-0.41	-0.28	-0.19	-0.12	-0.07	-0.03
D6S474	-∞	-2.26	-1.02	-0.41	-0.07	0.11	0.20	0.22	0.19	0.11
D6S1040	-∞	-2.16	-1.35	-0.91	-0.63	-0.44	-0.29	-0.19	-0.11	-0.05
D6S1009	-∞	-1.93	-1.16	-0.77	-0.54	-0.39	-0.24	-0.21	-0.15	-0.08
Chromosome 7										
D7S1802	-∞	-1.75	-0.95	-0.55	-0.32	-0.17	-0.01	0.01	0.02	0.02
D7S1808	-∞	-2.77	-1.66	-1.07	-0.70	-0.44	-0.26	-0.14	-0.06	-0.01
D7S817	-∞	-2.80	-1.74	-1.18	-0.82	-0.58	-0.48	-0.28	-0.17	-0.08
D7S2846	-∞	-2.08	-1.09	-0.61	-0.33	-0.17	-0.07	-0.02	0.01	0.01
D7S1818	-∞	-1.48	-0.80	-0.48	-0.32	-0.23	-0.17	-0.13	-0.09	-0.05
GATA118G10	-∞	-2.84	-1.54	-0.88	-0.48	-0.24	-0.10	-0.02	0.01	0.01
D7S2204	-∞	-3.48	-1.92	-1.13	-0.65	-0.34	-0.14	-0.02	0.04	0.05
D7S820	-∞	-4.37	-2.74	-1.84	-1.24	-0.81	-0.50	-0.28	-0.12	-0.03
D7S821	-∞	-1.86	-1.12	-0.74	-0.49	-0.31	-0.19	-0.09	-0.03	-0.00
D7S2195	-∞	-2.28	-1.44	-1.00	-0.71	-0.52	-0.37	-0.25	-0.15	-0.07
GATA189C06	-∞	-1.74	-0.78	-0.33	-0.09	0.03	0.08	0.08	0.07	0.04
Chromosome 8										
D8S264	-∞	-2.17	-1.31	-0.85	-0.55	-0.35	-0.21	-0.11	-0.05	-0.01
D8S277	-∞	-0.81	-0.32	-0.10	0.02	0.08	0.10	0.09	0.07	0.04
D8S1106	-∞	-1.63	-1.01	-0.66	-0.43	-0.27	-0.16	-0.08	-0.04	-0.01

Marker	LOD score (Z) at recombination (θ) of									
	0	0.05	0.1	0.15	0.20	0.25	0.30	0.35	0.40	0.45
D8S1145	-∞	-3.03	-1.52	-0.74	-0.28	-0.00	0.15	0.22	0.21	0.14
D8S136	-∞	-4.06	-2.61	-1.82	-1.29	-0.93	-0.65	-0.45	-0.28	-0.13
D8S1477	-∞	-2.04	-1.27	-0.89	-0.69	-0.45	-0.36	-0.27	-0.17	-0.08
D8S1110	One allele only									
D8S1113	-∞	-2.74	-1.66	-1.09	-0.72	-0.48	-0.30	-0.18	-0.09	-0.03
Chromosome 14										
D14S261	-∞	-2.79	-1.68	-1.09	-0.71	-0.45	-0.24	-0.14	-0.06	-0.01
D14S283	-3.59	-0.87	-0.62	-0.47	-0.34	-0.24	-0.16	-0.10	-0.05	-0.02
D14S742	1.89	1.59	1.30	1.00	0.72	0.49	0.29	0.14	0.05	0.01
D14S972	-∞	-0.84	-0.36	-0.16	-0.07	-0.03	-0.01	-0.01	-0.00	-0.00
D14S80	-∞	-1.78	-1.18	-0.85	-0.62	-0.46	-0.33	-0.23	-0.15	-0.07
D14S1280	-∞	-0.81	-0.46	-0.34	-0.30	-0.28	-0.25	-0.21	-0.15	-0.08
D14S608	-∞	-1.33	-0.60	-0.24	-0.05	0.06	0.11	0.12	0.11	0.06
D14S306	-∞	-4.27	-2.78	-1.95	-1.41	-1.02	-0.72	-0.49	-0.30	-0.13
D14S592	0.12	0.17	0.19	0.19	0.18	0.16	0.14	0.11	0.07	0.04
D14S588	-∞	-4.42	-1.09	-0.67	-0.44	-0.29	-0.19	-0.12	-0.07	-0.04
D14S606	-∞	-0.96	-0.47	-0.24	-0.11	-0.03	0.01	0.03	0.04	0.02
GATA168F06	-∞	-0.91	-0.34	-0.06	0.10	0.17	0.20	0.18	0.14	0.08
GATA136B01	-∞	-2.37	-1.52	-1.04	-0.73	-0.50	-0.34	-0.21	-0.12	-0.05
Chromosome 16										
D16S748	-∞	-3.28	-2.16	-1.53	-1.11	-0.81	-0.57	-0.38	-0.22	-0.10
D16S764	-∞	-2.35	-1.15	-0.52	-0.14	0.08	0.20	0.24	0.22	0.14
D16S516	-∞	-4.15	-2.63	-1.79	-1.23	-0.83	-0.54	-0.33	-0.17	-0.06
D16S402	-∞	-0.53	-0.10	0.07	0.14	0.16	0.15	0.12	0.08	0.04
D16S539	-∞	-2.02	-1.02	-0.54	-0.25	-0.08	0.02	0.07	0.08	0.05

Marker	LOD score (Z) at recombination (θ) of									
	0	0.05	0.1	0.15	0.20	0.25	0.30	0.35	0.40	0.45
D16S515	-∞	-2.54	-1.49	-0.95	-0.61	-0.39	-0.23	-0.13	-0.06	-0.01
D16S752	-0.11	-0.02	0.04	0.06	0.07	0.06	0.05	0.03	0.01	0.00
D16S621	-∞	-3.81	-2.25	-1.40	-0.86	-0.50	-0.25	-0.09	-0.00	0.03
Chromosome 17										
D17S1308	-∞	-2.10	-1.31	-0.90	-0.64	-0.45	-0.31	-0.20	-0.12	-0.05
D17S1298	-∞	-3.42	-2.17	-1.46	-1.00	-0,67	-0.43	-0.26	-0.14	-0.05
D17S794	-∞	-1.82	-1.06	-0.67	-0.44	-0.29	-0.19	-0.12	-0.07	-0.04
D17S1303	-∞	-0.46	0.12	0.34	0.41	0.39	0.32	0.23	0.12	0.03
D17S947	-∞	-3.99	-2.45	-1.61	-1.07	-0.71	-0.44	-0.26	-0.13	-0.04
GATA185H04	-∞	-1.97	-0.88	-0.34	-0.03	0.14	0.23	0.24	0.20	0.12
D17S1294	-∞	-0.01	0.22	0.31	0.32	0.30	0.25	0.19	0.13	0.06
D17S1293	-∞	-0.43	0.06	0.26	0.33	0.32	0.28	0.21	0.14	0.07
D17S1299	-∞	-1.39	-0.66	-0.30	-0.10	0.00	0.05	0.06	0.05	0.00
D17S1290	-∞	-2.49	-1.59	-1.09	-0.76	-0.52	-0.35	-0.22	-0.13	-0.05
D17S219	One allele only									
D17S1301	-∞	-3.58	-2.31	-1.61	-1.15	-0.83	-0.59	-0.41	-0.26	-0.12
D17S784	-∞	-1.59	-0.84	-0.46	-0.24	-0.11	-0.03	0.01	0.02	0.02
D17S928	-∞	-2.51	-1.48	-0.95	-0.62	-0.41	-0.26	-0.16	-0.09	-0.04
Chromosome 18										
D18S481	-∞	-2.80	-1.90	-1.12	-0.76	-0.52	-0.35	-0.22	-0.12	-0.06
Chromosome 19										
D19S586	-∞	-5.87	-3.88	-2.77	-2.01	-1.46	-1.03	-0.68	-0.41	-0.18
D19S433	-∞	-1.44	-0.88	-0.57	-0.37	-0.24	-0.14	-0.08	-0.03	-0.01

Marker	LOD score (Z) at recombination (θ) of									
	0	0.05	0.1	0.15	0.20	0.25	0.30	0.35	0.40	0.45
D19S245	-∞	-3.16	-2.03	-1.40	-0.98	-0.68	-0.45	-0.28	-0.15	-0.06
D19S178	-∞	-4.62	-3.00	-2.12	-1.54	-1.11	-0.78	-051.	-0.30	-0.13
D19S246	-∞	-4.55	-2.88	-1.97	-1.37	-0.95	-0.65	-0.42	-0.24	-0.11
D19S589	-∞	-4.05	-2.46	-1.58	-1.02	-0.65	-0.39	-0.23	-0.12	-0.05
D19S254	-∞	0.89	1.21	1.28	1.23	1.11	0.95	0.76	0.53	0.28
Chromosome 20										
D20S103	-∞	-0.69	-0.21	-0.02	0.12	0.18	0.19	0.17	0.13	0.08
D20S482	-∞	-1.02	-0.55	-0.32	-0.20	-0.13	-0.09	-0.07	-0.05	-0.02
D20S851	-∞	-1.44	-0.89	-0.59	-0.39	-0.25	-0.15	-0.09	-0.05	-0.02
D20S604	-∞	-2.83	-1.75	-1.18	-0.81	-0.55	-0.36	-0.23	-0.12	-0.05
D20S470	-∞	-2.66	-1.36	-0.79	-0.32	-0.10	0.01	0.05	0.05	0.02
D20S477	-∞	-2.27	-1.42	-0.96	-0.67	-0.46	-0.32	-0.20	-0.12	-0.05
D20S478	-∞	-4.75	-2.85	-1.80	-1.13	-0.67	-0.36	-0.16	-0.04	0.01
D20S481	-∞	-1.90	-1.09	-0.65	-0.38	-0.21	-0.10	-0.03	0.10	0.17
D20S480	-∞	-3.26	-2.09	-1.44	-1.01	-0.70	-0.47	-0.30	-0.17	-0.07
D20S171	-∞	-3.83	-2.46	-1.72	-1.23	-0.88	-0.62	-0.41	-0.25	-0.11
Chromosome 21										
D21S1432	0.63	0.56	0.49	0.42	0.35	0.29	0.23	0.17	0.11	0.07
D21S1437	-∞	-2.32	-1.40	-0.90	-0.58	-0.35	-0.20	-0.10	-0.03	-0.00
GATA129D11	-∞	-3.77	-2.33	-1.54	-1.03	-0.67	-0.42	-0.24	-0.12	-0.04
D21S1440	-∞	-0.46	-0.26	-0.21	-0.21	-0.23	-0.22	-0.19	-0.14	-0.07
GATA188 F04	-∞	-2.31	-1.07	-0.44	-0.08	0.12	0.23	0.26	0.22	0.13
D21S1446	-∞	0.07	0.52	0.69	0.74	0.70	0.61	0.49	0.33	0.16

Marker	LOD score (Z) at recombination (θ) of									
	0	0.05	0.1	0.15	0.20	0.25	0.30	0.35	0.40	0.45
Chromosome 22										
D22S420	-∞	-2.37	-1.37	-1.14	-0.84	-0.62	-0.45	-0.23	-0.17	-0.07
GCT10C10	-∞	-4.08	-2.72	-1.97	-1.48	-1.12	-0.83	-0.58	-0.37	-0.18
D22S689	-∞	-2.53	-1.54	-0.98	-0.62	-0.37	-0.20	-0.09	-0.02	0.01
D22S685	-∞	-0.87	-0.32	-0.06	0.08	0.15	0.17	0.16	0.12	0.07
D22S683	-∞	-1.63	-0.91	-0.56	-0.37	-0.26	-0.20	-0.15	-0.12	-0.07
D22S445	-∞	-2.76	-2.33	-0.61	-0.19	0.06	0.19	0.24	0.21	0.13
Chromosome 11										
D11S898	5.27	4.75	4.21	3.66	3.09	2.50	1.89	1.29	0.73	0.27
D11S908	-∞	2.25	2.37	2.22	1.96	1.63	1.26	0.87	0.49	0.19

3.13 Creation of a mouse cDNA resource

RNA was extracted from whole mouse lens homogenates and reverse transcription used to create a stable cDNA resource. To confirm and establish the quality of RNA extracted, primers were used to amplify a region of the mouse actin gene which is ubiquitously expressed in mouse cells. Two mouse fibroblast cell lines were used as positive controls and zebrafish DNA used as a negative control (figure 56). The primers amplify a region of the gene that spans an intron. Thus if any contaminating genomic DNA was present a second heavier band would be observed (figure 56*a*, arrowed). Dnase treatment of the preparation (figure 56*b*) completely eradicated this band.

Figure 56: detection of mouse γ-actin cDNA in cDNA of extracted mouse lens mRNA
a, before DNase; *b*, after DNase

Lane:
1ϕ x174/HaeIII ladder
2 negative control
3 positve control (mouse γ-actin)
4 positve control (mouse γ-actin)
5 mouse cDNA
6 negative control
7 positve control (mouse γ-actin)
8 positve control (mouse γ-actin)
9 mouse cDNA
* = DNA contamination

Primer annealing temperature lanes 1-5: 55°C, lanes 6-9: 58°C

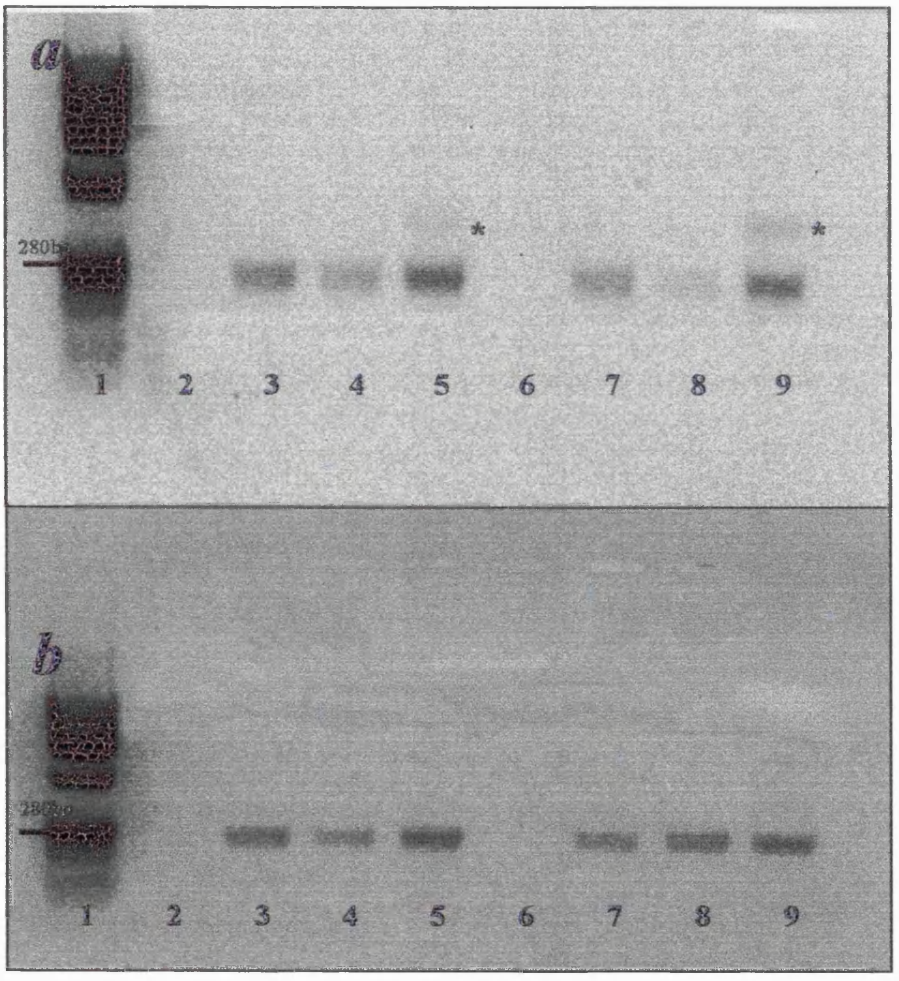

4. Discussion

4.1 General Comments

This is the largest study of congenital isolated non-syndromic cataract to date. Patients with cataracts of other aetiologies were excluded. In a two year period five hundred and eighty six individuals from 79 pedigrees were examined, phenotyped and blood or buccal swab samples taken for DNA extraction and linkage analysis and mutation detection.

4.1.1 Project Methodology

There are several methods of mapping human disease genes. As a condition, human inherited cataract is particularly genetically heterogeneous. Furthermore, a number of strong candidate genes have yet to be implicated in the disease and in all probability a number of presently unknown genes will be shown to be cataractogenic. In such circumstances, to maximise the efficiency with which novel mutations may be identified, a positional-candidate gene approach was employed where pedigrees were large enough for genetic linkage studies. A genome-wide search was then anticipated if linkage to known candidate loci was excluded. For small families, direct screening of cataract candidate genes by heteroduplex analysis or SSCP is most appropriate.

Particular logistical problems are raised if the disease of interest is uncommon, as is the case with inherited cataract where the incidence is probably less than 1 - 2 per 10000 live births. However, the wealth of clinical material at Moorfields Eye Hospital in addition to the enthusiastic response we have received country-wide from clinicians and patients alike, facilitated the identification of a large number of families suitable for linkage analysis. It is for these reasons, the methodology for the project was chosen.

The project structure is summarised in table 50.

Table 50: project structure

Stage	Activity	Period (months)
1	a) Establishing protocols b) Acquiring techniques c) Identifying families d) Initial contact letters sent	2
2	Patient ascertainment	6
3	a) Gene mapping b) Mutation detection c) Functional analysis	10
4	Patient ascertainment	2
5	a) Gene mapping b) Mutation detection c) Functional analysis	8
6	Preparation for the future a) future funding b) collaborations c) ascertainment of further clinical material	2

It was pragmatic to compartmentalise the project since patient ascertainment required a flexibility of time that conflicted with the rigour of laboratory technique. However many of the small families were acquired piecemeal during sections 3 and 5.

4.1.2 Ethical considerations

Careful consideration of the ethics of the project were made most particularly since the majority of individuals examined, ie unaffected individuals and spouses, were not under the care of any consultant ophthalmologist. Ethical committee approval for the examination and collection of tissue samples was granted by the Moorfields Eye Hospital ethics committee prior to the commencement of the study and renewed at appropriate intervals.

Written consent was obtained from all patients. Significant time was spent informing patients of the nature and methodology of the study. Furthermore, it was made clear that participation did not guarantee that the genetics underlying their condition would be revealed by the study, nor was the exercise diagnostic.

Every care was taken to inform patients of the scientific context of the project to avoid unrealistic hopes of cure and treatment in the immediate future. This point was particularly pertinent in some highly motivated families in whom many individuals were severely visually disabled.

Important issues of patient confidentiality were raised by the project. Firstly, contact letters were sent to probands at their current or last known address. To avoid any possible breach of confidentiality, no directly identifiable clinical details were included in these letters and a return-to-sender address always shown on each envelope. Examples of the correspondence can be found in appendix 1. Secondly, clinical information was not divulged to other family members during the course of the study.

Patients were invited to participate in the study by indicating their willingness on a form (included with a stamped addressed envelope, see appendix 1). Those that declined were not re-contacted. Those that did not reply were not pursued. In every instance, ophthalmic consultants and GPs were notified of their patient's intent to participate in the project to facilitate communication and to avoid any potential research conflict.

Other general ethical considerations regarding for example issues of non-paternity, consanguinity, divorce and separation were also heeded.

Patient information was kept in paper format in ring binder folders and stored in a locked cupboard in the Department of Molecular Genetics at the Institute of Ophthalmology. Patients' samples were also stored at the same site.

4.2 Phenotypes

4.2.1 What is a cataract?

Opacification of part or all of the crystalline lens of the eye is referred to as a cataract. An opacity is observed when a significant proportion of light in the visible spectrum, passing through that portion of the lens, is reflected. Such a loss of transparency could arise in several ways: (a) the accumulation or precipitation of abnormal material as was hypothesised to be the situation following the activation of the γE-pseudogene[156]; (b) precipitation of a normal lens constituent either as the result of insolubility, for example a mutated crystallin protein or as the result of disturbed homeostasis as may be the case in cataracts resulting from connexin mutations; (c) disturbance of ordered packing of the crystallin arrays, essential for transparency. Examples could be a mis-folded mutant crystallin molecule or if a cytoskeletal element is mutated; (d) disorganisation of the ordered packing of the lens fibres themselves as might result from abnormal cell-to-cell adherence or severe disturbance or the cellular environment. In almost all instances functional analyses are still awaited before precise pathophysiological mechanisms can be established.

4.2.2 The sample

Sampling in this study was opportunistic and for the most part limited to pedigrees of those probands referred to Moorfields Eye Hospital or other regional ophthalmic hospitals. The study was also limited to large families that were suitable for linkage analysis or smaller pedigrees in whom an inheritance pattern was clear. Both raise the possibility of ascertainment bias. However, given the large number of participants and the very low number of refusals, it is reasonable to assume that this may not have affected the distribution of phenotypes, the patient group therefore being representative of the non-syndromic inherited cataract population as a whole.

Overall, we found that nuclear cataract was the most common phenotype. Other frequently encountered phenotypes included posterior polar, lamellar and pulverulent. The remainder were uncommon. There are several possible explanations for these variations in prevalence. The poor visual prognosis for nuclear cataract may result in over-representation of this phenotype due to referral bias or this phenotype may encompass several as yet undefined subgroups of inherited cataract. Alternatively, certain phenotypes may be more rare because they may be more biologically disadvantageous resulting in eradication of the mutation by selection pressures. Assuming that low-copy eukaryotic genomic DNA has a constant mutation rate, it is possible that more (or larger!) genes will be implicated in the more common phenotypes.

4.2.3 Phenotypic heterogeneity

This study has revealed the remarkable phenotypic heterogeneity of human inherited cataract. No agreed nomenclature for the appearances seen is agreed though several classification and clinical grading systems have been suggested, exclusively for adult cataract and mainly for the assessment of severity and visual impact[197 212-219].

We propose that all pedigrees with human isolated non-syndromic cataract encountered can be classified as one of the ten following types: anterior polar, posterior polar (stationary or progressive), nuclear, lamellar, coralliform, blue-dot (cerulean), cortical, pulverulent, polymorphic or lattice. Given that some of these phenotypes mainly describe the geographical location of opacification, it is possible that subgroups within these categories may exist and further sophistication of this nomenclature is therefore anticipated. Other phenotypes not encountered in this study have been reported but have either been described in individual cases (and not in families) or are very uncommon. Furthermore, it has not been possible to accommodate those eponymous cataracts, such as the "Coppock-like"[156] or "Marner"[175] phenotypes since no accurate clinical description is available.

Although an attempt was made to examine the phenotypes of all family members at risk of inheriting the affected gene, the description of intra-familial variation in the phenotypes was limited by the number of patients who had already undergone surgery. This is a limitation inherent in all studies of early onset inherited cataract and as detailed a description as possible was obtained from the hospital records in such cases.

The penetrance of cataracts in the families was complete though expressivity was highly variable. With the exception of the polymorphic and pulverulent pedigrees, cataract morphology was consistent amongst all individuals within each family. Several authors have described intra-familial clinical heterogeneity in human inherited cataract, including inter-ocular variability in some individuals[212 229 284]. This was certainly the case with the polymorphic pedigree (see below). Inter-ocular variability in the distribution of cataract was observed in the pulverulent pedigrees, though the nature of the "dust-like" opacification was always preserved.

4.2.4 Novel phenotypes

Two novel phenotypes distinctive for both the distribution and appearance of the opacification were defined.

4.2.4.1 "Polymorphic" cataract

We documented a new inherited cataract phenotype (family A, figure 25) resulting from a mutation in the gene that encodes the major intrinsic protein of the lens (MIP), the most abundant membrane protein in the mature lens fibre cell. The genetic and functional analyses are described in detail below.

Growth of the crystalline lens throughout life results from the continual elongation and differentiation of equatorial epithelial cells to form concentric lamellae. In this way, the lamellar distribution of opacities seen in this family most probably reflects a distinct period of disturbance. Given that MIP is

a marker of secondary lens fibre differentiation, mutations would not be expected to result in opacification of the embryonic nucleus and indeed opacification is not observed in this portion of the lens in any of the affected members of the family.

To reflect the variable appearance between eyes and amongst individuals, the cataract phenotype was termed "polymorphic". In accordance with the polymorphic nature of opacification, the vision of affected individuals was highly variable (table 16) and largely reflected the established relationship between position of cataract within the lens and visual handicap[23].

The discrete punctate opacities are similar to the pulverulent phenotype, which is characterised by fine dust-like opacification. However the opacities in this pedigree are larger and critically, their position within the lens is consistent, contrasting markedly with the variable distribution of pulverulent opacities. Polar opacification is also not a feature of the pulverulent phenotype.

The phenotype observed in our family is also clearly distinct from the incompletely penetrant non-progressive polymorphic cataract mapped to chromosome 2q33-35 by Rogaev et al[230] in the Turkmen populations of the former Soviet Union. In this cataract opacities resembled lumps of grapes or cotton anywhere from the fetal nucleus to the equator. Polar opacification is also not a feature.

Although the mature lens fibre cell is metabolically inert, aquaporin mediated water-transport would be expected to continue, as it is not energy dependent. Thus, the progressive nature of the cataract might well be explained as the cumulative effect of cellular dysfunction over time. The presence of polar cataract is less easily explained but parallels the distribution observed in the *Cat*^{Fr} mouse.

Screening our panel of other families with isolated inherited congenital cataract identified a second pedigree (family J, figure 33, detailed below) with a different dominant missense mutation in the *MIP* gene[285]. Lens opacification in this family was non-progressive and confined to a peri-nuclear lamella. Such an observation is intriguing because it is not clear why two missense mutations in similar parts of

the gene would produce such strikingly different phenotypes. Furthermore, this provides the first confirmation of allelic heterogeneity in human inherited cataract.

4.2.4.2 "Lattice" cataract

In this phenotype, opacification, inherited as a fully penetrant autosomal dominant condition, is limited to the outermost layers cortical lens fibres (figure 26). The distribution of cataract suggests a defect in a gene expressed in later life and would appear to be a very rare phenotype. We have observed in our previous studies, another family with a cortical cataract. Contrastingly, opacification in this pedigree is limited to a portion of the superior lens cortex. We are in addition, aware of a pair of twins, genealogically unrelated to this family, with a similar phenotype.

Linkage analysis in these families will be intriguing. A good candidate would be α-crystallin whose predominant expression is in the adult lens. Widely expressed lens genes, for example phakinin, would be less likely to cause cortical cataract.

4.2.4.3 The "Coppock" cataract

The first description of a family with inherited isolated non-syndromic cataract was provided by Nettleship[9] in 1906. In this, the "Coppocks", all were residents of the Oxfordshire village of Headington Quarry, Headington. Indeed, of the original 1500 inhabitants , more than 300 were direct descendants of the founder. No photographs of the phenotype are available. Nettleship describes the cataract as "partial and often incomplete" and the patient is "often unaware ... and frequently shows no symptom". "The opacity takes the form of a sharply-defined circular disc placed deep in the lens between the nucleus and the posterior pole."

Until the 1960s, several of the Coppock family routinely attended for ophthalmic examinations at the Oxford Eye Infirmary (verbal communication Professor A Bron). Contact was then apparently lost

and this extensive family has never been the subject of a formal linkage study. Significant efforts were therefore made to identify and investigate the Coppock family. Unfortunately, despite consultation of relevant patient databases, a mail-shot and a visit to the village to examine direct descendants of family members described in the original article, no evidence of the original cataract could be found. The identification of visually insignficant peripheral punctate lens opacities in a grandmother, son and grandson is unfortunately unlikely to be of any significance.

It is clear that failure to find the Coppock cataract could be due to sampling error as it was not possible to identify all family members. It is probable that a number have moved out of the area and indeed, female descendants will have lost their maiden names through marriage. Alternatively, it is possible that the underlying mutation has been eliminated by chance or alternatively, confers a significant reproductive disadvantage. This latter supposition though is not born out by our family study.

4.3 Visual outcome and complications

4.3.1 The outcome for isolated inherited cataract is better than for other cataract aetiologies

This study is the largest series of patients with congenital cataract reported. In contrast to previous studies, in which cataracts of all aetiologies are included, our cohort consists of only those with isolated cataract. While cases were identified retrospectively, we examined all patients to improve data accuracy. Although opportunistic sampling of patient databases raises the possibility of ascertainment bias, the large number of eyes reported and the high response rate among those contacted suggests that our results reasonably reflect those of the study population as a whole. Although the outcome and prognosis for an eye is more likely to be similar to its fellow than to the rest of the study group, opacification was commonly asymmetric and un-adjusted data on all eyes is presented.

Overall, 50.1% (46.8% of those operated) in this study achieved a VA of 20/40 or better, 35.9% (36.1% of those operated) a VA between 20/50 and 20/200 and 14.0% (17.1% of those operated) worse than 20/200. These results compare favourably with previous reports[5 248]. Although visual acuity alone is a crude measure of visual function, it is probable that eyes affected by isolated inherited cataract do have a better prognosis; complications are less frequent following surgery (see below) and the patterns of opacification are probably less amblyogenic. To corroborate the latter, table 18 shows that opacities that are more diffuse or do not lie close to the visual axis (lamellar, pulverulent, polymorphic, coralliform and cortical) are associated with a better prognosis for vision.

In a recent study, Rahi et al[286] established that only 33% of patients in the United Kingdom with congenital cataract (all aetiologies) were diagnosed after one year of age. In our study, the mean age at diagnosis was 5.2 years and 4.5 years for those who underwent surgery. These results probably reflect changing practice and access to healthcare over several decades. However, the diagnosis of cataract seems surprisingly delayed given that in every family there was a history of congenital cataract.

In contrast to other studies[287 288], final visual acuity improved with later surgery in our patients, which may to some degree be as a result of improving surgical techniques. It is also likely that our results reflect the variable expressivity of dominant cataract. Opacification can be mild and surgical intervention reasonably delayed until a better surgical outcome is anticipated. In addition, some cataracts may be initially inconsequential but later progress, for example the progressive posterior polar and polymorphic phenotypes.

The reported incidence of glaucoma following surgery for cataracts of all aetiologies varies from 6-24%(ref. [245 246]). Secondary glaucoma can occur soon after surgery, for example pupil block or after many years (open angle). Eyes with co-existing ocular abnormalities including microphthalmia, microcornea, Nance-Horan ("floppy" iris), Lowe's oculocerebrorenal syndrome (trabecular dysgenesis), anterior segment dysgenesis and persistent hyperplastic primary vitreous have an increased risk of developing glaucoma following surgery[256]. The incidence of glaucoma (7.0%) in our patients is at the lower limit reported, most likely reflecting the absence of associated ocular abnormalities.

In the course of the study secondary open-angle glaucoma was diagnosed *de novo* in two individuals. Since it was not part of the study protocol to screen exhaustively for glaucoma, it is conceivable that a small number of cases remain undiagnosed.

Glaucoma developed more frequently in patients who underwent surgery before the age of 5 years probably because of the technical problems associated with surgery on the infant eye. Interestingly, the occurrence of glaucoma was exclusively bilateral suggesting that these eyes had some predisposition to the development of glaucoma.

As might be expected, the visual outcome for these patients was significantly prejudiced with only 24.0% of eyes achieving vision of 6/12 or better (as compared to 51.3% of the patient group as a whole) and 20.0% being absolutely blind.

Reports that the retinal detachment (RD) rate following congenital cataract surgery is similar to that following adult surgery are probably both anachronistic and underestimates given modern surgical techniques and the relatively short follow-up in the paediatric studies[245]. The incidence in our patients was 5.0% and the interval from cataract surgery to detachment was 22.3 years. It is suggested that certain surgical approaches and re-operations increase the risk of RD[263]. Adding weight to this view, the absence of concomitant ocular abnormalities in our patients did not appear to reduce the risk of RD. Furthermore, 65% of retinal detachments arose in those patients who underwent surgery before the age of 5 years, most likely reflecting the technical problems associated with surgery in this group.

4.3.2 Conclusions

Patients with isolated inherited congenital cataract have a better visual and surgical outcome than those with co-existing ocular and systemic abnormalities. The improved prognosis is related in part to the lack of other developmental abnormalities of the eye and also to the fact that inherited cataract is often partial at birth and surgery may be delayed to later infancy and childhood when there is a lower incidence of surgical complications. Certain inherited phenotypes (lamellar, pulverulent, polymorphic, coralliform and cortical) also appear to have a better prognosis and this should be born in mind when counselling these families.

4.4 Missense mutations in the gene encoding MIP, the major intrinsic protein of the lens (aquaporin-0) underlie cataract formation in humans

4.4.1 The aquaporin family of water channels

Water is the major component of all life forms, so the entry and exit of water from cells is a fundamental process of life. Physiologists have long recognised that plasma membranes of certain tissues must have water-selective pores to explain their high degree of water permeability. Attempts to identify molecular water channels initially proved difficult and discovery of the first aquaporin water-channel protein (AQP1) was serendipitous[76].

Studies of AQP1 expressed in *Xenopus laevis* oocytes demonstrate that this protein is a water-selective pore. Analysis of pure AQP1 reconstituted into membranes indicates a lack of permeability by other solutes including protons. Sequence analysis and membrane crystallographic studies predict a six transmembrane-domain protein that folds to resemble an "hourglass" with a central channel[77].

The presence of AQP1 in other tissues has been extensively documented and includes red blood cells, proximal tubules and descending loops of Henle in the kidney, aqueous humor-secreting epithelia in the eye and vascular endothelia. Humans with mutations in AQP1 (identified by the absence of the Colton blood group antigens) have a sub-clinical defect in renal urine concentration[289].

Failure to identify AQP1 in other water permeable tissues suggested the presence of a number of other aquaporins and nine sequence-related members have since been documented. These include aquaporin-0, formerly known as MIP, the major intrinsic protein of the lens, which is primarily and very abundantly found in the mature lens fibre cell membrane[76].

Prior to identification of mutations in MIP that cause cataracts in humans (discussed below) only AQP2 had been implicated in human disease. AQP2 is expressed in the principal cells of the renal

collecting duct, where vasopressin leads to the re-distribution of intracellular vesicles to the cell surface. Individuals with AQP2 mutations suffer from nephrogenic diabetes insipidus[93]. Interestingly, over expression of AQP2 is observed in rodent models of several clinical states such as lithium-induced polyuria, congestive heart failure and pregnancy[290].

4.4.2 Mutations in MIP, AQP0

Our data constitutes the first evidence implicating the major intrinsic protein of the lens, MIP or AQP0, in human cataract. MIP is synthesised as a 28kDa precursor and proteolysed by N and C terminal cleavage to produce a 22kDa protein which constitutes more than 50% of the total membrane protein. Although the monomeric protein has been shown to have water-channel properties (figure 57*e*), crystallographic analyses (figure 57*b* and 57*d*) strongly suggest that MIP molecules exist as homo-tetramers at the cell membrane[97].

The two mutations identified, C3795G and A3783G, result in the substitution of residues (T138R and E134G respectively), highly conserved not only amongst other members of the human aquaporin family but also between the AQP0 proteins from different species (figures 35, 36 and 55*a*). Alignment indicates that the threonine at codon 138 is conserved in all human aquaporins and the glutamic acid at codon 134 conserved in all but the aquaglyceroporins AQP -3, -7 and -9.

Based on amino acid sequence similarity, members of the aquaporin family are predicted to share a common topology consisting of six transmembrane domains (1-6) connected by five cytoplasmic loops (A-E). The two residues, E134 and T138 are located within transmembrane helix 4 (figure 37) and are probably equivalent to E142 and T146 respectively in AQP1.

Cryoelectron crystallographic studies[97 291] have determined the 3D density map of AQP1 at 6Å and 4.5Å which clearly show the monomer consists of six highly tilted, membrane-spanning α-helices that form two right handed bundles. The bundles consist of transmembrane helices 1-2-3, 4-5-6 and form

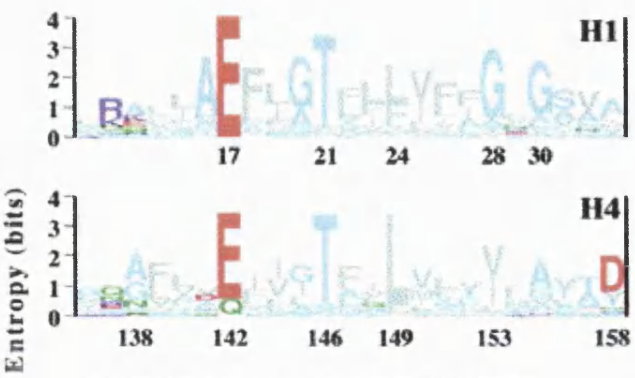

Figure 57: topography of the aquaporins (reproduced courtesy of Prof P. Agre)

a, multiple alignment of 164 AQP/GLP sequences and subsequent phylogenetic analyses yielded 46 subtypes. To identify critical residues, the 46 characteristic sequences were aligned and the conservation of each residue calculated. Sequence logos, whose heights are a measure of conservation, are drawn with the residue numbers for AQP1. They reveal the conservation patterns of helices H1 and H4. Colours: gray, hydrophobic; light blue, polar; green, amide; red, acidic; dark blue, basic.

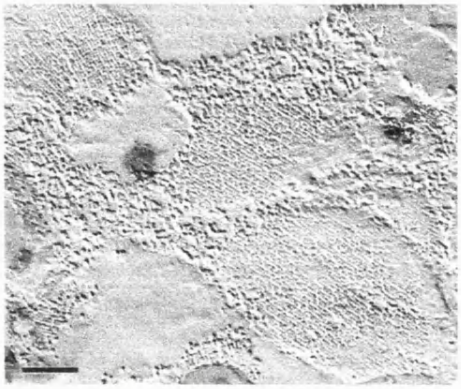

b, tetragonal arrays in lens fiber cell membranes are revealed by freeze-fracture techniques. The arrays are assembled from the major intrinsic protein, MIP, the first member of the water channel protein family to be sequenced (scale bar, 100nm)

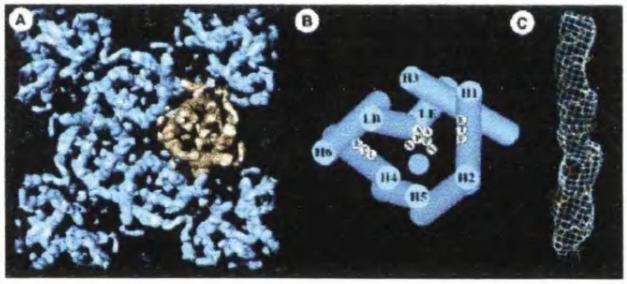

c, projection maps of water channel proteins acquired by cryo-electron microscopy. The maps reveal the structural similarity of the protein core that is embedded in the lipid bi-layer and well conserved during sample preparation in spite of surface tension and interaction with the supporting carbon film. (A) The red cell water channel, AQP1, at 3.5 Å resolution. AQP1 packs into arrays with P4212 symmetry, housing two tetramers per unit cell of size 96 Å. (B) The lens fiber cell water channel, MIP (AQP0), at 5.7 Å resolution. AQP0 packs into P4 arrays with a single tetramer per unit cell of 64 Å side length. The area shown comprises two unit cells. (C) The bacterial water channel, AqpZ, at 8 Å resolution. AqpZ is packed in an up-and-down orientation, as is AQP1, into unit cells of 94 Å width. All projections are viewed from the cytoplasmic side.

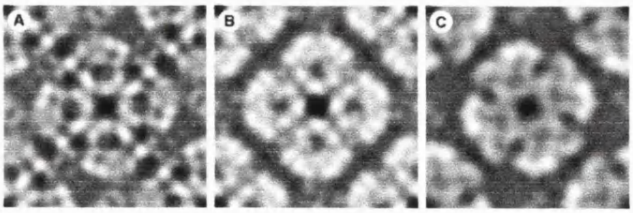

d, the tetrameric arrangement of AQP1 and its molecular architecture is demonstrated three-dimensionally at 6 Å resolution. (A) Cytoplasmic view of one unit cell comprising the central tetramer and four monomers in the opposite orientation at the corners. Gaps within the tetramer indicate the monomer boundary. (B) Helix assignment derived from multiple sequence alignment. The two NPA motifs are shown in the middle, and the hydrophobic residues on H1 (F) and H4 (L) are proposed to lie close to the channel (blue circle). (C) At 4.5 Å resolution, the helical nature of a membrane-spanning segment is revealed.

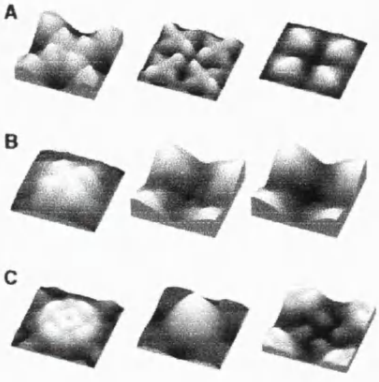

e, surface topographies of water channel proteins are distinctly different, reflecting the differences in their sequences that are found mainly in the helix-connecting loops. (A) Two-dimensional crystals assembled from AQP0 tetramers possess a P4 symmetry with one tetramer per unit cell of 64 Å width. Four bi-lobed domains protrude by 14 Å from the extracellular surface of AQP0 (left). They are involved in a 'tongue and groove' interaction in junctions formed by two packed crystal layers. The cytoplasmic surface exhibits four domains of 8 Å in height surrounding a depression about the 4-fold axis (center). Carboxy-peptidase Y treatment on mica removes these domains and identifies them as carboxylic (right). (B) AQP1 crystals have a symmetry and a corrugated extracellular surface with four protrusions of 12 Å in height (left). The cytosolic surface with four elongated peripheral and four small central domains produce a windmill-shaped structure with a height of 6 Å (centre). The C-terminus is located at a similar position as in AQP0. (C) AqpZ has an extracellular surface with four elongated peripheral protrusions and four central protrusions of 7 Å in height (left). Horizontal and vertical scaling are identical, but the gray level range is adapted to go from black to full white within each topograph.

the scaffold of the molecule (figure 57*c*). They are unusual in that the three helices form a roughly linear arrangement but not according to their position in the primary structure with the first helix of each bundle sandwiched between the other two helices: 2-1-3 and 5-4-6. The first two helices of each bundle (1 and 2, 4 and 5) run almost parallel to each other, tilting roughly to the same direction in the membrane. Whereas, the third helix is perpendicularly oriented to the axis defined by the first two and strongly cross-interacts with residues of its fellow bundle leading to intimate linking of the two protein halves. After helix 2, which crosses the membrane adjacent to helix 1, loop B immediately folds back into the membrane positioning an N-P-A motif in the middle of the two helical bundles, close to the centre of the lipid bi-layer. Loop E performs similarly thereby establishing the internal "hourglass" configuration.

Overall, folding in this way was thought to bring into close proximity several amino acids, principally E17, Q101, N76, N192, E142 (MIP E134) and T146 (MIP T138) in the core of the protein, providing a chain of polar residues predicted to line the water pore[77]. A refinement of this model suggests in fact that a highly conserved motif (E x x x T x x F/L) present in both the first and fourth transmembrane domains, lines the aqueous channel within each bundle[87]. The E and T residues are predicted to reside on the internal face of the fourth transmembrane α-helix. Significantly, these residues correspond exactly to the sites of the two mutations in our families.

Each of these substitutions will affect the change balance within the pore and might disrupt the passage of water molecules through the pore. Replacement of the negatively charged residue glutamate (E142, MIP E134) with glycine, a smaller but uncharged residue, eliminates a fixed charge lining the aqueous pathway (figure 38). Replacement of the polar residue threonine (T146, MIP T138) with the large residue arginine, introduces a strong positive charge in the channel (figure 38).

Alternatively, it is possible that the mutant proteins may mis-fold with failure to exit the endoplasmic reticulum (ER) or Golgi body. This has been observed experimentally in other mutated membrane

proteins, such as rhodopsin, the rod photoreceptor integral membrane protein and the cystic fibrosis transmembrane conductance regulator (CFTR)[292 293].

The topology of most eukaryotic membrane proteins is established co-translationally in the ER through a series of co-ordinated translocation and membrane integration events[294]. For AQP1, the initial topology of the protein synthesised in the ER includes four transmembrane α-helices and differs from the topology of the mature protein at the cell membrane which has six. Using epitope-tagged AQP1 constructs, it has been possible to show that maturation of the protein in the ER membrane involves a novel topological reorientation of three of the transmembrane domains (TD) and two of the connecting loops. During the synthesis of TDs 4-6, TD3 undergoes a progressive 180° rotation in which residues at the C-terminusare translocated from the cytosol to the lumen of the ER and vice versa its N-terminus, resulting in the mature six-TD protein. This re-orientation process is thought to be co-ordinated by sequence determinants N-terminal to TD2 and C-terminal to TD3. Although, from hydropathy plots, the mutations we have described do not substantially alter the hydrophobicity of TD4 as a whole, they do represent a significant change in amino acid size and hydrostatic charge and may thus affect topological reorganisation of the protein in the ER[295].

Failure to exit the ER is observed in the spontaneously-occurring mouse cataract mutant, *lop*, which has a dominant missense mutation resulting in the non-conservative substitution of alanine for proline at codon 51[75]. Human AQP2 missense mutants resulting in *recessive* forms of nephrogenic diabetes insipidus are usually retained in the ER (figure 58). *Dominant* AQP2 mutants are in contrast, sequestered at the Golgi apparatus. It is therefore suggested that the ability of this latter mutant to hetero-tetramize with wild-type AQP2 impairs further routing of functional water channels to the plasma membrane (figure 59), providing an explanation for dominance in this condition[296].

The functional implications for lens fibre physiology of MIP dysfunction are unknown. The main function of aquaporins is most likely to mediate rapid iso-osmolar fluid fluxes between the cytosolic and extracellular compartments. The consequences of a significant and geographically variable

reduction in functional water channels at the plasma membrane may thus be disturbance of water homeostasis resulting in for example localised precipitation of the lens crystallin arrays.

4.4.3 Phenotypic considerations

The ocular lens comprises a single layer of epithelial cells on its anterior surface and fibre cells that make up its volume. After formation of the embryonic nucleus, equatorial epithelial cells continuously elongate and differentiate into layers of new cells, which cover the previously synthesised fibre cells. Thus, the oldest fibres are surrounded and embedded into the center of the lens.

Lens opacities in individuals with the T138R mutation are discrete, progressive and distributed throughout the lens, implicating widespread ongoing lens fibre dysfunction. In contrast, the E134G cataract is limited to a specific lamella, within lens fibres that differentiated probably around the time of birth. This possibly suggests a "sensitive" period of lens development, where the lens fibre cells are more susceptible to disturbances in water homeostasis. Alternatively, MIP, which is present in very great numbers on the plasma membrane, may subserve a second as yet unknown, perhaps structural, role.

4.4.4 Conclusions

The identification of mutations in the *MIP* gene confirms that the major intrinsic protein of the lens plays an important role in the maintenance of optical clarity in the crystalline lens of the human eye. It is likely that the observed lens opacities result from abnormal water flux in mature lens fibres and possibly to structural changes induced by abnormal MIP molecules within the cell membrane.

It will be intriguing to establish whether MIP has a role in aged-related cataract, where the aetiology may be related to periods of dehydration[297].

4.5 Functional impairment of lens aquaporin in these two families with dominantly inherited cataracts

In order to establish pathophysiological relevance to cataract formation, the *Xenopus laevis* oocyte expression system was employed to evaluate functional defects in the mutant proteins, human MIP-E134G and MIP-T138R.

Xenopus laevis oocytes which are readily available, robust, large single cells are to date, the best method for examining aquaporin function. Previously, many studies have validated the model. Critically, it is well established that synthesis and cellular routing of aquaporins mimic that of the mammalian cell[76 281].

4.5.1 Preliminary experiments

Xenopus oocytes do not express aquaporin homologs at the cell membrane and have a low endogenous permeability to water molecules. Oocyte studies have established that orthologs of human MIP have a lower permeability to water molecules (P_f approximately 20 fold less) than other aquaporins, for example AQP1[64]. The P_f induced by *human* MIP has previously never been established. We therefore performed a number of preliminary experiments to calibrate the system.

Western blotting (using a rabbit anti-hMIP antibody directed towards MIP C-terminus) of oocyte total cell membrane preparations (including endoplasmic reticulum and Golgi apparatus) confirmed translation of wild type and both mutant proteins. Figure 39 shows that uninjected and water injected oocytes (negative controls) have a low basal water permeability. Oocytes micro-injected with 5ng bovine MIP exhibited an approximately four-fold increase in permeability to water when exposed to hypo-osmolar conditions at a physiological pH of 7.5. This is in agreement with other reports[64]. Oocytes micro-injected with 5ng human MIP exhibited an approximately three-fold increase in permeability to water in the same conditions suggesting that the molecules perform similar roles in the

lens. Doubling or halving the amount of cRNA injected did not significantly increase water permeability suggesting that the oocyte "protein translational apparatus" was saturated and changes in P_f were not dose-related.

4.5.2 Water permeabilities of oocytes expressing mutant MIP

Oocytes injected with 5ng cRNA of either of the mutants (MIP-T138R and MIP-E134G) abolished aquaporin-induced water permeability (figure 39*a*). Western blotting of total membrane preparations showed that less mutant protein was expressed compared to wild-type. However, increasing the cRNA micro-injected stepwise to 20ng did not increase P_f above basal levels. These results suggest that the mutations either result in disruption of water channel activity as predicted by sequence and structural analyses or that the mutant proteins are not trafficked to the cell membrane to participate in water transport (or some combination of both).

When wild-type and mutant proteins were co-injected in equal quantities, water permeabilities above basal levels were measured. These were however, not more than 25% above base-line, in contrast to the 3-fold increase induced by expression of the wild-type alone confirming that the mutants are able by some means to exert a dominant-negative effect.

Following the report that aquaporin function is further facilitated in more acidic conditions[298], we repeated the experiments at pH 6.0. The P_f of oocytes expressing bMIP rose to fivefold basal levels. A concomitant rise was observed with hMIP (Figure 39*b*). The P_f of mutant-expressing oocytes remained at basal levels.

By immunoblots, oocytes co-injected with wild-type and the E134G mutant were observed to express equal or greater amounts of MIP protein than oocytes injected with only wild-type AQP0 cRNA. In contrast, immunoblots of oocytes co-injected with wild-type AQP0 plus the T138R mutant cRNA always showed lower MIP protein expression. Since the antibody employed is directed towards the C-

terminus of the MIP protein and therefore has no selectivity for wild type or mutant, it was not possible to distinguish the relative contributions of each to the immunoblot bands. Nor was it possible to know the location of the protein (endoplasmic reticulum or plasma membrane). However, the results suggest that the T138R mutation either inhibits biosynthesis or increases degradation.

4.5.3 Immunohistochemical analyses

The possibility that the mutant proteins fail to traffic to the oocyte plasma membrane was investigated by confocal immunofluorescence microscopy. Control oocytes exhibited negligible immunofluorescence as expected, whereas oocytes injected with wild-type confirmed correct targeting of the protein correctly to the cell membrane.

In contrast, oocytes expressing MIP-E134G or -T138R showed immunofluorescence signal over the cytoplasmic space but no signal at the plasma membrane showing that the protein was sequestered in the cytosolic compartment and incorrectly targeted. Oocytes co-expressing wild-type plus E134G or T138R mutant exhibited immunofluorescence signal at the plasma membrane (reduced relatively to wild-type alone) as well as signal over the cytoplasmic space. Because the detecting antibody has no selectivity for wild-type or mutant MIP, it was not possible to know the distribution of the proteins in either compartment. It is reasonable to deduce however that the major constituent of the plasma membrane was wild-type MIP and since qualitatively less MIP was detected here when co-expressed with the mutant, it suggests that not only are the mutants not targeted but also that they interfere with trafficking of wild-type protein.

4.5.4 Summary

The oocyte swelling studies, immunoblots, and confocal immunofluorescence studies indicate that the human mutant polypeptides are expressed less efficiently than the wild-type protein and fail to traffic to the plasma membrane. Moreover, when co-expressed, both mutants interfere with function or

trafficking of the wild-type protein. This is very similar to the pathophysiology underlying cataract formation in the *lop* mouse and in families with dominantly inherited nephrogenic diabetes insipidus detailed above. A model of protein trafficking is thus proposed in figure 60.

It is strongly suggested by sequence and structural analyses that that the mutations would disrupt the water pore in the aquaporin molecule[291]. However since very little mutant protein appears to reach the plasma membrane it is not possible to know whether this is the case.

4.5.5 Phenotypic considerations

These functional analyses provide a coherent explanation of the dominant nature for the missense mutations. Furthermore, cataract formation, as the final common pathway of lens fibre dysfunction seems a reasonable outcome; a general reduction in membrane water permeability is likely to reduce the ability of cells to maintain solute homeostasis. Such a situation has been shown experimentally to result in precipitation of normally soluble cytosolic components, for example the crystallins, resulting in a loss of transparency/opacification.

Lens opacities in the E134G family are stationary and limited to specific central lamellae, corresponding to those fibres that differentiated at an early stage of life, possibly the late fetal period. Why the E134G mutation should result in cataract only localised to these lens fibres cannot be explained by the experiments. E134 is slightly less conserved phylogenetically than T138. The lens may be resistant to the consequences of the E134G mutation except during this developmental interval and most rapid period of lens growth[299].

The reduced overall AQP0 protein expression seen in the MIP-T138R/wild-type model suggests that it may be more disruptive to lens fibre physiology and may in part explain the more severe, widespread and progressive opacification observed clinically. Although the mature lens fibre cell is metabolically inert, aquaporin water transport would be expected to continue, as it is not energy dependent. Thus,

the progressive nature of the T138R cataract might well be explained as the cumulative effect of cellular dysfunction over time.

In many instances (table 51), the phenotypic appearances of murine cataract do not parallel closely that of the human. This is the case with both the Fraser and *lop* mice, which have progressive nuclear and polar opacification respectively. The lack of correlation makes comparison difficult.

Although distinct from the phenotype resulting from lens-specific connexin mutations, the punctate nature and distributional variability of opacification of the T138 mutation has some resemblance. Connexins, which co-oligomerise to form connexons, are also membrane proteins, involved in voltage-mediated intercellular solute transfer. It is possible that phenotypic similarities arise either from the same pathway to cataract formation or a possible intimate functional relationship with aquaporin role in maintaining the iso-osmotic cellular environment. Recent evidence suggests that at least some of the membrane-bound MIP molecules may, by virtue of their surface topology, form tongue-and-groove connections with MIP proteins of adjacent cells facilitating intercellular water flux. This mode of function is akin to connexins and may explain similarities in cataract phenotypes[87].

Taking the results and clinical observations together provides perhaps a strong clue to the fact that in the lens, MIP has been recruited for two different purposes. Firstly as a water channel and secondly as a structural protein, involved in maintaining the rigid and highly ordered lens fibre cell membrane but mediating cell-to-cell adherence. A model of such "gene sharing" already exists in the lens, *q.v.* the crystallins[53].

Figure 58: MIP targeting in *recessive* nephrogenic diabetes insipidus

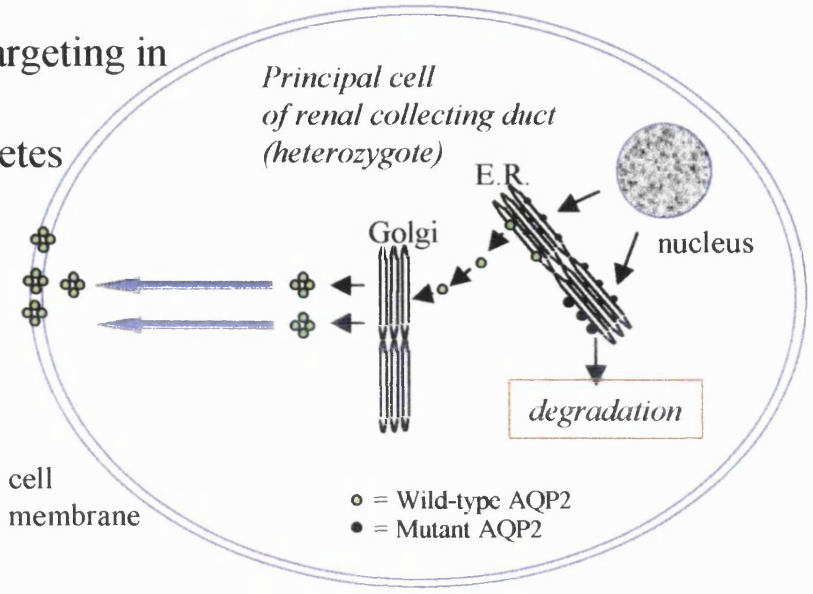

Figure 59: MIP targeting in *dominant* nephrogenic diabetes insipidus

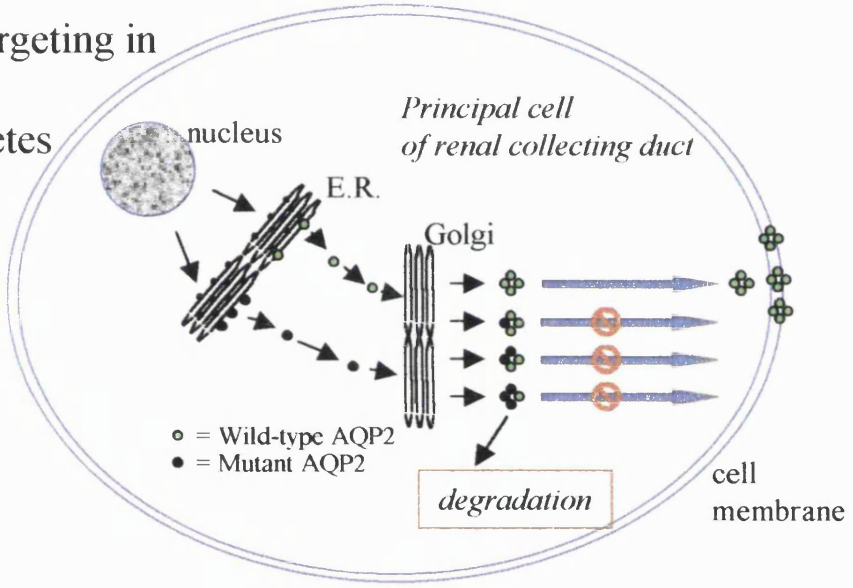

Figure 60: MIP targeting in *dominant* cataract

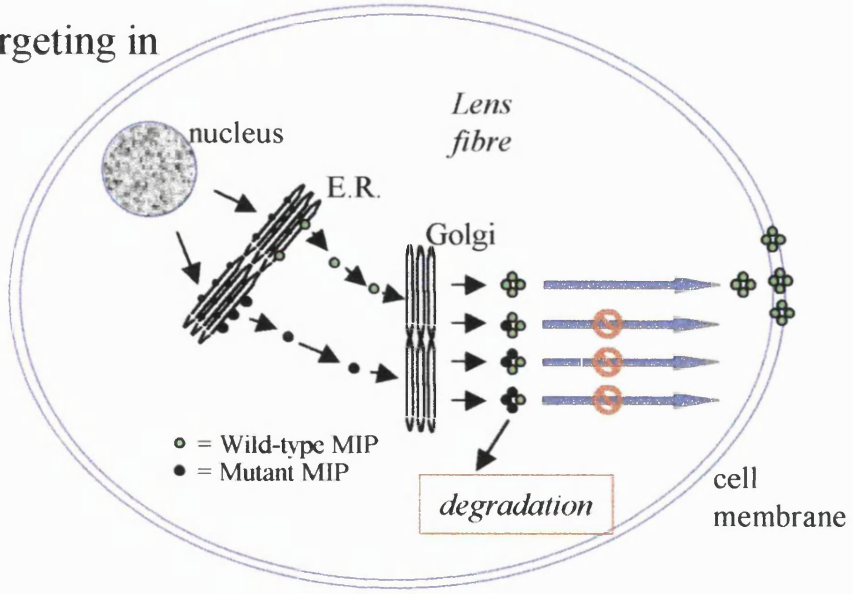

Table 51: mouse cataract models for which a human homologue is known

Mouse Model	Mutated Mouse Gene (human gene, if different)	Mouse Phenotype	Reference	Human Phenotype
No2	*connexin 50*	nuclear	[120]	pulverulent
Cat2^{t}	*γE-crystallin*	total opacity with microphthalmia	[119]	Coppock-like
Cat2^{elo}	*γ-E crystallin*	eye lens obsolescence (microphakia)	[121]	
ak	*Pitx3*	aphakia	[122]	total
	α3-connexin (connexin 46)	nuclear	[123]	pulverulent
Po	*βA3 crystallin*	nuclear	[124]	sutural
lop18	*αA-crystallin*	nuclear	[125]	zonular central nuclear
Philly (Phil)	*βB2-crystallin*	nuclear	[126]	cerulean / Coppock-like

4.5.6 Conclusions

The genetic analyses and functional studies of the mutant human proteins confirm that AQP0 provides critical functions in the human lens. Furthermore, it is unquestionable that the mutations identified in the two families are causative of the cataracts observed.

It remains uncertain whether the biochemical differences identified in the E134G and T138R mutants are directly responsible for the different clinical features of cataract in the two families. For example, it is unclear if the reduction in osmotic water permeability in oocytes expressing both wild-type AQP0 plus the E134G or T138R mutant polypeptides is only due to reduced membrane trafficking of tetramers containing a mix of wild-type and mutant subunits, or whether tetramers containing a mix of both subunits simply have a reduction in the unit water permeability. Nevertheless, our studies predict that other inherited or acquired defects in the AQP0 protein may underlie other forms of congenital cataracts in humans. Thus, it may also be informative to determine the deduced amino acid sequence encoded by genomic *AQP0* from cataract patients with predisposing conditions, such as diabetes mellitus, as well as from patients with the common, sporadic forms of adult cataract which are frequently found in older populations.

4.5.7 Future experimental strategies

We have been able to obtain lens material from a patient with the T138R mutation. H&E staining of fixed and mounted sections indicates normal lens fibre architecture. There are however no characteristic features that can reliably differentiate between cataractous and non-cataractous fibres. Unfortunately, we were unable by the end of this project to obtain human anti-MIP antibody. It will however be interesting to establish the distribution of MIP in these mature, probably cortical, lens fibres. It would be surprising if significant cytoplasmic fluorescence was observed given the absence of cellular organelles in these differentiated cells. To quantitate the levels of plasma membrane MIP and its distribution, comparison with normal control lenses and with a constitutively expressed protein

will be necessary. We also hope in the future to be able to obtain lens fibres from a patient with the E134G mutation.

Furthermore, the anterior capsule from this patient (with attached anterior epithelial cells) was sent to Dr Roy Quinlan, Dundee Hospital to be immortalised in a transformed cell line. Lens epithelial cells express only aquaporin-1. When it becomes technically feasible to direct these cells to differentiate into mature lens fibres, it may be possible to examine the cellular localisation and function of MIP in lens fibres themselves "in vitro".

The missense mutations detected are predicted to disrupt the channel through which water molecules pass. Since the mutant proteins were not trafficked to the cell membrane, we have not been able to directly measure abnormalities in water flux. The three-dimensional structure of several aquaporins has now been resolved to approximately 4.5 Å. We are engaged in discussions whether it may be possible to determine the secondary structure of our mutants by cryoelectron microscopy.

Another strategy would be to reconstitute purified MIP and the T138R/E134G mutants into liposomes[300]. The osmotic water permeability can then be measured in these proteoliposomes compared with control liposomes by for example stopped-flow light scattering[301]. It would not be useful to express the mutant in known mammalian cells lines and undertake water permeability studies as other aquaporins expressed by these cells would most likely compensate for any defect in AQP0 functionality.

The existence of two spontaneously occurring mouse strains with cataract that have mutations in the murine ortholog of MIP have disinclined us from creating a knock-in animal model though this remains a strategy to study the specific mutations we have detected.

Recent evidence from a twin study suggests that genotype may contribute up to 50% in determining development of adult cataract[302]. The primary and abundant expression *MIP*, the phenotypes and the

aetiological implication of dehydrational episodes in cataractogenesis[297], indicate that the gene would be a good candidate for this condition. We have already established collaboration with the St Thomas' Twin Study Unit[303] and are currently designing polymorphic markers around the MIP gene locus to enable detection of genetic linkage to *MIP* by transmission disequilibrium[304].

4.6 Mapping of the first family with isolated X-linked cataract

This is the first description of a family with isolated non-syndromic X-linked cataract. The existence of familial congenital cataract inherited in this way has been debated. The only possibly convincing X-linked pedigree previously described is that by Krill et al[192]. In this family, hemizygous males had sutural cataracts.

The differential diagnosis of X-linked cataract includes the syndromes of Nance-Horan, Lenz and Lowe. It has been suggested on the one hand that X-linked isolated cataract may be synonymous with Nance-Horan while others have proposed that since the conditions each map to Xp, all may be due to deletions of varying size within the region[185].

In our family, X-linked inheritance (with complete penetrance in heterozygous females) was suggested by affected individuals in successive generations, consistently severely affected males (requiring cataract surgery in the first months of life), contrasting markedly with asymptomatic or mildly visually disabled carrier females. Unfortunately, there were no male offspring born to affected males. Further support was lent by the cataract phenotype that consisted of a sea-fan of nuclear opacity in affected females and total opacity in hemizygous males; a combination of appearances not seen in autosomal dominant cataract. One female child with a unilateral cataract of a different phenotype, born to a mother and grandmother with no lens opacification was assumed to be a phenocopy.

Complex congenital cardiac anomalies were also noted in four of the six affected males and were not present in any unaffected individuals. The possibility that these abnormalities segregate with cataract formation in our family may prove instructive in identifying candidate genes. Several syndromes have been documented where congenital cataract and cardiac anomalies form a part. Arrhythmogenic right ventricular dysplasia associated with anterior polar cataract has been tentatively mapped to 14q[305 306] and the association of cataract, microphthalmia, septal heart defects and deafness has been reported as a dominantly inherited syndrome[307 308]. The oculo-facio-cardio-dental (OFCD) syndrome comprises cataract, microphthalmia, facial abnormalities, cardiac defect (atrial septal defect and VSD) together with dental abnormalities[309 310]. Interestingly, the condition appears to be X-linked and is lethal in hemizygous males, raising the possibility that a less deleterious mutation in the same gene might account for the spectrum of anomalies seen in our family.

To test the inheritance hypothesis, linkage analysis was performed across the X chromosome using the Genethon 5-10cM microsatellite marker set. Linkage to markers at Xp22.2 was detected and disease interval refined to lie between DXS9902 and DXS999 (Z_{max}=3.64 at θ=0 for marker DXS8036). The interval (*CXN, congenital X-linked nuclear cataract locus*) which is less than 2.5cM is encompassed by the Nance-Horan locus (DXS1053 – DXS443)[194 195]. This most likely suggests that allelic heterogeneity within the same gene can result in either isolated cataract or cataract associated with other systemic anomalies and thus refines the disease locus. Alternatively, in accord with the Warburg hypothesis and with the recognition that a microdeletion of Xp22.3 results in ocular anomalies (microphthalmia, sclerocornea) and cardiac anomalies associated with linear skin defects[311], a lens gene and one or more other genes may reside within the disease interval.

Although the *CXN* locus is gene rich, there is no obvious cataract candidate gene. As an initial strategy, the retinoic acid induced –2 (*RAI2*) gene was screened. This gene has been considered a strong candidate for Nance-Horan though recently excluded[194]. The precise function of RAI2 is unknown. The protein is one of several transcription factors upregulated by retinoic acid which have been implicated in the control of cellular differentiation[42]. *RAI2* has been shown to be expressed in

several tissues including the retina. Its presence in the lens is not established, however evidence that hypervitaminosis A in late fetal development results in congenital cataracts and ectopic expression produces lens opacification, indicates that RAI2 should be considered a candidate for human cataractogenesis[44]. Direct sequencing of the entire coding region including almost four hundred base pairs upstream did not reveal a segregating mutation.

A Bio-informatics approach was then used to identify novel genes within the disease interval. The PAC clone 245G19 (NCBI: Z92542) contains the sequence for *RS1*, the *retinoschisin* gene (mutations within which are responsible for X-linked retinoschisis). The gene is positioned within the *CXN* locus. A short distance upstream (120Kb) lies a sequence with homology to *connexin 43* (*CX43*). Connexin 43 (the actual gene resides on 6q14) is possibly expressed in the early embryonic human lens nucleus and thus activation of this pseudogene might cause cataract[106]. Interestingly, CX43 is also found in the heart, anomalies of which appear to segregate in our family[107]. On the basis of sequence evidence the sequence on Xp has been termed a *CX43* pseudogene (direct submission, C Bird, Sanger Centre, Cambridge, UK, 30/11/98); the first exon lacks an ATG start codon (present in *CX43*) and contains two STOP codons a short distance 3' by virtue of a frame shift induced by a single nucleotide deletion. For these reasons, this sequnce was not screened for mutations within the family.

Although the defect underlying X-linked cataract is unknown, it is tempting to speculate about the nature and function of the gene involved. Many X-linked dominant diseases are lethal to hemizygous males. In many instances, this is presumably because the complete absence or loss of functionality of a widely expressed protein is incompatible with life. It is therefore likely that the gene underlying cataractogenesis in our family is primarily expressed in the lens.

A number of progenitor cells differentiate to form the structures of the eye. It is suspected that the process of Lyonisation occurs shortly afterwards[312]. Cataract in our family is fully penetrant in heterozygous females. In each case, opacification is similar and limited to a portion of the lens nucleus and possibly in those cells derived from one or more lens progenitor cells in which Lyonisation has

inactivated the non-disease allele[313 314]. It is not clear however why transparency is maintained throughout life in those cortical lens fibre cells derived from those equatorial epithelial cells similarly Lyonised, though it is reasonable to suppose that the gene is not expressed in later life.

4.7 Mapping of a family with coralliform cataract to 2q33-q35

This study has shown that the coralliform phenotype is particularly rare amongst families with autosomal dominant congenital cataract. We were however fortunate to be able to make contact with a branch of the family originally described by Nettleship[239]. None of the affected individuals were phakic at the time of examination, so description of the cataract was taken from the original article.

At the time of the study, no mutation had been shown to underlie coralliform cataract formation. Given the remarkable phenotypic heterogeneity of the condition and evidence that a single gene could be responsible for two distinct phenotypes, a rigorous examination of all candidate loci by linkage analysis was appropriate. Following the exclusion of a number these candidate regions, positive lod scores (Z_{max}= 3.47 at θ=0 for D2S325) were obtained for markers within the locus 2q33-q35. The interval could not be refined beyond 33.8 cM owing to family size and informativeness of microsatellite markers in this region.

The prime cataract candidate genes within this locus are the γ-crystallin genes. However, direct sequencing of the *γ-A*, *γ-B*, *γ-C* and *γ-D* did not reveal a mutation. The sequencing data from the γS-crystallin gene is eagerly awaited. In 1994, Brackenhoff et al[156] described a mutation in the promoter region of the *γE*-pseudogene. The result was thought to be the abnormal accumulation of the protein product of this gene in the lens, giving rise to the Coppock-like cataract. Recently, this data has been critically evaluated and instead a missense mutation in the *γC-crystallin* gene shown to be causative[157]. Candidacy of this gene and the *γF* and *γG* gene fragment is therefore no longer advocated.

The result suggests that the mutation lies within a non-coding or regulatory element, another as yet unidentified gene expressed within the lens resides within the locus or that evidence of linkage has occurred as a result of the play of chance. Surveillance continues for publication of any new candidate genes within the disease locus.

Interestingly, a family described as having the aceuliform phenotype (synonymous with coralliform) has been mapped to the same interval and a missense mutation in the *γ-D crystallin* gene shown to underlie cataract formation[157 315]. This would strongly implicate the *γ-crystallin* genes as causative in our pedigree. However, the published images do not resemble those hand-drawn by Nettleship.

4.8 Mapping a locus for a novel ocular phenotype consisting of cataract, nanophthalmia, retinitis pigmentosa and glaucoma to chromosome 11p

4.8.1 Clinical considerations

The combination of developmental anomalies segregating in this family (N) represents a novel ocular phenotype. Nanophthalmia, in which the eye has a reduced ocular volume and axial length is an uncommon bilateral ocular finding that usually occurs in isolation. Often the lens:ocular-volume ratio is high or choroidal effusions may arise, both of which shallow the anterior chamber, narrowing the trabecular angle and predisposing to glaucoma[202 210]. Such a process is likely to account for the acute-on-chronic glaucoma in affected individuals in our family.

Retinitis pigmentosa (RP) is a common inherited retinal degeneration. A large number of genes have been implicated in its pathogenesis and autosomal dominant, autosomal recessive and X-linked inheritance patterns are seen. RP is characterised by progressive photoreceptor loss resulting in night blindness (nyctalopia), progressive visual field constriction and eventual loss of acuity. Typical clinical features include depigmentation of the retinal pigment epithelium with intra-retinal bone

spicule pigmentation, waxy pallor of the optic disc and narrowed retinal vessels[316]. The co-segregation of an autosomal dominant form of RP with nanophthalmia has not previously been recorded. In our family, the distribution of bone-spicule pigmentation was most unusual in that it was peripheral and limited posteriorly by a clearly defined band of RPE depigmentation. The optic disc was large, flat, pale and irregularly edged and the peripapillary retina and macula thinned.

There are only two reports of nanophthalmia associated with retinal pathology. Mackay et al.[209] described seven related individuals with apparently recessive cystic macular and retinal degeneration, synechial angle-closure glaucoma and nanophthalmia following an initial report by Ghose et al.[317] of an isolated case. In both of these articles, the distribution, appearance and electrophysiology of the retinal pathology was distinct from that in our family. It might be argued that in fact the retinal changes noted could be secondary phenomena resulting from choroidal effusions. However the electrophysiological abnormalities are consistent with a primary retinal dystrophy.

Cataract and nanophthalmia have also not previously been associated. Significantly, lens opacification is often seen in microphthalmic eyes (a more common and closely related congenital ocular anomaly to nanophthalmia) suggesting that candidate genes for this condition should be included in any search. Cataract is commonly seen in individuals with RP though the phenotype and onset of cataractogenesis suggest that in family N there is no aetiological relationship.

4.8.2 Linkage analysis

The constellation of congenital ocular abnormalities implicates a mutation in a major developmental control gene or a defect in its regulation. The candidate list therefore included those transcription factors essential for mammalian eye development. We were particularly concerned to exclude linkage to the microphthalmia and nanophthalmia loci on 14q (*CMIC*)[211] and 11p (*NNO1*)[204] respectively. Other strong candidates considered (whose human chromosomal location is known) were *PAX6*, *CHX10*, *MITF* and the human homologues of the drosophila genes *sine oculis*, (*Six3*) and *eyes absent* (*Eya1*, *Eya2*, *Eya3*).

After excluding linkage to one of these (table 33), significantly positive lod scores were obtained for markers D11S1765 and D11S4191. Owing to family size and informativity of markers, the disease interval could not be refined beyond a 33cM interval bounded by 11pter and microsatellite marker D11S908 which encompasses the *NNO1* locus and the coding region of the *PAX6* gene. The chance that a mutation in *PAX6* underlies the phenotype in this family is an intriguing possibility as this would the first implication of this master control gene of eye development in inherited retinal pathology. The results of direct sequencing are eagerly awaited. Another quite plausible possibility is that the mutation resides within a control element of the *PAX6* gene altering transcriptional regulation and resulting in a gene dosage effect.

4.9 Mapping of a family with progressive posterior polar cataract (PPC)

The results of positional candidate-gene linkage analysis performed on a three generation family with posterior polar cataract indicate that the gene underlying cataract formation in this pedigree resides at chromosomal band 10q25. Previously, human families with dominantly inherited cataracts of this appearance have been mapped to 1p36[173], 16q[318], and 20p12-q12[191]. In each instance, cataract has been stationary, contrasting markedly with the progressive nature of opacification in our family. From

linkage exclusion data relating to our other families with PPC, we have strong evidence implicating other genes in this phenotype (see below).

In 1998, Semina et al.[37], reported the identification of a deletion in the gene encoding the eye developmental regulator, PITX3 (ref. [122]), responsible for the development of anterior segment mesodermal dysgenesis (ASMD). The gene resides within the 10q25 locus. In the same paper, the authors concluded that a missense mutation in the same gene which segregated with isolated total cataract formation in a mother and her child was causative of opacification in this family.

Our results are therefore the first confirmation that a gene, most likely *PITX3*, residing on 10q25 is responsible for PPC. Furthermore, this is the first description of the genetic mapping of a progressive form of this phenotype.

PITX3 gene structure and primer sequences were not made available in the original paper. A Bioinformatics approach was therefore used to determine exon-intron boundaries, 5' and 3' UTRs and promoter region (figure 53). Like other homeobox genes the *PITX3* coding region is G/C rich. The homeobox region resides in exons 3 and 4.

Direct sequencing of exons 3 and 4 of the gene in our family has not revealed a segregating mutation. Amplification of the remaining two exons is eagerly awaited, once technical problems, for example primer design, have been overcome. The possibility that the mutation may either reside in a non-coding region of the gene cannot be excluded though this would be a novel mutational mechanism amongst pedigrees with human inherited cataract. The manner by which mutant PITX3 proteins may cause cataract is not known. PITX3 clearly has an important role in directing anterior segment development in the eye. Evidence suggests that the homologous gene in the mouse, *Pitx3*, is expressed in the developing lens vesicle[37]. Alternatively, another gene within the interval, as yet unknown, may be responsible.

4.10 Screening of a panel of inherited cataract patients for mutations in filensin and LEP503

The feasibility of directly screening a panel of affected individuals for mutations in a particular gene demands careful consideration. The strategy is most attractive when the panel is large, phenotypically homogeneous, the gene of interest is a very strong candidate for the disease, has a coding region which is manageable in size and likely to contain the mutation. Investigators must also be confident that any sequence change can be shown to be pathogenic, for example by co-segregation or linkage analyses, control population screening or by functional analysis.

The genes encoding the proteins LEP503 and filensin which meet these criteria were therefore screened using heteroduplex analysis. Samples in which heteroduplexes were identified were then sequenced. Segregation of any sequence change was then examined within all relatives of the affected panel member and a control population screened.

Although the function of LEP503 is unknown, its expression has been shown to be lens specific. The gene consists of two exons[108]. No mutations or polymorphisms were detected in our panel. Although, it must be conceded that screening in this way does not have a sensitivity of 100%[319], in all probability mutations in the coding sequence of this gene are not cataractogenic.

The gene encoding the differentiated lens fibre cell-specific cytoskeletal protein, filensin, is considered a very strong candidate for human cataract. The protein assembles with CP49 (phakinin, BFSP2) to form the unique intermediate beaded filament; a mutation in the phakinin gene has already been shown to cause cataract[160]. The filensin gene has eight exons. The complete gene structure was derived from alignment of the mRNA with known genomic clone sequences.

Two polymorphisms were detected. The first (exon 6, nucleotide position 806, C→T, Asn268Asn) is a synonymous nucleotide substitution. The second (exon 7, nucleotide position 1035, G→A) results in

the conservative substitution of serine for glycine at codon 345. This sequence change was present in 19 unrelated members of our panel of ninety-five families and in 22% of our control population.

The filensin protein has a three-domain structure consisting of a head, a tail and an intervening rod segment. Codon 345 resides within the tail domain outside any recognised motif or conserved sequence. Comparison of filensin sequences identifies bovine (71%), rat (68%) and chicken (50%) orthologs as sharing greatest homology. Alignment with these indicates that glycine at position 345 is conserved in bovine filensin but not in rat or chick.

Protein modelling suggests that the amino acid substitution produces some interesting variations in the protein. The presence of serine at position 345 introduces a potential phosphorylation site for protein kinase C (recognition motif S-G-K) and casein kinase II (S-G-K-D)[279]. Furthermore, the polymorphism lies within the area of maximum flexibility of the molecule. Although it does not alter this characteristic, the substitution probably foreshortens the turn region and inhibits the formation of a coil.

Our genetic evidence therefore corroborates the prediction that these minor changes do not significantly affect the structure or function of the protein. However, it is entirely possible that the deleterious effects of the polymorphism may accumulate over a long period of time predisposing to the development of lens opacity later in life. A reasonable strategy to test this hypothesis would be to look for an over-representation of the polymorphism in patients with age-related cataract compared with controls. While such a finding would provide further evidence of association, causality might plausibly be confirmed by ultrastructural analyses and the study of animal models.

4.11 Linkage exclusion data: candidate gene analyses and partial genome-wide scan

Although the number of candidate genes and loci for isolated non-syndromic cataract is large, our linkage exclusion data from several large pedigrees suggests that a number of additional genes are yet to be identified. Specifically, our data excluding linkage in families M (nuclear), E (pulverulent) and O (posterior polar) indicate that one or more genes for each of these phenotypes must exist.

4.12 Mapping a family with stationary posterior polar cataract

Having demonstrated exclusion to all candidate regions, family O was chosen for a genome-wide scan because the pedigree was large, the phenotype consistent and candidate gene analysis indicated that members of the family displayed a high degree of heterozygosity for the microsatellite markers.

Table 49 shows the lod scores calculated for linkage between the posterior polar cataract locus of family O and markers in the Genethon 10cM microsatellite marker set[272]. The order of chromosomal exclusion was arbitrary. The strategy was first to exclude those chromosomes with cataract candidate regions and then to move to the rest. Markers were amplified in a sequential order from the telomere using our standard PCR conditions.

Classically, values of θ between a disease and a marker locus are considered "excluded" (highly implausible) if the lod score is less than or equal to –2 (corresponding to a likelihood ratio of 1:100 or less)[271]. Thus where markers are closely spaced (~10cM as is in our study), the region of exclusion may eventually become continuous (in our case, where $Z<=-2$ at $\theta >=0.05$). It is worth bearing in mind that this approach assumes independence. In reality, a gene excluded from one region must have a higher probability of being in another region of the genome.and therefore the exclusion criterion could be less stringent[265]. Haplotype analysis was also employed as an additional safeguard: a double recombinant event between closely spaced markers being rare.

In this "first pass" therefore, a skeleton exclusion map was drawn; thereafter, areas were revisited where exclusion was not confirmed or markers did not amplify. Using this methodology, exclusion was obtained for chromosomes 1, 2, 19, 20, 21 ,22 and substantial regions of 3, 4, 5, 6, 7, 8, 14, 16 and 17. Significantly positive 2-point lod scores were then obtained for markers D11S898 and D11S908 (11q). The pressure of time did not allow further analysis of this linkage.

5 Future Perspectives

5.1 A voyage towards an understanding of the genotype-phenotype correlation

Congenital cataract is startlingly heterogeneous, both clinically and genetically. To date, 23 independent loci and mutations in 11 genes have been identified. Advances in microsatellite-based linkage technology and progress in the mapping of mammalian genomes suggest that the positional-candidate gene linkage approach will provide an increasingly efficient and powerful methodology for the identification of the remaining genes causing human cataracts.

Whilst this study has documented ten clearly distinguishable human congenital cataract phenotypes, it is an intriguing prospect for the future that functional analyses of the genetic defects identified in our families will better elaborate this clearly complex genotype-phenotype interrelationship. In certain ways, this study serves to exemplify the critical role molecular genetics has in challenging established clinical disease classification systems.

5.2 The genetics of age-related cataract

It is estimated that despite surgical removal and subsequent optical correction, a third of patients with congenital cataract will remain legally blind[5]. The removal of adult cataract with intra-ocular lens insertion, though not without risk, carries a much better prognosis and vision is often restored to pre-

morbid levels. In the developing world however, health provision is often inadequate to meet the eye-care needs of the population. Even in developed countries, patients incur significant morbidity from cataracts before surgery.

It is hoped that identification of the genetic mutations causing congenital cataract will not only improve our understanding of the pathogenesis of infantile cataract and the developmental biology of the lens but also adult-onset cataract. Mutations of the *TIGR* gene[320] were first identified in families with juvenile-onset glaucoma and were subsequently found to play a role in the pathogenesis of adult-onset glaucoma. More controversially it has been argued that mutations in the *ABCA4* (formally *ABCR*) gene[321] which cause a juvenile-onset macular dystrophy, may have a role in the pathogenesis of age related macular degeneration[322]. Genes implicated in inherited congenital cataract may therefore play a role in determining susceptibility to age-related cataract, which is known to have a significant genetic component in its aetiology. This is particularly the case with such genes encoding MIP and the lens specific connexins as these proteins are expressed in all lens fibres and modulate inter-fibre communication and water transport.

In the longer term, the identification of genetic variation associated with a high risk of developing cataract may lead to new strategies for the prevention of cataract or for slowing the progression of early lens opacity thus reducing the demand for surgery.

We have recently established collaboration with the St Thomas's United Kingdom Adult Twins Study group who have studied and phenotyped 506 pairs of female twins (226 monozygotic and 280 dizygotic)[302]. The study of twins has been described as the "perfect natural experiment"[323] from which to determine the relative importance of genetic and environmental factors, complex traits and genetic diseases[303]. We plan to investigate whether several of the genes implicated in congenital cataract (*MIP* described above) have a role in determining susceptibility to its age-related counterpart by performing association studies[324] utilising transmission disequilibrium[325] of intragenic polymorphic markers, for example single nucleotide polymorphisms (SNPs)[265].

6. Summary and concluding comments

This is the largest study of human inherited cataract yet reported, from which it has been possible to construct a clinical classification system based on ten recognisable phenotypes. The study has also shown that patients have better visual and surgical outcomes than those with cataracts of other aetiologies probably relating the lack of attendant developmental abnormalities and because surgery may often be delayed.

The results of our molecular linkage studies show the importance of identifying the genetic defects underlying single-gene Mendelian disorders in humans as they often provide incisive insights into biological processes and pathophysiological states. Four novel cataract loci have been identified. The recognition of mutations in MIP confirms the importance of this protein in both normal lens physiology and cataractogenesis. Furthermore, the functional analyses provide a molecular basis for the cataracts observed.

The lens is a unique biological structure, whose highly ordered molecular and cellular components are essential for transparency. Although disturbances in lens cell physiology are readily identified as opacification or cataract there is still much to learn about the normal structure and function of the lens and the mechanism of cataract formation. In the next few years, all the genes involved in inherited cataract will be identified. Clearly, a detailed understanding will not only be beneficial to those affected families (offering opportunities for prenatal diagnosis and better counselling) but is likely to lead to novel therapeutic avenues for age-related cataract, the most common cause of blindness in the world.

7. References

1. Albert D, Jakobiec F. *Principles and Practice of Ophthalmology*. Philadelphia: WB Saunders, 1994.

2. Evans J, Rooney C, Ashwood F, Dattani N, Wormald R. Blindness and partial sight in England and Wales: April 1990- March 1991. *Health Trends* 1996;28:5-12.

3. Lambert S, Drack A. Infantile Cataracts. *Surv Ophthalmol* 1996;40:427-458.

4. Parks M, Johnson D, Reed G. Long term visual results and complications in children with aphakia: a function of cataract type. *Ophthalmol* 1993;100:826-41.

5. Lambert S. Lens. In: Taylor D, editor. *Paediatric Ophthalmology*. Oxford: Blackwell Scientific, 1997:453.

6. Francois J. Genetics of cataract. *Ophthalmologica* 1982;184:61-71.

7. McKusick V. Online Mendelian Inheritance in Man, OMIM (TM): Centre for Medical Genetics, John Hopkins University (Baltimore, MD) and National Centre for Biotechnology Information, National Library of Medicine (Bethesda, MD), 1997.

8. Population genetic study on blinding diseases in Japan. Proceedings of the Second International Congress of Human Genetics; 1961; Rome.

9. Nettleship F, Ogilvie F. A peculiar form of congenital cataract. *Trans Ophth Soc UK* 1906;26:191-206.

10. Renwick J, Lawler S. Probable linkage between a congenital cataract locus and the Duffy blood group locus. *Ann Hum Genet* 1963;27:67-84.

11. Donahue R, Bias W, Renwick J, McKusick V. Probable assignment of the Duffy blood group locus to chromosome 1 in man. *Proc Natl Acad Sci USA* 1968;61:949-955.

12. Snell R, Lemp M. *Clinical Anatomy of the Eye*. Oxford: Blackwell Scientific, 1989.

13. Mann I. *The development of the human eye*. New York: Grune and Stratton, 1950.

14. Kronfeld P. *The gross anatomy and embryology of the eye*. 2 ed. New York: Academic Press, 1969.

15. McAvoy J. Developmental biology of the lens. In: Duncan G, editor. *Mechanisms of cataract formation in the human lens*. London: Academic Press, 1981:7-46.

16. Weekers R, Delmarcelle Y, Luyckx-Bacus J. *Morphological changes of the lens with age and cataract*. Amsterdam: Elsevier, 1973.

17. Sivak J, Dovrat A. Embryonic lens of the human eye as an optical structure. *Am J Optom Physiol Opt* 1987;64:599-603.

18. Kuszak J, Bertram B, Macsai M, Rae J. Sutures of the crystalline lens: a review. *Scan Elec Micr* 1984;111:1369-1378.

19. Chylack L. Sugar cataracts - possibly the beginning of medical anti-cataract therapy. In: Duncan G, editor. *Mechanisms of cataract formation in the human lens*. London: Academic Press, 1981:237-252.

20. Vogt A. Lens. *Klin MBL Augenheilk* 1919;62:582.

21. Koretz J, Cook C, Kuzak J. The zones of discontinuity in the human lens: development and distribution with age. *Vis Res* 1994;34:2955-62.

22. Garland D, Duglas-Tabor Y, Jimenez-Assensio J, Datiles M, Magno B. The nucleus of the human lens: Demonstration of a highly characteristic protein pattern by two-dimensional electrophoresis and introduction of a new method of lens dissection. *Exp Eye Res* 1996;62:285-291.

23. Duke-Elder S. *The practice of refraction*. Edinburgh: Churchill Livingstone, 1978.

24. Elkington A, Frank H. *Clinical Optics*. Oxford: Blackwell, 1984.

25. Eccles M, Schimmenti L. Renal-coloboma syndrome: a multi-system developmental disorder caused by PAX2 mutations. *Clin Genet* 1999;56:1-9.

26. Matsuo T. The genes involved in the morphogenesis of the eye. *Jpn J Ophthalmol* 1993;37(3):215-51.

27. Robinson M, Ohtaka-Maruyama C, Chan C, Jamieson S, Dickson C, Overbeek P, et al. Disregulation of ocular morphogenesis by lens-specific expression of FGF-3/int-2 in transgenic mice. *Dev Biol* 1998;198(1):13-31.

28. Hill R, Hanson I. Molecular genetics of the Pax gene family. *Curr Opin Cell Biol* 1992;4:967-972.

29. Quiring R, Walldorf U, Kloter U, Gehring W. Homology of the eyeless gene of Drosophila to the small eye gene in mice and aniridia in humans. *Science* 1994;265:785-789.

30. Hill R, Favor J, Hogan B, Ton C, Saunders G, Hanson I, et al. Mouse *Small eye* results from mutations in a paired-like homeobox-containing gene. *Nature* 1991;354:522-525.

31. Matsuo T, Osumi-Yamashita N, Noji S, Ohuchi H, Koyama E, Myokai F, et al. A mutation in the Pax-6 gene in rat small eye is associated with impaired migration of midbrain crest cells. *Nat Genet* 1993;3:299-304.

32. Hanson I, Heyningen Vv. Pax6: more than meets the eye. *Trends Genet* 1995;11:268-272.

33. Grindley J, Davidson D, Hill R. The role of Pax-6 in eye and nasal development. *Development* 1995;121(5):1433-1442.

34. Cveki A, Sax C, Bresnick E, Piatigorsky J. A complex array of positive and negative elements regulates the chicken alpha A-crystallin gene: involvement of Pax6, USF, CREB and/or CREM, and AP-1 proteins. *Mol Cell Biol* 1994;14(11):7363-7376.

35. Cveki A, Piatigorsky J. Lens development and crystallin gene expression: many roles for Pax-6. *Bioessays* 1996;18:621-630.

36. Duncan M, Haynes J, Cveki A, Piatigorsky J. Dual roles for Pax-6: a transcriptional repressor of lens fiber cell-specific beta-crystallin genes. *Mol Cell Biol* 1998;18(9):5579-86.

37. Semina E, Ferrell R, Mintz-Hittner H, Bitoun P, Alwar W, Reiter R, et al. A novel homeobox gene PITX3 is mutated in families with autosomal dominant cataracts and ASMD. *Nat Genet* 1998;19:167-170.

38. Lossli F, Koster R, Carl M, Krone A, Wittbrodt J. Six3, a medaka homologue of the drosophila homeobox gene sine oculis is expressed in the anterior embryonic shield and the developing eye. 1997.

39. Winchester C, Ferrier R, Sermoni A, Clark B, Johnson K. Characterization of the expression of DMPK and SIX5 in the human eye and implications for pathogenesis in myotonic dystrophy. *Hum. Mol. Genet.* 1999;8(3):481-492.

40. Smith S, Dickman E, Power S, Lancman J. Retinoids and their receptors in vertebrate embryogenesis. *J Nutr* 1998;128 (suppl 2):467S-470S.

41. Lohnes D, Mark M, Mendelsohn C, Dolle P, Decimo D, LeMeur M, et al. Developmental roles of the retinoic acid receptors. *J Steroid Biochem Mol Biol* 1995;53:475-486.

42. Glass C, DiRenzo J, Kurokawa R, Hans Z. Regulation of gene expression by retinoic acid receptors. *DNA Cell Biol* 1991;10:623-638.

43. Flagiello D, Apiou F, Gibaud A, Poupon M, Dutrillaux B, Malfoy B. Assignment of the genes for cellular retinoic acid binding protein 1 (CRABP1) and 2 (CRABP2) to human chromosome band 15q24 and 1q21.3, respectively, by in situ hybridisation. *Cytogenet Cell Genet* 1997;76(1-2):17-8.

44. Walpole S, Hiriyana K, Nicolaou A, Bingham E, Durham J, Vaudin M, et al. Identification and characterisation of the human homologue (*RAI2*) of a mouse retinoic acid-induced gene in Xp22. *Genomics* 1999;55:275-283.

45. Perez-Castro A, Tran V, Nguyen-Huu M. Defective lens fiber differentiation and pancreatic tumorigenesis caused by ectopic expression of the cellular retinoic acid-binding protein 1. *Development* 1993;119:363-375.

46. Li X, Cveki A, Bassnett S, Piatigorsky J. Lens-preferred activity of chicken delta 1- and delta 2-crystallin enhancers in transgenic mice for retinoic acid-responsive regulation of the delta 1-crystallin gene. *Trends Genet* 1997;20:258-266.

47. Patterson C. The lens. In: Hart W, editor. *Adler's physiology of the eye*. St Louis: Mosby, 1992:348-390.

48. Bhuyan K, Bhuyan D. Regulation of hydrogen peroxide in eye humors; effect of 3-amino-1H-1,2,4-triazole on catalase and glutathione peroxidase of rabbit eye. *Biochem Biophys Acta* 1977;497:641.

49. Reddy N, Giblin F. Metabolism and function of glutathione in the lens. In: Nugent J, Whelan J, editors. *Human cataract formation. Ciba Foundation Symposium 106*. London: Pitman, 1984:65-87.

50. Spector A. Oxidative stress-induced cataract: mechanism of action. *FASEB J* 1995;9:1173-1182.

51. Delaye M, Tardieu A. Short-range order of crystallin proteins accounts for eye lens transparency. *Nature* 1983;302:415-417.

52. Lubsen N, Aarts H, Schoenmakers J. The evolution of lenticular proteins: the beta and gamma crystallin supergene family. *Prog Biophys Mol Biol* 1988;51:47-76.

53. Piatigorsky J. Multifunctional lens crystallins and corneal enzymes. More than meets the eye. *Ann N Y Acad Sci* 1998;842:7-15.

54. Piatigorsky J, Kantorow M, Gopal-Srivastava R, Tomarev S. Recruitment of enzymes and stress proteins as lens crystallin. *EXS* 1994;71:241-250.

55. IJessel Pvd, Norman D, Quinlan R. Small heat shock proteins in the limelight. *Curr Biol* 1999;9(3):R103-5.

56. Derham B, Harding J. Alpha-crystallin as a molecular chaperone. *Prog Retina Eye Res* 1999;18(4):463-509.

57. Piatigorsky J. Gene Sharing in lens and cornea: facts and implications. *Prog Retina Eye Res* 1998;17(2):145-74.

58. Alcala J, Maisel H. Biochemistry of lens plasma membranes and cytoskeleton. In: Maisel H, editor. *The ocular lens: structure, function and pathology*. New York: Marcel Dekker, 1985:169-222.

59. Kibbelaar M, Selton-Versteigen A, Dunia I, Benedetti E, Bloemendal H. Actin in mammalian cells. *Eur J Biochem* 1979;95:543-549.

60. Sandilands A, Prescott A, Carter J, Hutcheson A, Quinlan R, Richards J, et al. Vimentin and CP49/filensin form distinct networks in the lens which are independently modulated during lens fibre cell differentiation. *J Cell Sci* 1995;108:1397-406.

61. Fitzgerald P. Methods for the circumvention of problems associated with the study of the ocular lens plasma membrane-cytoskeleton complex. *Curr Eye Res* 1990;9:1083-97.

62. Carter J, Hutcheson A, Quinlan R. In vitro studies on the assembly properties of the lens proteins CP49,CP115: coassembly with alpha-crystallin but not with vimentin. *Exp Eye Res* 1995;60:181-192.

63. Hess J, Casselman J, Fitzgerald P. Gene structure and cDNA sequence identify the beaded filament protein CP49 as a highly divergent type 1 intermediate filament protein. *J Biol Chem* 1996;271(12):6729-6735.

64. Mulders S, Preston G, Deen P, Guggino W, Os Cv, Agre P. Water channel properties of the major intrinsic protein of the lens. *J Biol Chem* 1995;270(15):9010-6.

65. Lea E. Main intrinsic polypeptide and water movement - recent developments and future prospects. *Ophth Res* 1996;28 Suppl 1:69-72.

66. Park J, Saier M. Phylogenetic characterisation of the MIP family of transmembrane channel proteins. *J Membr Biol* 1996;153(3):171-180.

67. Jarvis L, Lewis C. Purification and oligomeric state of the major lens fiber cell membrane proteins. *Cur Eye Res* 1995;14(9):799-808.

68. Brown D, Katsura T, Kawashima M, Verkman A, Sabolic I. Cellular distribution of the aquaporins: a family of water channel proteins. *Histochem Cell Biol* 1995;104(1):1-9.

69. Mulders J, Woorter C, Lamers C, deHaard-Hoekman W, Montecucco C, Wen Wvd, et al. MP17, a fiber-specific intrinsic membrane protein from mammalian eye lens. *Curr Eye Res* 1988;7:207-219.

70. Tenboek E, Arneson M, Jarvis L, Louis C. The distribution of fiber cell intrinsic membrane proteins MP20 and connexin 46 in the bovine lens. *J Cell Sci* 1992;103:245-57.

71. Steele E, Wang J, Lo W, Saperstein D, Li X, Church R. $Lim2^{To3}$ transgenic mice establish a causative relationship between the mutation identified in the Lim2 gene and cataractogenesis in the To3 mouse mutant. *Mol Vis* 2000;6:85-94.

72. Fraser F, Schabtach G. "Shrivelled": a hereditary degeneration of the lens in the house mouse. *Genet Res* 1962;3:383-387.

73. Lyon M, Jarvis S, Sayers I, Holmes R. Lens opacity: a new gene for congenital cataract on chromosome 10 of the mouse. *Genet Res* 1981;38:337-341.

74. Muggleton-Harris A, Festing M, Hall M. A gene location for the inheritance of the Cataract Fraser (*CatFr*) mouse congenital cataract. *Gen Res Camb* 1987;49:235-239.

75. Shiels A, Bassnett S. Mutations in the founder of the *MIP* gene family underlie cataract development in the mouse. *Nat Genet* 1996;12:212-215.

76. Borgnia M, Nielsen S, Engel A, Agre P. Cellular and Molecular Biology of the aquaporin water channels. *Ann Rev Biochem* 1999;68:425-428.

77. Heymann J, Agre P, Engel A. Progress on the structure and function of aquaporin 1. *J Struct Biol* 1998;121:191-206.

78. Moon B, Friedman J. The molecular basis of the obese mutation in *ob2J* mice. *Genomics* 1997;42:152-156.

79. Muggleton-Harris A, Higbee N. An in vivo and in vitro study of the embryonic and adult Lop mutant congenital cataractous lens. *Exp Eye Res* 1987;44:805-815.

80. Chrispeels M, Agre P. Aquaporins: water channel proteins of plant and animal cells. *Trends Biochem Sci* 1994;19:421-425.

81. Calamita G, Bishai W, Preston G, Guggino W, Agre P. Molecular cloning and characterisation of AqpZ, a water channel from Escherichia coli. *J Biol Chem* 1995;270:29063-29066.

82. Hohmann S, Bill R, Kayingo G, Prior B. Microbial MIP channels. *Trends in microbiology* 2000;8:33-38.

83. Tamas M, Luyten K, Sutherland F, Hernandez A, Valadi H, Li H, et al. Fps1p controls the accumulation and release of the compatible solute glycerol in yeast osmoregulation. *Mol Microbiol* 1999;31(4):1087-1104.

84. Yasui M, Kwon T-H, Knepper M, Nielsen S, Agre P. Aquaporin-6: An intracellular vesicle water channel protein in renal epithelia. *Proc Natl Acad Sci USA* 1999;96:5808-5813.

85. Agre P. Aquaporin null phenotypes: The importance of classical physiology. *Proc Natl Acad Sci USA* 1998;95:9061-9063.

86. Hamann S, Zeuthen T, Cour ML, Nagelhus E, Ottersen O, Agre P, et al. Aquaporins in complex tissues: distribution of aquaporins 1-5 in human and rat eye. *Am J Physiol* 1998;274(5):C1332-C1345.

87. Heymann J, Engel A. Structural clues in the sequences of the aquaporins. *J Mol Biol* 2000;295(4):1039-53.

88. Lagrec V, Froger A, Deschamps S, Hubert J-F, Delamarche C, Bonnec G, et al. Switch from an aquaporin to a glycerol channel by two amino-acids substitution. *J Biol Chem* 1999;274(11):6817-6819.

89. Cooper G, Boron W. Effect of PCMBS on CO2 permeability of Xenopus oocytes expressing aquaporin-1 or its C189S mutant. *Am J Physiol* 1998;275:C1481-C1486.

90. Meinild A-K, Klaerke D, Zeuthen T. Bidirectional water fluxes and specificity for small hydrophilic molecules in aquaporins 0-5. *J Biol Chem* 1998;273(49):32446-32451.

91. Lee M, King L, Agre P. The aquaporin family of water channel proteins in clinical medicine. *Medicine (Baltimore)* 1997;76(3):141-56.

92. Echevarria M, Ilundain A. Aquaporins. *J Physiol Biochem* 1998;54(2):107-18.

93. Tamarappoo B, Yang B, Verkman A. Misfolding of mutant aquaporin-2 water channels in nephrogenic diabetes insipidus. *J Biol Chem* 1999;274(49):34825-34831.

94. Deen P, Verdijk M, Knoers N, Wieringa B, Monnens L, Os Cv, et al. Requirement of human renal water channel aquaporin-2 for vasopressin-dependent concentration of urine. *Science* 1994;264:92-95.

95. Mulders S, Bichet D, Rijss J, Kamsteeg E, Arthus M, Lonergan M, et al. An aquaporin-2 water channel mutant which causes autosomal dominant nephrogenic diabetes insipidus is retained within the Golgi complex. *J Clin Invest* 1998;102:57-66.

96. Daniels G. Functional aspects of red cell antigens. *Blood Rev* 1999;13(1):14-35.

97. Engel A, Fujiyoshi Y, Agre P. The importance of aquaporin water channel protein structures. *EMBO J* 2000;19(5):800-6.

98. Gorin M, Yancey S, Cline J, Revel J-P, Horwitz J. The major intrinsic protein (MIP) of the bovine lens fiber membrane: characterisation and structure based on cDNA analysis. *Cell* 1984;39:49-59.

99. Bok D, Dockstader J, Horwitz J. Immunolocalisation of the lens intrinsic protein (MIP26) in communicating junctions. *J Cell Biol* 1982;92:213-220.

100. Bassnett S, Missey H, Vucemilo I. Molecular architecture of the lens fiber cell basal membrane complex. *J Cell Sci* 1999;112:2155-2165.

101. Varadaraj K, Kushmerick C, Baldo G, Bassnett S, Shiels A, Mathias R. The role of MIP in lens fiber cell transport. *J Membr Biol* 1999;170(3):191-203.

102. Fotiardis D, Hasler L, Muller D, Stahlberg H, Kistler J, Engel A. Surface tongue-and-groove contours on lens MIP facilitate cell-to-cell adherence. *J Membr Biol* 2000;300:779-789.

103. Beyer E, Paul D, Goodenough D. Connexin family of gap junctions. *J Membr Biol* 1990;116:187-194.

104. Goodenough D, Goliger J, Paul D. Connexins, connexons and intercellular communication. *Ann Rev Biochem* 1996;65:475-502.

105. Kumar N, Gilula N. The gap junction communication channel. *Cell* 1996;84:381-388.

106. Yang D, Louis C. Molecular cloning of ovine connexin 44 and temporal expression in gap junction proteins in a lens culture. *Invest Ophthalmol Vis Sci* 2000;41(9):2658-64.

107. Saffitz J, Green K, Kraft W, Schechtman K, Yamada K. Effects of diminished expression of connexin 43 on gap junction number and size in ventricular myocardium. *Am J Physiol Heart Circ Physiol* 2000;278(5):H1662-70.

108. Wen Y, Sachs G, Athmann C. A novel lens epithelium gene, LEP503, is highly conserved in different vertebrate species and is developmentally regulated in postnatal rat lens. *Exp Eye Res* 2000;70:159-168.

109. Isaacs A, Davies K, Hunter A, Nolan P, Visor L, Peters J, et al. Identification of two new pmp22 mouse mutants using large scale mutagenesis and a novel rapid mapping strategy. *Hum Mol Genet* 2000;9(12):1865-71.

110. Graw J. Cataract mutations as a tool for developmental geneticists. *Ophth Res* 1996;28(suppl 1):8-18.

111. Lang R, Metcalf D, Cuthbertson R, Lyons I, Stanley E, Kelso A, et al. Transgenic mice expressing a hemopoetic growth factor gene (GM-CSF) develop accumulations of macrophages, blindness and a fatal syndrome of tissue damage. *Cell* 1997;51:675-686.

112. Egwuagu C, Sztein J, Chan C, Reid W, Mahdi R, Nussenblatt R, et al. Ectopic expression of gamma interferon in the eyes of transgenic mice induces ocular pathology and MHCII gene expression. *Inv Ophth Vis Sci* 1984;35:332-341.

113. Griep A, Herber R, Jeon S, Lohse J, Dubielzig R, Lambert P. Tumorigenicity by human papillomavirus type 16 E6 and E7 in transgenic mice correlates with alterations in epithelial cell growth and differentiation. *J Virol* 1993;67:1373-1384.

114. Dunia I, Smitt J, Valk Mvd, Bloemendal H, Borst P, Benedetti E. Human multidrug resistance 3-P-glycoprotein expression in transgenic mice induces lens membrane alterations leading to cataract. *J Cell Biol* 1996;132:701-716.

115. Bloemendal H, Raatsd J, Pieper F, Benedetti E, Dunia I. Transgenic mice carrying chimeric or mutated type III intermediate filament proteins. *Cell Mol. Life Sci.* 1997;53:1-12.

116. Brady J, Garland D, Duglas-Tabor Y, Robison W, Groome A, Wawrousek E. Targeted disruption of the mouse alpha crystallin gene induces cataract and cytoplasmic inclusion bodies containing the small heat shock protein alpha B-crystallin. *Proc Nat Acad Sci USA* 1997;94:884-889.

117. Mitton K, Kamiya T, Tumminia S, Russell P. Cysteine protease activated by expression of HIV-1 protease in transgenic mice. MIP26 (aquaporin-0) cleavage and cataract formation in vivo and ex vivo. *J Biol Chem* 1996;271:31803-31806.

118. Hejtmancik J. The genetics of cataract: our vision becomes clearer. *Am J Hum Genet* 1998;62:520-525.

119. Klopp N, Favor J, Loster J, Lutz R, Neuhauser-Klaus A, Prescott A, et al. Three murine cataract mutants (CAT2) are defective in different gamma-crystallin genes. *Genomics* 1998;52:152-158.

120. Steele E, Lyon M, Favor J, Guillot P, Boyd Y, Church R. A mutation in the connexin 50 (Cx50) gene is a candidate for the No2 mouse cataract. *Curr Eye Res* 1998;17(9):883-9.

121. Cartier M, Breitman M, Tsui L. A frameshift mutation in the gammaE-crystallin gene of the ELO mouse. *Nat Genet* 1992;2:42-45.

122. Semina E, Reiter R, Murray J. Isolation of a new homeobox gene belonging to the Pitx/Rieg family: expression during lens development and mapping to the aphakia region on mouse chromosome 19. *Hum Mol Genet* 1997;6:2109-2116.

123. Gong X, Li E, Klier G, Huang Q, Wu Y, Lei H, et al. Disruption of alpha3 connexin gene leads to proteolysis and cataractogenesis in mice. *Cell* 1997;91(6):833-43.

124. Graw J, Jung M, Loster J, Klopp N, Soewarto D, Fella C, et al. Mutation in the betaA3/A1-crystallin encoding gene cryba1 causes a dominant cataract in the mouse. *Genomics* 1999;62(1):67-73.

125. Chang B, Hawes N, Roderick T, Smith R, Heckenlively J, Horwitz J, et al. Identification of a missense mutation in the alphaA-crystallin gene of the lop18 mouse. *Mol Vis* 1999;5:21.

126. Chambers C, Russell P. Deletion mutation in an eye lens beta-crystallin. *J Biol Chem* 1991;266:6742-6746.

127. Everett C, Glenister P, Taylor D, Lyon M, Kratochvilova-Loester J, Favor J. Mapping of six dominant genes in the mouse. *Genomics* 1994;20:429-434.

128. Hess E, Collins K, Copeland N, Jenkins N, Wilson M. Deletion map of the coloboma (Cm) locus on mouse chromosome 2. *Genomics* 1994;21:257-261.

129. Kersher S, Glenister P, Favor J, Lyon M. Two new cataract loci Cur and To3, and functional mapping of the Npp and Opj cataracts in the mouse. *Genomics* 1996;36:17-21.

130. Zhou E, Grimes P, Favor J, Koeberlein B, Pretsch W, Neuhauser-Klaus A, et al. Genetic mapping of a mouse ocular malformation locus, Tcm, to chromosome 4. *Mamm Genome* 1997;8:178-181.

131. Sanyal S, Nie Rv, Moes Jd, Hawkins R. Map position of the dysgenic (*dy*) locus on chromosome 4 in the mouse. *Genet Res Camb* 1986;48:199-200.

132. Kador P, Fukui H, Fukushi S, Jernigan H, Kinoshita J. A new model of hereditary cataract. *Exp Eye Res* 1980;30:59.

133. Hulsebos T, Gilbert D, Delattri O, Smith L, Dunham I, Westerveld A, et al. Assignment of the betaB1-crystallin gene (CRYBB1) to human chromosome 22 and mouse chromosome 5. *Genomics* 1995;29:712-718.

134. Griffin C, Shiels A. Localisation of the gene for the major intrinsic protein of the eye-lens-fibre cell membranes to mouse chromosome 10 by in situ hybridisation. *Cytogenet Cell Genet* 1992;59:300-302.

135. Harris AM, Higbee N. An in vivo and in vitro study of the embryonic and adult Lop mutant congenital cataractous lens. *Exp Eye Res* 1987;44:805-815.

136. Graw J. Cataract mutations and lens development. *Prog Retina Eye Res* 1999;18(2):235-267.

137. Loster J, Immervoll T, Schmitt-John T, Graw J. Cat3vi and Catvao cataract mutations on mouse chromosome 10: phenotypic characterisation, linkage studies and analysis of candidate genes. *Mol Gen Genet* 1997;257:97-102.

138. Loster J, Graw J, Neuhauser-Klaus A, Schmitt-John T. A new murine cataract gene on chromosome 10. *Exp Eye Res* 1994;59 (suppl 1):S152.

139. Burmeister M, Novak J, Liang M, Basu S, Ploder L, Hawes N, et al. Ocular retardation mouse caused by Chx 10 homeobox null allele: impaired retinal progenitor proliferation and bipolar cell differentiation. *Nat Genet* 1996;12:376-384.

140. Matsushima Y, Kamoto T, Iida F, Abujiang P, Honda Y, Hiai H. Mapping of rupture lens cataract (rlc) on mouse chromosome 14. *Genomics* 1996;36:553-554.

141. Sidjanin D, Grimes P, Pretsch W, Neuhauser-Klaus A, Favor J, Stambolian D. Mapping of the autosomal dominant cataract mutation (Coc) on mouse chromosome 16. *Invest Ophthalmol Vis Sci* 1997;38:2502-2507.

142. Zwaan J, Kirkland B. Malorientation of mitotic figures in the early lens rudiment of aphakia mouse embryos. *Anat Rec* 1975;182:345-354.

143. Semina E, Murray J, Reiter R, Hrstka R, Graw J. Deletion in the promoter region and altered expression of Pitx3 homeobox gene in aphakia mice. *Hum Mol Genet* 2000;9(11):1575-1585.

144. Grimes P, Favor J, Koeberlein B, Silven W, Fitzgerald P, Shambolian D. Lens development in a dominant X-linked congenital cataract in the mouse. *Exp Eye Res* 1993;57:587-594.

145. Steingrimsson E, Moore K, Lamoreux M, Ferre-D'Amare A, Burley S, Zimring D, et al. Molecular basis of mouse microphthalmia (mi) mutations helps explain their developmental and phenotypic consequences. *Nat Genet* 1994;8:256-263.

146. Gunther T, Struwe M, Aguzzi A, Schugart K. *Open brain*, a new mouse mutant with severe neural tube defects, shows altered gene expression patterns in the developing spinal cord. *Devel* 1994;120:3119-3130.

147. Chase H. Studies on an anophthalmic strain of mice. IV. A second major gene for anophthalmia. *Genet* 1944;29:264-269.

148. Webster E, Silver A, Gonsalves N. The extracellular matrix between the optic vesicle and presumptive lens during lens morphogenesis in an anophthalmic strain of mice. *Devel Biol* 1984;103:142-150.

149. Kobayashi S, Kasuya M, Itoi M. Changes in the lens proteins induced at the early stage of cataractogenesis in cac (Nakano) mice. *Exp Eye Res* 1989;49:553-559.

150. Iwata S, Kinoshita J. Mechanism of development of hereditary cataract in mice. *Invest Ophthalmol* 1971;10:504-512.

151. Kuck J, Kuwabara T, Kuck K. The Emory mouse cataract: an animal model for human senile cataract. *Cur Eye Res* 1981;1:643.

152. West J, Fisher G. Inherited cataracts in inbred mice. *Genet Res Camb* 1985;46:45.

153. Tissot R, Cohen C. A new congenital cataract in the mouse. *J Hered* 1972;63:197.

154. Mathew S, Chauduri A, Murty V, Pogo A. Confirmation of Duffy blood group antigen locus (FY) at 1q22-q23 by fluorescence in situ hybridisation. *Cytogenet Cell Genet* 1994;67:68.

155. White T, Bruzzone R, Goodenough D, Paul D. Mouse Cx50, a functional member of the connexin family of gap junction proteins, is the lens fibre protein MP70. *Mol Cell Biol* 1992;3:711-720.

156. Brackenhoff R, Heskens H, Rossum Mv, Lunsen N, Schoenmakers J. Activation of the gamma-E-crystallin pseudogene in the human hereditary Coppock-like cataract. *Hum Mol Genet* 1994;3:279-283.

157. Heon E, Priston M, Schorederet D, Billingsley G, Girard P, Lubsen N, et al. The gamma-crystallins and human cataracts: a puzzle made clearer. *Am J Hum Genet* 1999;65(5):1261-7.

158. Stephan D, Gillanders E, Vanderveen D, Freas-Lutz D, Wistow G, Baxevanis A, et al. Progressive juvenile-onset punctate cataract characterised by mutation of the gamma-D-crystallin gene. *Proc Natl Acad Sci USA* 1999;96:1008-1012.

159. Conley Y, Erturk D, Keverline A, Mah T, Keravala A, Barnes L, et al. A juvenile-onset cataract locus 3q21-q22 is associated with a missense mutation in the beaded filament structural protein-2. *Am J Hum Genet* 2000;66:1425-31.

160. Jakobs P, Hess J, Fitzgerald P, Kramer P, Weleber R, Litt M. Autosomal dominant congenital cataract associated with a deletion mutation in the human beaded filament protein gene BFSP2. *Am J Hum Genet* 2000;66:1432-1436.

161. Mackay D, Ionides A, Kibar Z, Rouleau G, Berry V, Moore A, et al. Connexin46 mutations in autosomal dominant congenital cataract. *Am J Hum Genet* 1999;64(5):1357-64.

162. Kannabiran C, Rogan P, Olmos L, Basti S, Rao G, Kaiser-Kupfer M, et al. Autosomal dominant zonular cataract with sutural opacities is associated with a splice mutation in the betaA3/A1-crystallin gene. *Mol Vis* 1998;4:21.

163. Litt M, Kramer P, LaMorticella D, Murphey W, Lovrien E, Weleber R. Autosomal dominant congenital cataract associated with a missense mutation in the human alpha crystallin gene CRYAA. *Hum Mol Genet* 1998;7(471-474).

164. Litt M, Carrero-Valenzuela R, LaMorticella D, Schultz D, Mitchell T, Kramer P, et al. Autosomal dominant congenital cataract is associated with a chain termination mutation in the human beta-crystallin gene CRYBB2. *Hum Mol Genet* 1997;6:665-668.

165. Gill D, Klose R, Munier F, McFadden M, Priston M, Billingsley G, et al. Genetic heterogeneity of the Coppock-like cataract: a mutation in CRYBB2 on chromosome 22q11.2. *Invest Ophthalmol Vis Sci* 2000;41(1):159-165.

166. Shiels A, Mackay D, Ionides A, Berry V, Moore A, Bhattacharya S. A missense mutation in the human connexin 50 gene (GJA8) underlies autosomal dominant "zonular pulverulent" cataract, on chromosome 1q. *Am J Hum Genet* 1998;62:526-532.

167. Berry V, Mackay D, Khaliq S, Francis P, Hameed A, Anwar K, et al. Connexin 50 mutation in a family with congenital "zonular nuclear" pulverulent cataract (CZNP) of Pakistani origin. *Hum. Genet.* 1999;105(1-2):168-170.

168. Mackay D, Ionides A, Berry V, Moore A, Bhattacharya S, Sheils A. Autosomal dominant congenital cataract linked to chromosome 13. *Am J Hum Genet* 1997;60:1474-1478.

169. Suchyna T, Xu L, Gao F, Fourtner C, Nicholson B. Identification of a proline residue as a transduction element involved in voltage gating of gap junctions. *Nature* 1993;365:847-849.

170. Rees M, Watts P, Fenton I, Clarke A, Snell R, Owen M, et al. Further evidence of autosomal dominant congenital zonular nuclear pulverulent cataracts linked to 13q11 (CZP3) and a novel mutation in connexin 46 (GJA3). *Hum Genet* 2000;106(2):206-9.

171. Lubsen N, Renwick J, Tsui L-C, Breitman M, Schoenmakers J. A locus for human hereditary cataract is closely linked to the gamma-crystallin gene family. *Proc Nat Acad Sci USA* 1987;84:489-492.

172. Eiberg H, Lund A, Warburg M, Rosenberg T. Assignment of congenital cataract Volkmann-type (CCV) to chromosome 1p36. *Hum Genet* 1995;96:33-38.

173. Ionides A, Berry V, Mackay D, Moore A, Bhattacharya S, Shiels A. A locus for autosomal dominant posterior polar cataract on chromosome 1p. *Hum Mol Genet* 1997;6:47-51.

174. Marner E. A family with eight generations of cataract. *Acta Ophthalmol* 1949;27:537-551.

175. Eiberg E, Marner E, Rosenberg T, Mohr J. Marner's cataract (CAM) assigned to chromosome 16: linkage to haptoglobin. *Clin Genet* 1988;34:272-275.

176. Berry V, Ionides A, Moore A, Plant C, Bhattacharya S, Shiels A. A locus for autosomal dominant anterior polar cataract on chromosome 17p. *Mol Genet* 1996;5:415-419.

177. Padma T, Ayyagari R, Murty J, Basti S, Fletcher T, Rao G, et al. Autosomal dominant zonular cataract with sutural opacities localised to chromosome 17q11-12. *Am J Hum Genet* 1995;57:850-845.

178. Armitage M, Kivlin J, Ferrel R. A progressive early onset cataract gene maps to human chromosome 17q24. *Nat Genet* 1995;9:37-40.

179. Moross T, Vaithilingam S, Styles S, Gardner H. Autosomal dominant anterior polar cataracts associated with a familial 2;14 translocation. *J Med Genet* 1984;21:52-53.

180. Miller B, Jaafar M, Capo H. Chromosome 14-terminal deletion and cataracts. *Arch Ophthalmol* 1992;110:1053.

181. Yokoyama Y, Narahara K, Tsuji K, Ninomiya S, Seino Y. Autosomal dominant congenital cataract and microphthalmia associated with a familial t(2;16) translocation. *Hum Genet* 1992;90:177-8.

182. Brewer C, Holloway S, Zawalnyski P, Schnizel A, Fitzpatrick D. A chromosomal deletion map of human malformations. *Am J Hum Genet* 1998;63:1153-1159.

183. Yamaguchi H, Okubo Y, Tanaka M. A note on possible close linkage between the Ii blood locus and a congenital cataract locus. *Proc Jap Acad* 1972;48:625-628.

184. Bierhuizen M, Mattei M, Fukuda M. Expression of the developmental 1 antigen by a cloned human cDNA encoding a member of the beta-1,6-N-acetylglucosaminyltransferase gene family. *Genes Dev* 1993;7:468-478.

185. Warburg M. X-linked cataract and X-linked microphthalmos: how many deletion families? *Am J Med Genet* 1989;34:451-453.

186. Bixler D, Higgins M, Hartsfield J. The Nance-Horan syndrome: a rare X-linked ocular-dental trait with expression in heterozygous females. *Clin Genet* 1984;26(1):30-5.

187. Seow W, Brown J, Romaniuk K. The Nance Horan syndrome of dental anomalies, congenital cataracts, microphthalmia and anteverted pinnae: case report. *Pediatr Dent* 1985;7(4):307-11.

188. Toutain A, Ayrault A, Mouraine C. Mental retardation in Nance-Horan syndrome: clinical and neuropsychological assessment in four families. *Am J Med Genet* 1997;71(3):305-14.

189. Franco E, Hodgson S, Lench N, Roberts G. Nance-Horan syndrome: a contiguous gene syndrome involving deletion of the amelogenin gene? A case report and molecular analysis. *Oral Dis* 1995;1(1):8-11.

190. Ogata H, Okubo Y, Akabara T. Phenotype i associated with congenital cataract in Japanese. *Transfusion* 1979;19:166-168.

191. Yamada K, Tomita H, Yoshiura K, Kondo S, Wakui K, Fukushima Y, et al. An autosomal dominant posterior polar cataract locus maps to human chromosome 20p12-q12. *Eur J Hum Genet* 2000;8(7):535-9.

192. Krill A, Woodbury G, Bowman J. X-chromosomal-linked sutural cataracts. *Am J Ophth* 1969;68:867-872.

193. Shambolian D, Lewis R, Buctow K, Bond A, Nussbaum R. Nance-Horan syndrome: localisation within the region Xp22.1-22.3 by linkage analysis. *Am J Hum Genet* 1990;47:13-19.

194. Walpole S, Ronce N, Grayson C, Dessay B, Yates J, Trump D, et al. Exclusion of RAI2 as the causative gene for Nance-Horan syndrome. *Hum Genet* 1999;104:410-411.

195. Toutain A, Ronce N, Dessay B, Robb L, Francannet C, Merrer ML, et al. Nance-Horan syndrome: linkage analysis in 4 families refines localisation to Xp22.31-p22.13. *Hum Genet* 1997;99:256-261.

196. Stambolian D, Favor J, Silvers W, Avner P, Chapman V, Zhou E. Mapping the X-linked cataract (Xcat) mutation, the gene implicated in the Nance Horan syndrome, on the mouse X chromosome. *Genomics* 1994;22(2):377-80.

197. Ionides A, Francis P, Berry V, Mackay D, Bhattacharya S, Shiels A, et al. Clinical and genetic heterogeneity in autosomal dominant congenital cataract. *Br J Ophthalmol* 1999;83(7):802-808.

198. Thut C, Rountree R, Hwa M, Kingsley D. A large scale in situ screen provides molecular evidence for the induction of eye anterior segment development by the developing lens. *Dev Biol* 2001;231(1):63-76.

199. Beebe D, Coats J. The lens organises the anterior segment: specification of neural crest differentiation in the avian eye. *Dev Biol* 2000;220(2):424-31.

200. Semina E, Reiter R, Leysens N, Alward W, Small K, Datson N, et al. Cloning and characterisation of a novel bicoid-related homeobox transcription factor gene RIEG, involved in Rieger syndrome. *Nature Genetics* 1996;14:392-399.

201. Phillips J, Bono ED, Haines J, Pralea A, Cohen J, Greff L, et al. A second locus for Rieger syndrome maps to 13q14. *Am J Hum Genet* 1996;59:340-341.

202. Weiss A, Kouseff B, Ross E, Longbottom J. Simple microphthalmos. *Arch Ophthalmol* 1989;107:1625-1630.

203. Othman M, Sullivan S, Skuta G, Cockrell D, Stringham H, Downs C, et al. Autosomal dominant nanophthalmos (NNO1) with high hyperopia and angle-closure glaucoma maps to chromosome 11. *Am J Hum Genet* 1998;63:1411-1418.

204. Vingolo E, Steindl K, Forte R, Zompatori L, Iannaccone A, Sciarra A, et al. Autosomal dominant simple microphthalmos. *J Med Genet* 1994;31:721-725.

205. Serrano J, Hodgkins P, Taylor D, Gole G, Kriss A. The nanophthalmic macula. *Br J Ophthalmol* 1998;82(3):276-9.

206. Yamani A, Wood I, Sugino I, Warner M, Zarbin M. Abnormal collagen fibrils in nanophthalmos: a clinical and histologic study. *Am J Ophthalmol* 1999;127:106-108.

207. Shaffer R, Calhoun F. The management of glaucoma in nanophthalmos. *Trans Am Ophthalmol Soc* 1975;73:119-122.

208. Singh O, Sofinski S. Nanophthalmos: guidelines for diagnosis and therapy. In: Albert D, Jakobiec F, editors. *Principles and Practice of Ophthalmology*. Philadelphia: WB Saunders, 1997:1535.

209. Mackay C, Shek M, Carr R, Yanuzzi L, Gouras P. Retinal degeneration with nanophthalmos, cystic macular degeneration and angle closure glaucoma: a new recessive syndrome. *Arch Ophthalmol* 1987;105:366-371.

210. Warburg M. Classification of microphthalmos and coloboma. *J Med Genet* 1993;30:664-669.

211. Bessant D, Khaliq S, Hameed A, Anwar K, Mehdi S, Payne A, et al. A locus for autosomal recessive congenital microphthalmia maps to chromosome 14q32. *Am J Hum Genet* 1998;62:1113-6.

212. Francois J. *Congenital cataracts*. Springfield, Illinois: Charles C Thomas, 1963.

213. Duke-Elder S. The lens. In: Duke-Elder S, editor. *A system of ophthalmology*: Henry Kimpton, 1964:715-759.

214. Clapp C. *Cataract: its aetiology and treatment*. London: Henry Kimpton, 1934.

215. Harman N. Treasury of Human Inheritance. Part 4. Section XIIIa, Congenital Cataract. *Eugenics Library Memoirs XI* 1910.

216. Vogt A. *Lens and zonule*. Bonn: JP Weyenborgh, 1979.

217. Sparrow J, Bron A, Brown N, Ayliffe W, Hill A. Oxford clinical cataract grading and classification. *Int Ophthalmol* 1986;9:207-225.

218. Merin S. *Congenital cataracts*. Boston: Little Brown, 1974.

219. Brown N, Bron A, Ayliffe W, Sparrow J, Hill A. The objective assessment of cataract. *Eye* 1987;1:234-245.

220. Vogt A. Weitere Ergebnisse der Spaltlampenmikroskopie des vorderen Bulbusabschnittes. III. (Abschnitt-Fortsetzung). Angeborene und fruh aufgetretene Linsenveranderungen. *Graefes Arch Clin Exp Ophthalmol* 1922;108:182-191.

221. Smith P. A pedigree of Doyne's discoid cataract. *Trans Ophth Soc UK* 1910;30:37-42.

222. Harman N. Ten pedigrees of congenital and infantile cataract; lamellar, coralliform, discoid and posterior polar with microphthalmia. *Trans Ophth Soc UK* 1910;30:251-274.

223. Harman N. Congenital cataract: a pedigree of five generations. *Trans Ophth Soc UK* 1909;29:101-108.

224. Nettleship E. Seven new pedigrees of hereditary cataract. *Trans Ophth Soc UK* 1909;29:188-211.

225. Poos F. Ueber eine familiar aufgetretene besondere Schichtstarform: "Cataracta zonularis pulverulenta". *Klin Monatsbl Augenheilkd* 1926;76:502-7.

226. Waardenburg P, Franceschetti A, Klein D. *Genetics and Ophthalmology*. Oxford: Blackwell Scientific, 1961.

227. Girardet M. Une nouvelle famille de cataracte poussiereuse centrale (cataracta centralis pulverulenta). *Ophthalmologica* 1943;105:24-36.

228. Marner E, Rosenberg T, Eiberg H. Autosomal dominant congenital cataract. Morphology and genetic mapping. *Acta Ophthalmol* 1989;67:151-8.

229. Scott M, Hejtmancik J, Wozencraft L, Reuter L, Marshall M, Parks M, et al. Autosomal dominant congenital cataract. Interocular phenotypic variability. *Ophthalmol* 1994;101:866-871.

230. Rogaev E, Rogaeva E, Korovaitseva G, Farrer L, Petrin A, Keryanov S, et al. Linkage of polymorphic congenital cataract to the gamma-crystallin locus on human chromosome 2q33-35. *Hum Mol Genet* 1996;5:699-703.

231. Cridland A. Three cases of hereditary cortical cataract, with a chart showing the pedigree of a family in which they occurred. *Trans Ophth Soc UK* 1918;38:375-376.

232. Clementi M, Rossetti A, Pesenti P, Tenconi R. Microphthalmia-congenital anterior polar cataract. *Ophth Paed Genet* 1985;6:189-192.

233. Bouzas A. Anterior polar congenital cataract and corneal astigmatism. *Ped Ophth Strab* 1992;29:210-212.

234. Helveston E, Ellis F. *Paediatric Ophthalmology Practice*. St Louis: Mosby, 1980.

235. Nettleship E. A pedigree of presenile or juvenile cataract. *Trans Ophth Soc UK* 1912;32:337-352.

236. Vogt A. Die spezifitat auder borener und erworbener starformer fur die einzelnen linsezouene. *Albrecht Von Graefes Arch Clin Exp Ophth* 1922;108:219-228.

237. Kivlin J, Lovrien E, George C, Cannon L, Maumenee I. Linkage between cerulean cataract and PGP. *Cytogenet Cell Genet* 1985;40:669.

238. Bodker F, Lavery M, Mitchell T, Lovrien E, Maumenee I. Microphthalmos in the presumed homozygous offspring of a first cousin marriage and linkage analysis of a locus in a family with autosomal dominant cerulean congenital cataracts. *Am J Med Genet* 1990;37:54-59.

239. Nettleship E. On heredity in the forms of cataract. *The Royal Lond Ophth Hosp Rep* 1906;17:218-222.

240. Gunn RM. Peculiar coralliform cataract with crystals in the lens. *Trans Ophth Soc UK* 1895;XV:119.

241. Souied E, Rozet J, Gerber S, Dufier J, Soubrane G, Coscas G, et al. Two novel missense mutations in the peripherin/RDS gene in two unrelated French families with autosomal dominant retinitis pigmentosa. *Eur J Ophthalmol* 1998;8(2):98-101.

242. Nakazawa M, Kikawa E, Chida Y, Wada Y, Shiono T, Tamai M. Autosomal dominant cone-rod dystrophy associated with mutations in codon 244 and codon 184 of the peripherin/RDS gene. *Arch Ophthalmol* 1996;114(1):72-8.

243. Trujillo M, Bueno J, Osorio A, Sanz R, Garcia-Sandoval B, Ramos C, et al. Three novel RDS-peripherin mutations (689delT, 857del17, G208D) in Spanish families with autosomal dominant retinal degenerations. *Hum Mutat* 1998;12(1):70.

244. Sinskey R, Amin P, Lingue R. Cataract extraction and intraocular lens implantation in an infant with a monocular congenital cataract. *J Cataract and Refract Surg* 1994;74:564-565.

245. Chrousos G, Parks M, O'Neill J. Incidence of chronic glaucoma, retinal detachment and secondary membrane surgery in pediatric aphakic patients. *Ophthalmology* 1984;91:1238-1241.

246. Simon J, Mehta N, Simmons S. Glaucoma after pediatric lensectomy/vitrectomy. *Ophthalmology* 1991;98:670-674.

247. Kanski J, Elkington A, Daniel R. Retinal detachment after congenital cataract surgery. *Br J Ophthalmol* 1974;58:92-95.

248. Gelbart S, Hoyt C, Jastrebeski G, Marg E. Long term results in bilateral congenital cataracts. *Am J Ophthalmol* 1982;93:615-621.

249. Lambert S, Boothe R. Amblyopia: basic and clinical science perspectives. *Focal Points* 1994;12:1-12.

250. Morgan K. Pediatric cataract and lens implantation. *Curr Opin Ophthalmol* 1995;6(1):9-13.

251. Taylor D. Congenital cataract: the history, the nature and the practice. The Doyne lecture. *Eye* 1998;12:9-36.

252. Elston J, Timms C. Clinical evidence for the onset of the sensitive period in infancy. *Br J Ophthalmol* 1992;76:327-328.

253. Lorenz B, Worle J. Visual results in congenital cataract with the use of contact lenses. *Graefes Arch Clin Exp Ophthalmol* 1991;229(2):123-32.

254. Yamamoto M, Dogru M, Nakamura M, Shirabe H, Tsukahara Y, Sekiya Y. Visual function following congenital cataract surgery. *Jpn J Ophthalmol* 1998;42(5):411-6.

255. Spierer A, Desatnik H, Rosner M, Blumenthal M. Congenital cataract surgery in children with cataract as an isolated defect and in children with a systemic syndrome: a comparative study. *J Pediatr Ophthalmol Strabismus* 1998;35(5):281-5.

256. Ariturk N, Oge I, Mohajery F, Erkan D, Turkoglu S. Secondary glaucoma after congenital cataract surgery. *Int Ophthalmol* 1999;22(3):175-180.

257. Neumann D, Weissman B, Isenberg S. The effectiveness of daily wear contact lenses for the correction of infantile aphakia. *Arch Ophthalmol* 1993;111:927-930.

258. Bradford G, Keech R, Scott W. Factors affecting visual outcome after surgery for bilateral congenital cataracts. *Am J Ophthalmol* 1994;117:58-64.

259. Ainsworth J, Cohen S, Levin A, Rootman D. Pediatric cataract management with variations in surgical technique and aphakic optical correction. *Ophthalmology* 1997;104(7):1096-1101.

260. Zwaan J, Mullaney P, Awad A, al-Mesfer S, Wheeler D. Pediatric intraocular lens implantation. Surgical results and complications in more than 300 patients. *Ophthalmology* 1998;105(1):112-8.

261. Cavallaro B, Madigan W, O'Hara M, Kramer K, Bauman W. Posterior chamber intraocular lens use in children. *J Pediatr Ophthalmol Strabismus* 1998;35:254-263.

262. Sharma N, Pushker N, Dada T, Vajpayee R, Dada V. Complications of pediatric cataract surgery and intraocular lens implantation. *J Cataract Refract Surg* 1999;25:1585-1588.

263. Taylor D. The Doyne lecture. Congenital cataract: the history, the nature and the practice. *Eye* 1998;12(1):9-36.

264. Strachan T, Read A. *Human Molecular Genetics*. Oxford: BIOS Scientific Publishers, 1996.

265. Ott J. *Analysis of human genetic linkage*, 1997.

266. Baltimore D. Our genome unveiled. *Nature* 2001;409(6822):814-816.

267. Roberts L. New game plan for genome mapping. *Science* 1989;245:1438-1440.

268. Sudbery P. *Human Molecular Genetics*. Harlow, UK: Addison Wesley Longman, 1998.

269. Davies K, Read A. *Molecular basis of inherited disease*. Second ed. Oxford: Blackwell Scientific, 1992.

270. Adams M, Kerlavage A, Fleischmann R, Fuldner R, Bult C, Lee N, et al. Initial assessment of human gene diversity and expression patterns based upon 83 million nucleotides of cDNA sequence. *Nature* 1995;377 (Suppl.):3-17.

271. Strachan T, Read A. *Human Molecular Genetics*. Oxford: Bios Scientific Publishers, 1997.

272. Dib C, Faure S, Fizames C, Samson D, Drouot N, Vignal A, et al. A comprehensive genetic map of the human genome based on 5,264 microsatellites. *Nature* 1996;380:152-154.

273. Mange A, Mange E. *Genetics: Human Aspects*. Second ed: Sinauer, 1990.

274. Morton N. Sequential tests for the detection of linkage. *Am J Hum Genet* 1955;7:277-318.

275. Lathrop G, Lalouel J, Julier C, Ott J. Strategies for multipoint linkage analysis in humans. *Proc Natl Acad Sci (USA)* 1984;81:3443-3446.

276. Curtis D, Gurling H. A procedure for combining two-point lod scores into a summary multipoint map. *Hum Hered* 1992;43:173-185.

277. Keen J, Lester D, Inglehearn C, Curtis A, Bhattacharya S. Rapid detection of single base mismatches as heteroduplexes on hydrolink gels. *Trends Genet* 1991;7:5.

278. Gudbartsson D, Jonasson K, Frigge M, Kong A. Allegro, a new computer program for multipoint linkage analysis. *Nat Genet* 2000;25:12-13.

279. Bairoch A, Bucher P, Hofmann K. The PROSITE database, its status in 1997. *Nucl Acids Res* 1997;25:217-221.

280. Johnson G, Foster A. Prevalence, incidence and distribution of visual impairment. In: GJ Johnson MD, Weale R, editor. *The epidemiology of eye disease*. London: Chapman and Hall, 1998:8-9.

281. Preston G, Carroll T, Guggino W, Agre P. Appearance of water channels in Xenopus oocytes expressing red cell CHIP28 protein. *Science* 1992;256:385-387.

282. Kushmerick C, Rice S, Baldo G, Haspel H, Mathias R. Ion, water and neutral solute transport in Xenopus oocytes expressing frog lens MIP. *Exp Eye Res* 1995;61:351-362.

283. Chandy G, Zampighi G, Kreman M, Hall J. Comparison of the water transporting properties of MIP and AQP1. *J Membr Biol* 1997;159:29-39.

284. Lund A, Eiberg H, Rosenberg T, Warburg M. Autosomal dominant cataract; linkage relations; clinical and genetic heterogeneity. *Clin Genet* 1992;41:65-69.

285. Berry V, Francis P, Kaushal S, Moore A, Bhattacharya S. Missense mutations in the human *MIP* gene, encoding the major intrinsic protein of the lens, underlie autosomal dominant "polymorphic" and lamellar cataracts on 12q. *Nat Genet* 2000;(in print).

286. Rahi J, Dezateux C. National cross sectional study of detection of congenital and infantile cataract in the United Kingdom: role of childhood screening and surveillance. *BMJ* 1999;318:362-365.

287. Taylor D. Developments in the treatment of cataract. *Trans Ophthalmol Soc UK* 1982;102:441-452.

288. Lloyd I, Gross-Sampson M, Jeffrey B, Kriss A, Russell-Eggitt I, Taylor D. Neonatal cataract: aetiology, pathogenesis and management. *Eye* 1992;6:184-196.

289. King L, Yasui M, Agre P. Aquaporins in health and disease. *Mol Med Today* 2000;6(2):60-5.

290. Wen H, Frokiaer J, Kwon T, Nielsen S. Urinary excretion of aquaporin-2 in rat is mediated by a vasopressin-dependent apical pathway. *J Am Soc Nephrol* 1999;10:1416-1429.

291. Mitsuoka K, Murata K, Walz T, Hirai T, Agre P, Heymann J, et al. The structure of aquaporin-1 at 4.5 angstrom resolution reveals alpha helices in the center of the monomer. *J Struct Biol* 1999;128(1):34-43.

292. Kaushal S, Khorana H. Structure and function in rhodopsin. 7 point mutations associated with autosomal dominant retinitis pigmentosa. *Biochemistry* 1994;33(20):6121-8.

293. Xiong X, Chong E, Skach W. Evidence that endoplasmic reticulum (ER)-associated degradation of cystic fibrosis transmembrane conductance regulator is linked to retrograde translocation from the ER membrane. *J Biol Chem* 1999;274(5):2616-24.

294. Moss K, Helm A, Lu Y, Bragin A, Skach W. Coupled translocation events generate topological heterogeneity at the endoplasmic reticulum membrane. *Mol Biol Cell* 1998;9(9):2681-97.

295. Shi L, Skach W, Ma T, Verkman A. Distinct biogenesis mechanisms for the water channels MIWC and CHIP28 at the endoplasmic reticulum. *Biochemistry* 1995;34(26):8250-6.

296. Kamsteeg E, Wormhoudt T, Rijss J, Os Cv, Deen P. An impaired routing of wild-type aquaporin-2 after tetramerisation with an aquaporin-2 mutant explains dominant nephrogenic diabetes insipidus. *EMBO J* 1999;18(9):2394-400.

297. Minassian D, Mehra V, Verrey J. Dehydrational crises: a major risk factor in blinding cataract. *Br J Ophthalmol* 1989;73(2):100-5.

298. Nemeth-Cahalan K, Hall J. pH and calcium regulate the water permeability of aquaporin 0. *J Biol Chem* 2000;275(10):6777-82.

299. Hess J, Casselman J, Kong A, Fitzgerald P. Primary sequence, secondary structure, gene structure and assembly properties suggests that the lens-specific cytoskeletal protein filensin represents a novel class of intermediate filament protein. *Exp Eye Res* 1998;66(625-644).

300. Yang B, Fukuda N, Hoek Av, Matthay M, Ma T, Verkman A. Carbon dioxide permeability of aquaporin-1 measured in erythrocytes and lung of aquaporin-1 null mice and in reconstituted liposomes. *J Biol Chem* 2000;275(4):2686-2692.

301. Yang B, Hoek Av, Verkman A. Very high single channel water permeability of aquaporin-4 in baculovirus-infected insect cells and liposomes reconstituted with purified aquaporin-4. *Biochemistry* 1997;36:7625-7632.

302. Hammond C, Sneider H, Spector T, Gilbert C. Genetic and environmental factors in age-related nuclear cataracts in monozygotic and dizygotic twins. *N Engl J Med* 2000;342(24):1786-90.

303. MacGregor A, Snieder H, Schork N, Spector T. Twins. Novel uses to study complex traits and genetic diseases. *Trends Genet* 2000;16(3):131-4.

304. Spielman R, Ewens W. The TDT and other family-based tests for linkage disequilibrium and association. *Am J Hum Genet* 1996;59:983-989.

305. Frances R, Benitez AR, Cohen D. Arrhythmogenic right ventricular dysplasia and anterior polar cataract. *Am J Med Genet* 1997;73(2):125-6.

306. Krutovskikh V, Yamasaki H. Connexin gene mutations in human genetic diseases. *Mutat Res* 2000;462(2-3):197-207.

307. Wilkie A, Taylor D, Scambler P, Baraitser M. Congenital cataract, microphthalmia and septal heart defects in two generations: a new syndrome. *Clin Dysmorphol* 1993;2(2):114-9.

308. Aalfs C, Oosterwijk J, Schoeneveld Mv, Begeman C, Wabeke K, Hennekam R. Cataracts, radiculomegaly, septal heart defects and hearing loss in two unrelated adult females with normal intelligence and similar facial appearance: confirmation of a syndrome. *Clin Dysmorphol* 1996;5(2):93-103.

309. Gorlin R, Marashi A, Obwegeser H. Oculo-facio-cardio-dental (OFCD) syndrome. *Am J Med Genet* 1996;63(1):290-3.

310. Schulze B, Horn D, Kobelt A, Tariverdian G, Stellzig A. Rare dental abnormalities seen in oculo-facio-dental (OFCD) syndrome: three new cases and review of nine patients. *Am J Med Genet* 1999;82(5):429-35.

311. Lindor N, Michels V, Hoppe D, Driscoll D, Leavitt J, Dewald G. Xp22.3 microdeletion syndrome with microphthalmia, sclerocornea, linear skin defects, and congenital heart defects. *Am J Med Genet* 1992;44(1):61-5.

312. Bech-Hansen N, Pearce W. X-linked retinitis pigmentosa: re-evaluation of fundus findings and the use of haplotype analysis in clarification of carrier female status. *Ophthalmic Genet* 1995;16(3):113-8.

313. Happle R, Kuchle H. Sectoral cataract: a possible example of lyonisation. *Lancet* 1983;15(2(8355)):919-920.

314. Wilson C, Aftimos S. X-linked dominant chondrodysplasia punctata: A peroxisomal disorder. *Am J Med Genet* 1998;78(3):300-302.

315. Heon E, Liu S, Billingsley G, Bernasconi O, Tsifildis C, Schorderet D, et al. Gene localisation for aculeiform cataract, on chromosome 2q33-35. *Am J Hum Genet* 1998;63:921-926.

316. Berson E. Retinitis Pigmentosa and allied diseases. In: Albert D, Jakobiec F, editors. *Principles and Practice of Ophthalmology*. Philadelphia: WB Saunders, 1997:1213.

317. Ghose S, Sachev M, Kumar H. Bilateral nanophthalmos, pigmentary retinal dystrophy, and angle-closure glaucoma- a new syndrome. *Br J Ophthalmol* 1985;69(8):624-8.

318. Richards J, Maumenee I, Rowe S, Lovrien E. Congenital cataract possibly linked to haptoglobin. *Cytogenet Cell Genet* 1994;37:570.

319. Inglehearn C, Keen T, Bashir R, Jay M, Fitzke F, Bird A, et al. A completed screen for mutations of the rhodopsin gene in a panel of patients with autosomal dominant retinitis pigmentosa. *Hum Mol Genet* 1992;1:41-45.

320. Stone E, Fingert J, Alward W, Nguyen T, Polansky J, Sunden S, et al. Identification of a gene that causes primary open angle glaucoma. *Science* 1997;275:668-670.

321. Allikmets R, Shroyer N, Singh N, Seddon J, Lewis R, Bernstein P, et al. Mutation of the Stargardt disease gene (ABCR) in age related macular degeneration. *Science* 1997;277:1805-1807.

322. Allikmets R. Simple and complex ABCR: genetic predisposition to retinal disease. *Am J Hum Genet* 2000;67(4):793-799.

323. Martin N, Boomsma D, Machin G. A twin-pronged attack on complex traits. *Nat Genet* 1997;17:387-92.

324. Johnson G, Todd J. Strategies in complex disease mapping. *Curr Opin Gen Devel* 2000;10:330-334.

325. Kaplan N, Martin E, Weir B. Power studies for the transmission/disequilibrium tests with multiple alleles. *Am J Hum Genet* 1997;60:691-702.

8. Appendix 1

Department of Molecular Genetics
Institute of Ophthalmology
(Associated with Moorfields Eye Hospital)
University College London
11-43 Bath Street
London EC1V 9EL
UK
Telephone +44 (0)171 608 6806
Fax +44 (0)171 608 6863

30 August 1999

Dear,

Following your recent clinic at Moorfields Eye Hospital with Mr Moore, I write to ask for your help in our research study. We are trying to find the causes of inherited cataract.

I am a member of a team of doctors and scientists at Moorfields Eye Hospital and the Institute of Ophthalmology in London who are undertaking a study to identify the genes that cause cataract in families. To do this, we need to examine the eyes of all members of a family, both those who have cataracts and those that do not. We will also ask you to provide a small sample of blood.

I would be very grateful if you would indicate on the enclosed form whether you would be interested in helping us and return it to me.

If you have any questions, please do not hesitate to contact me at the Institute on 0171 608 6932 or 0585 688847 (mobile).

Thank you for your help with our study.

Yours sincerely,

Professor S S Bhattacharya - Head of Department Telephone 0171 608 6806 Email sbhatach@hgmp.mrc.ac.uk
Professor D M Hunt Telephone 0171 608 6820 Email d.hunt@ucl.ac.uk
Dr M J Warren - Senior Lecturer Telephone 0171 608 6943 Email m.warren@ucl.ac.uk

I would like to help with the study on inherited cataract and wish to discuss this further.

Signature..... Date.....

I can be contacted on the following telephone number:

.....

I prefer not to participate in the study on inherited cataract.

Signature..... Date.....

Department of Molecular Genetics
Institute of Ophthalmology
(Associated with Moorfields Eye Hospital)
University College London
11-43 Bath Street
London EC1V 9EL
UK
Telephone +44 (0)171 608 6806
Fax +44 (0)171 608 6863

I consent to participate in the study into the genetics of congenital cataract which involves an eye examination and providing a blood sample.

Name.....

Signature..... Date.....

Signature of investigator.....

Professor S S Bhattacharya - Head of Department Telephone 0171 608 6806 Email sbhatach@hgmp.mrc.ac.uk
Professor D M Hunt Telephone 0171 608 6820 Email d.hunt@ucl.ac.uk
Dr M J Warren - Senior Lecturer Telephone 0171 608 6943 Email m.warren@ucl.ac.uk

Department of Molecular Genetics
Institute of Ophthalmology
(Associated with Moorfields Eye Hospital)
University College London
11-43 Bath Street
London EC1V 9EL
UK
Telephone +44 (0)171 608 6806
Fax +44 (0)171 608 6863

5 July 1999

Dear Mr

re: study into inherited cataract

Just a quick note to thank you all for your help with our study.

If you have any questions, please do not hesitate to contact me at the Institute on 0171 608 6932.

Best Wishes,

Dr Peter Francis
Clinical Research Fellow
and Honorary Specialist Registrar

Professor S S Bhattacharya - Head of Department Telephone 0171 608 6806 Email sbhatach@hgmp.mrc.ac.uk
Professor D M Hunt Telephone 0171 608 6820 Email d.hunt@ucl.ac.uk
Dr M J Warren - Senior Lecturer Telephone 0171 608 6943 Email m.warren@ucl.ac.uk

INSTRUCTIONS FOR BLOOD COLLECTION

Thank you for taking the blood in the EDTA tubes provided.
Please label the tubes with name and date of birth.
Then, in order to comply with post office regulations, please seal in plastic bag, wrap in bubble-wrap and seal in the box provided. The package can then be posted in the normal fashion.
If you have any queries please phone 0171 608 6932 or 0585 688847

Department of Molecular Genetics
Institute of Ophthalmology
(Associated with Moorfields Eye Hospital)
University College London
11-43 Bath Street
London EC1V 9EL
UK
Telephone +44 (0)171 608 6806
Fax +44 (0)171 608 6863

INSTRUCTIONS FOR CELL COLLECTION

It is best if the sample is collected early in the morning prior to having a drink

Remove brush from the plastic bag, touching only the "stick" end.

Open mouth and twirl the brush on the inner cheeks and tongue for 30 seconds. Be firm but don't scrape so hard as to make the cheek bleed!

Carefully place the brush end of the collector into the fluid filled plastic tube and snap off (this should be quite easy as the brush has been scored in the correct position).

Repeat the procedure using the other brushes.

When all brushes are in the fluid, ensure the container is shut tightly, then return it in the bag, wrapped in bubble-wrap and sealed in the box.

Professor S S Bhattacharya - Head of Department Telephone 0171 608 6806 Email sbhatach@hgmp.mrc.ac.uk
Professor D M Hunt Telephone 0171 608 6820 Email d.hunt@ucl.ac.uk
Dr M J Warren - Senior Lecturer Telephone 0171 608 6943 Email m.warren@ucl.ac.uk

3 February 1999

Dear Mr Coppock,

Please forgive any intrusion. I am a member of a team of doctors and scientists at Moorfields Eye Hospital and the Institute of Ophthalmology in London. We are undertaking a study to identify the causes of inherited cataract (opacity of the lens in the eye).

In 1906, the first report of a family with inherited cataract was published in the medical literature. This family, by the name of Coppock, came from the parish of Headington Quarry and the villages of Headington and Milton/ Great Milton in Oxfordshire. We are interested in making contact with this family once again.

I would be very grateful if you could indicate on the enclosed form whether you would be able to help us or if you have any information that might be of use in tracing this family.

Thank you for your help with this study and once again please forgive any intrusion. If you have any questions, please do not hesitate to contact me at the Institute on 0171 608 6932.

Yours sincerely,

Dr Peter Francis BM BSc FRCOphth
Clinical Research Fellow and Honorary Specialist Registrar

9. Appendix 2

9 Mutation detection in exons 9,10 and 11 of the *OPA1* gene in patients with normal tension glaucoma

9.1 Background

Normal tension glaucoma (NTG) is a subtype of glaucoma characterised progressive glaucomatous optic nerve damage in the presence of usually a normal or low normal intraocular pressure.

The recent identification of mutations in the *OPA1* gene (personal communication, M Votruba, 2000) that underlie dominant optic atrophy, a disease primarily of the optic nerve head, not dissimilar from NTG, point to this gene at a strong candidate for patients with inherited NTG. At present no other gene or chromosomal locus is known for this condition.

9.2 Methods

Using the primers shown below, exons 9, 10 and 11 of the *OPA1* gene of 95 patients with NTG were amplified. Heteroduplex analysis was then undertaken (Materials and Methods) as a screening method. Heteroduplexes identified were directly sequenced (Materials and Methods) as were other members of the family where possible.

9.3 Results

Table 2a shows the primers used to amplify the relevant exons.

Gene – exon	Forward primer 5' –3'	Reverse primer 5' – 3'	Annealing temp (°C)
OPA1 exon 9	AGA GCA GCA TTA CAA ATA GGT TT	CAG GTT TCC CTG AAG CAG TT	58
OPA1 exon 10, intron 10, exon 11	GAC AGA TCT GGT GTA TGC CCG ACA CCC	CCA TAA AAC GTC ACT GAA ATG AAT	55

Heteroduplexes were identified with assurity in individuals 9 and 60 (exon 10, 11, intron 10). An extra band was seen for individuall 20, but this may have resulted from overflow of some 1kb ladder from the adjacent lane. Direct sequencing confirmed the observed change in lane 20 as artifactual. The A→C transversion at nucleotide 158568 was observed in both samples 9 and 60 (figure 2a). No heteroduplexes were seen in exon 9

9.4 Discussion

The aetiology of normal tension glaucoma is unknown. The disease is primarily one of the optic nerve and is characterised by progressive retinal ganglion cell degeneration resulting, if untreated, in progressive glaucomatous visual field loss. Although small families with dominantly inherited NTG have been described the condition is usually sporadic. Recently, mutations in the *OPA1* gene have been shown to underlie the development of dominant optic atrophy. Similarity in the apparent disease processes implicates *OPA1* as a candidate gene for NTG.

The results of the heteroduplex analysis and direct sequencing have identified the same sequence alteration in intron 10 in two genealogically distinct individuals. Since the missense change occurs within a non-coding region, the likelihood is that the transversion represents a polymorphism. Pathological significance could be established if the mutation segregates within the family and is not shown to be present in a normal control population.

Figure 2a: sense strand sequence analysis of *OPA1* exons 10 , 11 and intron 10 showing: ***a***, non-segregating A→ C transversion at nucleotide 158568(arrowed); ***b***, wild-type sequence

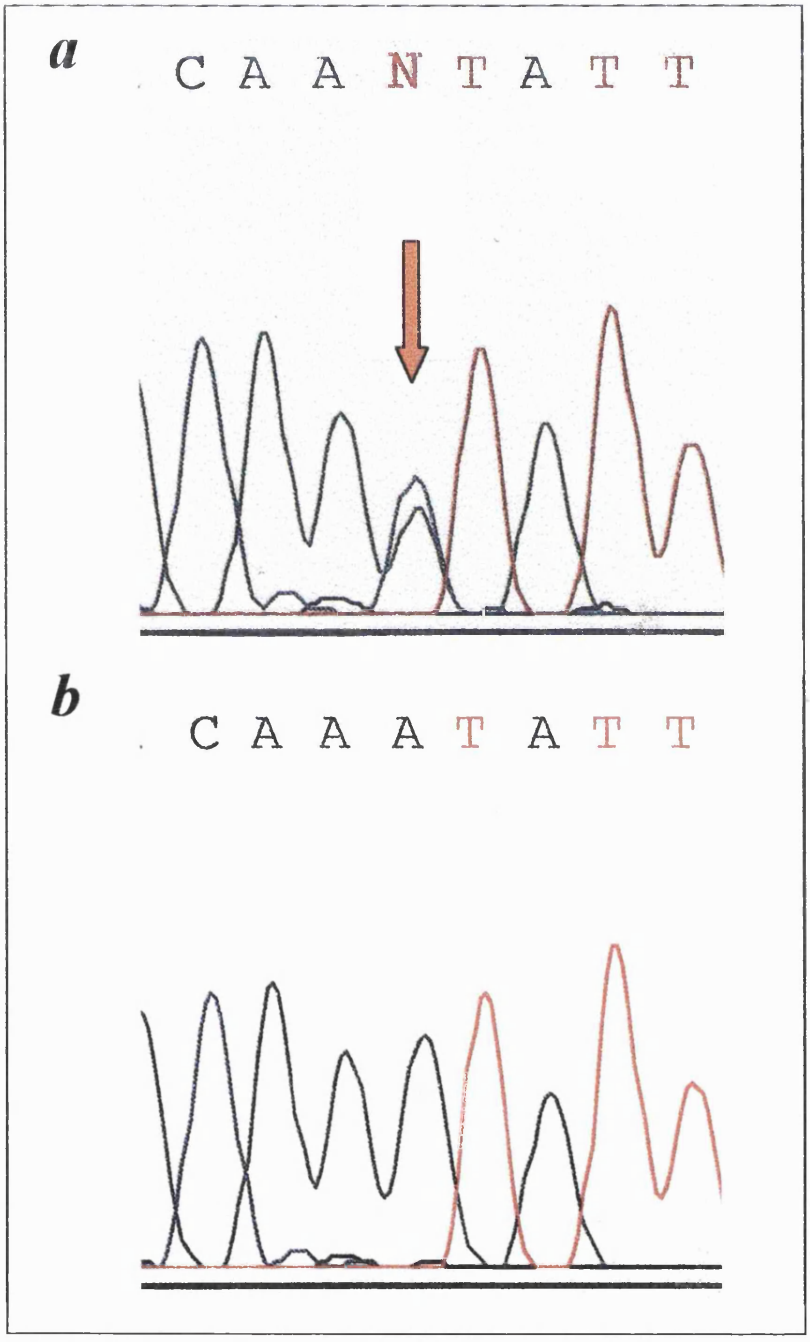

10. Appendix 3

Table 3a: Direct sequencing panel

No.	Status
1	A
2	U
3	A
4	U
5	A
6	U
7	A
8	U
9	A
10	U
11	A
12	U
13	A
14	U
15	A
16	U
17	A
18	U
19	A
20	U
21	A
22	A
23	A
24	U
25	A
26	U
27	A
28	U
29	A
30	U
31	A
32	U
33	A
34	U
35	A
36	U
37	A
38	U
39	A
40	U
41	A
42	U
43	A
44	U
45	A
46	U
47	A
48	U
49	A
50	U
51	A
52	U
53	A
54	U
55	A
56	U
57	A
58	A
59	A
60	U
61	A
62	A
63	A
64	A
65	U
66	A
67	U
68	A
69	A
70	U
71	A
72	A
73	U
74	A
75	A
76	A
77	A
78	U
79	A
80	U
81	A
82	U
83	A
84	U
85	A
86	U
87	A
88	A
89	U
90	A
91	U
92	A
93	A
94	A
95	A
96	A
97	A
98	A
99	A
100	A
101	A
102	A
103	A
104	A
105	A
106	A
107	A
108	A
109	A
110	A
111	A
112	A
113	A
114	A
115	A
116	A
117	A
118	A
119	A
120	A
121	A
122	A
123	A
124	A
125	A
126	A
127	A
128	A
129	A
130	A
131	A
132	A
133	A

A = affected
U = unaffected